# Investigating the Mechanisms Governing Humoral Immunity in Autoimmune Kidney Disease

By

Tho-Alfakar Al-Aubodah

Department of Microbiology & Immunology, Faculty of Medicine and Health Sciences

McGill University

Montréal, Québec, CANADA

August 2024

A thesis submitted to McGill University in partial fulfillment of the requirements of the degree of Doctor of Philosophy

*To Esra and Manar*

**TABLE OF CONTENTS**

**ABSTRACT**

Autoimmune kidney diseases are a heterogeneous family of disorders caused by immune-mediated damage to the glomerulus, the major filtering structure of the kidney. Without intervention, loss of protein into the urine and the accumulation of wastes in circulation can progress to end-stage kidney disease, requiring lifelong hemodialysis or a kidney transplantation for survival. While the autoreactive immune responses that lead to autoimmune kidney disease are highly variable both in terms of the anatomic location of the target antigen and the degree of inflammation within the kidney, autoantibodies are ubiquitous and are often the primary drivers of pathogenesis. *Nevertheless, the immune mechanisms underlying the break in tolerance and the development of autoimmune kidney disease remain poorly defined*. Here, we investigated these questions in two distinct settings: childhood idiopathic nephrotic syndrome (INS) and rapidly-progressive glomerulonephritis (RPGN).

Childhood INS is a relapsing-remitting glomerular disease characterized by non-inflammatory injury to the podocytes, the major cellular component of glomerular filtration. While the etiology of INS remains completely unknown, the recent therapeutic success of B cell depletion and the discovery of anti-podocyte antibodies (APAs) in subpopulations of affected individuals led us to hypothesize that *childhood INS is a humoral autoimmune kidney disease*. By dissecting the peripheral blood B cell compartment of affected children, we show that active disease is associated with the expansion of autoimmune-associated extrafollicular memory B cells (eMBCs) and short-lived plasma cells (SLPCs) (*Chapter 2*). Through B cell receptor sequencing, we demonstrated that the eMBCs and SLPCs expanded in INS are oligoclonal denoting their participation in *bona fide* B cell response, particularly in APA-positive children (*Chapter 3*). Moreover, we used a mouse model of INS and provided strong evidence that the generation of pathogenic APAs is dependent on MHC-II haplotype (*Chapter 4*). Taken together, these data support an autoimmune humoral origin for childhood INS.

Autoimmune kidney diseases are often associated with a defect in regulatory T ($T_{REG}$) cell number, though the nature of this defect is unknown. In RPGN, diminished $T_{REG}$ cell

suppressive function is predicted to contribute the inflammatory pathology seen in disease. Here, using an established mouse model for RPGN mediated by antibodies, we showed that the IL-1 family cytokines IL-1 and IL-33 released upon glomerular injury severely diminish $T_{REG}$ cell control of kidney-directed T and B cell responses (*Chapter 5*).

Taken together, our results identify a complex interplay of factors that contribute to the development of autoimmunity in autoimmune kidney disease and highlight possible therapeutic avenues for the modulation of these responses.

**RÉSUMÉ**

Les maladies rénales auto-immunes constituent une famille hétérogène de troubles causés par des lésions immunitaire du glomérule, la principale structure filtrante du rein. Sans intervention, la perte de protéines dans l'urine et l'accumulation de déchets métaboliques dans la circulation peut progresser jusqu'au stade de l'insuffisance rénale terminale, nécessitant une hémodialyse à vie ou une greffe de rein pour survivre. Bien que les réponses immunitaires auto-réactives à l'origine des maladies rénales auto-immunes soient très variables à la fois en termes de localisation anatomique de l'antigène cible et de degré d'inflammation dans le rein, les auto-anticorps sont omniprésents et sont souvent les principaux moteurs de la pathogenèse. Néanmoins, les mécanismes immunitaires qui sous-tendent la rupture de tolérance et le développement d'une maladie rénale auto-immune restent mal définis. Nous avons étudié ces questions dans deux contextes: le syndrome néphrotique idiopathique (SNI) de l'enfant, et la glomérulonéphrite aiguë.

Le SNI de l'enfant est une maladie glomérulaire récurrente-rémittente caractérisée par des lésions non inflammatoires des podocytes, la principale composante cellulaire de la filtration glomérulaire. Bien que l'étiologie du SNI reste totalement inconnue, le succès thérapeutique récent de la déplétion des cellules B et la découverte d'anticorps anti-podocytes (AAP) dans des sous-populations d'individus affectés nous ont amenés à émettre l'hypothèse que le SNI de l'enfant a une étiologie auto-immune humorale. En disséquant le compartiment des cellules B du sang périphérique des enfants atteints, nous montrons que la maladie active est associée avec l'expansion des cellules B mémoires extrafolliculaires (eMBC), qui sont associées avec l'auto-immunité systémique, et les plamablastes (*Chapitre 2*). Grâce au séquençage des récepteurs des cellules B, nous avons démontré que les eMBCs et plasmablasts sont oligoclonaux, en particulier chez les enfants séropositifs pour l'AAP, ce qui dénote leur participation à une véritable réponse induite par l'antigène (*Chapitre 3*). En outre, nous avons utilisé un modèle murin de SNI, et fourni des preuves solides que la génération d'AAP pathogènes dépend de l'haplotype du CMH-II (*Chapitre 4*). Dans l'ensemble de ces données soutiennent d'une origine humorale auto-immune pour le SNI de l'enfant.

Les maladies rénales auto-immunes sont souvent associées avec un défaut du nombre de cellules T régulatrices ($T_{REG}$). Bien que, la nature de ce défaut soit inconnue. Dans la glomérulonéphrite aiguë, la diminution de la fonction suppressive des cellules $T_{REG}$ devrait contribuer à la pathologie inflammatoire observée dans la maladie. En utilisant un modèle murin établi de la glomérulonéphrite aiguë médié par des anticorps, nous avons montré que les cytokines IL-1 et IL-33, qui sont libérées lors d'une lésion glomérulaire, diminuent fortement le contrôle exercé par les cellules $T_{REG}$ sur les réponses des lymphocytes T et B dirigées vers le rein (*Chapitre 5*).

Dans l'ensemble, nos résultats identifient une interaction complexe de facteurs qui contribuent au développement de réponses humorales dans les maladies rénales auto-immunes, et mettent en évidence des avenues thérapeutiques possibles pour la modulation de ces réponses.

**ACKNOWLEDGEMENTS**

Any attempt to acknowledge the people who have helped me realize this dream feels truly inadequate. Sentences, or my ability to formulate them, cannot sufficiently express my gratitude to the many who have that have left their mark on such a precious time of my life. First and foremost, I would like to thank my supervisors *Dr. Ciriaco Piccirillo* and *Dr. Tomoko Takano*. Their guidance over the years and their unwavering commitment to nurturing my curiosity have cemented my passion for science and my dedication to immunology. Thank you for the countless scientific and professional opportunities that you have given me and for always believing in my ability to excel. I will forever cherish your influence on my career and sincerely hope that our paths will cross again.

I would also like to express my deepest gratitude to my advisory committee members, *Dr. Jörg Fritz*, *Dr. Inés Colmegna*, and *Dr. Andrey Cybulsky*. Your valuable insights and mentorship were instrumental to my success and to the quality of the work presented in this thesis. I would also like to thank *Dr. Susan Samuel* (the director of CHILDNEPH) and *Dr. Martin Bitzan*, the primary caregivers for many of our study participants. Thank you for your dedication to our science, and for always providing the much-needed perspective of the treating physician, patient, and family. Importantly, I would like to thank *Dr. Joyce Rauch* for running the Immunology Journal Club – I am grateful to have been a part of it and wish that more students will benefit from the collegial environment that you have established.

I would also like to acknowledge my colleagues, from past and present, for their impact on my graduate training: *Helen Mason*, *Fernando Alvarez*, *Roman Istomine*, *Mikhaël Attias*, *Céleste Pilon*, *Zhiyang Liu*, *Harshita Patel*, *Ashley Ste-Croix*, *Sebastian Grocott*, *Geneviève Genest*, *Lamine Aoudjit*, *Giuseppe Pascale*, *Simon Leclerc*, *Sabrina Bartolucci*, *Harry Yang*, and *Laura Widawski*. Your friendship and support throughout my Ph.D. have been essential to my success and my happiness. I would especially like to thank *Roman*, my first friend and mentor in the lab. Thank you for all the adventures, both in and out of the lab – you will always be synonymous to the best of Montréal for me. To *Helen*, I am forever grateful for your bright personality, our invaluable discussions, your care for the lab, and your sincere friendship. To *Fernando Alvarez*, *Mikhaël Attias*, *Zhiyang Liu*, and *Ashley Ste-Croix* – I

will treasure our many discussions on science, culture, and philosophy; I'm humbled to have been your colleague and grateful to be your friend. To *Sebastian Grocott*, one of the brightest people I've ever met – thank you for all the memories and top-notch discussions. And finally, I would like to thank *Céleste Pilon* and *Harshita Patel* – I will continue to cherish the elite friendship we forged in our journeys; I will miss chasing sunsets, cooking dinners, playing board games, helmeted ice skating, having night picnics, and drinking endless amounts of bubble tea. To Céleste, thank you for standing with me on our little B cell island and for exposing me to la vraie culture québécoise. And to Harshita, thank you for your untiring support, even when at a Canada's length away.

I would also like to thank *Ekaterina Yurchenko*, *Hélène Pagé-Veillette*, and *Marie-Hélène Lacombe* of the Immunophenotyping Core for their technical support and guidance. Perhaps just as importantly, thank you for the often much-needed distracting conversation.

To *all of you*, the greatest learning I've done has not been in studying textbooks, reading articles and reviews, or watching seminars in solitude, but rather in my discussions with you, be they short or long, science-related or not.

Finally, I would like to thank my parents, *Hameed* and *Afrah*, and siblings, *Esra* and *Manar*, for their constant love, encouragement, and firm belief in my success.

## CONTRIBUTION TO ORIGINAL KNOWLEDGE

This thesis is manuscript-based. *Chapters 2*, *3*, *4*, and *5* significantly contribute to the field of autoimmune kidney disease, with *Chapters 2*, *3*, and *4* advancing our understanding of the immunopathogenesis of childhood idiopathic nephrotic syndrome (INS).

In published, *Chapter 2* (1), we identify the expansion of extrafollicular memory B cells as a feature of childhood INS. We demonstrate that:

1) *A B cell transcriptional program consistent with antigen-specific activation is the major immunological perturbation in the periphery in childhood INS.*
2) *Atypical B cells and marginal zone-like B cells are expanded in INS.*
3) *The APRIL-TNFRSF13B signaling axis is upregulated in INS.*
4) *The expansion of CD21$^{low}$ CD11c$^{+}$ T-bet$^{+}$ CD38$^{+}$ B cells, consistent with atypical B cells, and plasmablasts are a hallmark of childhood INS.*
5) *Plasmablasts are effectively controlled with glucocorticoid treatment and are removed following rituximab treatment, denoting a short-lived phenotype.*
6) *Relapses following rituximab treatment are associated with the resurgence of memory B cells.*

In *Chapter 3*, we demonstrate that the expansion of memory B cells and plasmablasts in childhood INS is clonal and associated with autoantibody generation. We show that:

1) *TNFRSF13B-expressing memory B cells and plasmablasts are expanded in INS.*
2) *The expansion of TNFRSF13B-expressing memory B cells are clonal, especially in individuals seropositive for anti-CRB2 antibody.*
3) *Clonally expanded memory B cells underwent significant somatic hypermutation, denoting the presence of a mature B cell response.*

In *Chapter 4*, we use a novel mouse model of INS and identify that polymorphisms in genes encoding the major histocompatibility complex impact the pathogenic potential of autoantibodies in INS. Our preliminary results demonstrate that:

1) *Childhood INS is associated with HLA-DQA1*02:01, HLA-DQB1*02:02, and HLA-DRB1*07:01 alleles.*
2) *C57BL/6 mice are completely protected from experimental autoimmune nephrotic syndrome (EANS) induced by immunization with the extracellular domain of mouse Crb2 (rmCrb2$_{601-940}$) while C3H/HeN and BALB/c mice are susceptible.*
3) *C57BL/6 mice developed high titers of anti-Crb2 antibodies, but they were unable to bind to podocytes in the glomerulus.*
4) *Germinal center responses in C57BL/6 mice failed to be recalled with subsequent challenge with rmCrb2$_{601-940}$.*

In *Chapter 5*, we use a mouse model of rapidly-progressive glomerulonephritis and identify that alarmins from the IL-1 family of cytokines impair regulatory T ($T_{REG}$) cell capacity to regulate nephritogenic $T_H1$ and B cell responses. We show that:

1) *In the nephrotoxic nephritis (NTN) model, renal $T_{REG}$ cells accumulate as GATA-3$^+$ ST2$^+$ cells during the $T_H1$-dominated autologous – or autoantigen-driven – phase of disease.*
2) *GATA-3$^+$ $T_{REG}$ cells arise in renal lymph nodes alongside $T_H1$ and B cell responses in the autologous phase.*
3) *GATA-3$^+$ $T_{REG}$ cell development is independent of IL-33 signaling, and IL-33 limits $T_{REG}$ cell control of autologous responses.*
4) *IL-1 signaling limits $T_{REG}$ cell control of renal $T_H1$ responses.*

## CONTRIBUTION OF AUTHORS

*Chapter 1: Introduction and Literature Review*

T.A. wrote the literature review and edited by T.T. and C.A.P.

*Chapter 2:*

Al-Aubodah T, Aoudjit L, Pascale G, Perinpanayagam MA, Langlais D, Bitzan M, Samuel SM, Piccirillo CA, Takano T. **The extrafollicular B cell response is a hallmark of childhood idiopathic nephrotic syndrome.** *Nature Communications*. 2023;14(1): 7682.

T.A., C.P., and T.T. conceptualized the study and designed all the experiments. T.A. conducted the experiments and performed all the data analysis. T.A., L.A., and M.P. processed all the blood samples. G.P. and M.P. consented the children into the study. T.A., L.A., M.P., M.B., S.S., and T.T. coordinated sample collection and biobanking at the McGill University Health Centre and Alberta Children's Hospital. T.A., D.L., C.P., and T.T. planned all the bioinformatics analyses. T.A., C.P., and T.T. wrote the initial draft of the manuscript. All authors critically reviewed the manuscript, discussed the results, interpreted the data, and contributed to the formulation and agreed on the submission of the final draft of the manuscript.

*Chapter 3:*

Al-Aubodah T, Leclerc S, Aoudjit L, Istomine R, Pascale G, Perinpanayagam MA, Samuel SM, Piccirillo CA, Takano T. **Memory B cells are clonally expanded in anti-CRB2-positive children with idiopathic nephrotic syndrome.** *Manuscript in preparation*.

T.A., C.A.P. and T.T. conceptualized the study and designed all the experiments. T.A. conducted the flow cytometry and scRNA-seq experiments and performed all the data analyses. T.A., L.A., M.A.P. processed all the blood samples. T.A. and R.I. thawed the PBMC and prepared them for cell sorting. L.A. generated the recombinant human CRB2, and S.L. conducted the ELISAs to determine anti-CRB2 serostatus. G.P. and M.A.P. obtained consent from the parents/legal guardians of all participating children and further obtained assent

from subjects between 7 and 18 years of age. T.A., L.A., G.P., M.A.P., A.B.D., S.M.S. and T.T. coordinated sample collection and biobanking at the McGill University Health Centre, Alberta Children's Hospital, and the Children's Hospital Research Institute of Manitoba. T.A., C.A.P. and T.T wrote the initial draft of the manuscript.

*Chapter 4:*

Al-Aubodah T, Aoudjit L, Grocott S, Leclerc S, Suzuki S, Piccirillo CA, Takano T. **The susceptibility to Crb2-induced experimental autoimmune nephrotic syndrome is mouse strain-dependent.** *Manuscript in preparation*.

T.A., C.A.P. and T.T. conceptualized the study and designed all the experiments. T.A. completed all the data analysis. T.A. and L.A. processed the blood samples for HLA typing. T.A., S.G., S.L., and S.S. performed all immunizations. T.A. and S.G. collected urine and blood. T.A. performed urine and serum ELISAs, sacrificed the mice and harvested the organs, performed flow cytometry, and ran the *in vitro* Crb2-specific T cell culture. L.A. performed the immunofluorescence experiments. T.A., C.A.P and T.T. wrote the initial draft of the manuscript.

*Chapter 5:*

Al-Aubodah T, Istomine R, Alvarez F, Takano T, Piccirillo CA. **IL-1 and IL-33 limit $T_{REG}$ control of autologous responses in rapidly-progressive glomerulonephritis.** *Manuscript in preparation*.

T.A., T.T., and C.A.P. conceptualized the study and designed all the experiments. T.A., R.I., and F.A. conducted all the investigations. Formal analysis was completed by T.A.. T.A., T.T., and C.A.P. wrote the initial draft of the manuscript.

*Chapter 6: Conclusion and General Discussion*

T.A. wrote the conclusions and edited by T.T. and C.A.P.

I am also preparing the following manuscript co-authored with Sebastian Grocott investigating the heterogeneity of SARS-CoV-2 Spike-specific $CD4^+$ T cell responses in infected and vaccinated adults:

Al-Aubodah T*, Grocott S*, Liu Z, Ismailova N, Koh W, Fritz JH, Ostrowski MA, Piccirillo CA. **Activation-induced marker expression patterns identify distinct SARS-CoV-2-specific $CD4^+$ T cells.** *Manuscript in preparation*.

*Co-first authorship

I have also co-authored the following report with Dr. Khashayar Esfahani detailing a case of kidney transplant rejection during immune checkpoint inhibition for the treatment of melanoma.

Esfahani K*, Al-Aubodah T*, Thebault P, Lapointe R, Hudson M, Johnson NA, Baran D, Bhulaiga N, Takano T, Cailhier JF, Piccirillo CA, Miller WH. **Targeting the mTOR pathway uncouples the efficacy and toxicity of PD-1 blockade in renal transplantation.** *Nature Communications*. 2019;10(1): 4712.

*Co-first authorship

I have also co-authored this review with Dr. Mikhaël Attias reviewing $T_{REG}$ cell functions in homeostasis and diseases.

Attias M*, Al-Aubodah T*, Piccirillo CA. **Mechanisms of human $FoxP3^+$ Treg cell development and function in health and diseases.** *Clinical & experimental immunology*. 2019;197(1): 36-51.

*Co-first authorship

**I, Tho-Alfakar Al-Aubodah, have read, understood, and abided by all norms and regulations of academic integrity of McGill University.**

**LIST OF FIGURES**

**ABBREVIATIONS**

α3(IV)NC1 – Non-collagen domain of the α3 chain of type IV collagen

AAV – ANCA-associated vasculitis

ABC – Age-associated B cell

AChR – Acetylcholine receptor

ACPA – Anti-citrullinated protein antibody

AICD – Activation-induced cytidine deaminase

ANA – Anti-nuclear antibody

ANCA – Anti-neutrophil cytoplasmic antibody

APA – Anti-podocyte antibody

APLS – Anti-phospholipid syndrome

APRIL – A proliferation induced ligand

ASC – Antibody-secreting cell

atBC – Atypical B cell

BACH2 – BTB domain and CNC homology 2

BAFF – B cell-activating factor

BAFF-R – BAFF receptor

BCDT – B cell depletion therapy

BCMA – B cell maturation antigen

BCL-2/6 – B cell lymphoma-2/6

BCR – B cell receptor

BCL-6 – B cell lymphoma 6

BLIMP1 – B lymphocyte maturation protein 1

CAR – Chimeric antigen receptor

CD2AP – CD2 associated protein

CDR – Complementarity-determining region

CKD – Chronic kidney disease

cMBC – Classical memory B cell

CSR – Class switch recombination

DN – Double negative

dsDNA – Double-stranded DNA

EBF1 – Early B cell factor 1

EBI2 – Epstein-Barr virus-induced G-protein coupled receptor 2

EBV – Epstein-Barr virus

eMBC – Extrafollicular memory B cell

ESKD – End-stage kidney disease

FcγR – Fc fragment of IgG receptor

FCRL – Fc receptor-like protein

FDC – Follicular dendritic cell

FOXP3 – Forkhead box P3

FSGS – Focal segmental glomerulosclerosis

GC – Glucocorticoid

gdIgA1 – Galactose-deficient IgA1

GlialCAM – Glial cell adhesion molecule

GWAS – Genome-wide association studies

HHEX – Hematopoietically expressed homeobox

HIV – Human immunodeficiency virus

HLA – Human leukocyte antigen

ICAM – Intracellular adhesion molecule

IFN-I – Type-I interferon

IL – Interleukin

IFN - Interferon

IgAN – IgA Nephropathy

IPEX – Immunodysregulation polyendocrinopathy enteropathy X-linked

IRF – Interferon regulatory factor

ITP – Immune thrombocytopenia

LLPC – Long-lived plasma cell

M3R – Muscarinic acetylcholine receptor $M_3$

MBC – Memory B cell

MBP – Myelin basic protein

MCD – Minimal change disease

MG – Myasthenia gravis

MHC – Major histocompatibility complex

MOG – Myelin oligodendrocyte protein

MOGAD – Myelin oligodendrocyte protein antibody-associated disease

MPO – Myeloperoxidase

MS – Multiple sclerosis

MuSK – Muscle-specific kinase

MZ – Marginal zone

NF-κB – Nuclear factor-kappa B

NLR – Nucleotide-binding oligomerization domain-like receptors

PAX5 – Paired box 5

PBMC – Peripheral blood mononuclear cells

PC – Plasma cell

PLP – Proteolipid protein

PR3 – Proteinase 3

RA – Rheumatoid arthritis

RAG1/2 – Recombination activating genes 1/2

RF – Rheumatoid factor

RLR – RIG-I-like receptor

RNP – Ribonucleoprotein

RPGN – Rapidly progressive glomerulonephritis

RTX – Rituximab

SHM – Somatic hypermutation

SLE – Systemic lupus erythematosus

SLPC -Short-lived plasma cell

SjS – Sjögren's syndrome

SRNS – Steroid-resistant nephrotic syndrome

SSNS – Steroid-sensitive nephrotic syndrome

SSc – Systemic sclerosis

T1D – Type-1 diabetes

TACI – Transmembrane activator and CAML interactor

T-bet – T-box expressed in T cells

$T_{CONV}$ – Conventional T cell

TCR – T cell receptor

TD – T-dependent

TdT – Terminal deoxynucleotidyl transferase

$T_{EFF}$ – Effector T cell

$T_{FH}$ – Follicular helper T

$T_{FR}$ – Follicular regulatory T

TGF – Transforming growth factor

$T_{H}$ – Helper T

TI-1/2 – T-independent-1/2

TLR – Toll-like receptor

TNF – Tumor necrosis factor

$T_{PH}$ – Peripheral helper T

$T_{REG}$ – Regulatory T

XBP1 – X-box binding protein 1

ZEB2 – Zinc finger E-box binding homeobox 2

ZO-1 – Zonula occludens-1

## CHAPTER 1: INTRODUCTION AND LITERATURE REVIEW

Chronic kidney disease (CKD) afflicts an estimated 700 million people worldwide – that is, nearly 10% of the global population – with this figure only expected to rise alongside our aging demographics (2). Already standing as the third fastest growing cause of global deaths, claiming approximately 1.2 million lives annually, CKD is projected to become the fifth leading cause of mortality by 2040 (2, 3). Many affected individuals are unaware of their CKD status resulting in delayed diagnoses. Consequently, many will progress into end-stage kidney disease (ESKD) requiring lifelong kidney replacement therapy, namely dialysis or kidney transplantation, for survival. Tragically, up to 20% of those commencing dialysis will succumb to the complications associated with renal failure within a year (2). The burden of CKD on affected individuals is profound and places significant strains on healthcare systems worldwide.

Autoimmune kidney disease is the third major cause of CKD in adults and the primary cause in children. It encompasses a spectrum of disorders predominantly characterized by glomerulonephritis – inflammation in the principal filtering unit of the kidney, the glomerulus (4, 5). Situated at the proximal end of the nephron, the glomerulus is comprised of a capillary network surrounded by a permselective filtration barrier that maintains essential proteins and cells in circulation while filtering metabolic wastes from the blood. In autoimmune kidney disease, immune-mediated insults disrupt this filtration barrier leading to the accumulation of wastes in circulation that, if left untreated, can progress into ESKD (6). The immune mechanisms underlying the development and chronicity of autoimmune kidney disease remain elusive, and hence, treatments remain largely non-specific relying on broad immunosuppression with glucocorticoids and other immunosuppressive drugs despite their unfavourable safety profiles (4). *There is a pressing need for the development of safer and targeted therapeutics, and to do so, we need to better understand the pathogenesis of autoimmune kidney disease.*

Antibodies, or more precisely *auto*antibodies, are the primary culprits responsible for autoimmune kidney disease, produced by B cells that recognize either systemic/extrarenal or kidney-specific/renal autoantigens through their B cell receptors (4, 7). Consequently,

therapeutic strategies focusing on B cell modulation have gained traction utilizing monoclonal antibodies (e.g., belimumab, daratumumab, rituximab, and ofatumumab), recombinant fusion proteins (e.g., atacicept), and B cell-targeted chimeric antigen receptor (CAR)-T cell therapy, albeit with variable efficacy (8, 9). While some approaches indiscriminately deplete most B cells, compromising protective humoral immunity, others provide a more precise targeting strategy. Nevertheless, the etiology of humoral immune responses in autoimmune kidney disease remains largely ill-defined. *A comprehensive understanding of the factors dictating the development and progression of these autoreactive B cell responses, including their regulation, is imperative to orient therapeutic advancements accordingly.*

The work presented in this thesis is the result of our efforts to better understand the humoral autoimmune origins of one of the least understood forms of autoimmune kidney disease, namely childhood idiopathic nephrotic syndrome (10). An immune etiology was first proposed by the late Robert Shalhoub 50 years ago, but the pathogenesis of disease remains completely unknown (11). The success of B cell depletion with rituximab seen in the last decade positioned B cells as central contributors to pathogenesis. *Nevertheless, the pathogenetic roles of B cells in childhood INS remain elusive.*

~ ~ ~

*Chapter 1* will provide an overview of the foundations of humoral immunity – the development of B cells and the processes eliciting antibody production – and its contribution to autoimmunity, with a particular emphasis on the role of B cells in the generation of autoimmune kidney disease.

### 1.1 Overview of humoral immunity

> *"We're always shown evolution portrayed something like this, a monkey and a chimpanzee, some extinct humans, all on a forward and steady march to becoming us… We're not the goal of evolution. Think of us all as young leaves on this ancient and gigantic tree of life – connected by invisible branches not just to each other, but to our extinct relatives and our evolutionary ancestors."*
>
> Prosanta Chakrabarty
> Ichthyologist

I begin this literature review on autoimmune kidney disease with the above quote not only because Dr. Chakrabarty is a McGill alumnus, but also because he vulgarises in it what I believe is a central tenant of the life sciences – that evolutionary forces work to grow the tree of life through *diversity* but are utterly careless of its individual units. And, perhaps just as importantly, quoting an ichthyologist makes sense when we are discussing adaptive immunity. Indeed, the adaptive immune system of mammals originated 500 million years ago in our gnathastomata (jawed fish) ancestors, evolving to enable us to respond to an incredible diversity of pathogens all-the-while maintaining memory of these encounters (12). At the basis of adaptive immunity are two lymphocyte populations, the T and B cell, each carrying a receptor, the T cell receptor (TCR) and B cell receptor (BCR), specific for a certain antigen. By generating large numbers of T and B cells, the adaptive immune system ensures a great diversity of antigen-specificities, one clone of which will be selected following insult by a foreign agent (e.g., virus, bacteria, toxin).

The types of the adaptive responses that follow antigen encounter are diverse and rely on the nature of the antigen, the environment of the immunogenic insult, and the quality of the responding lymphocytes. We are particularly interested in adaptive responses that result in the production of antibodies by B cells – or *humoral immunity*. Here, BCRs bind to a three-dimensional region, termed epitope, on their cognate antigen triggering numerous

signaling cascades that lead to B cell activation. Activated B cells, after internalizing the BCR with cognate antigen, process the antigen and present it on class II major histocompatibility complexes (MHC-II) to activated T cells, which will in turn provide signals that promote B cell development into memory cells and, ultimately, antibody-secreting plasmablasts and plasma cells (PC). In *Chapter 1.1*, we will review how adaptive immunity develops its tremendous repertoire of antigen diversities and provide a detailed overview of the generation of antibody responses.

### *1.1.1 B cell development*

Mammalian B cell development starts in primary lymphoid organs, namely the bone marrow and fetal liver, with the goal of generating an antigen-specific immunoglobulin receptor (13, 14). This occurs through somatic rearrangement of BCR H (*h*eavy) chain V (*v*ariable, *IGHV*), D (*d*iversity, *IGHD*), J (*j*oining, *IGHJ*), and C (*c*onstant) genes and L (*l*ight) chain V (*IGLV* or *IGKV*) and J (*IGLJ* or *IGKJ*) genes via an error-prone process – a discovery made by Susumu Tonegawa and that was awarded the Nobel Prize in 1987 (15, 16). Together, the heavy ($VDJ_H$) and light ($VJ_L$) chains form the variable, antigen-binding region of the BCR. The resulting immature B cells express a BCR consisting of two heavy chains of the IgM isotype, each covalently linked to a light chain. These immature B cells then traffic to secondary lymphoid organs (spleen, lymph nodes, tonsils, and Peyer's patches) for further development.

*A) Recombination of the BCR in the bone marrow*

Expression of the transcription factor Early B cell factor 1 (EBF1) by the common lymphoid progenitor in the bone marrow promotes the development of early pro-B cells (17, 18). EBF1, acting with E2A, opens the H chain locus allowing for the first set of somatic rearrangements to take place between $D_H$ and $J_H$ gene segments. Here, Recombination activating genes 1 and 2 (RAG1/2), in concert with other enzymes, break the DNA at specific recombination signal sequences, excise the DNA between $D_H$ and $J_H$ segments, which then are subsequently ligated via non-homologous end-joining (15). During joining, Terminal deoxynucleotidyl transferase (TdT) add non-templated nucleotides which enhance the

diversity of the variable region. With the successful recombination of $DJ_H$, pro-B cells gain expression of Paired box 5 (PAX5), a direct target of EBF1, which commits the cell to the B lineage largely through its repressor functions (17). In cooperation with signals from bone marrow stromal cells including the cytokines interleukin (IL)-7 and stem cell factor, PAX5 drives the next major recombination event, now between $V_H$ and the newly synthesized $DJ_H$ (19). Productive $VDJ_H$ recombination successfully generates a heavy chain that utilizes the μ constant gene. The resulting Igμ chain pairs with a surrogate light chain ($\lambda_5$ and VpreB) and is exported to the cell surface as the pre-BCR (20). At this stage, the B cell is referred to as a large pre-B cell.

In the large pre-B cell, Igα and Igβ, signaling side chains of the BCR encoded by *CD79A* and *CD79B* and whose expression is dependent on EBF1, associate with the pre-BCR and deliver a potent proliferative signal (20). The expression of RAG1/2 enzymes is repressed at this point, preventing further rearrangement of the H chain locus on the other allele (21). This process, termed allelic exclusion, ensures that only pre-B cells with a single antigen-specificity can progress in development (22). Cells that fail to generate a productive $VDJ_H$ through either allele do not receive this signal and undergo apoptosis (checkpoint 1) (23).

As large pre-B cells divide, they downregulate the genes encoding the surrogate light chain thereby diluting the number of pre-BCRs available for daughter cells (24, 25). The diminishing of pre-BCR signals effectively halts cell division generating resting, small pre-B cells that regain expression of RAG1/2. At this stage, RAG1/2 catalyze $V_L$ to $J_L$ recombination at both alleles and at both κ and λ loci. Productive $VJ_L$ rearrangement yields light chains that pair with the heavy chain generating an intact IgM BCR on the surface of a, now, immature B cell. Due to the nature of recombination at the L chain loci, productive rearrangement can take place at multiple loci (26). B cells that fail to generate a productive $VJ_L$ chain undergo apoptosis (checkpoint 2) (23).

To maximize diversity of antigen-specificities in the B cell repertoire, the combinatorial rearrangement of VDJ segments leading to the generation of the BCR are, by and large, random. As a result, as many as 75% of the resulting B cells are capable of recognizing autoantigen (27). To limit the autoreactivity of the repertoire, B cells carrying

BCRs that recognize autoantigen within their environment will continue editing their L chain loci until they lose autoreactivity (28-30). B cells that do not successfully lose their autoreactivity via receptor editing will either undergo *clonal deletion* (checkpoint 3), especially following high avidity interactions with autoantigen, or enter the periphery as anergic B cells – B cells that will not respond to cognate antigen (23). The negative selection of autoreactive B cells in the bone marrow is referred to as *central tolerance* and eliminates up to 85% of emerging B cells (31). Despite this, it is estimated that 40% of the B cells exported to the periphery remain autoreactive (27).

*B) Maturation in the secondary lymphoid organs*

In humans, immature B cells that exit the bone marrow travel to the spleen via the bloodstream as transitional naïve B cells characterized by expression of CD10, CD24, CD38 and all essential components of the BCR complex (e.g., IgM, CD19, CD20, CD22, Igα, Igβ) and represent approximately 4% of all B cells in peripheral blood (32, 33). Early on, transitional B cells are not immune competent, with BCR signaling often triggering apoptosis. At this stage, many transitional B cell clones receive strong antigenic signals and undergo negative selection, thereby eliminating them from the repertoire (checkpoint 4) (23). The few that receive moderate antigenic signals gradually upregulate expression of pro-survival factors, including the receptor for the B cell activating factor (BAFF-R) encoded by *TNFRSF13C*, and gain competence to respond to future antigen signals with activation (34, 35). These immune competent B cells are considered mature and are distinguished from immature B cells by loss of expression of CD10, RAG1/2, and TdT. The negative selection of transitional B cell clones in the spleen is referred to as *peripheral tolerance* and is responsible for pruning the B cell repertoire, dropping autoreactivity rates to 20% in the mature population (27).

Most mature naïve B cells will differentiate into *follicular B cells*, trafficking to B cell follicles in the white pulp of the spleen and cortical regions of lymph nodes, tonsils, and Peyer's patches (36). Expression of CXCR5 by follicular B cells is critical for their homing to the CXCL13-rich follicles (37). These B cells are fully capable of recirculating between

secondary lymphoid organs to aid in their search for cognate antigen. Alongside their IgM BCRs, follicular B cells gain the expression of IgD. In contrast, 15-20% of mature naïve B cells will migrate to the *marginal zone (MZ)* within the red pulp of the spleen, often after receiving weaker antigenic stimuli than their follicular counterparts (36, 38). These MZ B cells express high levels of IgM, Toll-like receptors (TLR), CD1c, CD21, CD22, CD24, and the Fc fragment of IgG receptor (FcγR)IIB, low expression of IgD, and are the main source of IgM antibodies in the body (39, 40). In humans, MZ B cells also recirculate in the blood and are present in the subcapsular sinus of lymph nodes, the epithelium of tonsillar crypts, and mucosa-associated lymphoid tissues. In contrast to follicular B cells, which express monoreactive BCRs, MZ B cells tend to be enriched with polyreactive and autoreactive clones and play an important innate-like role in the clearance of bloodborne pathogens and cellular debris.

### *1.1.2 Germinal center responses by follicular B cells*

The processes giving rise to the mature B cell repertoire were designed to maximize its diversity while curtailing its capacity for autoreactivity. The resulting $10^{13}$ specificities not only enables our humoral immunity to recognize virtually any invading pathogen or toxin, but also provides the genetic diversity needed for the selection of the best B cell clones to generate the highest quality antibodies (*clonal selection*).

*A) Follicular B cell activation*

Follicular B cells constantly monitor the reticular networks of follicular dendritic cells (FDC) in the B cell follicles and subcapsular macrophages within secondary lymphoid organs for cognate antigen (36, 41). Upon a successful encounter, signaling events downstream CD19 and Igα/β chains of the BCR complex lead to B cell activation and the subsequent internalization of the BCR-antigen unit (42). Internalized antigens travel to lysosomes where they are enzymatically processed into peptides and are loaded onto MHC-II molecules for presentation on the surface of the activated B cell. Early following activation, B cells upregulate the chemoattractant receptors Epstein-Barr virus-induced G-protein coupled receptor 2 (EBI2/GPR183) and CCR7 (43, 44). EBI2 and CCR7 sensing 7α,25-

dihydroxycholesterol in the interfollicular regions and CCL19/21 in the T cell-zone, respectively, guide the activated B cell to the interface of the follicle and T cell zone (44-48) (**Figure 1**). Here, pre-activated $CD4^+$ helper T ($T_H$) cells that recognize the peptide-MHC-II on the surface of the B cell via their TCRs generate an intimate T-B cell crosstalk crucial for the generation of high affinity antibody (49).

The molecular players involved in the T-B cell crosstalk are vast. Intracellular adhesion molecules (ICAM)-1/2 on the surface of the B cell bind integrins on the cognate $T_H$ cell, lowering the threshold needed for robust B cell activation (50). Interactions between B cell CD80 and CD86, costimulatory molecules upregulated shortly following B cell activation, and CD28 on the $T_H$ cell provide signals to both cells promoting their survival and further functionalization. Importantly, interactions between CD40 on the surface of the B cell with CD40L on the $T_H$ cell delivers a potent proliferative signal to the B cell through nuclear factor-kappa B (NF-κB) (51, 52). Thus, B cells receiving T cell help are capable of proliferating and subsequently changing their BCR isotypes, differentiating into memory B cells (MBC) and, eventually, giving rise to antibody-secreting plasmablasts and PCs. Meanwhile, cognate $CD4^+$ $T_H$ cells differentiate into follicular helper T ($T_{FH}$) cells that continue to support the maturation of the B cell response by orchestrating the *germinal center* reaction within the B cell follicle (53).

*B) Germinal center reaction: Maturation of the antibody response*

The T cell-dependent activation of follicular B cells results in the formation of germinal centers within seven days of primary antigen exposure (54). These are specialized microanatomical structures within the B cell follicles where B cell responses mature to generate high affinity antibody. To generate these structures, both B and $T_{FH}$ cells downregulate EBI2 and CCR7 and gain high CXCR5 expression causing their migration to the centre of the B cell follicle, where the ligands for EBI2 and CCR7 are minimal and stromal-derived CXCL13 is abundant (45, 46, 55) (**Figure 1**). Here, $T_{FH}$ cell-derived signals through CD40, ICOSL, and the cytokines IL-4 and IL-21 induce the expression of the transcription

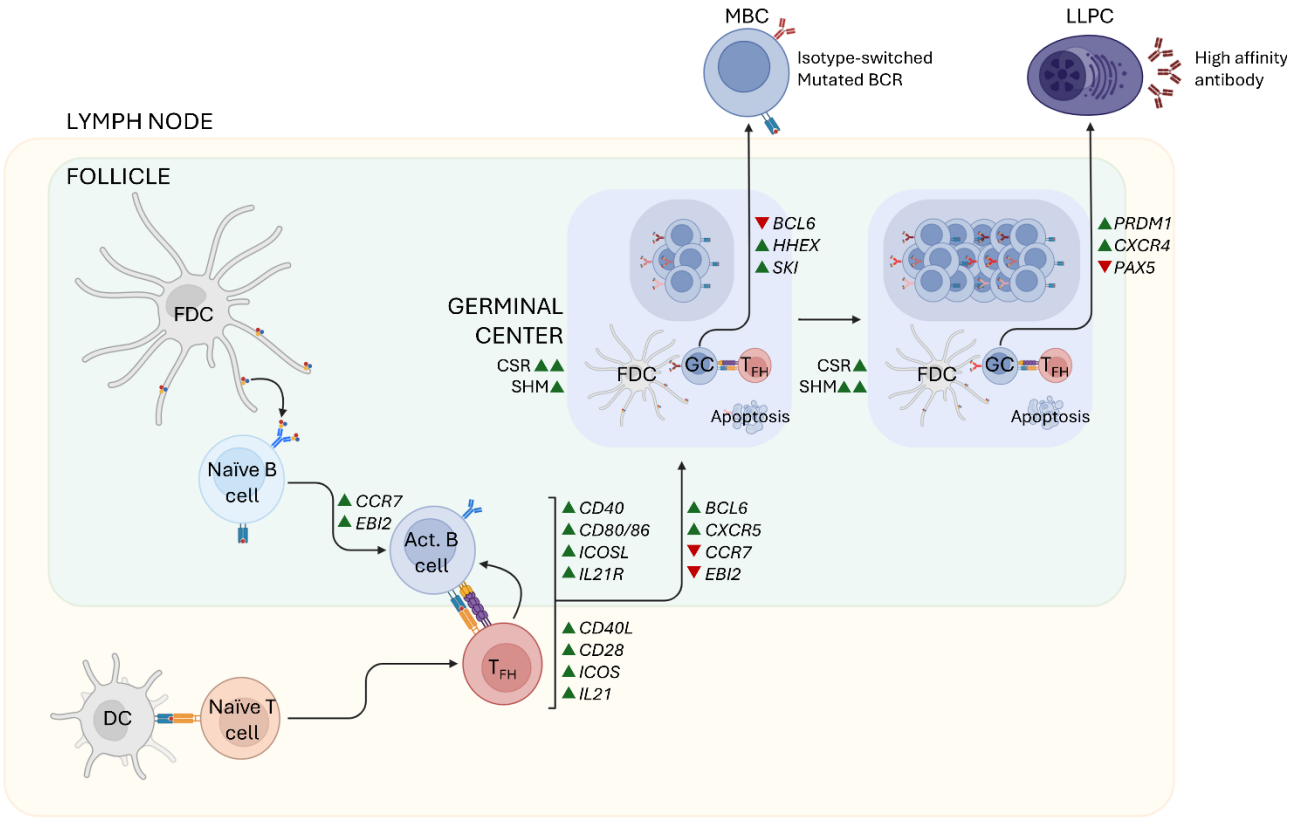


***Figure 1 - Follicular B cell response.*** Naïve B cells encounter cognate antigen from follicular dendritic cells (FDCs) or subcapsular macrophages within the lymph node. The antigen-BCR complex is internalized, processed, and epitopes are presented on MHC-II on the surface of the activated B cell. CCR7 and EBI2 guide the activated (Act.) B cell to the interface of the follicle and T cell zone, where the B cell will crosstalk with cognate follicular helper T ($T_{FH}$) cells. $T_{FH}$-B cell interactions including CD40L-CD40, ICOS-ICOSL, and IL-21-IL-21R deliver a signal that promotes BCL-6 expression in the B cell, and its homing into the middle of the follicle by CXCR5. Germinal centers are generated within the follicle consisting of an inner dark zone comprised of $CXCR4^{high}$ germinal center B cells that undergo somatic hypermutation (SHM), and an outer light zone consisting of $CXCR4^{low}$ germinal center B cells, $T_{FH}$ cells, and FDCs. In the light zone, germinal center B cells that are best able to uptake antigen from the FDC and/or receive strong stimulatory signals from $T_{FH}$ cells due to a high affinity BCR will cycle between the light and dark zones (cyclic re-entry). Those with lower affinity BCRs will undergo apoptosis. Initially, light zone B cells will preferentially undergo class-switch recombination (CSR) and give rise to memory B cells (MBC). As the germinal center progresses and BCR affinity increases, germinal center B cells will preferentially progress into antibody-secreting long-lived plasma cells (LLPC) expressing the lineage-defining transcription factor BLIMP1/PRDM1. Created with BioRender.com.

factor B-cell lymphoma (BCL)-6 in B cells (56-58). BCL-6, acting primarily as a transcriptional repressor, orchestrates key aspects of the germinal center B cell phenotype, including keeping germinal center B cells in a proapoptotic state by repressing expression of the anti-apoptotic molecule BCL-2, while concomitantly protecting them from DNA damage-induced apoptosis by repressing expression of TP53, CDKN1A, and ATR (59-62). Moreover, BCL-6 retains B cells within the germinal center by silencing expression of the B lymphocyte-induced maturation protein 1 (BLIMP1), the master transcription factor responsible for

germinal center exit via differentiation into plasmablasts and PCs (63). Other transcription factors essential in generating the germinal center response are Octamer-binding protein 2 (OCT2/POU2F2) and OCT-binding factor 1 (OBF1/POU2AF1) as they regulate the expression of several signal transducers involved in the $T_{FH}$-B cell crosstalk (64, 65).

Germinal center B cells proliferate rapidly, pushing surrounding naïve B cells to the boundaries of the follicle. After continued proliferation, two anatomical compartments appear within the germinal center: a dark zone composed of highly proliferative B cell blasts, and a light zone consisting of less proliferative germinal center B cells interspersed within the FDC reticular network (54). The positioning of germinal center B cells within these zones is maintained by gradients of the chemokines CXCL12 and CXCL13 (66). High CXCR4 expression traffics germinal center B cells to the CXCL12-rich dark zone while low CXCR4 expression enables CXCR5 to guide germinal center B cells to the CXCL13-rich light zone. In the dark zone, $CXCR4^{high}$ B cell blasts undergo *somatic hypermutation (SHM)* of their rearranged $VDH_H$ and $VJ_L$ loci, attempting to improve the affinity of their BCRs for their cognate antigen (67). Here, activation-induced cytidine deaminase (AICD) deaminates cytidine nucleotides generating uracil residues largely within the complementary-determining regions (CDR) of these loci – the regions of the heavy and light chains that directly contact the antigen (68-70). Error-prone base excision repair mechanisms follow introducing new mutations.

In the light zone, $CXCR4^{low}$ germinal center B cells compete with one another for cognate antigen on the FDCs and pro-survival signals with $T_{FH}$ cells. B cells with higher affinity BCRs outcompete other B cells, receiving signals that will promote their re-entry into the dark zone for further SHM (54). Most germinal center B cells, which are already primed for apoptosis via BCL-6, will be eliminated in the light zone. Through repeated rounds of transition between dark and light zones, referred to as cyclic re-entry, the affinity of BCRs for cognate antigen gradually increases (71). Therefore, while follicular responses begin as monoclonal responses from a single BCR (or an oligoclonal response from a few BCRs), germinal centers drive further diversification for the selection of the highest affinity clones to produce highly specific antibodies.

*C) Germinal center reaction: Class-switch recombination*

One of the major events in the light zone is the isotype-switching of the BCR via *class-switch recombination (CSR)* driven by CD40, IL-4, and IL-21 signals received during $T_{FH}$-B cell crosstalk (53, 72). This process usually occurs early during the germinal center reaction, preceding any significant SHM, and also relies on AICD (68). AICD deaminates cytidines in S (*s*witch) regions upstream the $C_H$ genes thereby instigating the formation of double-strand breaks. For initial class-switching, AICD will specifically deaminate Sμ (upstream Cμ and Cδ for the IgM and IgD chain) and the S region of another $C_H$ gene. The DNA between the Sμ and new S, which includes both Cμ and Cδ, will be excised by chromosome looping and non-homologous end-joining resulting in the expression of $VDJ_H$ with a new $C_H$ gene. CSR to a particular isotype is dependent on both the nature of the antigen as well as cytokine cues the B cell receives from the $T_{FH}$ cell and the environment (70).

Each isotype has its own unique properties and functions. IgM, the first immunoglobulin expressed by B cells, is eventually secreted by $IgM^+$ plasmablasts as a pentamer (73). The high avidity of the pentameric unit endows IgM antibodies with a high capacity for complement fixation and opsonization. IgG, which in humans includes the IgG1/2/3/4 subclasses, are the most abundant antibodies in healthy individuals and are secreted as monomers (74). IgG1 and IgG3 are induced by soluble and membrane-bound protein antigens including viruses, while IgG2 is often generated against bacterial capsular polysaccharides. Antibodies of these three isotypes are excellent at opsonization and complement fixation by binding to activating FcγR and complement receptors. Class-switching to IgG4 is induced following long-term exposure to antigen, often in a non-inflammatory setting, and antibodies of this isotype are not capable of complement fixation or opsonization (75). As such, IgG4 is thought to play a regulatory role in an antibody response. Like IgG, IgE is secreted as a monomer but represents the rarest antibody isotype (76). Class-switching to IgE relies on IL-4 and IL-13 signals, often from $T_H2$ cells, in response to helminth infection or innocuous environmental allergens. Antibodies of this isotype bind Fcε receptors on mast cells and basophils that, when cross-linked via antigen, induces

degranulation and release of lipid mediators (e.g., prostaglandins, leukotrienes, thromboxanes). Finally, class-switching to IgA, which includes the IgA1/2 subclasses, largely takes place within mucosal tissues, especially the within the Peyer's patches of the gut (77). Mucosal IgA antibodies are predominantly polymeric (2-4mers), joined by the J chain, and line mucosal surfaces to prevent pathogens from accessing the epithelium. In contrast, serum IgA is monomeric.

*D) Germinal center exit: Memory formation*

A key event in the light zone of the germinal center is the decision of positively selected B cells to differentiate into either MBCs or *long-lived PCs (LLPC)* (78). As of now, the mechanisms controlling this decision are not fully elucidated with evidence suggesting that MBCs are generated first followed by LLPCs, possibly guided by changes in BCR affinity and $T_{FH}$ cell phenotype (79) (**Figure 1**). This is supported by lower SHM rates in MBCs than LLPCs. Weaker interactions between germinal center B cells and $T_{FH}$ cells in the light zone are associated with MBC formation (80). Here, decreased expression of BCL-6 and increased BTB containing and CNC homology 2 (BACH2), a transcriptional regulator, results in the induction of anti-apoptotic genes (e.g., *BCL2*, *BCL2L1*) and the repression of proliferative genes (e.g., *CDKN1A*, *CDKN2A*) (81, 82). Repression of Hematopoietically expressed homeobox (HHEX*)* by BCL-6 is also alleviated, enabling HHEX to induce expression of the transcription factor SKI, which was recently identified to drive MBC generation (83). In humans, MBCs are defined by surface CD27 expression and can survive for decades (78). MBCs that retain their IgM and IgD BCR are *non-switched MBCs* while those that lose IgM and IgD in favour of other isotypes are *isotype-switched MBCs*. Their highly diversified BCRs and their primed status as MBCs enables them to respond rapidly to subsequent immunogenic insults, particularly in the case of variant viruses. In the case of influenza virus re-infection and vaccination, selection of clones from the clonally expanded but diversified MBC pool is thought to enable the generation of broadly neutralizing antibodies (84, 85).

LLPCs, on the other hand, arise from stronger interactions with $T_{FH}$ cells (78). Elevated BCR and CD40 signaling induces high levels of Interferon regulatory factor (IRF)4 in germinal

center B cells, which silences the expression of BCL-6 and thereby alleviates its repression of the master transcription factor of the PC program, BLIMP1 (64, 86). BLIMP1, in turn, destabilizes the B cell program by repressing PAX5 expression and induces expression of X-box binding protein 1 (XBP1), a transcription factor that regulates the PC secretory program (87-89). The resulting LLPCs exit the lymph node and traffic to the bone marrow, guided by CXCR4, where they will receive stromal cell-derived survival cues, namely IL-6, a proliferation-induced ligand (APRIL/TNFSF13), and B cell activating-factor (BAFF/TNFSF13B) (90, 91). B cell maturation antigen (BCMA/TNFRSF17), a receptor of APRIL and BAFF, is expressed on LLPCs and is essential for their long-term survival (92). Of note, the extinguishing of the B cell transcriptional program by BLIMP1 causes PCs to downregulate CD20 expression, and as such, LLPCs are not eliminated using CD20-targeting monoclonal antibodies.

### *1.1.3 Extrafollicular B cell responses*

While the germinal center represents a major mechanism for protective antibody generation, it is not the only means that B cells achieve this. For primary antigen exposures, the germinal center develops after 4-7 days, peaks at approximately 14 days and involutes thereafter, though recent work in humans vaccinated against SARS-CoV-2 demonstrated that germinal centers could persist for months (54, 93). Prior to germinal center formation, activated B cells rapidly convert into plasmablasts/*short-lived PCs (SLPC)* outside of the B cell follicle providing an immediate source of protective antibodies (94). Due to their localization outside of B cell follicles, such responses are referred to as *extrafollicular B cell responses* (**Figure 2**).

*A) Extrafollicular activation by T cell-dependent and -independent antigens*

The decision for an activated B cell to participate in a germinal center or extrafollicular response is determined by the strength of the antigen signal it receives (78). Moderate interactions with cognate antigen promote the development of germinal centers while higher affinity interactions result in the extrafollicular generation of SLPCs. Unlike

activated B cells destined for generation of germinal centers, extrafollicular B cells maintain expression of EBI2 and CCR7, retaining them outside of follicles (95). These cells will also upregulate CXCR4, which promotes their migration to the medullary cords of the lymph nodes. A population of IL-21-producing $CXCR4^+$ $CD40L^+$ $T_{FH}$-like cells – termed peripheral helper T ($T_{PH}$) cells – that lack CXCR5 also migrate to the medullary cords where they are thought to support the generation of extrafollicular responses (96). Within these extrafollicular niches, strong BCR and CD40 signals instruct the extrafollicular B cells to proliferate and upregulate IRF4, thereby inducing the development of the PC program (97). Unlike LLPCs, SLPCs do not travel to the bone marrow but rather remain within the extrafollicular niches of secondary lymphoid organs or enter circulation and survive for only a few days. Most PCs measured in the blood of healthy individuals correspond to SLPCs.

Extrafollicular B cell responses were historically associated with antigens capable of activating B cells in the absence of T cell help (94). Unlike T-dependent (TD) antigens, which are monovalent (or lowly valent) proteins that bind the BCR, T-independent (TI) antigens are multivalent and often polymeric, either activating the B cell via binding to pathogen recognition receptors (TI-1: e.g., CpG binding TLR9) or via crosslinking multiple BCRs (TI-2, e.g., bacterial capsular polysaccharides). Strong mitogenic signals from TI-1 antigens and BCR signals from TI-2 antigens promote B cell proliferation and the generation of SLPCs.

The B cell survival factors APRIL and BAFF are critical for the formation of extrafollicular responses (94, 98). Both cytokines are produced by myeloid cells, primarily monocytes, macrophages, and dendritic cells, and signal through the receptor Transmembrane activator and calcium-modulator and cyclophilin ligand interactor (TACI/TNFRSF13B) on B cells. B cells gain TACI following BCR stimulation and its expression is maintained within the extrafollicular population. Germinal center B cells, on the other hand, downregulate its expression (99). Supporting its role in extrafollicular responses, mutations in *TNFRSF13B* are a cause of common variable immunodeficiency in humans, specifically impairing TI-2 B cell responses, a finding that is also supported in TACI-deficient mice (100-102). While the majority of SLPCs that arise from extrafollicular responses are IgM-secreting, TACI signaling enables extrafollicular B cells to undergo CSR by inducing the

expression of AICD (103). As such, sustained extrafollicular responses have the capacity to generate antibodies of non-IgM isotypes. Moreover, extrafollicular responses also support the secondary diversification of BCRs via SHM, albeit to a lower extent than germinal centers (104). Indeed, human B cells and PCs obtained from sites of persistent extrafollicular responses, for example from the synovium of people with rheumatoid arthritis, show both CSR and SHM (105). More recently, CSR and SHM were also observed in the extrafollicular B cells and SLPCs elicited by SARS-CoV-2 infection (106).

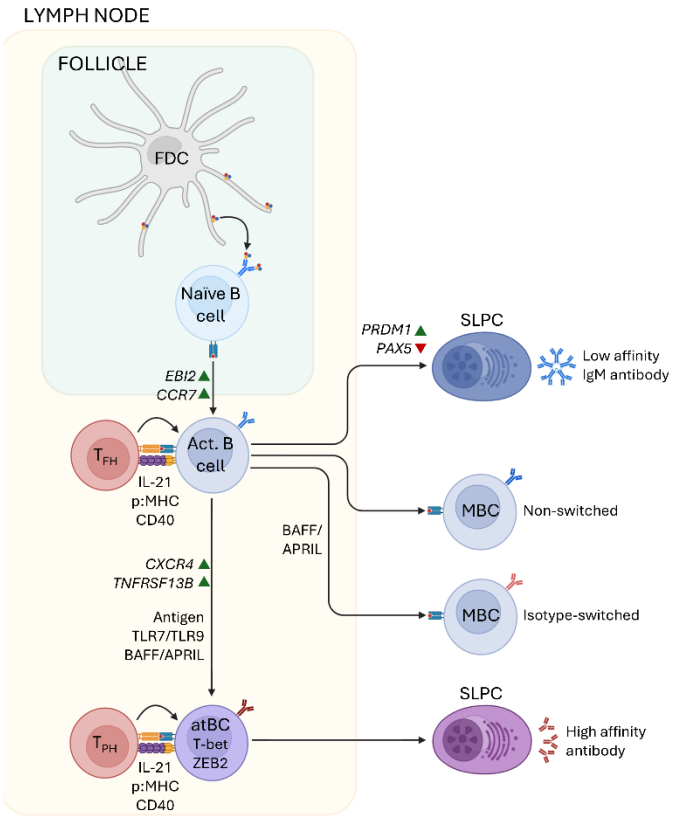


***Figure 2 – T-dependent extrafollicular B cell response.*** Activated (Act.) B cells retain expression of EBI2 and CCR7 and upregulate CXCR4, which promotes their migration into extrafollicular regions of the lymph node (e.g., interfollicular regions, medullary sinuses). Initial strong interactions T-B interactions promote the generation of low affinity IgM-secreting short-lived plasma cells (SLPC). Subsequent proliferation of B cells dilutes the availability of T-B signals, thus promoting the generation of memory B cells (MBC). While class-switch recombination and somatic hypermutation are not a primary feature of extrafollicular responses, BAFF/APRIL signaling through TACI induces a degree of class-switching and hypermutation. Chronic antigenic signals, ligation of endosomal TLR7 and TLR9 by microbial genetic material, and BAFF/APRIL signaling through TACI promotes the generation of $CD21^{low}$ T-$bet^{+}$ $CD11c^{+}$ atypical B cells (atBCs) in a ZEB2-dependent manner. Peripheral helper T ($T_{PH}$) cell production of IL-21 and IFN-γ are instrumental for their generation. T-$bet^{+}$ atBC rapidly give rise to SLPCs, and their elevated SHM rates indicate that these SLPCs may contribute to the production of high affinity antibodies. Created with BioRender.com.

*B) Extrafollicular memory B cells: Atypical B cells*

Not all activated B cells participating in extrafollicular responses are destined to become SLPCs. As initial high affinity antigen interactions drive B cell proliferation and differentiation into SLPCs, antigen availability and T cell help become limited, thereby delivering lower strength BCR signals that facilitate the development of *extrafollicular MBCs (eMBC)* and germinal center-destined B cells (78). Amongst the MBCs generated by TD extrafollicular responses are *'atypical' MBCs (atBCs)* that reside within the interfollicular

regions of secondary lymphoid organs and the red/white pulp border of the spleen (107-109). These cells were initially discovered in human tonsils as B cells expressing the inhibitory receptor Fc receptor-like protein (FCRL)4 and lacked the expression of the classical memory marker CD27 and the complement receptor CD21 – hence the use of 'atypical' differentiating them from $CD27^+$ $CD21^+$ *classical MBCs (cMBC)* (110). Lack of BCL-6, BLIMP1, XBP1, and IRF4 ruled out a germinal center B cell or PC identity, whereas evidence of SHM in the $V_H$ gene (*IGHV*) and expression of key MBC transcription factors denoted a memory phenotype (111).

In humans, chronic infections with *Plasmodium falciparum* (malaria) and human immunodeficiency virus (HIV), and vaccination against or infection with influenza virus or SARS-CoV-2 are associated with an expansion of atBCs (106, 112-119). Moreover, driven by single-cell RNA-sequencing (scRNA-seq), atBCs have been identified in numerous human tissues including the blood, lymph nodes, spleen, kidneys, liver, cerebrospinal fluid, and synovium, with a very consistent phenotype and often associated with autoimmune pathology (discussed further in *Chapter 1.2.3*) (120-123). On their surface, atBCs preferentially express high levels of CD19, the integrin CD11c (ITGAX), and FCRL5 and lack CXCR5, CD27, and CD21. An analogous population of $CD11c^+$ $CD27^-$ $CD21^-$ B cells were identified in mice that expand rapidly in response to viral infection and accumulate with age – these are referred to as age-associated B cells (ABC) (124, 125). Both human atBCs and murine ABCs upregulate the transcription factors T-box expressed in T cells (T-bet/TBX21), Zinc finger E-box binding homeobox 2 (ZEB2), and ZBTB32. T-bet and ZEB2 were recently identified as the major drivers of the atBC/ABC phenotype in humans and mice promoting the expression of several genes including *ITGAX*, *ZBTB32*, and *IL21R* (107, 126, 127). Nevertheless, the development of atBCs is not fully characterized (128). Recent studies looking at human atBC development following chronic infections with malaria or HIV suggest that interferon (IFN)-γ and TLR7/9 signaling are likely involved the process (114, 119, 129). In mouse studies, TLR7 signaling in the presence of IFN-γ and IL-21 were all shown to be involved in ABC formation (124, 130). $T_{FH}$ and $T_{PH}$ cells, as IFN-γ and IL-21 producing cells, are likely needed for human atBC development with mutations in *CD40*, *CD40L*, *IFNG*,

*IFNGR1*, and *IL21R* causing lower frequencies of peripheral CD21$^{low}$ T-bet$^{+}$ B cells (131). Despite this, whether atBCs are an exclusive feature of extrafollicular responses or can also be generated by chronic antigen exposure in germinal centers remains unclear.

Initially, it was thought that atBCs were exhausted-like B cells since they were unresponsive to *in vitro* BCR stimulation (110, 113). Supporting this, several human studies showed that atBCs contract rapidly following clearance of an insulting pathogen (114, 125, 128, 132, 133). Nevertheless, atBCs also have the capacity to convert rapidly into PCs, particularly following TLR7 signaling and have hence been suggested to function as PC precursors (124, 125, 134, 135). Of note, atBC/ABCs express high levels of MHC-II and CD86 on their surface and are specifically localized in niches where they can interact with T cells as antigen-presenting cells (107, 119, 136). It is becoming increasingly appreciated that atBC/ABCs are needed for optimal $T_{FH}$ cell development and generation of germinal centers (107, 137).

*C) Marginal zone B cells*

One of the primary locations of extrafollicular B cell responses is the spleen. Here, MZ B cells situated between the blood-filled splenic cords and the white pulp provide innate-like protection from bloodborne pathogens (e.g., *Streptococcus pneumoniae* and *Haemophilus influenzae*) and cellular debris via the rapid production of IgM, IgG, and IgA antibodies (36, 38, 39). Unlike the follicular B cell repertoire, MZ B cells are enriched with polyreactive BCRs that recognize diverse microbial antigens captured by splenic macrophages, dendritic cells, and the extracellular traps of neutrophils. These antigens tend to be TI-2 antigens that crosslink multiple BCRs and often also engage TLRs enabling the MZ B cell to rapidly differentiate into SLPCs. These antigen signals also trigger high expression of TACI, which enables MZ B cells to undergo CSR in response to BAFF and APRIL produced by local myeloid cells (103). Nevertheless, MZ B cells are also capable of responding to TD antigens and receiving T cell help. Here, MZ B cells uptake bound antigen and present them to $T_{FH}$ cells at the periphery of the white pulp where they can undergo extrafollicular responses or migrate into the B cell follicle for germinal center responses (138). Accordingly,

the majority of non-switched cMBCs ($IgM^+$ $IgD^+$ $CD27^+$) B cells in human blood are derived from MZ B cells and have undergone SHM, though not to the same extent as PCs and isotype-switched cMBCs (38, 139, 140).

### *1.1.4 Regulating the B cell response*

Multiple checkpoints in B cell development ensure the production of a largely non-autoreactive B cell repertoire, including clonal deletion and receptor editing in the bone marrow (checkpoint 3) and negative selection in the periphery (checkpoint 4). However, continued editing of the BCR in germinal centers or in extrafollicular foci via SHM risk introducing autoreactivity into the MBC and PC pools. As such, B cell responses need to be regulated – they should arise during a pathogenic insult and halt upon clearance. Several intrinsic regulatory mechanisms were already discussed: the shift from MBC to LLPC development in the germinal center, the apoptosis of germinal center B cells that fail to improve the affinity of their BCRs towards the target antigen, and the transition from SLPC to MBC generation during extrafollicular responses. Nevertheless, extrinsic mechanisms of regulation are also essential.

*A) Regulatory T cells: master regulators of self-tolerance*

Regulatory T ($T_{REG}$) cells are a class of $CD4^+$ T cell that are crucial in maintaining peripheral tolerance (141). They arise in the thymus from thymocytes (immature T cells) wielding a TCR capable of intermediate to high affinity interactions with autoantigen (142, 143). The transcription factor FOXP3 distinguishes $T_{REG}$ cells from conventional T ($T_{CONV}$) cells – T cells capable of differentiating into distinct effector T ($T_{EFF}$) cell lineages including $T_{FH}$ and $T_{PH}$ cells – and orchestrates a vast transcriptional program that endows $T_{REG}$ cells with a robust capacity to suppress B and T cell responses (141). The importance of these cells in peripheral tolerance is exemplified by loss-of-function *FOXP3* polymorphisms giving rise to a severe multiorgan autoimmune disorder known as immunodysregulation polyendocrinopathy enteropathy X-linked (IPEX) syndrome featuring $T_{EFF}$ cell-mediated tissue inflammation (144, 145). Notably, individuals with IPEX syndrome also accumulate

autoreactive B cells and autoantibodies, demonstrating that $T_{REG}$ cells play a role in regulating humoral immunity (146). Early work demonstrated that some $T_{REG}$ cells in lymph nodes acquire CXCR5 while concomitantly losing CCR7 and migrate into germinal centers following antigen exposure (147, 148). These $T_{REG}$ cells, now called follicular $T_{REG}$ ($T_{FR}$) cells, adopt the expression of BCL-6, which normally instructs the $T_{FH}$ cell phenotype, alongside FOXP3 enabling them to acquire the transcriptional programming needed for their transition to germinal centers (149-151). $T_{FR}$ cells accumulate at the peak of germinal center reactions and stop B cell responses by direct suppression of B and $T_{FH}$ cells. Abrogation of $T_{FR}$ cells in mice results in spontaneous germinal centers and autoantibody generation (152, 153).

This functional specialization of $T_{REG}$ cells into $T_{EFF}$-like lineages by adopting the expression of $T_{EFF}$ cell lineage-defining transcription factors and associated chemokine receptors has also been observed with $T_H1$-like $T_{REG}$ cells expressing T-bet and CXCR3 and $T_H17$-like $T_{REG}$ cells expressing RORγt and CCR6 particularly within tissues like the gut, skin, lungs, and kidneys (154-157). As with $T_{FR}$ cells specializing in suppressing $T_{FH}$ and B cells, T-bet$^+$ and RORγt$^+$ $T_{REG}$ preferentially target $T_H1$ and $T_H17$ cell responses, respectively. Investigations on the functional specialization of $T_{REG}$ cells have been largely driven by mouse studies, due to the relative inaccessibility of human tissues. Nevertheless, ample evidence for $T_{REG}$ cell functional specialization has been uncovered in humans as well (158, 159).

### *1.1.5 Conclusions*

The adaptive immune system is a highly successful component of animal biology. Since it first arose 500 million years ago, the amount of genetic material dedicated to the genes encoding its various components has only expanded, creating extensive genetic diversity and a greater capacity to defend against pathogens (12, 160, 161). In this chapter, we outlined how this diversity is utilized throughout the human lifespan to generate a broadly protective B cell repertoire (VDJ recombination), limit the possibility for autoreactivity via central and peripheral tolerance mechanisms (clonal deletion), and finally, select the best B cell clones for antibody production (clonal selection). Analogous mechanisms of VDJ recombination, clonal deletion, and selection run in parallel in the thymus to generate our

highly diversified T cell repertoire. While most of the population will benefit from the protection afforded by generating such an expansive array of antigen-specificities, certain individuals will face its consequences – evolutionary forces work to grow the tree of life through diversity but are utterly careless of its *individual* units.

## 1.2 B cells in autoimmune disease

Most of the B cells that make it to the periphery and gain immunocompetency are incapable of responding to self. The remaining approximately 20% of B cells that can bind autoantigens via their BCR must either be kept anergic/tolerant or participate in key physiological functions (27). MZ B cells are an example of the latter – these B cells possess a poly/autoreactive repertoire that enables them to generate low-affinity autoantibodies that facilitate the removal of cellular debris (39). In approximately 8% of people, B cell tolerance alongside T cell tolerance, is broken resulting in autoimmunity, where autoreactive lymphocytes orchestrate injurious immune responses to the body's own tissues (162). In *Chapter 1.2*, we will review the mechanisms leading to the general loss of B and T cell tolerance and overview some of the pathological roles that autoreactive B cells play in autoimmune diseases. We will also discuss some of the established and emerging B cell-targeting strategies that can be used in the treatment of these diseases.

### *1.2.1 Breaking tolerance*

The disruption of B and T cell tolerance is a multifactorial process that relies on an interplay between genetics and the environment. In any given autoimmune disease, the exact identities of the factors involved in pathogenesis are difficult to pinpoint since tissue pathology often arises long after the initial break in tolerance and the development of autoimmune effectors (e.g., autoantibodies) – a stage referred to as pre-clinical autoimmunity (163). Nonetheless, a common immunogenetic architecture for autoimmunity is emerging, wherein polygenic factors predispose individuals to respond to certain environmental triggers with autoreactive B and T cell activation (164).

*A) Genetic predispositions*

While most autoimmune diseases are themselves not inherited in a Mendelian fashion, susceptibility to autoimmunity is demonstrably heritable (165). Accordingly, several autoimmune diseases, while not necessarily being prevalent within a single family, are more abundant in certain ethnic groups than others. Genome-wide association studies (GWAS)

have uncovered several genetic predispositions for autoimmune diseases. These polymorphisms are vastly heterogeneous and can be involved in both the genesis and perpetuation of disease.

***Human leukocyte antigen (HLA).*** The human leukocyte antigen (HLA) locus is the most polymorphic component of the human genome encoding the components of MHC-I and MHC-II. Most genetic susceptibility – and protection – to autoimmunity is attributed to this locus (166). Polymorphisms here are usually in linkage disequilibrium making it difficult to tease out the functional importance of single mutations but are largely thought to predispose to autoimmunity by breaking T cell tolerance. This is achieved by increasing MHC expression to augment antigen presentation to T cells or by altering the geometry of the MHC peptide-binding groove thereby favouring the selection and activation of inflammatory T cells (167-169).

Anti-glomerular basement (GBM) nephritis, or Goodpasture syndrome, is an autoimmune disease characterized by severe kidney and lung inflammation caused by a loss of B and T cell tolerance to the non-collagen domain of the α3 chain of type IV collagen [α3(IV)NC1] present within the basement membranes of the kidney and lungs (discussed further in *Chapter 1.3*) (4). Predisposition is strongly associated with the *HLA-DRB1**15 (HLA-DR15) allele while *HLA-DRB1**01 (HLA-DR1) and *HLA-DRB1**07 (HLA-DR7) confer dominant protection (170, 171). In a recent study, Ooi and Peterson et al. demonstrated that the immunodominant epitope of the Goodpasture antigen ($\alpha3_{135\text{-}145}$) was shifted by a single amino acid when presented on HLA-DR15 versus HLA-DR1 (168). Patient $CD4^+$ T cells recognizing the peptide on the risk-associated HLA-DR15 were enriched in proinflammatory $T_H1$ and $T_H17$ cells, while HLA-DR1-restricted $\alpha3_{135\text{-}145}$-specific $CD4^+$ T cells were largely $T_{REG}$ cells. Similarly, transgenic mice expressing HLA-DR15 (DR15/DR15) developed significant disease with autoreactive $T_H1$ and $T_H17$ cells infiltrating the kidneys, whereas DR1/DR1 transgenic mice were completely protected. Mice heterozygous for DR15/DR1 generated HLA-DR1-restricted $\alpha3_{135\text{-}145}$-specific $T_{REG}$ cells that provided dominant protection from disease. These results demonstrate that changes in the configuration of antigen presentation due to HLA polymorphisms dictate the development of tolerized ($T_{REG}$) and non-

tolerized ($T_H1$ and $T_H17$) T cells, likely at the thymus level. Importantly, the onset of anti-GBM nephritis, as the name implies, is primarily driven by autoantibodies against the GBM (4, 170). While a direct mechanistic link between HLA-DR15 and autoreactive B cells has not been made, we can envision that the B cell responses giving rise to anti-GBM antibody are supported by HLA-DR15-restricted autoreactive $T_{FH}$ cells.

Rheumatoid arthritis (RA) is also associated with *HLA-DRB1* polymorphisms that change the geometry of the peptide-binding groove. Here, T cell autoreactivity to citrullinated proteins present in synovial tissue leads to chronic inflammation of the joints, with *HLA-DRB1**04:01 and *HLA-DRB1**04:04 conferring risk (172, 173). It was shown that positive charges in the peptide-binding groove of *HLA-DRB1**04:01/04 excluded the arginine of non-citrullinated autoantigens (vimentin and aggrecan) but accommodated citrulline (169). In *HLA-DRB1**04:01$^+$ individuals with RA, the presentation of citrullinated vimentin on DRB1*04:01 selected for CD4$^+$ $T_{CONV}$ cells, while in *HLA-DRB1**04:01$^+$ healthy individuals, it selected for $T_{REG}$ cells. Notably, *HLA-DRB1**04$^+$ RA is strongly associated with the presence of anti-citrullinated protein antibodies (ACPA) (174). Thus, as with anti-GBM nephritis, it is highly likely that *HLA-DRB1**04:01/04-restricted autoreactive $T_{FH}$ cells can support ACPA production by promoting autoreactive B cell activation. Nevertheless, for most autoimmune diseases, how risk-associated or protective HLA polymorphisms are involved in the pathological process is not known.

***Common genetic drivers.*** Some polymorphisms are shared across multiple autoimmune diseases, suggesting that the affected genes might be involved in driving overall propensity to autoimmunity (163). One such gene is *PTPN22*, the Arg260Trp variant of which is strongly implicated in RA, systemic lupus erythematosus (SLE), and type-1 diabetes mellitus (T1D), all of which are associated with autoantibody formation (165, 175). This gain-of-function mutation enhances its phosphatase functions downstream TCR and BCR signaling, thereby diminishing T and B cell activation (176). In doing so, this variant promotes the escape of autoreactive B cells from clonal deletion at checkpoints 3 and 4 (central and peripheral tolerance), which ordinarily relies on strong BCR signals to autoantigen. Accordingly, individuals carrying the *PTPN22*$^{Arg260Trp}$ polymorphism have greater frequencies

of transitional naïve B cells in the periphery (177). Other genes carrying such driver polymorphisms include *CD28*, which is essential for T cell activation, *CTLA4*, which is necessary for $T_{REG}$ cell suppressive function, *IL2RA*, which is needed for $T_{REG}$ cell survival, *TNFAIP3*, which encodes the NF-κB inhibitor A20, and *CLEC16A*, which is involved in endosomal trafficking during antigen presentation (178).

***Monogenic drivers.*** While most autoimmune disorders have a complex polygenic basis, certain manifestations can arise from single mutations. As mentioned in *Chapter 1.1.4*, IPEX syndrome is caused by single nucleotide mutations in *FOXP3*, the lineage-defining transcription factor for $T_{REG}$ cells, which features early onset multi-organ T cell-dependent inflammation (144, 145). The extent of tissue pathology coincides with the severity of the resulting $T_{REG}$ cell defect with mutations abrogating *FOXP3* expression mediating rapidly progressive and fatal IPEX manifestations (179). The $T_{REG}$ cell defect in IPEX syndrome is also associated with the generation of spontaneous germinal centers and autoantibodies due to uncontrolled autoreactive B cell activation (180).

SLE is the prototypical multifactorial autoimmune disease (181, 182). It develops primarily in females after 30-years of age and is featured by recurrent flares of systemic inflammation leading to progressive multiorgan damage. The pathogenesis of SLE involves a breakdown of B cell tolerance to nucleic acids released by cell death, and the production of type-I IFN (IFN-I) by plasmacytoid dendritic cells following TLR7 signaling (181). High affinity autoantibodies against the nuclear components of a cell like double-stranded DNA (dsDNA) and ribonucleoproteins (RNP), collectively termed antinuclear antibodies (ANA), are a robust feature of SLE and likely drive pathology. Hundreds of risk alleles have been identified in SLE by GWAS, the interaction of which contributes to disease onset (182, 183). Nevertheless, monogenic variants have been described, usually arising in childhood. Most recently, a gain-of-function variant of *TLR7* (*TLR7*$^{Tyr264His}$) was identified in a 7-year-old girl with SLE (184). In mice, *Tlr7*$^{Tyr264His}$ was sufficient at inducing lupus and ANAs, and drove plasmablast development through the extrafollicular pathway (discussed further in *Chapter 1.2.3*)

*B) Environmental factors*

Genetic predispositions provide the underlying conditions needed for the development of autoimmunity but are not themselves sufficient for pathogenesis. For example, HLA-DR15, the strongest single genetic factor associated with the chronic demyelinating autoimmune disorder multiple sclerosis (MS), is present in up to 15% of the European population but affects only 142.81/100,000 people (185). Indeed, despite our genetics having largely remained the same, rates of autoimmunity and other inflammatory conditions have steadily increased since industrialization, thus positioning the environment as a key factor in eliciting autoimmunity (186). Several environmental factors have been associated with autoimmune diseases, including dietary factors, decreased parasitic burden, pollution, smoking, and UV radiation (187).

***Molecular mimicry.*** Immune cell interactions with commensal or pathogenic microorganisms are likely the primary mechanism of triggering autoreactive responses. These interactions lead to B and T cell activation either through bystander activation, largely mediated by the sensing of microbial components through pathogen recognition receptors (e.g., TLRs, RLRs, NLRs), or by molecular mimicry, where microbial components elicit autoreactive responses due to structural similarity with autoantigens (163, 188). One example of molecular mimicry leading to autoreactive B and T cell responses is observed in MS with Epstein-Barr virus (EBV) (189). The pathogenesis of MS is orchestrated by pro-inflammatory $T_H1$ and $T_H17$ cells that direct immune responses against myelin components in the central nervous system like myelin basic protein (MBP), myelin oligodendrocyte glycoprotein (MOG), and proteolipid protein (PLP) (190). Autoantibodies against the same components are also prevalent in the cerebrospinal fluid, though their role in pathogenesis remains to be established. EBV infection has long been associated with MS, but this association was recently turned to causation in a longitudinal study showing that EBV infection is necessary for MS development (163). $T_H1$ cells specific to the EBV nuclear antigen 1 (EBNA1) isolated from MS individuals can cross-react with MBP, suggesting the presence of molecular mimicry (191). In a recent study, mimicry was directly demonstrated between EBNA1 and another myelin component, glial cell adhesion molecule (GlialCAM),

through their overlapping SPPR(R/A)P amino acid motifs (192). Accordingly, anti-GlialCAM antibodies generated by plasmablasts in the cerebrospinal fluid of MS individuals were capable of cross-reacting with EBNA1.

*C) Epitope spreading*

Once tolerance is breached, the scope of B and T cell autoreactivity often expands beyond the initial epitope to include others on the same (intramolecular) or new (intermolecular) antigens (193). This phenomenon, termed epitope spreading, can initiate long before symptom onset, giving rise to a myriad of autoreactive effectors that will collectively add to the burden of autoimmunity. This is evident in SLE, where the likelihood of developing disease increases with the proliferation of distinct ANA species (194).

Autoreactive B cells are key mediators of epitope spreading. By selectively taking up autoantigen that is in complex with other proteins (e.g. RNPs in SLE), they can present multiple epitopes of from distinct antigens to T cells thereby expanding the breadth of autoreactivity (195). Indeed, this B cell-mediated epitope spreading was recently demonstrated in two studies using mixed chimera mice carrying transgenic autoreactive B cells (clone 564Igi recognizing RNA) and wildtype B cells (196, 197). Initial autoimmunity triggered by 564Igi B cell clones expanded to RNA-directed autoimmunity mediated by wildtype B cells. Notably, this occurred in a TLR7-dependent manner, reminiscent of SLE (196). Moreover, the group demonstrated that this epitope spread was fully dependent on 564Igi B cells acting as antigen-presenting cells to $CD4^+$ T cells (197). Beyond autoantigen presentation, the diversification of the BCR by SHM may also promote epitope spreading (198).

*D) Defects in immunoregulation: the case for FOXP3$^+$ $T_{REG}$ cells*

$T_{REG}$ cells, being key mediators of peripheral tolerance, directly suppress B and T cells to safeguard from autoimmunity (199). However, they are not a monolithic population; while the majority of $T_{REG}$ cells possess potent suppressive capabilities, certain clones (25-30%) exhibit an unstable $T_{REG}$ program, which contributes to their diminished suppressive

function, even in healthy individuals (200). These $T_{REG}$ cells can be differentiated by their expression of the transcription factor Helios, with Helios$^+$ $T_{REG}$ cells being enriched in stable $T_{REG}$ cells (201, 202). Autoimmune diseases consistently show perturbations in the $T_{REG}$ cell pool, often showing as a reduction in the frequencies of $T_{REG}$ cells in peripheral blood, denoting a defect in immunoregulation (203). Nevertheless, few studies in humans have attempted to qualify this perturbation beyond simple enumeration of $T_{REG}$ cells.

Several mechanisms can lead to $T_{REG}$ cell dysregulation in autoimmune disease (204). First, mutations in genes involved in $T_{REG}$ cell development, maintenance, and suppressive function can lead to a paucity of suppressive $T_{REG}$ cells; *IL2RA* and *PTPN2* mutations in T1D result in decreased IL-2 sensitivity and consequently diminish $T_{REG}$ cell survival (205, 206). Next, HLA polymorphisms can skew against $T_{REG}$ selection in the thymus and the periphery; as previously discussed, HLA-DR15 preferentially selects α3(IV)NC1-specific $T_{CONV}$ cells over $T_{REG}$ cells in anti-GBM nephritis (168). Finally, pro-inflammatory factors can directly counteract $T_{REG}$ cell suppressive function. This is of particular interest in the progression towards and the perpetuation of autoimmune diseases within affected tissues, where pro-inflammatory cytokines are in abundance. For example, IL-6 and tumor necrosis factor (TNF)-α dampen $T_{REG}$ cell-mediated suppression, and this is predicted to promote $T_H1$ cell responses in RA (207-210). Moreover, the IL-1 family of cytokines IL-1α/β and IL-33 have also been implicated in $T_{REG}$ cell stability. Unlike other cytokines, IL-1 and IL-33 are released immediately upon tissue injury and thus alarm the immune system to react – and hence are qualified as 'alarmins'. IL-33, signaling through its receptor ST2, drives the expansion of Helios$^+$ $T_{REG}$ cells expressing the $T_H2$-associated transcription factor GATA-3. The suppressive function of these Helios$^+$ GATA-3$^+$ $T_{REG}$ cells has been implicated in restricting $T_H1$ and $T_H17$ cell responses in mouse models of colitis, MS, and T1D (211-214). IL-1, on the other hand, restricts the expansion of this population favouring the expansion of unstable Helios$^-$ $T_{REG}$ cells, which contributes to increased pathology (212, 215). As the effects of these cytokines take place within tissues, human studies remain scarce.

Given the importance of $T_{REG}$ cells in immunoregulation, several $T_{REG}$ cell-based therapies are currently in development. These include autologous $T_{REG}$ cell transfer and CAR-

$T_{REG}$ cells to treat T1D, RA, MS, amongst others (199). Other approaches are utilizing IL-2 mutant proteins (muteins) and IL-2-IL-33 fusions to selectively expand endogenous Helios$^+$ $T_{REG}$ cells thereby enhancing immunoregulation (216, 217).

### *1.2.2 B cells in autoimmune pathogenesis*

The generation of autoimmune disease relies on interactions between autoreactive T and B cells. The outcomes of these interactions leading to tissue pathology are diverse but can be broadly categorized into autoantibody-mediated injury (e.g., SLE) or T cell-mediated inflammation (e.g., MS, RA, T1D) (163). Autoreactive B cells are vital to pathogenesis in both categories; in addition to producing autoantibodies, autoreactive B cells serve as antigen-presenting cells that can trigger autoreactive T cell responses (218). The success of B cell depletion therapies (BCDT) in the treatment of both autoantibody-mediated and T cell-mediated autoimmune diseases underscores the central position of B cells in the broad autoimmune architecture.

*A) B cells as autoantibody-secreting cells*

The production of autoantibodies by B cells is one of the primary features of autoimmune disorders. Unlike the physiological autoantibodies produced by MZ B cells, pathogenetic autoantibodies exhibit significant SHM and CSR, resulting in high specificity towards their target antigen (219, 220). As such, autoantibodies can focus the scope of an immune response towards even the rarest autoantigen resulting in significant tissue injury. The mechanisms by which autoantibodies can cause pathology are many and are predominantly dependent on the antibody isotype and the nature of the autoantigen (221).

***Target antagonism*.** The direct binding and neutralization of a target antigen is one mechanism by which autoantibodies can mediate tissue pathology. For example, up to 90% of myasthenia gravis (MG) cases, a neurological autoimmune disorder characterized by progressive skeletal muscle weakness, involve autoantibodies that antagonize the nicotinic acetylcholine receptor (AChR) (222, 223). These predominantly IgG1 and IgG3 anti-AChR antibodies bind to AChR at postsynaptic neuromuscular junctions causing cross-linking and

internalization, thereby rendering muscle fibres unresponsive to acetylcholine. IgG4 autoantibodies against muscle-specific kinase (MuSK), a transmembrane kinase integral for AChR clustering, also contributes to MG pathology by antagonizing AChR signaling (222, 223). Similarly, in Sjögren's syndrome (SjS), autoantibodies against the muscarinic acetylcholine receptor $M_3$ (M3R) on the salivary and lacrimal epithelia prevent acetylcholine-triggered calcium signaling downstream M3R, leading to decreased saliva and tear production (224).

***Complement activation.*** Autoantibodies of the IgM and IgG1/2/3 isotypes can also cause pathology by activating the complement system. Complement deposition on the target tissue can either lead to cell destruction by membrane attack complex formation or inflammation by the recruitment of innate immune cells. For example, the IgG1 and IgG3 anti-AChR antibodies prevalent in MG can trigger the formation of the membrane attack complex at neuromuscular junctions, thereby contributing to muscle weakness in affected individuals (223). Complement fixation by autoantibody also contributes to the severe systemic thrombotic pathology in anti-phospholipid syndrome (APLS) (225, 226). Here, IgG1 and IgG2 autoantibodies against phospholipid-associated proteins like β2 glycoprotein 1 (β2GP1) present on a wide range of cell surfaces leads to complement fixation, the activation of platelets, and clot formation. Finally, complement activation can also result in the demyelination observed in various demyelinating autoimmune disorders including MOG antibody-associated disease (MOGAD) (227).

***Cell activation.*** Autoantibody binding of certain antigens on immune and non-immune cells can also cause cell activation. In APLS, the binding of anti-β2GP1 antibodies to vascular endothelial cells promotes expression of adhesion molecules, thereby elevating the thrombotic state of blood vessels (228). Moreover, anti-β2GP1 antibodies can also bind neutrophils, inducing their degranulation and the release of pro-thrombotic extracellular traps (229). This autoantibody-mediated triggering of neutrophil degranulation is also the primary pathomechanism in antineutrophil cytoplasmic antibody (ANCA)-associated vasculitis (AAV) (230). ANCAs bind and cross-link the granule proteases myeloperoxidase (MPO) and proteinase 3 (PR3) present on the surface of cytokine-primed neutrophils leading

to their degranulation within the small arteries of the lungs and kidneys resulting in substantial inflammation and impaired organ function (discussed further in *Chapter 1.3*).

***Opsonization.*** In some cases, the binding of autoantibodies to target autoantigens destines the cell carrying the autoantigen for phagocytosis by FcγR-laden macrophages (231). This is the primary pathomechanism in immune thrombocytopenia (ITP). The opsonization of platelets by IgG1 and IgG3 autoantibodies targeting the platelet-specific surface glycoproteins GPIIb/IIIa and GPIb/IX marks these cells for destruction by splenic macrophages. Consequently, the paucity of platelets renders affected individual susceptible to bleeding.

***IgG4 autoimmune diseases.*** Certain autoimmune disorders are almost exclusively associated with autoantibodies carrying an IgG4 isotype. Unlike IgG1/2/3 autoantibodies, IgG4 autoantibodies have a greatly reduced capacity to activate complement, opsonize antigen, and induce cross-linking, and instead primarily mediate pathology by blocking autoantigen interactions with their ligands – namely target antagonism (75). Pemphigus vulgaris and pemphigus foliaceus, autoimmune diseases featuring severe skin blistering, are predominantly caused by IgG4 autoantibodies targeting desmogleins 1 and 3 (232). These autoantibodies block desmoglein-desmoglein interactions, thereby preventing desmosome formation between keratinocytes and ultimately compromising the integrity of the skin barrier.

***Immune complexes.*** The pathology of some autoimmune disorders is linked with the capacity of autoantibodies to form immune complexes with target antigen. Immune complexes of ANAs with dsDNA/RNA-containing autoantigens are central to SLE pathogenesis as they can ligate TLR7/9 and FcγRs on innate immune cells, particularly plasmacytoid dendritic cells, leading to IFN-I production, the primary pathogenic factor in SLE (181). Moreover, BCR and TLR7 ligation in B cells by ANAs is thought to drive germinal center formation thereby promoting further autoantibody production and epitope spreading. In 40-60% of SLE cases, these immune complexes also embed within the filtration barrier of the kidney resulting in severe inflammation, termed lupus nephritis (discussed further in *Chapter 1.3*) (233).

***Autoantibodies of unknown pathogenicity.*** Several autoimmune disorders are strongly associated with the presence of autoantibodies, but their involvement in the pathomechanism remains to be determined. Approximately two thirds of people with RA are seropositive for ACPAs, and 80% have autoantibodies targeting the Fc portion of IgG (rheumatoid factor, RF) (234). Both ACPAs and RFs are thought to participate in RA pathogenesis by forming immune complexes with target antigens and directly embedding within synovial tissue where they bind to activating FcγRs on osteoclasts, macrophages, and neutrophils leading to bone resorption at the joints (235, 236). ACPAs are highly specific to RA, thereby denoting a likely involvement (237). However, ACPAs are insufficient at driving disease in mouse models. RFs, on the other hand, are prevalent even in the healthy elderly population and may simply represent an epiphenomenon of defective B cell tolerance (238).

Similarly, the importance of myelin-targeting autoantibodies in MS is also unknown. The expansion of oligoclonal bands within the cerebrospinal fluid, corresponding with plasmablast-derived intrathecal IgG antibodies, is the most characteristic feature of MS. Antigenic mapping of these bands has identified several myelin targets including MBP, MOG, GlialCAM, and PLP (192, 239, 240). While the autoantibodies against these antigens are hypothesized to mediate pathology via complement activation, this remains controversial; these autoantibodies are present in variable frequencies in people with MS and many autoantibodies within the oligoclonal bands are directed towards ubiquitous intracellular antigens instead of myelin (241, 242).

*B) B cells as autoantigen-presenting cells*

Successful response to BCDT is not consistently associated with reduced autoantibody levels indicating that autoantibody-independent B cell functions are involved in the pathogenesis of autoimmune diseases (218). Autoreactive B cells, given their autoantigen-specific BCRs, are in a unique position to uptake and present autoantigen to autoreactive T cells and can thereby orchestrate T cell-mediated mechanisms of tissue pathology. The strongest evidence for autoantigen presentation by autoreactive B cells in human autoimmune disease comes from MS. MS pathology is predominantly driven by

myelin-specific T cells, and this is supported by several key findings: $CD4^+$ T cells are present in central nervous system lesions, myelin-specific $CD4^+$ T cells are abundant in MS blood, and myelin-specific $CD4^+$ T cells are capable of mediating MS pathology in mice in the absence of B cells (243-247). Nevertheless, the efficacy of BCDT at mediating remission and the prevalence of expanded oligoclonal bands in the cerebrospinal fluid denote B cell involvement. The autoantigen-presenting capacity of autoreactive B cells was recently implicated in MS pathogenesis with the observation that peripheral blood MBCs could activate autologous $T_H1$ cells *ex vivo* in the absence of any exogenous antigen (248). TCRVβ chain-sequencing of the activated T cells demonstrated significant overlap with T cells present in MS lesions, and these T cells recognized the antigen RASGRP2 present in both MS brain tissue and peripheral blood MBCs. In a subsequent study, the same group expanded on their work showing that MS $CD4^+$ T cells could respond to a wide variety of MHC-II-bound autoantigens presented by MBCs from MS individuals, including MBP, RASGRP2, and HLA-DR peptides (249). Together, these studies strongly suggest that B cells have an autoantigen-presenting role in MS. While there is still a paucity in research on the autoantigen-presenting capacity of human B cells in autoimmunity, this will likely improve with detailed examination of affected tissues and associated lymph nodes via scRNA-seq and spatial transcriptomics.

### *1.2.3 Atypical B cells: Implicating the extrafollicular response*

Immunophenotyping studies in the last two decades established the expansion of $CD21^{low}$ MBCs as a common feature of various autoimmune disorders, including SLE, RA, MS, SjS, systemic sclerosis (SSc) (134, 135, 250-253). Recently, a striking similarity was demonstrated between these autoimmune-associated $CD21^{low}$ B cells and the extrafollicular $CD21^{low}$ T-bet$^+$ $CD11c^+$ atBCs that arise during chronic viral and parasitic infections, thereby implicating the extrafollicular response in autoimmune pathogenesis (119). The predicted involvement of extrafollicular B cell responses in autoimmunity is not new, with the extrafollicular generation of plasmablasts/SLPCs having been observed in synovial tissue and salivary glands in RA and SjS, respectively (254-257). Moreover, the development of autoreactive plasmablasts in SLE-prone MRL/$FAS^{lpr}$ mice occurs

predominantly extrafollicularly (258). In humans the involvement of atBCs remains correlational, nevertheless strong evidence supports a pathogenic role for these eMBCs in SLE and RA (95).

The severity of SLE is associated with the expansion of two clonally-related B cell populations that correspond with CD11c$^+$ T-bet$^+$ atBCs: CD19$^{high}$ CD21$^{low}$ IgD$^-$ CD27$^-$ T-bet$^+$ CD11c$^+$ CXCR5$^-$ FcRL5$^+$ B cells termed double negative (DN)2 B cells and CD19$^{high}$ CD21$^{low}$ IgD$^+$ CD27$^-$ CD11c$^+$ CXCR5$^-$ B cells termed activated naïve B cells, the latter population serving as precursors for the former (135, 250, 259). Consistent with an extrafollicular origin, DN2 B cells exhibit lower SHM than cMBCs and are able to convert rapidly into plasmablasts/SLPCs when provided with TLR7 signals in the presence of IFN-γ, IL-2, IL-21, and BAFF (135, 250, 260). Moreover, the atBC repertoire overlaps with the expanded plasmablast/SLPC repertoire in SLE and is enriched with autoreactive clones, denoting their likely involvement in SLE pathogenesis (135). Indeed, TLR7 is highly implicated in SLE, giving rise to spontaneous ectopic germinal centers that are thought to be the source of high affinity ANAs (261). Accordingly, the recently described *TLR7*$^{Tyr264His}$ gain-of-function mutation causing childhood SLE was shown to drive the formation of atBCs, germinal centers, and ANAs in mice, with SLE developing even when germinal centers were ablated (184, 262). Thus, it is hypothesized that atBCs participate in SLE pathology through the extrafollicular generation of ANA-producing plasmablasts/SLPCs in a TLR7-dependent manner. Moreover, as was recently demonstrated in chronic *P. falciparum* infection, we can theorize that atBCs may also promote SLE by supporting autoreactive germinal centers through antigen-presentation to $T_{FH}$ cells (107, 137, 263).

In RA, expanded atBCs are present in both the blood and synovial tissue, with the abundance of atBCs in the blood correlating with disease severity (123, 264-266). As with atBCs in SLE, atBCs in RA are clonally expanded, exhibit SHM, and are enriched with autoreactive clones, indicating their likely involvement in autoantibody generation (266-268). Accordingly, $T_{PH}$ cells, which support atBC generation via IFN-γ and IL-21 production, are also expanded in peripheral blood of both RA and SLE (131, 269, 270). *Studies investigating the mechanisms by which atBCs may be implicated in other autoimmune*

*diseases remain sparse and are still in their infancy. Nevertheless, the prevalence of atBCs in multiple autoimmune entities denotes their contribution to a greater architecture of autoimmunity – one which can be exploited by B cell-targeting therapeutics.*

### *1.2.4 B cells as therapeutic targets*

Initially developed for the treatment of B cell lymphoma, BCDT is quickly emerging as a cornerstone of therapy in autoimmune diseases (218). The expanding arsenal of B cell-targeting biologics directed towards distinct aspects of B cell biology offers a more tailored approach to the treatment of autoimmune diseases than traditional broad immunosuppression with glucocorticoids (GC), cytostatics, and calcineurin inhibitors. BCDTs can largely be categorized by the format of the drug (monoclonal antibody, fusion protein, CAR-T cells) and their targets.

*A) Monoclonal antibodies*

***Anti-CD20.*** Monoclonal antibodies targeting CD20, a B cell-specific cell surface protein involved in BCR signaling, are the foundation of BCDT. They bind to and eliminate all B cells expressing CD20 (pre-B cells to MBCs) but do not target pro-B cells and PCs as they lack surface CD20. Anti-CD20 monoclonal antibodies are categorized into type-I antibodies that cause CD20 clustering in lipid rafts (e.g., rituximab (RTX) and ocrelizumab), and type-II antibodies that do not cause redistribution (e.g., ofatumumab and obinutuzumab) (271, 272). The clustering of type-I anti-CD20 monoclonal antibodies on the surface of B cells results in strong complement activation and cell elimination by complement-dependent cytotoxicity (CDC), but are also susceptible to FcγRIIb-mediated internalization leading to treatment resistance (273). Type-II antibodies bind uniformly across the B cell surface and are thus not susceptible to internalization (272). Lower CDC is observed using type-II antibodies, which preferentially act through antibody-dependent cell cytotoxicity (ADCC) performed by FcγRIIa-expressing NK cells. BCDT with anti-CD20 monoclonal antibodies is effective in treating multiple autoimmune diseases including MS, RA, and ITP (274-277). However, relapses eventually occur, often corresponding with B cell recovery, and therefore

maintained remission usually requires multiple treatments. While the mechanisms driving relapses following BCDT are not fully elucidated, the incomplete depletion of autoreactive MBCs and the generation of new autoreactive B cells likely play a role. Indeed, it was recently demonstrated that pre-existing RTX-resistant germinal center B cells and newly generated MBCs residing in the spleen participated in post-RTX relapses of ITP (278).

While LLPCs are not directly targeted by anti-CD20 monoclonal antibodies, plasmablasts/SLPCs are susceptible since their replenishment is dependent on their CD20-expressing MBC precursors. This may explain the efficacy of anti-CD20 targeting drugs in treating certain autoantibody-mediated diseases (e.g., ITP, AAV, MG, MOGAD, neuromyelitis optica spectrum disorders (NMOSD)) (277, 279-282). While SLE, whose pathology is reliant on autoantibody production, has seen some success with anti-CD20 BCDT, the effects are inconsistent and providing minimal benefit in severe cases (283).

***Anti-CD19.*** To broaden the scope of B cell depletion to include PCs, monoclonal antibodies were generated against CD19, a co-receptor of the BCR present on all B cells except for the most terminally differentiated LLPCs in the bone marrow. One anti-CD19 monoclonal antibody, inebilizumab, has been approved for the treatment of NMOSD and is in trials for MS and SSc (284, 285). Both anti-CD20 and anti-CD19 monoclonals induce a largescale B cell deficiency, eliminating even the B cell precursors in the bone marrow. As such, both BCDT strategies are associated with infections, warranting the development of more targeted drugs (284, 286).

***Anti-BAFF.*** The anti-BAFF monoclonal antibody belimumab is the only monoclonal BCDT approved for the treatment of SLE (287). Anti-BAFF monoclonals function by preventing the binding of BAFF to its receptors BAFF-R, TACI, and BCMA, which are differentially expressed on B cell subsets; BAFF-R is expressed on transitional naïve B cells and decreases with maturation, TACI is expressed on all activated B cells with elevated expression on extrafollicular subsets (atBCs and MZ B cells) and is absent from germinal center B cells, and BCMA is expressed exclusively by PCs (288). Thus, anti-BAFF monoclonal antibodies reduce naïve B cell, activated B cell, and PC survival without affecting MBCs and

B cell precursors in the bone marrow (289). Nevertheless, anti-BAFF monoclonal antibodies do not disrupt APRIL signaling through TACI or BCMA, which may limit its efficacy.

***Anti-CD38.*** CD38 is expressed on numerous immune cells but is present at higher levels on the surface of PCs. As such, anti-CD38 monoclonal antibodies (daratumumab) were developed to target PCs directly, with the hope of eliminating the bone marrow-residing LLPCs (290). Accordingly, daratumumab was effective in treating refractory SLE resulting in a significant decrease in ANAs, as was outlined in a recent case series (291). Nevertheless, larger trials are needed to demonstrate the efficacy of anti-CD38 monoclonal antibodies in autoimmune diseases.

*B) Recombinant fusion proteins*

***TACI-Ig.*** Atacicept/telitacicept is a fusion protein consisting of the extracellular domain of TACI, a receptor capable of binding both BAFF and APRIL, and a modified Fc domain of human IgG1. Unlike anti-BAFF monoclonal antibodies, TACI-Ig neutralize both BAFF and APRIL signals and are thus predicted to have a stronger effect on SLPCs and LLPCs (288). Currently, TACI-Ig is being investigated in the treatment of IgA nephropathy (IgAN) (292). Surprisingly, trials in RA and SLE did not pass, and TACI-Ig increased relapse rates in MS (293-295).

*C) CAR-T cell therapy*

***CD19 CAR-T.*** The newest class of therapeutics adopted for BCDT are CAR-T cells, wherein autologous $CD8^+$ T cells are engineered to express a CAR directed towards a certain antigen. Unlike monoclonal antibodies and recombinant fusion proteins, CD19 CAR-T cells are predicted to have greater tissue penetrance and thereby provide a stronger depletion of B cells (296). Initial reports using CD19 CAR-T cells in individuals with severe refractory SLE showed effective depletion of B cells and long-term drug-free remission (296, 297).

### *1.2.5 Conclusions*

Humanity's transition into sedentary, agricultural-based societies 12,000 years ago was met with an explosion in the burden of communicable diseases (185). Substantial adaptation of our immune genes enabled us to deal with the new heavy pathogen burden but inadvertently predisposed us for the development of inflammatory and autoimmune conditions in the modern age (185, 298, 299). In this chapter, we provided an overview of a conserved immunogenetic architecture that facilitates a breach in B and T cell tolerance in some individuals (164). We highlighted the roles autoreactive B cells play in autoimmune pathogenesis, and outlined an emerging pathway by which atBCs cells may contribute to the pathogenesis of multiple autoimmune disorders. With the arrival of tools that enable us to track and dissect individual pathogenic B cell clones within blood and tissue, conceptual leaps made in one autoimmune setting will undoubtedly translate to another.

## 1.3 Autoimmune kidney disease

The kidneys are the critical orchestrators of water and electrolyte homeostasis in the body. They filter out metabolic wastes, excess ions, and water from the blood, regulate blood pressure through the renin-angiotensin-aldosterone system, and stimulate red blood cell production via erythropoietin. Nephrons are the discrete functional units of the kidney. Each consists of a renal corpuscle, the primary site of blood filtration, and a tubule, which mediates reabsorption of the filtered substances and further secretion of metabolic wastes. Progressive injury to nephrons leads to deterioration of kidney function and the development of CKD. In severe cases, this can progress into ESKD necessitating lifelong dialysis or kidney transplantation for survival (2).

Immune-mediated kidney injury, largely due to autoimmunity, is the primary non-preventable cause of CKD in children and adults (4, 5). The immune mechanisms involved in injury are diverse, but autoantibodies represent an overarching feature of autoimmune kidney diseases. In *Chapter 1.3*, we will review the humoral etiologies of several distinct autoimmune kidney diseases, highlighting their similarities and differences. The *Literature Review* will be completed by a discussion on the immunopathogenesis of childhood INS, the primary focus of this thesis.

### *1.3.1 Glomerular filtration barrier*

The renal corpuscle is composed of two structures: the capillaries of the glomerulus and the surrounding sack-like Bowman's capsule (**Figure 3**). Fenestrated endothelial cells form the walls of the glomerular capillaries and specialized smooth muscle cells, called mesangial cells, located between the capillaries maintain glomerular structure. Surrounding the glomerulus at its interface with the Bowman's capsule is a tripartite proteinaceous layer known as the GBM. This basement membrane is produced and maintained by highly specialized glomerular epithelial cells called podocytes. Long processes emanating from podocyte cell bodies, termed foot processes, wrap around the glomerular capillaries and interdigitate with each other forming a contiguous cellular junction across the glomerulus known as the slit diaphragm (300). The fenestrated endothelium, GBM, and slit diaphragm

together constitute the *glomerular filtration barrier* (301). As blood enters the glomerulus, its non-cellular components traverse the endothelial fenestrae and encounter the GBM. The inner and outermost layers of the GBM, rich in negatively charged heparan sulfate, impede the passage of negatively charged molecules, while a network of type IV collagen and laminin in the middle layer restricts the passage of large proteins. Subsequently, the fluid is sieved by the slit diaphragm, which permits water and small solutes to pass into the urinary space of the Bowman's capsule, while proteins remain in circulation. The resulting ultrafiltrate is processed further within the nephron tubule to produce urine.

*A) Slit diaphragm*

The slit diaphragm is a unique cellular junction that serves as the major ultrastructural determinant of glomerular filtration. It is composed primarily of Nephrin (*NPHS1*), NEPH1, and Podocin (*NPHS2*) expressed on the surface of the podocyte (302). Homotypic Nephrin-Nephrin and heterotypic Nephrin-NEPH1 interactions bridge a 40 nm gap between adjacent podocyte foot processes generating a fishnet-like structure that mediates size-selective filtration (303, 304). Podocin acts as a scaffold for the slit diaphragm, recruiting both Nephrin and NEPH1 into lipid rafts at the junction of the foot processes (305). Intracellularly, several proteins, like Zonula occludens-1 (ZO-1) and CD2 associated protein (CD2AP), link the slit diaphragm to the actin cytoskeleton, thereby enabling it to regulate podocyte structure in response to physical stress (e.g., changes in glomerular pressure) (306-309). The importance of the slit diaphragm in glomerular filtration is exemplified by mutations in slit diaphragm proteins that cause congenital nephrotic syndrome (e.g., *NPHS1*, *NPHS2*) (310, 311). Here, podocyte foot processes are retracted resulting in the massive loss of proteins into the urine (nephrotic-range proteinuria, >3.5 g protein lost in urine per day in adults or >1 g/$m^2$ of body surface area per day in children) (**Figure 3**). This foot process effacement is the diagnostic lesion of nephrotic syndrome and is observable only by electron microscopy.

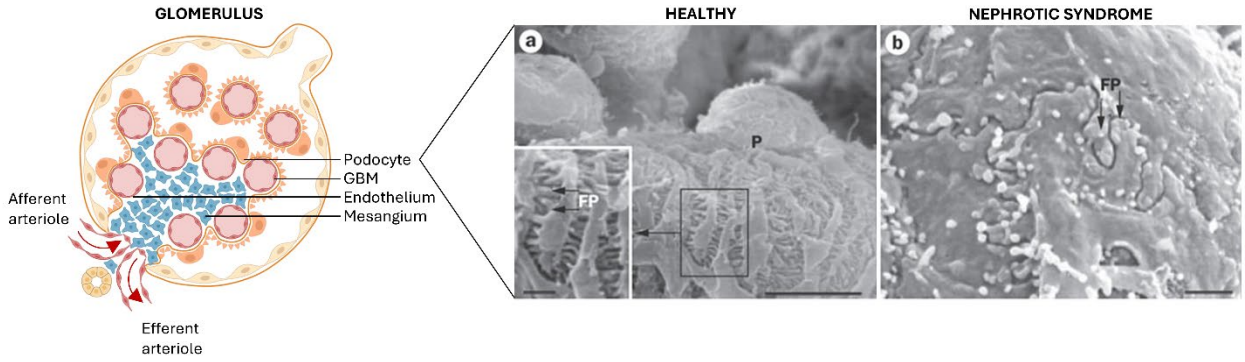


***Figure 3 - Glomerular filtration barrier.*** The glomerulus is the principal filtering unit of the kidney. It filters blood by passing it through a highly selective filtration barrier composed of an innermost layer of fenestrated endothelial cells, the glomerular basement membrane (GBM), and podocytes (P). Podocyte foot processes (FP) wrap around the glomerular capillaries and interdigitate forming the slit diaphragm. In nephrotic syndrome, foot processes are effaced, and the slit diaphragm is lost result in massive proteinuria. Electron microscopy images obtained from ref (300). Created with BioRender.com

### *1.3.2 Glomerulonephritis: immune-mediated injury to the glomerulus*

Glomerulonephritis is the main consequence of pathological immunity within the kidney. It can arise from immune responses triggered by infection but is most often caused by autoimmunity. In either case, it is characterized by immune-mediated injury to the glomerulus and its filtration barrier that impedes its filtering function (4). The mechanisms underlying pathogenesis are diverse and can proceed through either an inflammatory or a non-inflammatory course. Inflammatory injury to the glomerulus is acute, recruiting innate immune cells that mediate necrotizing tissue destruction by the release of reactive oxygen species (312). Clinically, this manifests as a nephritic syndrome (*Chapter 1.3.3*), characterized by the loss of red blood cells into the urine (hematuria) alongside varying degrees of proteinuria and kidney failure. In contrast, non-inflammatory injury to the glomerulus primarily induces podocyte foot process effacement, thereby resulting in nephrotic syndrome (*Chapter 1.3.4*) (313). In the case of autoimmune kidney diseases, pathology is predominantly elicited by autoantibodies following a breach in tolerance to either a systemic or renal autoantigen (7) (**Figure 4**). While the immune mechanisms driving disease following autoantibody-mediated injury are partially characterized, *the factors leading to the loss of tolerance in autoimmune kidney diseases remain largely undefined*.

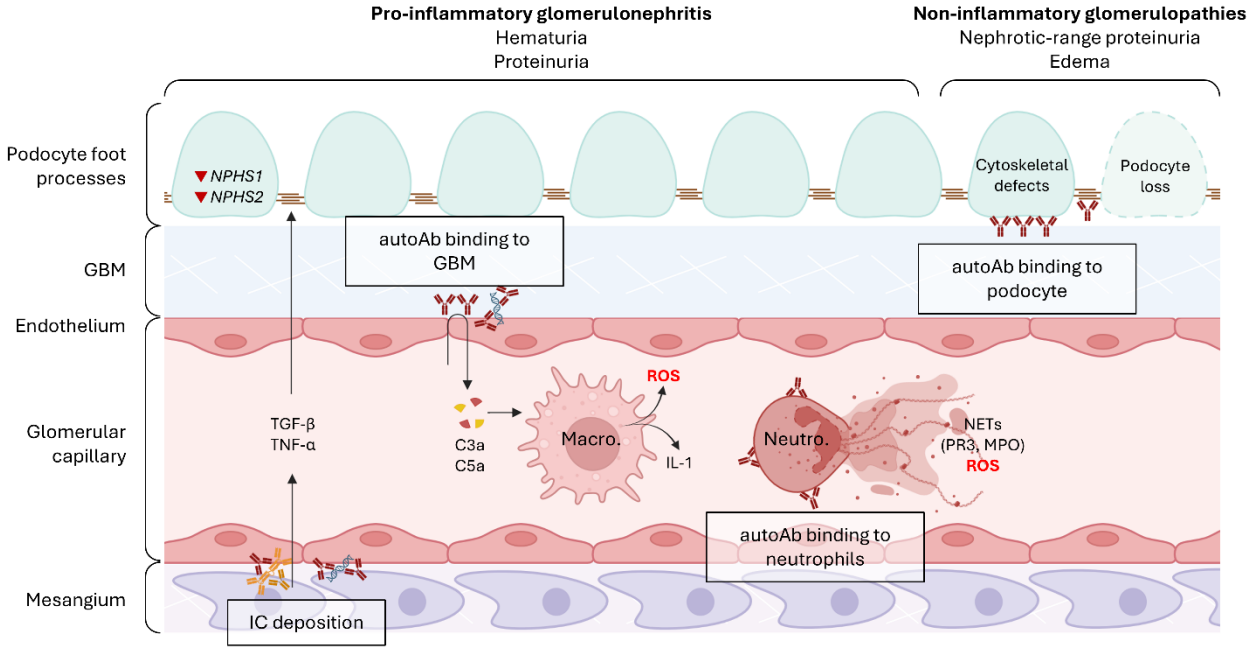


***Figure 4 - Autoantibodies in glomerular diseases.*** Pathology in autoimmune glomerulonephritis is elicited by autoantibodies. The resulting injury may either be inflammatory resulting in a rupture of the filtration barrier and the development of nephritic disease (hematuria and proteinuria) or non-inflammatory causing podocyte foot process effacement and eventual detachment from the filtration barrier resulting in nephrotic syndrome (nephrotic-range proteinuria and edema). Nephritic disorders are mediated by immune complexes (IgA nephropathy, lupus nephritis) that entrap within the mesangium or subendothelial space, autoantibodies that bind to the glomerular basement membrane (anti-GBM nephritis), or autoantibodies that bind neutrophils (ANCA glomerulonephritis). These antibodies can activate mesangial cells to produce podocyte-injuring cytokines like TNF-α and TGF-β, activate complement, recruit pro-inflammatory macrophages and neutrophils, and trigger neutrophil degranulation. The production of reactive oxygen species (ROS) by macrophages and neutrophils mediates the rapidly-progressive destruction of kidney tissue. Nephrotic disorders are mediated by anti-podocyte antibodies (APAs) that bind subepithelially (membranous nephropathy) resulting in cytoskeletal changes in the podocyte. APAs that bind to the slit diaphragm are predicted to be involved in the pathogenesis of idiopathic nephrotic syndrome (INS: minimal change disease and focal segmental glomerulosclerosis). Created with BioRender.com.

Immediate treatment of autoimmune kidney disease is essential for preventing further decline in kidney function. Therapeutic strategies have historically relied on long-term general immunosuppression with GCs and the cytostatic drugs cyclophosphamide and mycophenolate mofetil, despite the toxicity associated with extended use (314). The lack of targeted treatment approaches is the result of *a paucity in biomarkers that can inform an early diagnosis* – which often relies on biopsies – and an *incomplete understanding of disease pathogenesis*. Nevertheless, BCDT has been successful in treating several autoimmune kidney diseases (178, 315). *Thus, by dissecting the roles of B cells in the pathogenesis of these diseases, we will likely uncover novel biomarkers and potential therapeutic targets.*

### *1.3.3 Inflammatory glomerulonephritis: Nephritic syndrome*

Inflammatory injury to the kidney is most often elicited by autoantibodies directed towards systemic autoantigens and can have both renal and systemic manifestations (7). These autoimmune kidney diseases usually involve the formation of immune complexes that embed within the glomerulus thereby triggering local inflammation. Inflammation proceeds in two phases; the acute phase is marked by complement activation and the recruitment of innate immune cells that mediate initial injury (4). In the subsequent chronic phase, lymphocytes, particularly T cells, accumulate within and around the glomeruli and perpetuate inflammation. The use of mouse models has propelled our understanding of these diseases, particularly during acute kidney injury, where the availability of human samples is sparse. More recently, analysis of immune cell infiltrates in kidney biopsies during the chronic phase by scRNA-seq has helped in our understanding of disease perpetuation, though these studies remain few (316, 317).

While initially restricted to the glomerulus, inflammation usually spreads to the tubules resulting in tubulointerstitial nephritis alongside glomerulonephritis. Severe cases will develop into rapidly progressive glomerulonephritis (RPGN), characterized by the emergence of irreversible crescent-shaped glomerular lesions caused by excessive fibrosis, rupture of the GBM, and the proliferation of parietal epithelial cells in the Bowman's capsule (318). As such, immediate immunosuppression is critical to preventing decline in kidney function. Often, this is done in conjunction with plasma exchange to rapidly eliminate circulating antibodies.

*A) IgA nephropathy: Immune complex-mediated glomerulonephritis*

IgAN is the most prevalent form of glomerulonephritis in adults, with ESKD developing in 30-40% of cases in 10-20 years (319). It affects both adults and children with a 2:1 male-to-female preponderance (1:1 in East Asia) and has a lower incidence in individuals of African ancestry (320). The disease follows a relapsing-remitting course with relapses frequently taking place alongside respiratory infections. Pathogenesis is mediated

by the mesangial deposition of systemic immune complexes consisting of polymeric hypogalactosylated IgA1 (gdIgA1) bound by glycan-specific IgG or IgA (321). Polymeric IgA1 induces mesangial cell activation, proliferation, and production of pro-fibrotic factors (e.g., matrix components, transforming growth factor (TGF)-β), pro-inflammatory cytokines (e.g., IL-6, TNF-α), and angiotensin II (322). IgA1 immune complexes also trigger complement C3 deposition and the production of C3a and C5a anaphylatoxins, altogether culminating in the recruitment of pro-inflammatory macrophages to the glomerulus. Progressive fibrosis, mesangial cell proliferation, and immune cell recruitment leads to the development of nephritis, hallmarked by hematuria and proteinuria (319). Additionally, angiotensin II results in tubular atrophy and systemic hypertension, with elevated glomerular pressure augmenting pathology. Lastly, TGF-β and TNF-α from mesangial cells cause podocytes to downregulate slit diaphragm proteins (e.g., Nephrin and Podocin) and promote apoptosis (323, 324).

The etiology of IgAN remains incompletely defined. Pathogenic models define at least two independent factors necessary for mediating disease: the generation of gdIgA1 and the loss of B cell tolerance to epitopes exposed on the hypogalactosylated IgA1. The production of gdIgA1 is at least partly heritable, with circulating gdIgA1 being more prevalent in relatives of affected individuals (325). Indeed, GWAS have identified several predisposing polymorphisms in genes involved in the *O*-glycosylation of IgA1, though they were variably present in independent cohorts (326, 327). The gdIgA1-producing PCs likely arise in mucosal sites given their predominantly polymeric format and their specificity for common mucosal antigens (328, 329). The association of IgA1 with respiratory infection and the interfollicular expansion of gdIgA1-producing B cells highlight an extrafollicular origin. Accordingly, TLR7, TLR9, BAFF, APRIL, and TACI, all factors that drive extrafollicular responses, have been implicated in disease pathogenesis (326, 330-332). As such, both therapeutic tonsillectomy and atacicept are being explored in the treatment of IgAN (292, 333).

The factors underlying the loss of tolerance to gdIgA1 are more difficult to pinpoint. Numerous predisposing and protective HLA-II polymorphisms were identified by GWAS, though their relevance to the pathomechanism remains unknown (326, 331, 334, 335).

Nevertheless, the loss of tolerance to gdIgA1 is necessary since gdIgA1 on its own is insufficient at mediating IgAN (325). Moreover, it was recently reported that certain individuals with IgAN carry IgA autoantibodies that directly target βII-spectrin in mesangial cells, possibly arising by intermolecular epitope spreading (336).

*B) Lupus nephritis: Immune complex-mediated glomerulonephritis*

Lupus nephritis develops in 40-60% of cases of SLE, with up to 30% of individuals progressing to ESKD (337). Pathogenesis is mediated by immune complexes deposited in the mesangium or endothelium-GBM interface (subendothelial) that direct local inflammatory responses. These immune complexes are composed of IgG, IgM, or IgA ANAs and nucleic acids derived from dying cells or neutrophil extracellular traps (338, 339). Acutely, immune complexes activate the complement system leading to neutrophil and macrophage recruitment, which are thought to drive immediate tissue pathology by the production of reactive oxygen species (340-343). As disease progresses, $CD4^+$ and $CD8^+$ T cells become the predominant immune infiltrate within the kidney (340). $T_H1$ cells are especially abundant and are predicted to facilitate macrophage activation and promote $CD8^+$ T cell cytotoxic functions (344). Moreover, IL-17A from infiltrating $T_H17$ cells likely promotes neutrophil recruitment and mediates direct tissue effects (e.g., epithelial-mesenchymal transition) (345). Like IgAN, lupus nephritis also manifests as a nephritic syndrome.

The etiology of lupus nephritis is vastly heterogeneous with numerous genetic and environmental contributors (181, 182). The loss of tolerance to chromatin content and the production of ANAs precedes SLE development by years, and the accumulation of distinct ANA species is correlated with the development of lupus nephritis (338). The induction of a IFN-I signature, possibly by the ligation of TLR7 in plasmacytoid dendritic cells, is an important determinant of SLE and lupus nephritis (181). Reduced capacity to clear dead cells is thought to play a role in the breach of tolerance towards nucleic acids. As discussed in *Chapter 1.2.3*, extrafollicular B cell responses are hypothesized to be involved in ANA production and may give rise to ectopic autoreactive germinal centers (95). Indeed, both

atBCs and ectopic germinal centers have been identified in kidneys from individuals with lupus nephritis (340, 346).

*C) ANCA glomerulonephritis: Pauci-immune glomerulonephritis*

ANCA glomerulonephritis is the most common cause of RPGN. It develops secondary to systemic AAV, though renal-limited manifestations exist, with incidence peaking between 65-75 years of age (347). ANCA glomerulonephritis is also referred to as 'pauci-immune' glomerulonephritis since antibodies are not a histopathological feature of disease. Instead, ANCAs bind to the granule proteases PR3 and MPO expressed on the surface of primed neutrophils (230). ANCA-bound neutrophils degranulate as they pass through the small vasculature of the glomerulus, releasing PR3- and MPO-containing extracellular traps and reactive oxygen species (348). Subsequent complement activation results in the release of anaphylatoxins that promote further neutrophil recruitment, priming, and activation (349). Following acute injury, $T_H1$ and $T_H17$ cells accumulate in the kidney driving further inflammation by activating macrophages, promoting $CD8^+$ T cell cytotoxicity, and neutrophil recruitment (350). The recruitment of these T cells to the kidney is predicted to occur either in an antigen-specific manner in response to PR3 and MPO, or through bystander activation of resident T cells (351, 352).

Loss of tolerance to PR3 and MPO is the primary cause of AAV. PR3-AAV is associated with the *HLA-DPB1**04:01 allele while MPO-AAV is associated with the *HLA-DRB1**09:01 and 11:01 alleles, though their relevance to pathogenesis is not yet known (353, 354). The *PTPN22* Arg260Trp variant is also a major predisposing factor in AAV, possibly by increasing the abundance of autoreactive B and T cells that enter the periphery (355). Accordingly, naïve B cells are elevated in circulation in individuals with AAV and are more responsive to BCR stimulation, and autoantigen-specific B and T cells are also present in peripheral blood (351, 352, 356-358). While ANCAs are capable of neutrophil activation on their own, neutrophils primed by pro-inflammatory cytokines or microbial components more readily degranulate upon ANCA binding (230). Its incidence primarily in the elderly individuals might be explained in part by the increase in inflammation associated with aging.

*D) Anti-GBM nephritis: Autoantibody-mediated glomerulonephritis*

Anti-GBM nephritis is the rarest form of glomerulonephritis with an incidence of approximately 1-2 per million people, primarily affecting men and women in their late twenties or between 65-75 years (359, 360). It follows a rapidly progressive disease course (RPGN) resulting in crescent formation. Anti-GBM nephritis is caused by autoantibodies that target α3(IV)NC1 within the collagenous layer of the GBM (170, 361). Autoantibodies against secondary antigens in type IV collagen and laminin can also participate in pathogenesis (362). Complement fixation leads to the release of anaphylatoxins that recruit neutrophils and macrophages (363). Their production of reactive oxygen species facilitates a rapidly progressing necrotizing tissue injury. Subsequently, $T_H1$ and $T_H17$ cells accumulate in the kidney resulting in the further recruitment and activation of macrophages and neutrophils, and $CD8^+$ T cell-mediated cytotoxicity (168, 364). As was the case in ANCA glomerulonephritis, T cell engagement can be autoantigen-driven or through bystander resident T cell activation (364). Anti-GBM antibodies can also target the alveolar basement membrane, leading to concomitant pulmonary inflammation and injury in 40-60% of cases (365). Disease with both renal and pulmonary manifestations is referred to as Goodpasture syndrome.

Loss of tolerance to α3(IV)NC1 is the primary underlying cause of anti-GBM nephritis. This is attributed to the predisposing *HLA-DRB1**15 (HLA-DR15) allele (171). Normally, α3(IV)NC1 expression in the thymus results in the deletion of α3(IV)NC1-reactive T cells and promotes the generation of α3(IV)NC1-specific $T_{REG}$ cells that provide dominant protection from disease (see *Chapter 1.2.1*). The presentation of the immunodominant α3(IV)NC1 peptide by HLA-DR15 permits the development of autoreactive $T_{CONV}$ cells that can drive kidney pathology (168). Autoreactive $T_{FH}$ cells are likely instrumental in the generation of the anti-GBM antibody that will initiate injury. *HLA-DRB1**15 is not exclusively associated with anti-GBM nephritis (e.g., MS) and is prevalent especially in the healthy European population and is therefore insufficient to drive disease. Prior pulmonary injury due to infection or smoking has been associated with the development of anti-GBM nephritis (366-368).

Notably, approximately 30% of individuals with anti-GBM nephritis also have ANCAs, denoting a shared etiology (369). Moreover, a polymorphism in *COL4A3* which encodes α3(IV)NC1 promotes anti-GBM formation in a familial form of the disease (170).

*E) $T_{REG}$ cells in RPGN*

Defects in $T_{REG}$ cell numbers is associated with all forms of glomerulonephritis (199). However, the cause of this defect is ill-defined. In mouse models of RPGN, $T_{REG}$ cells are essential at preventing the break in tolerance prior to the onset of disease and in limiting the $T_H1$ and $T_H17$ cell responses responsible for perpetuating kidney injury (370, 371). For the latter, $T_{REG}$ cell adoption of a $T_H1$-like or $T_H17$-like phenotype by gaining expression of the lineage-defining transcription factors T-bet and STAT3, respectively, is essential for their suppressive function (155, 372). In doing so, $T_{REG}$ cells acquire chemokine receptors (e.g., CXCR3 and CCR6) that promote their localization to renal $T_H1$ and $T_H17$ cells, to provide direct suppression. Nevertheless, glomerular injury in RPGN is associated with the release of highly pro-inflammatory cytokines that may destabilize $T_{REG}$ cell suppressive, as was outlined in *Chapter 1.2.1*. Amongst these are TNF-α and IL-6 from infiltrating myeloid cells, and IL-1 released by necrotic epithelial and endothelial cells, all of which are known to dysregulate the $T_{REG}$ cell phenotype (209, 210, 212, 215, 373). *Whether this contributes to the $T_{REG}$ defect in glomerulonephritis is currently unknown (investigated in Chapter 5)*.

### *1.3.4 Non-inflammatory glomerulopathies: Idiopathic nephrotic syndrome*

The etiology of non-inflammatory autoimmune kidney diseases are largely unknown, however, autoantibodies are predicted to underly disease pathogenesis (4). Podocyte foot process effacement results in nephrotic syndrome characterized by nephrotic-range proteinuria, hypoalbuminemia, and dyslipidemia (313). The most debilitating feature of disease is generalized edema, especially around the legs and eyes, caused by the reduction in serum albumin. Non-inflammatory podocytopathies are chronic, follow a relapsing-remitting course, and are primarily idiopathic, though they can arise secondary to other systemic autoimmune diseases (e.g., SLE) and cancer. Hence, non-inflammatory

glomerulopathies are collectively termed idiopathic nephrotic syndrome (INS). Despite their idiopathic etiology, BCDT with RTX is effective at mediating remission, denoting a clear B cell dependence (178).

INS is categorized histopathologically, though, with recent discoveries, a more immunological categorization is emerging (4). Membranous nephropathy (MN), one of three histopathological variants, is characterized by the thickening of the GBM (hence 'membranous'), glomerular sclerosis, and fibrosis by light microscopy. Under electron microscopy, podocyte foot process effacement alongside electron-dense regions between the GBM and podocyte (subepithelial) associated with antibody deposition are observed. Next, focal segmental glomerulosclerosis (FSGS) is characterized by varying degrees of sclerosis ('segmental') of some glomeruli ('focal') under light microscopy and podocyte foot process effacement by electron microscopy. Finally, minimal change disease (MCD) is solely characterized by podocyte foot process effacement ('minimal change'). Of the three INS manifestations, only MN has an established autoimmune origin, which will be reviewed below. In contrast, an autoimmune etiology of FSGS and MCD has long been predicted but remains controversial; these will be discussed in *Chapter 1.3.5*.

*A) Membranous nephropathy: Subepithelial autoantibody glomerulonephritis*

MN is the second most common cause of INS in adults representing about 30% of cases (374). Approximately 10-20% of affected individuals will progress to ESKD while one-third will spontaneously remit (375). It is defined by the binding of autoantibodies to podocytes in the subepithelial compartment of the filtration barrier. Numerous autoantigenic targets have been discovered since 2009: the M-type phospholipase $A_2$ receptor 1 ($PLA_2R1$; ~75% of cases), neural epidermal growth factor-like 1 (NELL1; ~15%), thrombospondin type 1 domain-containing 7A (THSD7A; 1-5%), amongst various others (376). Autoantibodies directed towards these antigens are predominantly of the IgG4 subclass, and therefore are inefficient activators of complement and do not bind activating Fcγ receptors (377). Their binding to the podocyte is thought to primarily trigger cytoskeletal defects that impair its anchoring to the GBM and disrupt the slit diaphragm (378-380).

Nevertheless, complement activation is observed in MN, with membrane attack complex formation leading to the production of reactive oxygen species and thromboxanes, ultimately destabilizing podocyte structure (381). Injured podocytes retract their foot processes and increase deposition of both type IV collagen and laminin leading to podocyte foot process effacement and GBM thickening. Immunostaining of kidney biopsies in MN show a characteristic granular IgG pattern along the filtration barrier and C3 deposition.

The etiology of MN is not well understood, but loss of tolerance to podocyte autoantigen is the initiating factor. Several polymorphisms have been associated with MN especially within the HLA-II locus but also in *PLA2R1* (382-384). *HLA-DQA1**05:01 and *HLA-DRB1**03:01 are strongly predisposing alleles, and *HLA-DRB1**15:01 is associated with risk specifically in East Asian populations, though their involvement in pathogenesis is not clear (171). An immunoregulatory defect is also proposed to play a role in disease pathogenesis, as frequencies of circulating $T_{REG}$ cells tend to be reduced (385, 386). Supporting this, MN can develop secondary to IPEX syndrome (387-389). Moreover, frequencies of $PLA_2R$-specific plasmablasts and MBCs are elevated, highlighting the humoral autoimmune etiology of the disease (386). Autoantibodies often develop years before disease onset and their isotype-switching to IgG4 is thought to be associated with chronic antigen exposure (390). The success of RTX at mediating remission, the abundance of circulating plasmablasts, and chronicity of antigen exposure may denote the involvement of an extrafollicular B cell response and an SLPC origin for pathogenic autoantibodies (391-393). Accordingly, there are increased frequencies of circulating IL-$21^+$ $T_{FH}$ cells in MN and their proportions correlate with the degree of proteinuria (394, 395). Nevertheless, a detailed phenotypic and molecular characterization of peripheral blood immune cells during active MN remains lacking, hence the nature of the B cell response giving rise to autoantibodies remains unknown.

### *1.3.5 MCD and FSGS: Glomerulopathies of unknown etiology*

INS is the most common chronic glomerular disorder of childhood, with an incidence of 1.4-6.1/100,000 children and a 3:2 male-to-female preponderance (10, 313). About 85% of

childhood INS is caused by MCD with the remaining cases manifesting largely as FSGS. This is in contrast to adult INS, where FSGS is the most frequent histopathological finding (50% of cases), followed by MN (30%), and MCD (20%) (374). Childhood INS responds strongly to treatment with GCs, with 90% of affected children achieving remission (steroid-sensitive nephrotic syndrome, SSNS) (313). The remaining are said to be steroid-resistant (SRNS) and often present with FSGS. Of the responding individuals, 60-90% will relapse with 55-60% relapsing four or more times a year. With frequent relapses, repetitive treatment with GCs is warranted and often results in significant side-effects. *As such, identifying GC-sparing treatment alternatives is a priority for the treatment of childhood INS* (396).

*A) MCD and FSGS are a spectrum of podocytopathy*

Despite their distinct histopathological features, ample evidence suggests that MCD and FSGS describe a continuum of disease (397, 398). In a seminal 1985 study, researchers obtained biopsies from 48 children with frequently relapsing SSNS shortly following disease onset, all of which showed MCD. Five years after, a second biopsy was obtained from 33 of the children, 15 of which showed progression to FSGS (399). This was also associated with a shift from GC sensitivity to resistance. The progression from MCD to FSGS strongly denotes a continuity in INS manifestations and is further supported by the older age of onset for childhood FSGS in comparison to MCD (400). Another piece of evidence comes from the recurrence of FSGS following transplantation. While childhood INS rarely progresses to ESKD, FSGS can eventually require a kidney transplant. In these cases, FSGS will recur in approximately 45% of recipients where it is preceded by a period of steroid-resistant nephrotic-range proteinuria with characteristic MCD histology (401, 402). This finding also suggests the presence of a circulating factor that induces podocyte injury in INS. Indeed, prophylactic plasma exchange can improve the chance of sustained remission following transplantation (403).

A mechanistic understanding of the transition from MCD to FSGS is lacking, at least in part due to the inaccessibility of kidney tissue from childhood INS. Indeed, biopsies are rarely performed in children with SSNS due to their minimal therapeutic value. Nevertheless,

a progression from foot process effacement in MCD to the eventual detachment of podocytes from the GBM and their replacement with sclerotic scars in FSGS is supported by mouse models (398). Transgenic mice with podocyte-specific doxycycline-inducible expression of constitutively-active Rac1, a Rho-GTPase involved in regulating the actin cytoskeleton, develop foot process effacement and nephrotic-range proteinuria within five days of doxycycline treatment, highly reminiscent of MCD (398). By one month, there were fewer podocytes in the glomerulus and significant sclerosis, characteristic of FSGS. *Nonetheless, the pathogenesis of MCD and FSGS remains completely unknown*.

*B) Evidence for an autoimmune humoral etiology*

***Autoimmune origin.*** Several features of childhood INS, including its high responsiveness to immunosuppressive treatment, suggest an autoimmune origin. As with most autoimmune disorders, GWAS consistently implicate the HLA-II locus in SSNS, with *HLA-DQA1**02:01, *HLA-DQB1**02:02, and *HLA-DRB1**07:01 all conferring increased risk (404-411). Predisposing polymorphisms in other immune-related genes have also been identified including *TNFSF15*, *CD28*, *MICA*, and *CLEC16A* (410). *Nevertheless, the relevance of these polymorphisms to the pathogenesis of childhood INS is not known (investigated in Chapter 4)*. Moreover, approximately 45% of relapses are associated with upper respiratory tract viral infections, with many others associated with EBV and cytomegalovirus infection/reactivation, skin infections, gastroenteritis, atopic flares, and allergy (412, 413). *The relationship between infections and proteinuric relapses in childhood INS is also unknown*. Finally, immunophenotyping studies consistently show a defect in $T_{REG}$ cell numbers during active disease that is normalized following GC-induced remission, and cases of MCD occurring secondary to IPEX have been reported (414-421).

***B cell origin.*** The finding that BCDT can effectively mediate remission in childhood INS was serendipitous and strongly implicated B cells in INS etiology. A 15-year-old boy with long-standing frequently relapsing SSNS developed ITP that was successfully treated with RTX. Concomitant with ITP remission, proteinuric relapses halted (422). Since this 2004 case, there was a proliferation of reports outlining the utility of RTX in childhood INS,

culminating in a landmark 2014 study demonstrating that B cell depletion with RTX is effective at mediating long-term remission (423). This finding strongly positioned B cells as central contributors to disease pathogenesis. Immunophenotyping studies since demonstrated that active INS is associated with the expansion of isotype-switched cMBCs ($IgD^{-}$ $IgM^{-}$ $CD27^{+}$), and that the resurgence of this population following RTX-mediated B cell depletion is strongly associated with relapse (424-428). *Nevertheless, the pathogenic role of B cells and whether the expansion of MBCs constitutes a bona fide autoreactive B cell response remained unknown (investigated in Chapters 2 and 3).*

*C) Anti-podocyte antibodies in childhood INS*

The implication of B cells in childhood INS strongly suggested the involvement of autoantibodies in the disease process. However, unlike MN where granular podocyte-associated IgG and complement are robust histopathological features, immunostaining for IgG in MCD is weak, though also podocyte-associated, and had historically been dismissed as background (429). Initial studies supported the presence of a circulating podocytopathic factor, since *in vitro* cultured immortalized human podocytes retract their foot process and internalize Nephrin and Podocin when exposed to plasma from affected children (430). Several proposed circulating factors (e.g., suPAR, ANGPTL4, CLCF1) have been proposed, but none were validated as the podocytopathic agent in INS (431). Screening of IgG in plasma fractions on cultured podocytes identified UCHL1 as a potential autoantigen, with anti-UCHL1 autoantibodies being identified in 36% (15/42) of INS children (432). In another study, SDS-PAGE with human podocyte lysates was used to identify Annexin A2 as another autoantigen, with anti-Annexin A2 IgG autoantibodies identified in the serum of 18% (106/596) of INS children (433). Most recently, antibodies against Nephrin were also identified in serum from 22% (9/41) of children and 43% (9/21) of adults with INS (429). The presence of anti-Nephrin autoantibodies were also associated with a shorter time to relapse, and diffuse punctate podocyte-associated IgG1 and IgG2 staining in biopsies. Thus, childhood INS, encompassing the spectrum of MCD and FSGS, is hypothesized to be mediated by anti-podocyte antibodies (APAs). *Nevertheless, the prevalence of APA-*

*mediated disease and whether childhood INS can be subdivided by distinct autoantibody species (as is done in MN) remains to be determined. Additionally, it is not known whether the expansion of MBCs observed in INS is associated with autoantibody production. Finally, it is unclear how RTX may promote long-lasting remission in an autoantibody-mediated disease.*

### 1.4 Rationale, Hypothesis, and Experimental Aims

The expansion of MBCs and the presence of autoantibodies in childhood INS strongly suggest a B cell-mediated autoimmune etiology. However, the efficacy of RTX at mediating long-term remission from proteinuria denotes either that autoantibody-independent functions of B cells might be involved in pathogenesis or that autoantibodies are derived from RTX-sensitive B cells (e.g., SLPC generated from extrafollicular B cell responses). As such, *we hypothesized that childhood INS is a humoral autoimmune kidney disease mediated by a RTX-sensitive B cell population*. We addressed this hypothesis in three major aims:

**AIM 1:** Provide a molecular characterization of the B cell perturbation in childhood INS.

This will be the focus of *Chapter 2*. Using scRNA-seq and multiparametric flow cytometry, we dissected the identities of the expanded MBCs in childhood INS and implicated the RTX-sensitive extrafollicular B cell response in disease pathogenesis.

**AIM 2:** Assess the clonality of the expanded MBCs in childhood INS.

This will be the focus of *Chapter 3*. Using scRNA-seq pairing gene expression and VDJ sequencing data, we evaluated the clonality of expanded MBC populations in childhood INS and demonstrated that their expansion is antigen-driven and likely dependent on TACI signaling.

**AIM 3:** Evaluate the role of MHC-II haplotype in regulating the production of APAs.

This will be the focus of *Chapter 4*. We used a novel mouse model of APA-mediated nephrotic syndrome with MHC-II distinct mice and demonstrated that the production of podocytopathic APAs is dependent on the mouse background.

Secondly, as was outlined in *Chapter 1*, defects in $T_{REG}$ cells are a common feature of autoimmune diseases including glomerulonephritis. Nevertheless, the underlying causes of the $T_{REG}$ cell defect are not unknown. Acute kidney injury leads to the release of pro-

inflammatory cytokines that are known to modulate the $T_{REG}$ cell phenotype in other tissues (e.g., gut, lungs, skin), including the IL-1 alarmins. As such, *we hypothesized that acute kidney injury destabilizes the $T_{REG}$ cell phenotype locally leading to uncontrolled kidney-targeting T and B cell responses*. We addressed this hypothesis in the following aim:

**AIM 4:** Evaluate the impact of IL-1 alarmins on $T_{REG}$ cell control of kidney-targeting adaptive responses following acute kidney injury.

This will be the focus of *Chapter 5*. Using a common mouse model of RPGN that is mediated by the injection of exogenous anti-GBM antibody, we showed that IL-33 and IL-1 released following kidney injury specifically impeded $T_{REG}$ cell control of kidney-targeting $T_H1$ and B cell responses.

# CHAPTER 2: The extrafollicular B cell response is a hallmark of childhood idiopathic nephrotic syndrome

**The extrafollicular B cell response is a hallmark of childhood idiopathic nephrotic syndrome.**

Tho-Alfakar Al-Aubodah[1,2,3,4,5], Lamine Aoudjit[3,5], Giuseppe Pascale[5,6], Maneka A. Perinpanayagam[7], David Langlais[1,8], Martin Bitzan[6,9], Susan M. Samuel[7], Ciriaco A. Piccirillo[1,2,4]*, Tomoko Takano[3,4,5]*

[1] Department of Microbiology & Immunology, Faculty of Medicine and Health Sciences, McGill University, Montréal, Québec
[2] Infectious Diseases and Immunity in Global Health Program, Research Institute of the McGill University Health Centre, Montréal, Québec
[3] Metabolic Disorders and Complications Program, Research Institute of the McGill University Health Centre, Montréal, Québec
[4] Centre of Excellence in Translational Immunology, Research Institute of the McGill University Health Centre, Montréal, Québec
[5] Division of Nephrology, Faculty of Medicine and Health Sciences, McGill University, Montréal, Québec
[6] Division of Nephrology, Department of Pediatrics, Faculty of Medicine and Health Sciences, McGill University, Montréal, Québec
[7] Section of Nephrology, Department of Pediatrics, Cumming School of Medicine, University of Calgary, Calgary, Alberta
[8] Department of Human Genetics, Faculty of Medicine and Health Sciences, McGill University Genome Centre, Montréal, Québec
[9] Kidney Centre of Excellence, Al Jalila Children's Hospital, and Mohammed Bin Rashid University of Medicine and Health Sciences, Dubai, UAE

*Correspondence should be addressed to:
**Dr. Tomoko Takano, M.D., Ph.D.**
Research Institute of the McGill University Health Centre (RI-MUHC),
Metabolic Disorders and Complications Program, Division of Nephrology
1001 Boulevard Décarie, Bloc E, Room EM1.3244
Montréal, Québec H4A 3J1, Canada
E-mail: tomoko.takano@mcgill.ca

**Dr. Ciriaco A. Piccirillo, Ph.D.**
Research Institute of the McGill University Health Centre (RI-MUHC),
Infectious Diseases and Immunity in Global Health Program
1001 Boulevard Décarie, Bloc E, Room EM2.3248
Montréal, Québec H4A 3J1, Canada
E-mail: ciro.piccirillo@mcgill.ca

Published in *Nature Communications*: *Nat Commun. 2023 Nov 24;14(1): 7682*

## 2.1 Bridging Statement

As discussed in *Chapter 1*, the etiology of childhood INS is currently unknown. However, the recent success of RTX at maintaining long-term remission positioned B cells as likely contributors to pathogenesis (423, 434). Moreover, the consistent observation that MBCs are expanded during active disease and the very recent discovery of APAs in a subset of affected individuals strongly suggest an autoimmune humoral etiology (429, 432, 433, 435). Nevertheless, the characterization of the B cell response beyond the simple enumeration of broad B cell subsets was lacking. In *Chapter 2*, we addressed this gap by performing scRNA-seq on peripheral blood mononuclear cells (PBMC) isolated from children with INS and age- and sex-matched healthy controls, and further validated our findings by multiparametric flow cytometry in a larger cohort. This work represents the first molecular characterization of B cells in childhood INS. In doing so, *we hypothesized that we would identify a phenotypic and transcriptional B cell response signature in active INS that supports the production of autoantibodies yet is sensitive to RTX treatment*.

## 2.2 Abstract

An autoimmune B cell origin for childhood idiopathic nephrotic syndrome (INS) is predicted based on the efficacy of rituximab (RTX) at maintaining long-term remission from proteinuria. Knowledge regarding the nature of the culprit B cell response is very limited. Using single-cell RNA-sequencing, we demonstrate that a B cell transcriptional program poised for effector functions represents the major immune perturbation in the blood of children with active INS. This was conferred by the engagement of an extrafollicular B cell response marked by the expansion of atypical B cells (atBCs), marginal zone-like B cells, and antibody-secreting cells (ASCs). In flow-based analyses of blood from 13 children with active INS and 24 healthy donors, this was reflected by the proliferation of RTX-sensitive extrafollicular ($CXCR5^{-}$) $CD21^{low}$ $T\text{-}bet^{+}$ $CD11c^{+}$ atBCs, and short-lived $T\text{-}bet^{+}$ ASCs. Together, our study provides evidence for an extrafollicular origin for humoral immunity in active INS.

## 2.3 Introduction

Idiopathic nephrotic syndrome (INS), the most common chronic glomerular disorder in children, features recurrent episodes of heavy proteinuria caused by injury to the principal filtering cell of the glomerulus, the podocyte[1,2]. The resulting podocyte lesion is often the sole histopathological manifestation of childhood INS – termed minimal change disease (MCD) – with fewer than 20% of cases presenting as more severe focal segmental glomerulosclerosis (FSGS) [1]. While an immune etiology is predicted given the efficacy of glucocorticoids (GC) and other broadly immunosuppressive drugs at reversing podocyte injury and mediating remission from proteinuria, the precise immune mechanisms involved in INS pathogenesis remain elusive. With frequent relapses, multiple rounds of GCs are warranted resulting in substantial GC-associated toxicity. Hence, a complete understanding of disease pathogenesis is a priority for the development of safe and targeted GC-sparing therapies[3].

The recent identification of rituximab (RTX), a CD20-targeting B cell-depleting monoclonal antibody, as an effective therapeutic option to maintain long-term remission in GC-treated individuals pointed to a previously unrecognized role for B cells in the immunopathogenesis of INS[4-7]. Indeed, several immunophenotyping studies have since demonstrated that elevated levels of circulating B cells is a robust feature of active disease in affected children and adults[8-11]. The expansion of isotype-switched classical memory B cells (cMBCs) and a converse reduction in transitional naïve B cells in the peripheral blood denotes the involvement of a classical follicular B cell response wherein B cells undergo class-switch recombination in germinal centres and generate long-lived antibody-secreting cells (ASCs) [4,11,12]. Accordingly, ASCs are elevated in adults and children with INS and circulating autoantibodies against several podocyte autoantigens have been identified in subpopulations of affected individuals, underlining a *bona fide* autoimmune humoral origin for INS[13-17]. Nevertheless, the exact nature of the nephrotic B cell response remains to be investigated beyond the enumeration of broad B cell subsets.

Although B cell depletion provides long-term remission from proteinuria, many patients will eventually relapse through an unknown mechanism[18,19]. Seminal work

demonstrated that post-RTX relapses of INS were associated with a resurgence of isotype-switched cMBCs, indicating that follicular B cell responses may be responsible for generating autoreactive ASCs[20]. However, B cell depletion with CD20-targeting biologics does not eliminate long-lived bone marrow-residing ASCs as they are devoid of surface CD20[21]. In contrast, short-lived ASCs in the periphery, while also lacking surface CD20, are effectively depleted after RTX therapy as the antigen-experienced B cell pools from which they arise are ablated. The impact of RTX on the ASC compartment in INS has not been investigated.

Unlike long-lived ASCs, short-lived ASCs are generated through extrafollicular B cell responses with lower degrees of class-switch recombination and somatic hypermutation than classical follicular responses[22,23]. Atypical B cells (atBCs), a population of T-bet$^+$ CD11c$^+$ B cells, are now recognized to be an important source for short-lived ASCs[24,25]. This population arises in chronic viral and parasitic infection and is enriched with autoreactive clones in autoimmunity[26-33]. Indeed, upper respiratory tract viral infections can precipitate and exacerbate relapses of INS[34-36]. Therefore, extrafollicular reactions giving rise to RTX-sensitive short-lived ASCs may represent a major source of podocytopathic antibodies in INS.

In this study, we characterize the nature of the nephrotic B cell response by defining an INS-associated B cell transcriptional signature and identifying the contributing pathogenic B cell populations in disease. Through single-cell RNA-sequencing (scRNA-seq) of peripheral blood mononuclear cells (PBMC) derived from four children with active INS and age-matched healthy controls (HC), we demonstrate that the mobilization of memory B cells through an extrafollicular route represents the major immunological abnormality in peripheral blood. Subsequent flow cytometric characterization of B cells in a cohort of 13 children with active INS and 24 HCs shows that this is associated with the expansion of RTX-sensitive CD21$^{low}$ CXCR5$^-$ T-bet$^+$ CD11c$^+$ atBCs and the accumulation of T-bet$^+$ ASCs. Finally, we show that the nascent reengagement of memory B cells in the extrafollicular pathway is associated with post-RTX relapses. In summary, we pinpoint the extrafollicular B cell response as a possible origin for autoreactive ASCs in childhood INS.

## 2.4 Results

### *2.4.1. Perturbation of the B cell transcriptional landscape is the major immunological abnormality in childhood INS.*

Since the transcriptional landscape of immune cells in pediatric INS had not yet been defined, we aimed to characterize the nephrotic immune signature by scRNA-seq. Following doublet and non-viable cell removal in standard, quality control steps (Supplementary Fig. 1a-c), we analyzed the transcriptomes of 69,994 immune cells in PBMC of four children during active INS without known viral infection (INS; 32,139 cells) and four age/sex-matched HCs (Supplementary Data 1). Following integrated clustering, we identified 18 distinct immune cell populations that were uniformly present in all donors (Fig. 1a and Supplementary Fig. 2a, b). Cluster identities were determined by the expression of canonical lineage-defining genes and were subsequently stratified into broad immune cell lineages: B cells (expression of *CD19*, *CD79A*, *CD79B*), $CD4^+$ T cells (*CD3G*, *CD4*), $CD8^+$ T cells (*CD3G*, *CD8*), double negative T cells (*CD3G* and lacking *CD4* and *CD8*), NKT cells *(CD3G*, *KLRB1*, *KLRG1*), NK cells (*ZBTB16*, *NKG7*, *GNLY*), monocytes/dendritic cells (*CD14* or *FCGR3A*), and plasmacytoid dendritic cells (*LILRA4*) (Fig. 1a and Supplementary Fig. 2c, d). Notably, the only lineage that was preferentially expanded in children with INS was the B cell lineage (Fig. 1b). Specifically, memory B cell-containing clusters C11, C12, and C13, which contained antibody-secreting cells (ASC), accumulated in INS indicating the induction of a humoral response (Supplementary Fig. 2b). A cluster of NK cells relating to $CD16^{dim}$ (C9) was the only other cluster expanded in INS.

To identify a transcriptional profile associated with INS, we performed pseudobulk differential gene expression analysis between INS and HC children for each broad immune cell lineage [37]. Through this pseudobulk approach, cells were aggregated at the level of the donor and broad immune cell lineages to account for biological replication. We identified 1,976 genes that were differentially expressed ($|\log_2 FC| > 0.65$, $P_{adj} < 0.05$) in at least one lineage and present in at least 10% of cells of that lineage (Fig. 1c, Supplementary Fig. 2e, and Supplementary Data 2). The largest transcriptional differences were amongst B cells encompassing 958 genes, 642 of which were upregulated in INS (Fig. 1c, d and

Supplementary Fig. 2e). We defined the nephrotic B cell signature as these 642 upregulated genes (Fig. 1d, Supplementary Data 2). Thus, perturbations in the B cell transcriptional landscape represents the major immune abnormality in the blood during active childhood INS.

### *2.4.2. B cells in INS are poised for acquisition of effector functions and ASC differentiation.*

Pathogenic B cells possess both antibody-dependent and -independent functions that can trigger and drive autoimmunity[21]. To assess the functional properties of B cells in INS, we performed pathway analysis in the nephrotic B cell signature and found a substantial enrichment of terms associated with the engagement of humoral immunity (Fig. 1e). INS B cells had elevated expression of genes encoding components of B cell receptor (BCR) signaling including the tyrosine kinases *SYK* and *BTK*, adaptors *BLNK*, *BANK1*, and *LAT2*, and the co-receptor *CD19* denoting an activated status (Fig. 1f). This activated phenotype was further supported by the increased expression of activation-associated genes like the APRIL/BAFF receptor TACI (*TNFRSF13B*), the memory marker *CD27*, and both chains of the activating integrin VLA-4 (*ITGA4*, *ITGB1*) (Fig. 1f). Moreover, the transcriptional landscape of INS B cells revealed the acquisition of key effector functions including immunoglobulin production as evidenced by the elevated expression of several variable heavy and light chain genes, *IGHG1*, *IGHG3*, *IGHA2*, and *IGHA1* (Fig. 1f). The molecular chaperone *MZB1* that mediates IgM and IgA secretion in marginal zone (MZ) B cells, B-1 cells, and ASCs was particularly enriched in INS B cells (Fig. 1f). Oxidative phosphorylation (OXPHOS) and fatty acid oxidation (FAO) pathways were also elevated in INS B cells consistent with a metabolic program essential for ASC development and antibody generation (Fig. 1e, f) [38,39]. Beyond antibody generation, INS B cells upregulated the expression of genes involved in antigen presentation, including *HLA-DPA1* and *HLA-DOB*, the cathepsin *CTSS*, and the lipid antigen presenter *CD1C* (Fig. 1e, f). We also observed an enrichment of genes involved in actin cytoskeleton dynamics including the Arp2/3 complex (*APRC1B*, *ARPC5*), actin nucleation factors (*WAS*), polymerization factors (*EVL*, *VASP*), and capping proteins (*CAPG*, *CAPZB*)

highlighting increased B cell motility in INS (Fig. 1e, f)[40]. This enrichment of BCR signaling, B cell activation, antigen presentation, actin polymerization, and fatty acid oxidation pathways in INS B cells was also observed by gene set enrichment analysis (GSEA) (Supplementary Fig. 3a).

Next, we sought to identify the putative transcriptional drivers of the nephrotic B cell signature using the web-based transcription factor enrichment analysis tool ChIP-X Enrichment Analysis 3 (ChEA3)[41]. Transcriptional targets for PU.1 (*SPI1*), SPI-B (*SPIB*), and OCT-2 (*POU2F2*), key transcription factors coordinating B cell activation and functionalization, were enriched in INS B cells (Fig. 1g and Supplementary Data 4)[42]. Consistently, the genes encoding these transcription factors were themselves upregulated (Fig. 1f). Collectively, these data underline that B cells in INS are activated and can exert potentially pathogenic effector functions.

We also observed possible transcriptional regulation by the speckled protein (SP) chromatin readers SP140, SP110, and SP140L, the expression of which were also strongly elevated in INS B cells (Fig. 1g, h). These transcription factors were recently implicated in antiviral type-I interferon (IFN) responses, though their function in B cells remain undefined[43,44]. Interestingly, we identified a type-I IFN signature in INS B cells conferred by genes downstream IFN-β signaling (e.g., *IFNAR2*, *OAS1*, *AIM2*, *IFITM2*, *IFITM3*, *XAF1*, *PYHIN1*, *MNDA*, *CAPN2*, *IKBKE*) (Fig. 1i and Supplementary Fig. 3b). Most of these genes were expressed in less than 10% of B cells and were thus not included in the nephrotic B cell signature. Nevertheless, these results indicate that type-I IFN signaling, a common driver of antiviral immunity and autoimmunity, may underline the generation of the nephrotic B cell response.

### *2.4.3. Childhood INS is characterized by the expansion of extrafollicular B cell populations.*

Having demonstrated the increased activation and functionality of B cells in children with active INS, we sought to identify the pathogenic cell subsets underlying the nephrotic B cell response. Integrated subclustering of the B cell lineage identified ten distinct

subpopulations corresponding with naïve B cells (*BACH2*-expressing subclusters B0, B4, and B7), memory B cells (*BCL2A1*-expressing subclusters B1, B2, B3, B5, and B6), and ASCs (*PRDM1*-expressing subclusters B8 and B9) (Fig. 2a, b, Supplementary Fig. 4a and Supplementary Data 5). The naïve clusters included transitional naïve B cells defined by *IGHM*, *NEIL1*, *HRK*, and *TCL1A* expression (subcluster B4), and mature naïve B cells defined by *IGHM*, *FCER2*, and *IL4R* expression (subclusters B0 and B7) (Fig. 2b and Supplementary Fig. 4b). Subcluster B0, representing the largest naïve B cell subcluster in all children, was significantly reduced in INS while two memory (B3 and B6) and all ASC subclusters (B8 and B9) were increased indicating elevated antigen-experience in INS (Fig. 2c).

To define the memory B cell subclusters, we performed differential gene expression analysis between each memory B cell subcluster identified (Fig. 2d). Cells in subcluster B1 expressed genes associated with activation (*CD69*, *FOS*, and *FOSB*) and IgM and IgD synthesis (*IGHM* and *IGHD*) denoting an isotype-unswitched phenotype and were accordingly termed activated memory B cells (actMBC) (Fig. 2d). Cells in the dominant, INS-associated subcluster B3 were also isotype-unswitched and expressed genes associated with extrafollicular MZ B cells (*CD1C*, *CD24, PLD4*)[45,46], they were thus termed MZ-like B cells (Fig. 2d). Consistent with an extrafollicular phenotype, MZ-like B cells also preferentially expressed *TNFRSF13B* (TACI), the APRIL/BAFF receptor that drives extrafollicular ASC generation[22], and *GPR183* (EBI2), the G protein-coupled receptor that orchestrates extrafollicular reactions by homing B cells to extrafollicular foci[47]. Cells in subcluster B5 corresponded with isotype-switched memory (SM) B cells as they lacked *IGHM* and *IGHD* expression and instead expressed *IGHG1*, *IGHA1*, and *IGHA2* (Fig. 2d). Both the MZ-like B cell and SM subpopulations exhibited a transcriptional profile consistent with memory B cells including *ANXA2*, *S100A10*, and *S100A4*. Subcluster B2, termed MBC-2, was similar to MZ-like and SM B cell subpopulations, albeit the extent of the memory B cell phenotype was diminished (Fig. 2d). Finally, the second INS-associated subcluster B6 corresponded with atBCs, a B cell population that participates in extrafollicular B cell responses arising in autoimmune and chronic viral infection settings[27,28,33]. Genes characteristic of atBCs were enriched in this subcluster including *FCRL5*, *FCLRA*, *FCRL2*, *ITGB2*, *ITGB7*, *ITGAX* (CD11c),

*FGR*, *ZEB2*, *NR4A2, ZBTB32*, and high *CD19* expression (Fig. 2d and Supplementary Fig. 4c). Of the immunoglobulin heavy chain genes, atBCs preferentially expressed *IGHD* and *IGHM* denoting reduced class-switching thereby supporting an extrafollicular origin (Fig. 2d). Interestingly, the two subclusters expanded in INS, namely MZ-like B cells and atBCs, preferentially expressed *POU2F2*, one of the putative transcriptional drivers of the nephrotic B cell signature (Fig. 2d).

Pseudobulk differential gene expression analysis showed significant upregulation of genes in all the B cell subclusters in INS, except for atBCs and ASCs (Fig. 2e and Supplementary Fig. 5a). Pathway analysis revealed an enrichment of functions associated with actin cytoskeletal dynamics in all B cell subclusters in INS, while some subclusters (Naïve-1, actMBCs, MBC-2, and MZ-like B cells) also showed an enrichment of B cell activation pathways (Supplementary Fig. 5b). The antigen-inexperienced and recently activated B cell subsets (Naïve-1 and actMBC) showed the greatest differences in gene expression suggesting that the transcriptional events leading to B cell dysregulation occur early during B cell activation (Fig. 2e and Supplementary Fig. 5a). There was a substantial overlap in the upregulated genes between Naïve-1 B cells, actMBCs, MBC-2, and MZ-like B cells including many atBC-associated genes (e.g., *ITGB2*, *ITGB7*, *FCRLA*, *FCRL2*), *POU2F2*, *POU2AF1*, and the extrafollicular response genes *TNFRSF13B* and *GPR183*, suggesting a possible developmental sequence or cooperation between these B cell subclusters in generating an extrafollicular B cell response in INS (Fig. 2e).

We sought to better identify relationships between the B cell subclusters by performing trajectory inference using Monocle3, a computational method that orders cells along a pseudotemporal trajectory informed by changes in gene expression to make inferences about cell development[48]. To this end, ASCs were removed from analysis and the remaining B cells were re-clustered before selecting the transitional naïve B cell cluster as the starting point for calculating pseudotime (Fig. 2f). SM B cells and atBCs formed the termini of two independent branches (II and III) that arose from a common branching point in the MBC-2 subcluster. Branch III was comprised of the INS-expanded MZ-like B cells and atBCs suggesting an origin for atBCs in MZ-like B cells, consistent with a recent study on

atBCs from malaria-infected adults[27]. As both atBCs and MZ-like B cells are extrafollicular B cell populations, trajectory III likely represents an extrafollicular developmental pathway for B cells. Indeed, the expression of both *TNFRSF13B* and *GPR183* was higher in trajectory III than trajectory II, with *TNFRSF13B* being only expressed in B cells from INS children (Fig. 2f).

Monocyte-derived dendritic cells within secondary lymphoid organs are established sources of TACI ligands (APRIL and BAFF) during extrafollicular B cell responses[49,50]. To identify potential sources of these TACI ligands in PBMC of INS children, we evaluated the APRIL and BAFF signaling networks by CellChatDB[51]. The APRIL signaling network consisting of APRIL (*TNFSF13*), TACI (*TNFRSF13B*), and BCMA (*TNFRSF17*) was specifically enriched in PBMC from INS children, with monocytes and dendritic cells being the predominant sources of APRIL (Fig. 2g, h). Accordingly, both ASC subclusters (subcluster B8 and B9) were identified as the predominant receivers of APRIL signal (Fig. 2g), and both were highly expanded in INS children blood (Fig. 2a, c). Collectively, these data demonstrate that memory B cells in childhood INS are engaged through an extrafollicular pathway with a capacity to generate ASCs.

### *2.4.4. Proliferating T-bet$^+$ atBCs and ASCs are a hallmark of active INS.*

The rapid extrafollicular expansion of ASCs was only recently recognized as a salient feature of antiviral immunity and has since been linked to multiple autoimmune conditions[25,27-29,31,52]. Since we identified a pronounced extrafollicular mobilization of memory B cells in INS, we sought to confirm the presence of extrafollicular B cells using the most up-to-date flow cytometric definitions for these cells in the peripheral blood of 13 children with active INS and 24 age-matched HCs. Total CD19$^+$ B cell frequencies did not differ between HC and INS children (Supplementary Fig. 6a). Following unsupervised high-dimensional clustering of B cells, we generated 14 distinct B cell metaclusters (M0-M13) present in HC and INS children (Fig. 3a, b). The metaclusters were broadly categorized into naïve (CD27$^-$CD21$^+$IgM$^+$IgD$^+$), classical memory (cMBC: CD27$^+$CD21$^+$CD20$^+$), CD21$^{low}$ memory (CD27$^{+/-}$CD21$^{low}$CD20$^+$CD38$^{-/low}$), and ASC (CD20$^-$) populations (Fig. 3b). INS children had lower frequencies of the largest naïve B cell metacluster (M0) and an expansion

of an isotype-switched ($IgM^-$ $IgD^-$) cMBC metacluster (M9), consistent with previous reports[4,10,53]. However, most of the metaclusters that were expanded in INS corresponded with isotype-switched $CD21^{low}$ memory B cells (M7, M11) and both isotype-unswitched (M13) and switched (M8, M12) $CD38^{high}$ ASCs (Fig. 3c-e). The INS-expanded $CD21^{low}$ metacluster M11 and all ASC metaclusters (M8, M12, M13) were Ki-$67^+$ denoting active cycling, and the proportions of Ki-$67^+$ B cells were significantly greater in INS compared to HC (Fig. 3d, e). Moreover, both INS-expanded $CD21^{low}$ populations had diminished levels of CXCR5, the key chemokine receptor orchestrating germinal centre responses, denoting an extrafollicular origin for these B cells (Fig. 3d, e). In contrast, the INS-expanded isotype-switched cMBC metacluster was $CXCR5^{high}$ Ki-$67^-$ denoting a follicular origin (Fig. 3d, e).

The expansion of $CD21^{low}$ B cells is an established feature of B cell dysregulation and frequently relates with atBC responses in autoimmunity and viral infections[31,54-57]. We sought to determine whether the expansion of $CD21^{low}$ B cells in INS correlated with the increased frequency of atBCs identified by scRNA-seq. T-$bet^+$ $CD11c^+$ B cells, one of the most widely accepted phenotypes for atBCs[30,32,58], were almost exclusively present within the $CD21^{low}$ B cell ($CD27^{+/-}CD21^{low}CD20^+CD38^{-/low}$) compartment representing approximately 40% of the cells (Fig. 4a). Accordingly, frequencies of T-$bet^+$ $CD11c^+$ B cells strongly correlated with frequencies of $CD21^{low}$ B cells (Fig. 4a). Indeed, atBCs (T-$bet^+$ $CD11c^+$ $CD27^{+/-}$ $CD21^{low}$ $CD20^+$ $CD38^{-/low}$), and more specifically the isotype-switched atBCs, were significantly expanded in INS (Fig. 4b). In line with previous reports and our scRNA-seq data, these atBCs expressed higher levels of CD19 than cMBCs (Supplementary Fig. 6b). Thus, the accumulation of $CD21^{low}$ B cells in INS corresponds with an expansion of atBCs. $IgD^-$ $CD27^-$ double negative (DN) B cells, another common definition for atBCs [24,25], were also increased in INS (Supplementary Fig. 6c).

To identify differences in INS and HC atBCs, we compared the expression of T-bet, a key driver of the atBC transcriptional program essential for their conversion into ASCs, and FcRL5, an inhibitory receptor that restricts BCR signaling[59]. atBCs in INS expressed higher levels of T-bet and lower levels of FcRL5 indicating a stronger tendency to develop into ASCs (Fig. 4c, d). Consistently, ASCs ($CD20^-$ $CD10^-$ $CD38^{high}$) were greatly expanded in INS, with a

greater proportion accumulating as isotype non-switched ASCs suggesting an extrafollicular origin (Fig. 4e). As with atBCs, ASCs from INS children had greater T-bet expression and were largely lacking FcRL5 (Fig. 4f, g). In summary, the expansion of isotype-switched atBCs and T-bet$^+$ ASCs in active INS positions the extrafollicular B cell response as a hallmark of active disease.

### *2.4.5. RTX effectively ablates INS-associated B cell populations.*

While relapses are effectively controlled using GCs, a more enduring remission state is achieved with subsequent RTX therapy despite the eventual resurgence of peripheral B cells[6]. As such, we aimed to compare the impact of GC alone and GC/RTX combination therapy on the INS-associated B cell populations (Fig. 5a, Supplementary Table 1 and Supplementary Data 1). We first compared B cell numbers in the blood of actively relapsing individuals (INS) to those in GC-induced remission (Rem-GC) and remission maintained by RTX (Rem-RTX). Treatment with GC strongly decreased peripheral ASC numbers with no major impact on earlier B cell subpopulations indicating a limited effect of GCs on the INS-associated B cell response (Fig. 5b-e). In contrast, children maintained in remission with RTX had lower total B cell numbers than RTX-inexperienced individuals, suggesting incomplete B cell recovery at the time of sampling post-RTX (Fig. 5c). At this time point, children had reconstituted the transitional naïve B cell compartment, but cMBCs, atBCs, and ASCs remained sparse in peripheral blood (Fig. 5b, d, e). Hence, while GC treatment was effective at restricting ASC abundance in the blood, a more extensive B cell deficiency that eliminated all INS-associated B cell populations was achieved with subsequent RTX administration.

Next, we aimed to evaluate the changes in the B cell compartment in relapses following remission maintained by RTX. B cell numbers were still largely suppressed in patients in post-RTX relapse (Supplementary Fig. 7a-c). Thus, we predicted that changes in B cell subset composition rather than total cell numbers may differentiate between post-RTX remission (Rem-RTX) and relapse (Rel-RTX). While frequencies of total B cells in PBMC were similar in both groups (Fig. 5f), those who relapsed had fewer proportions of transitional naïve B cells (confirmed in 3/5 longitudinal samples) and higher proportions of both isotype-

unswitched and switched cMBC (confirmed in 5/5 longitudinal samples), confirming an earlier finding that the resurgence of isotype-switched cMBCs is associated with post-RTX relapses of INS (Fig. 5b, g, h)[20]. Surprisingly, we did not observe any differences in atBC and ASC frequencies in post-RTX remission and relapse (Fig. 5b, h).

### *2.4.6. The nascent resurgence of MZ-like B cells is associated with post-RTX relapse.*

Given that the B cell compartment in post-RTX relapses was still largely skewed towards antigen-inexperienced populations, we hypothesized that this represented an early time point in the generation of the nephrotic B cell response. To investigate this, we performed scRNA-seq on peripheral B cells isolated from four of the children from whom we were able to obtain both relapse and remission samples following RTX treatment (Supplementary Data 1). Following integrated clustering, we obtained 12 clusters most of which represented antigen-inexperienced cells as is evidenced by *BACH2* expression (Fig. 6a, b, Supplementary Fig. 8a). Three clusters (clusters R4, R9, R10) expressed *BCL2A1* and corresponded to MZ-like B cells, SM B cells, and atBC subpopulations (Fig. 6a, b, Supplementary Fig. 8a). Only MZ-like B cells (cluster R4), the predominant B cell subset associated with active INS, were expanded in all relapsing individuals supporting an early resurgence of the nephrotic B cell response (Fig. 6c). Accordingly, the MZ-like B cell signature (3/4 children), and to a lesser extent the atBC signature (2/4 children), was enriched in B cells during post-RTX relapse (Fig. 6d, Supplementary Fig. 8b). This expansion of MZ-like B cells reflects a nascent resurgence of the extrafollicular B cell response in post-RTX relapse.

Finally, we sought to evaluate the similarity between this nascent extrafollicular response, and the B cell responses observed in active INS. Pseudobulk differential gene expression analysis did not yield significant results, likely due to the overwhelmingly naïve B cell landscape in the post-RTX setting. As such, we proceeded with a non-pseudobulk approach comparing gene expression in all memory B cells (clusters R4, R9, and R10) between relapse and remission timepoints. We identified small differences in gene expression represented by $\log_2$FC magnitudes of less than 0.2 (Fig. 6e, Supplementary Data 6). The most enriched genes ($|\log_2 FC| > 0.1$, $P_{adj} < 0.01$) in post-RTX relapse memory B cells

were present within the nephrotic B cell signature (Fig. 6f). These included genes associated with MZ-like B cells and atBCs (*POU2F2*, *CD19*, *PPP1R14A*, *COTL1*, *LY6E*, and *RGS2*), as well as genes involved in the type-I IFN response (Fig. 6f). Consistently, the response to IFN-β signaling GO term was highly enriched in post-RTX relapse memory B cells (Supplementary Fig. 8c). Similar findings were observed in the naïve compartment (clusters R0, R1, R2, R3, R5, R6, R7, and R8) during post-RTX relapse (Supplementary Fig. 9a). Here, there was an enrichment of GO terms associated with B cell activation and type-I IFN signaling (Supplementary Fig. 9b). These results support the early re-establishment of the extrafollicular nephrotic B cell response during post-RTX relapse.

## 2.5 Discussion

A B cell origin for the pathogenesis of childhood INS is supported by the efficacy of B cell-depleting biologics like RTX at maintaining long-term remission from proteinuria. Nevertheless, the precise nature of the pathogenic B cell response has thus far remained elusive. In this study, we used scRNA-seq and multi-parametric flow cytometry to identify, for the first time, a dysregulated B cell response and transcriptional signature associated with active INS. This signature was conferred by the expansion of $CD21^{low}$ $CXCR5^{-}$ $CD11c^{+}$ T-$bet^{+}$ atBCs – a B cell population that is associated with extrafollicular responses in chronic viral infection and systemic autoimmunity – and T-$bet^{+}$ ASCs. Moreover, we demonstrated that distinct immunosuppressive treatment strategies, namely GC and RTX, differentially targeted these INS-associated B cell populations with RTX providing more extensive coverage. Together, our study has uncovered a novel and prominent involvement of an extrafollicular B cell response in pediatric INS.

Using scRNA-seq on total PBMC isolated from INS and HC children, we showed that perturbations in the B cell compartment represented the major immunological abnormality in pediatric INS. In comparison to healthy B cells, INS B cells upregulated genes involved in BCR signaling, antibody production, antigen presentation, oxidative phosphorylation/fatty acid oxidation, and actin cytoskeleton dynamics. This transcriptional signature was likely endowed by PU.1 (*SPI1*), SPI-B (*SPIB*), OCT-2 (*POU2F2*), and OBF-1 (*POU2AF1*), transcription factors that coordinate the expression of multiple BCR signal transducers and receptors enabling B-T cell communication, and thereby take a central position in B cell acquisition of effector functions[42]. This data represents the first transcriptional signature of B cells in INS and indicates that B cells are receiving an activating signal and acquiring effector functions during active disease. The nephrotic signature was present in all four children with active INS despite participants being in very different stages of active disease (first episode before therapy, relapse before therapy, relapse on therapy) possibly denoting a uniform mechanism for B cell engagement at the time of active disease.

By further stratifying the B cell compartment into distinct subpopulations, we observed that INS patients had a reduction in naïve B cells and an expansion in MZ-like B

cells, atBCs, and ASCs. MZ-like B cells represented an isotype-unswitched memory B cell subset that was almost exclusively present in INS children, and expressed genes associated with MZ B cells (*IGHM*, *IGHD*, *CD24*, *CD1C*, *PLD4*), an extrafollicular B cell population that largely resides in the spleen giving rise to IgM-secreting ASCs in a T cell-independent manner[60,61]. The atBCs expanded in INS were equivalent to those recently identified in people with viral or parasitic infections (malaria, HIV, SARS-CoV-2), autoimmunity (SLE, rheumatoid arthritis, and multiple sclerosis), and immunodeficiencies (CVID, partial RAG deficiency) [25,27,28,31-33]. Recent reports demonstrate that this population is involved in extrafollicular B cell responses acting as an important source for short-lived ASCs. Thus, the expansion of both MZ-like B cells and atBCs is strongly indicative of an active, extrafollicular B cell response during active INS. We confirmed the expansion of atBCs by flow cytometry (T-bet$^{+}$ CD11c$^{+}$ CXCR5$^{-}$ CD27$^{+/-}$ CD21$^{low}$ CD20$^{+}$ CD38$^{-/low}$) in 13 children with active INS. A recent report characterizing circulating B cells in patients with GC-sensitive INS by cytometry by time-of-flight (CyTOF) also showed an expansion of a CD11c$^{+}$ T-bet$^{+}$ B cell population, though this population was not discussed by the authors[62]. Moreover, as both MZ-like B cell and atBC populations harbour autoreactive clones[61], the expansion of these populations highlights the potential for autoreactivity through the extrafollicular pathway in pediatric INS. Of note, trajectory inference predicted that MZ-like B cells may act as precursors for atBCs, consistent with a recent report in malaria-infected adults[27]. To investigate this relationship between MZ-like B cells and atBCs, future work should decipher individual B cell clonotypes operating in active INS.

Extrafollicular responses do not undergo the same degree of class-switch recombination and somatic hypermutation as germinal centre-dependent follicular responses resulting in the rapid generation of IgM-secreting short-lived ASCs[22]. T-bet, a transcription factor that promotes conversion into ASCs[63], was more strongly expressed in INS atBCs than atBCs from healthy children, thus further supporting their participation in antibody-producing responses. Accordingly, we also observed a strong expansion of actively cycling T-bet$^{+}$ ASCs in INS. Unlike ASCs in HC, INS-associated ASCs were skewed towards an unswitched phenotype (IgM$^{+}$ IgD$^{+}$) consistent with an extrafollicular origin. Both atBCs

and ASCs also showed lower expression of FcRL5, a receptor with ITIM domains that restricts BCR signaling[59], in INS children than HC suggesting a possible mechanism for the dysregulated activation of atBCs and their differentiation into ASCs. Our findings support earlier reports which demonstrated ASC expansion in adult and childhood GC-sensitive INS[13,14], and further point to the extrafollicular reaction as a possible mechanism for the generation of podocyte-targeting autoantibodies that have been recently reported in subsets of children with INS[15-17].

Evidence for an extrafollicular response was also found within the INS-associated gene signatures of B cell subclusters. The marked upregulation of genes associated with atBCs and the preferential expression of *GPR183* (EBI2) and *TNFRSF13B* (TACI) in naïve B cells and recently activated B cells shows that this preference for the extrafollicular response takes place early during B cell activation. Indeed, *TNFRSF13B* was specifically upregulated in INS B cells over HC B cells and was amongst the most highly enriched genes in the nephrotic B cell signature. Cell network analysis using CellChatDB showed that the APRIL signaling pathway was markedly elevated in INS PBMC. In INS, monocytes were identified as a major putative source of APRIL signal in INS, consistent with a recent report that monocyte-derived dendritic cells provide APRIL to promote the extrafollicular generation of ASCs[49].

The first episode and relapses of INS are usually preceded by a triggering immune event, often involving respiratory viral infections caused by influenza, parainfluenza, respiratory syncytial virus, adenoviruses, and, most recently, SARS-CoV-2[34-36,64]. Although the mechanism by which viral infections trigger relapse is unknown, viral infections are effective activators of humoral immunity in an IFN-γ- and type-I IFN-dependent manner[65]. Using scRNA-seq, we showed a possible role for type-I IFN signaling in driving the nephrotic B cell response. Interestingly, 5/13 children studied with active INS experienced upper respiratory tract infections in the two weeks prior to proteinuria onset (Supplementary Data 1). While we cannot rule out that the expansion of atBCs and ASCs defined herein may be driven by viral infections, future work will aim to determine whether these infections may precipitate INS relapses through the stochastic activation of autoreactive B cells.

Finally, we sought to investigate the impact of immunosuppressive treatment on the INS-associated B cell populations that we uncovered. While GC treatment specifically restricted the abundance of ASCs in the blood, RTX effectively ablated all INS-associated B cell populations and maintained B cells in a transitional naïve state well into the recovery phase. The broader and more sustained effects of RTX on B cell compartments may explain the longer remission times observed with GC/RTX combination therapy than GC alone[6]. Additionally, the ability of RTX to ablate ASCs in INS supports that these cells are short-lived ASCs that developed extrafollicularly.

As with RTX-maintained remission, post-RTX relapses also featured a highly naïve B cell profile. We therefore hypothesized that these relapses were taking place because of a nascent version of the nephrotic B cell response. We confirmed earlier findings that the post-RTX relapses were associated with a resurgence in isotype-switched cMBCs but were unable to detect an expansion of atBCs or ASCs in this setting[20]. A possible explanation for this observation is that post-RTX relapses may represent an early time point in the extrafollicular response before the export of pathogenic B cells to the peripheral blood. Supporting this, scRNA-seq of four children from whom we were able to acquire post-RTX relapse-remission paired PBMC revealed that there was an expansion of MZ-like B cells in post-RTX relapse, the memory B cell population predicted to act as an atBC precursor by trajectory inference. This finding was confirmed by flow cytometry with an expansion of $IgM^+$ $IgD^+$ cMBCs, a heterogeneous population that contains MZ-like B cells, in post-RTX relapse samples[46]. Additionally, post-RTX relapses may be associated with the accumulation of clonally expanded autoreactive B cell populations that persist following RTX treatment, the detection of which would warrant clonotyping of post-RTX B cells. Indeed, the post-RTX persistence of autoreactive memory B cells in the blood has been reported in SLE and ANCA-associated vasculitis[66], in the spleen in immune thrombocytopenia[67], and in the lymph nodes in kidney transplant recipients[68].

Differential gene expression analysis between post-RTX relapse and remission did not identify any significant differences when completed at the pseudobulk level. We reasoned that this was due to the paucity of pathogenic B cells in the naïve-enriched post-

RTX setting, a scarcity that was only compounded by the limited number of cells that we could analyze by scRNA-seq. To this end, we also conducted differential gene expression analysis by comparing all post-RTX relapse memory B cells to post-RTX remission B cells, without pseudobulk separation. Here, we identified significant enrichment of nephrotic B cell signature genes and genes relating to type-I IFN signaling in memory B cells during post-RTX relapse. However, as these differences were not consistently observed across donors, the post-RTX transcriptional signature needs to be verified with memory pre-enriched B cells derived from a greater number of children.

In summary, our results uncovered a previously unrecognized role for extrafollicular B cells in childhood INS. We propose that these B cells contain autoreactive clones that may give rise to ASCs that produce podocytopathic autoantibodies thereby contributing to the pathogenesis of INS. This work provides a rationale for further exploration of B cell-targeting therapeutics in pediatric INS, in particular the targeting of atBCs alongside other autoimmune conditions.

## 2.6 Methods

### *Human subjects and PBMC collection*

This observational longitudinal study follows thirty-one children with INS that were enrolled according to protocols approved by institutional Research Ethics Boards (REBs) at the Research Institute of the McGill University Health Centre (MUHC-14-466, T.T.) and the Alberta Children's Hospital (CHREB-16-2186, S.S.)[69]. Blood samples were collected during active disease (first onset or relapse; defined by a urinary protein-to-creatinine ratio (uPCR) ≥ 0.2 g/mmol, serum albumin ≤ 25 g/L, and edema), and in remission (negative/trace dipstick or uPCR ≤ 0.02 g/mmol). Samples from children with active INS were stratified into RTX-inexperienced (INS, N = 14; median age of 8.1 years, interquartile range 5.5-10.8 years; 7 females) and -experienced (Rel-RTX, N = 7; 9.7 years, IQR of 9.0-11.0 years; 2 females) groups based on previous exposure to RTX. In the RTX-inexperienced group, 12/13 children had GC-sensitive INS (1/12 biopsy proven FSGS) and one child was diagnosed with GC-resistant membranous nephropathy (identified by the yellow point in relevant graphs). Of these, 8/13 children were untreated at the time of sampling, the remainder received weaning doses of prednisone. In the RTX-experienced group, all children had GC-sensitive INS (2/6 biopsy proven MCD, 1/6 FSGS). Five of the RTX-experienced GC-sensitive INS samples were obtained while off therapy and the remaining sample was taken during a prednisone taper. Samples from children in remission were stratified into GC-induced remission (Rem-GC, N = 13; 9.9 years, IQR of 6.2-12.5 years; 6 females) and remission maintained by RTX (Rem-RTX, N = 14; 9.2 years, IQR of 7.0-11.1 years; 5 females). Rem-GC samples were taken after completion of prednisone taper, though two patients were receiving mycophenolate mofetil at the time of sample collection, and Rem-RTX samples were collected following the re-emergence of $CD19^+$ cells off therapy. For healthy controls, we enrolled twenty-four healthy children undergoing minor day surgery or healthy volunteers from the community into the study (11.6 years, IQR of 8.4-14.6 years; 13 females). All samples were used in accordance with our standard operating protocol (MUHC-15-341, T.T.).

***Single-cell and RNA preparation from PBMC***

Cryopreserved PBMC were thawed and rested for two hours at 37ºC and in 5% $CO_2$. Cells were then washed and resuspended in PBS + 2% FBS before fluorescence activated cell sorting using the BD FACSAria Fusion. Live cells from PBMC of HC (N = 4) and INS (N = 4) children (HC-INS scRNA-seq dataset) were isolated based on size and granularity, while live B cells ($CD19^+$ $CD4^-$ $CD8^-$) were sorted from Rel-RTX (N = 4) and Rem-RTX (N = 4) PBMC (Rel-Rem scRNA-seq dataset). Sorted cells were washed twice in PBS + 0.04% BSA and were brought to a concentration of 1,000 cells/µl. Samples were subsequently processed according to the 10x Genomics Single Cell 5' v1.1 user guide. Single cell PBMC suspensions were loaded onto the 10x Single Cell Chip G along with 10x Genomics NextGem scRNA 5' V1.1 reagents. We targeted 10,000 captured events on a 10x Genomics Chromium controller. Complementary DNA (cDNA) and 5' gene expression libraries were generated using the standard 10x Genomics protocol. Libraries were sequenced on a NovaSeq6000 (Illumina).

***scRNA-seq data preprocessing and quality control***

Raw FASTQ files were aligned to the GRCh38 reference genome and count matrices for cell barcodes and UMIs were generated for each sample by CellRanger (v3.0.1). Using the Seurat (v4.3.0) R package, samples were filtered from cells expressing any two lineage markers (*CD79A*, *CD3G*, *CD14*, and *LILRA4*) as these were considered doublets[70,71]. In the HC-INS dataset, doublet and nonviable cells were removed by excluding cells expressing <200 or >3000 genes, >10% mitochondrial genes, and <10% ribosomal protein genes. In the Rel-Rem dataset, cells expressing <200 or >2500 genes, >10% mitochondrial genes, and <7% ribosomal protein genes were filtered. Lingering doublets were predicted and removed using the DoubletFinder (v2.0) R package[72].

***Generating scRNA-seq clusters***

To generate clusters that were uniformly present in all samples, we used the reciprocal PCA method for integrated clustering in Seurat. Data were normalized and

variable features were identified for each sample separately. Integration features were identified (SelectIntegrationFeatures), scaled, and PCA was performed. Integration anchors were then generated from the integration features (FindIntegrationAnchors) and two integrated Seurat objects for the HC-INS and Rel-Rem datasets were produced (IntegrateData). The integrated objects were subsequently scaled on variable features and PCA was performed. UMAP clustering was completed using 35 (HC-INS) or 10 (Rel-Rem) PCs at a resolution of 0.5. For the Rel-Rem dataset, a single cluster comprised of contaminating T cells (expressing *CD3G* or *CD3E*) were removed, and the object was then re-clustered using 10 PCs and a resolution of 0.5.

For the HC-INS object, cluster identities were determined by expression of major lineage defining genes (Supplementary Fig. 1b). To generate B cell subclusters, the Bnaive, Bmem-1, Bmem-2, and ASC clusters were isolated, and re-clustered using the reciprocal PCA method with 10 PCs and a resolution of 0.5. Two small contaminating T and NK cell clusters (expressing *CD3G*, *CD3E*, or *NKG7*) were removed, and clustering was performed again.

***Differential gene expression***

Pseudobulk differential gene expression analysis was completed using the muscat R package (v1.14) [37]. First, the HC-INS Seurat object was converted into a Single Cell Experiment (SCE) object and gene counts were normalized and log-transformed. Counts were then aggregated at the level of the broad immune cell lineages ($CD4^+$ T cells, $CD8^+$ T cells, NK cells, NKT cells, B cells, and monocytes) for each sample using the aggregateData function in muscat and differential gene expression analysis between INS and HC individuals was carried out using edgeR. Gene lists for each broad immune cell lineage was filtered from genes present in fewer than 10% of cells and genes with a $|\log_2 FC| < 0.65$ (Supplementary Data 2). The genes upregulated in INS B cells comprised the nephrotic B cell signature while downregulated genes comprised the healthy B cell signature. To determine B cell subcluster identities, differential gene expression analysis between individual subclusters was done using the FindMarkers function in Seurat v4. Pseudobulk differential

gene expression analysis using the muscat R package (v1.14) was used as outlined above to identify differentially expressed genes between INS and HC in each B cell subcluster. For the Rel-Rem Seurat object, differential gene expression analysis was performed between Rel-RTX and Rem-RTX memory B cells using the FindMarkers function in Seurat v4 (Supplementary Data 6).

***Pathway analysis, gene set enrichment analysis, and module scores***

Pathway analysis on the nephrotic B cell signature and the INS-associated signature for each B cell subcluster was performed using g:Profiler with the Gene Ontology Biological Process and Reactome databases[73]. Terms that were significantly enriched ($P_{adj} < 0.05$) and consisting of at least five and no more than 500 genes were organized in 2D space using the EnrichmentMap plugin on Cytoscape v3.9.1[74]. Enriched terms were clustered into groups using the AutoAnnotate and ClusterMaker2 plugins. GSEA of Gene Ontology terms in unfiltered gene lists organized by $log_2FC$ was carried out using the GSEA App (Broad Institute).

***Trajectory inference analysis***

The ASC subclusters (B8 and B9) were removed and the remaining B cell subclusters (B0-B7) from both HC and INS individuals were re-clustered. Pseudotemporal trajectories were constructed on the new UMAP using the Monocle3 R package[48]. Pseudotime was calculated by selecting all trajectory nodes within the transitional naïve B cell subcluster as the starting point. Cells along distinct branches were isolated for downstream comparisons of *TNFRSF13B* and *GPR183* expression.

***Cell network analysis***

CellChatDB (v1.6) was used to infer cell networks between clusters in INS and HC PBMC following the accompanying tutorial[75]. Briefly, CellChatDB objects were generated from Seurat objects and overexpressed genes in each cluster were identified. The probability of each cluster in participating as a sender, modulator, or receiver of each signal was

determined using known networks of ligands, receptors, and co-factors. INS and HC PBMC were analyzed independently. We show the results for the APRIL signaling pathway.

***Flow cytometry***

Cryopreserved PBMC were thawed, rested, washed twice with PBS + 2% FBS, and counted using the hemocytometer. Over 90% viability was confirmed by trypan blue and no more than $1 \times 10^6$ cells were stained per flow cytometry panel. Cells were then incubated with Fixable Viability eFluor 780 Dye (ThermoFisher Scientific) at 4ºC for 15 minutes, washed with PBS + 2% FBS, and incubated for another 15 minutes at 4ºC in the presence of Fc receptor block (BD Biosciences). Antibody cocktails for surface proteins were prepared in PBS + 2% FBS and Brilliant Stain Buffer (50 µl/100 µl of cocktail, BD Biosciences) and added to the cells. Cells were incubated at 4ºC for 20 minutes before washing with PBS + 2% FBS and fixation/permeabilization was performed using the eBioscience Foxp3/Transcription Factor Staining Buffer Set (eBioscience). Cells were then washed with 1X permeabilization buffer (eBioscience) and incubated for 45 minutes at 4ºC with antibody cocktails detecting cytoplasmic and nuclear proteins. Two final washes, the first in 1X permeabilization buffer and the final in PBS + 2% FBS, were performed before cells were acquired on the BD LSRFortessa X-20.

Extracellular staining was performed using the following antibodies: anti-human CD3ε BV785 (1:50, OKT3, BioLegend), anti-human CD19 BV605 (1:20, SJ25C1, BD Biosciences), anti-human CD20 Alexa Fluor 700 (1:50, 2H7, BioLegend), anti-human CD21 BV421 (1:20, B-ly4, BD Biosciences), anti-human CD27 PE-Cy7 (1:20, M-T271, BD Biosciences), anti-human CD10 BUV737 (1:20, HI10a, BD Biosciences), anti-human CD38 BUV737 (1:20, HB7, BD Biosciences), anti-human CD11c PerCp-Cy5.5 (1:20, B-ly6, BD Biosciences), anti-human IgD BV510 (1:20, IA6-2, BioLegend), anti-human IgM Alexa Fluor 488 (1:40, MHM-488, BioLegend), anti-human FcRL5 APC (1:20, 509f6, BioLegend), anti-human CD24 PE (1:20, ML5, BD Biosciences), anti-human CD1c BV711 (1:20, L161, BioLegend), and anti-human CXCR5 APC (1:20, J252D4, BioLegend). Intracellular proteins were stained using the following antibodies: anti-human T-bet PE (1:20, 4B10, BioLegend),

and anti-human Ki-67 BUV395 (1:50, B56, BD Biosciences). Data were analyzed on FlowJo v10.8 software (FlowJo, LLC).

***FlowSOM clustering***

Unsupervised high-dimensional clustering of B cells was done using the FlowSOM plugin for FlowJo v10.8 software[76]. We randomly selected 15,000 or 8,125 B cells (live $CD19^+$ $CD3^-$) from 13 RTX-inexperienced children with active INS and 24 HC, respectively, for concatenation (195,000 INS B cells, 195,000 HC B cells). FlowSOM clustering was performed using ten B cell surface markers: CD19, CD20, CD21, IgD, IgM, CD27, CD38, CXCR5, CD1c, and CD24. Briefly, each B cell was plotted onto a 10×10 self-organizing map (SOM) yielding 100 distinct clusters. Minimal-spanning trees (MST) were built upon these clusters with branches containing cells with similar surface phenotypes. The clusters were further categorized into 14 metaclusters, the identities of which were determined by the expression of the ten surface markers.

***Statistical analysis***

Statistical analyses were performed on R or using the GraphPad Prism v9 software. Two-sided analyses between two groups were done using Mann-Whitney tests. For any comparison between more than two groups, a Kruskal-Wallis test was employed with multiple comparison's (Dunn's test). A two-way ANOVA was used for comparisons of two parameters between two groups with multiple comparisons (Tukey's test). Finally, a paired t-test was used for longitudinal analyses. Data are shown as median ± 95% confidence intervals with each point representing a single study participant. *P*-values < 0.05 were considered significant and significant *P*-values were depicted on graphs. No sample size calculations were conducted *a priori*. All samples obtained were used for the study.

**Data Availability**

Raw sequencing data and the processed count matrices included in this study were deposited in the NCBI Gene Expression Omnibus (GEO) as a super series under the

accession number GSE233277. The results of all differential gene expression analyses, pathway analysis, and transcription factor enrichment analysis are included in Supplementary Data files of this paper. All source data needed to evaluate the conclusions are included with this paper. Public data repositories used for analysis include ChEA3[41] (https://maayanlab.cloud/chea3/) and g:Profiler[73] (https://biit.cs.ut.ee/gprofiler/gost).

**Acknowledgements**

We are grateful to all study participants, their families, and the medical teams involved in their care. We thank the Canadian Childhood Nephrotic Syndrome Study (CHILDNEPH) for supplying PBMC, D. Muruve and the Biobank for the Molecular Classification of Kidney Disease (BMCKD) for processing and storing PBMC, and B. Mazer and B. Foster for supplying healthy children PBMC. We also thank I. Ragoussis, H. Djambazian, and Y. Wang at the McGill Genome Centre for sample processing through the 10X Genomics platform, sequencing, and generation of pre-processed count matrices, and M-H. Lacombe, E. Iourtchenko, and H. Pagé-Veillette at the Research Institute of the McGill University Health Centre Immunophenotyping Core for their support. This work was supported by a Canadian Institute of Health Research (CIHR) project grant (PFT-166006 to T.T., C.P., S.S.) and a Kidney Foundation of Canada Kidney Health Research grant (KHRG-190010 to T.T., C.P., S.S.). T.A. was supported by a CIHR Doctoral Award and a FRQS Doctoral Award.

**Author Contributions**

T.A., C.P., and T.T. conceptualized the study and designed all the experiments. T.A. conducted the experiments and performed all the data analysis. T.A., L.A., and M.P. processed all the blood samples. G.P. and M.P. consented the children into the study. T.A., L.A., M.P., M.B., S.S., and T.T. coordinated sample collection and biobanking at the McGill University Health Centre and Alberta Children's Hospital. T.A., D.L., C.P., and T.T. planned all the bioinformatics analyses. T.A., C.P., and T.T. wrote the initial draft of the manuscript. All authors critically reviewed the manuscript, discussed the results, interpreted the data, and

contributed to the formulation and agreed on the submission of the final draft of the manuscript.

### 2.9 Description of Online Supplementary Files

**Supplementary Data 1: Participant characteristics.** The demographic and clinical characteristics of all participants in this study.

**Supplementary Data 2: Differences in gene expression between HC and INS PBMC lineages.** The results of pseudobulk differential gene expression analysis between HC and INS for each PBMC lineage using the Muscat R package and the edgeR method. $P_{adj}$ values were calculated using Benjamini-Hochberg corrections for multiple-testing.

**Supplementary Data 3:** Pathway analysis on the nephrotic B cell signature. The list of g:Profiler results showing the enrichment of Gene Ontology Biological Processes and Reactome pathways in the nephrotic B cell signature. $P_{adj}$ (FDR) values were calculated using Benjamini-Hochberg corrections for multiple testing.

**Supplementary Data 4: Transcription factor enrichment analysis in the nephrotic B cell signature.** The list of the ChEA3 results showing the ranking of predicted upstream regulators of the nephrotic B cell signature.

**Supplementary Data 5: B cell subcluster gene expression.** The results of the differential gene expression analysis using Seurat comparing each B cell subcluster. $P_{adj}$ values were calculated by Wilcoxon rank sum testing with Bonferroni correction.

**Supplementary Data 6: Differentially expressed genes between HC and INS B cell subclusters.** The results of pseudobulk differential gene expression analysis between HC and INS for each B cell subcluster using the Muscat R package and the edgeR method. $P_{adj}$ values were calculate using Benjamini-Hochberg corrections for multiple-testing.

**Supplementary Data 7:** Differences in gene expression between post-rituximab relapse and remission in memory and naïve B cells. The results of the differential gene expression analysis using Seurat comparing post-rituximab relapse (Rel-RTX) and remission (Rem-RTX) memory and naïve B cells.

## 2.8 Figures

## Figure 1

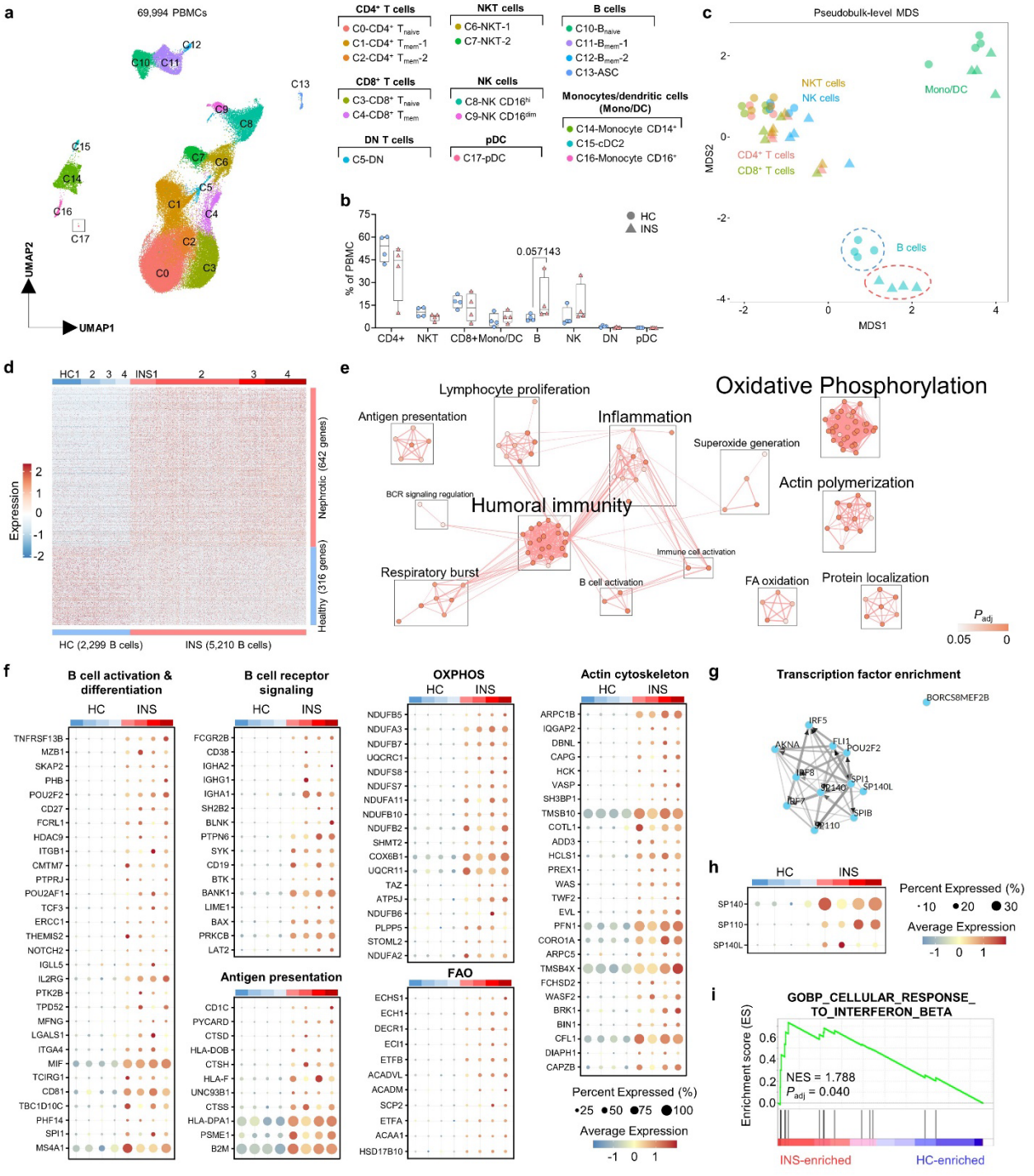

**Figure 1: B cells in INS are transcriptionally poised to acquire effector functions.**

**a.** Integrated Uniform Manifold Approximation and Projection (UMAP) of the 18 clusters of PBMC from HC (*n* = *4*) and INS (*n* = *4*) children. **b.** Proportions of each broad immune cell lineage; *p* values were determined using Mann-Whitney tests. **c.** Multi-dimensional scaling (MDS) plot of differentially expressed genes between INS and HC broad cell lineages. Genes with $|\log_2(\text{Fold Change})|>0.65$ and $P_{adj}<0.05$ were considered significantly differentially expressed. **d.** Heatmap of the normalized expression of differentially expressed genes between INS and HC B cells. **e.** Enrichment map depicting the pathway analysis results in the nephrotic B cell signature. OXPHOS denotes oxidative phosphorylation and FAO denotes fatty acid oxidation. **f.** Bubble plots showing the expression of genes associated with B cell effector functions in the nephrotic B cell signature. **g.** A network plot from ChEA3 depicting the transcription factors predicted to confer the nephrotic B cell signature. **h.** A bubble plot showing the expression of three ChEA3 hits. **i.** A gene set enrichment analysis (GSEA) plot of the Gene Ontology term “Cellular Response to Interferon Beta” (GO:0035458).

# Figure 2

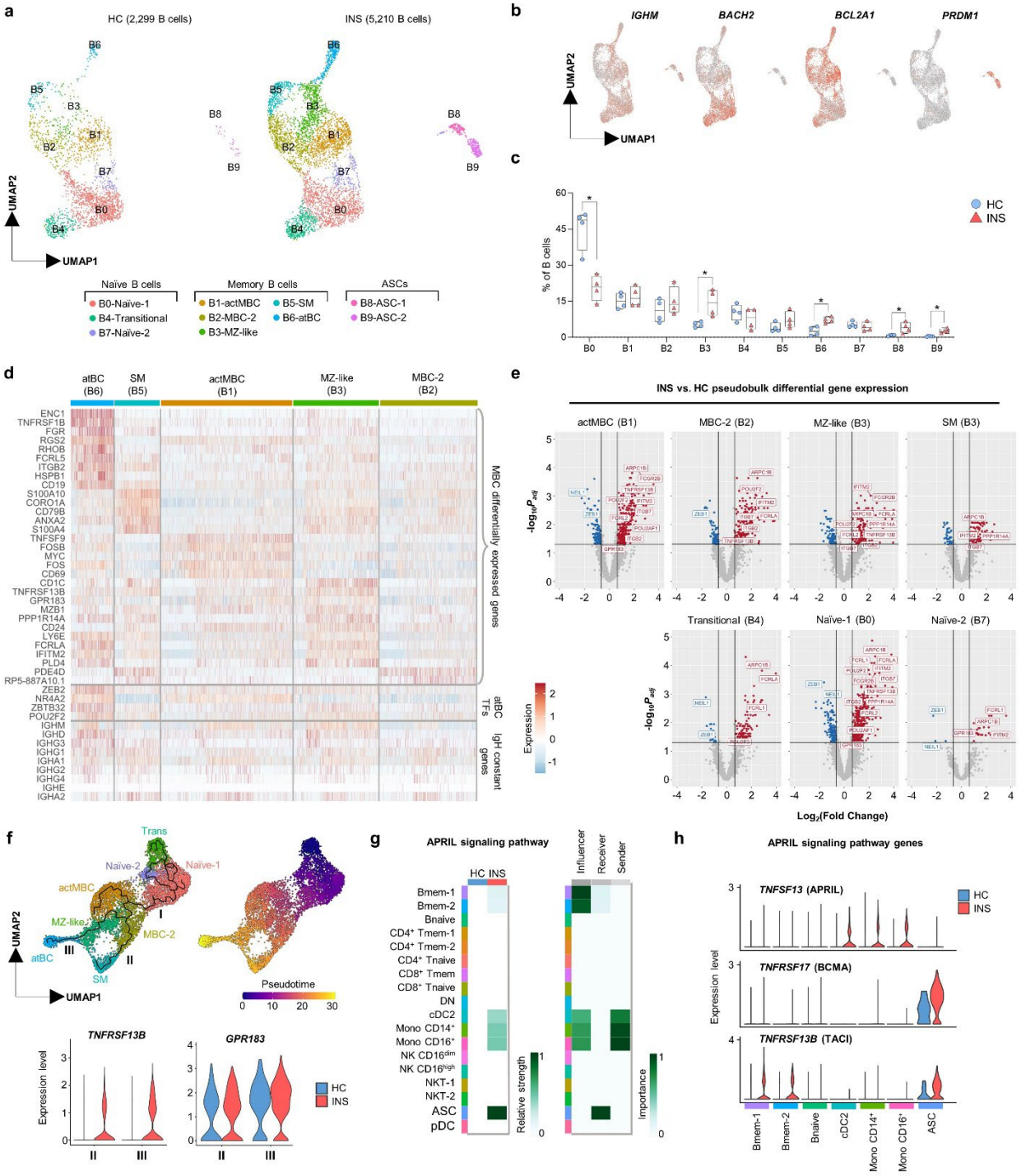
a
HC (2,299 B cells)
INS (5,210 B cells)
UMAP1
UMAP2
Naïve B cells
B0-Naïve-1
B4-Transitional
B7-Naïve-2
Memory B cells
B1-actMBC
B2-MBC-2
B3-MZ-like
B5-SM
B6-atBC
ASCs
B8-ASC-1
B9-ASC-2
b
IGHM
BACH2
BCL2A1
PRDM1
c
% of B cells
HC
INS
d
atBC (B6)
SM (B5)
actMBC (B1)
MZ-like (B3)
MBC-2 (B2)
MBC differentially expressed genes
atBC TFs
IgH constant genes
Expression
e
INS vs. HC pseudobulk differential gene expression
actMBC (B1)
MBC-2 (B2)
MZ-like (B3)
SM (B3)
Transitional (B4)
Naïve-1 (B0)
Naïve-2 (B7)
Log2(Fold Change)
f
Trans
Naïve-2
Naïve-1
actMBC
MZ-like
MBC-2
atBC
SM
Pseudotime
TNFRSF13B
GPR183
Expression level
g
APRIL signaling pathway
HC INS
Influencer
Receiver
Sender
Relative strength
Importance
h
APRIL signaling pathway genes
TNFSF13 (APRIL)
TNFRSF17 (BCMA)
TNFRSF13B (TACI)
Expression level

**Figure 2: The engagement of extrafollicular B cells is a feature of active INS.**

**a.** Integrated UMAP of the ten B cell subclusters shown for HC (*n = 4*, *left*) and INS (*n = 4*, *right*). **b.** Feature plots showing expression of *IGHM*, *BACH2*, *BCL2A1*, and *PRDM1* in B cells. **c.** Proportions of each B cell subcluster in HC and INS children; *p* values were determined using Mann-Whitney tests (*$p<0.05$). **d.** Heatmap showing the expression of the most highly enriched genes in each memory B cell subcluster. **e.** Volcano plots showing the differentially expressed genes between INS and HC in each B cell subcluster. Genes with $|\log_2(\text{Fold Change})|>0.65$ and $P_{adj}<0.05$ were considered significantly differentially expressed. **f.** UMAP plots showing re-clustering of all B cell subclusters except ASC-1 and ASC-2 alongside the trajectory (*left*) and pseudotime (*right*) as determined by Monocle3, and violin plots showing the expression of *TNFRSF13B* and *GPR183* in branches II and III (*bottom*). **g.** Heatmaps from CellChatDB showing the relative strength of the participation of each PBMC cluster in the APRIL signaling network in HC and INS (*left*), and the importance of each PBMC cluster in INS as acting as "sender", "modulator", or "receiver" cell types within the APRIL signaling network. **i.** Violin plots showing the expression of genes within the APRIL signaling network across participating PBMC clusters in HC and INS.

## Figure 3

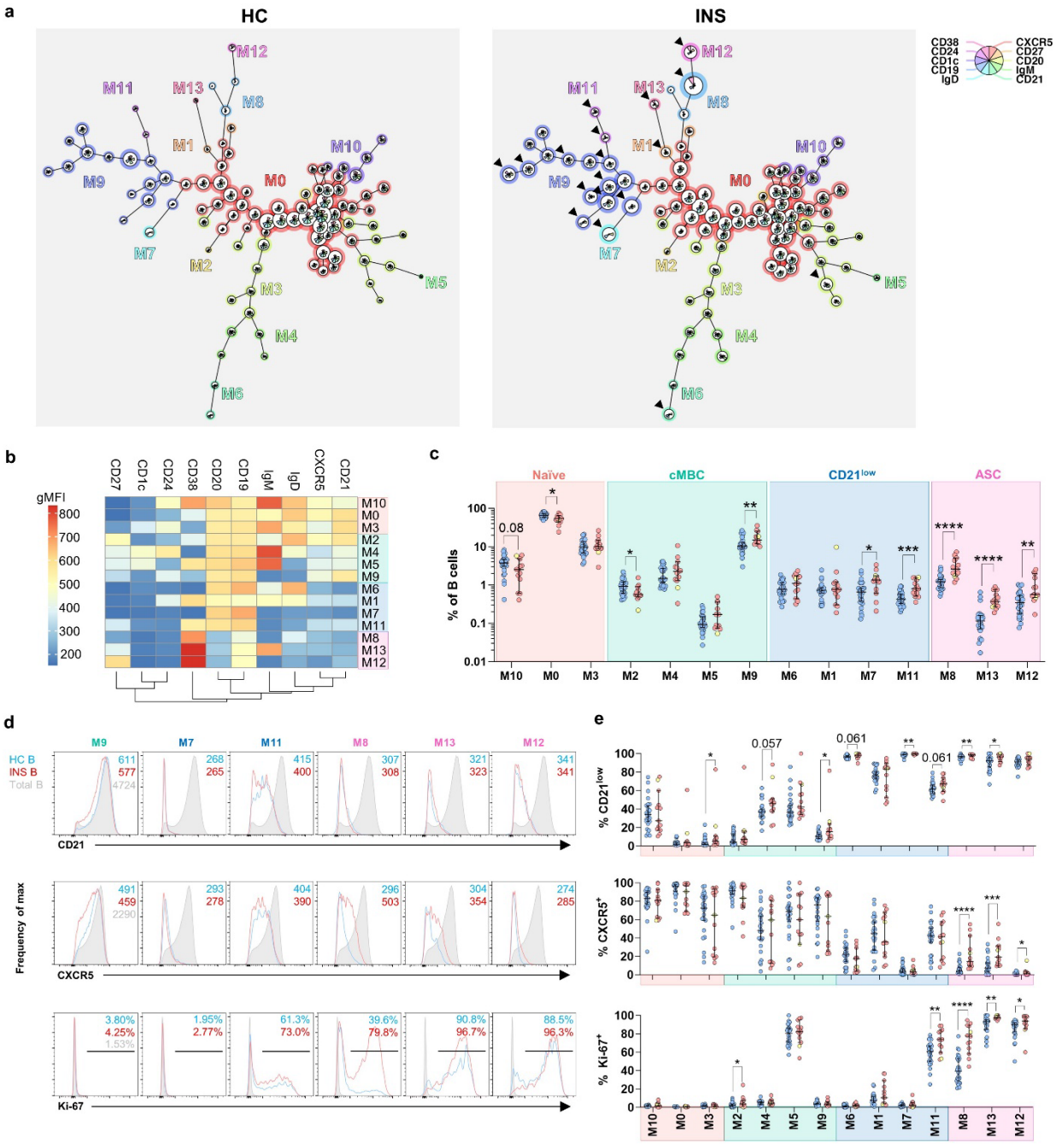
a
HC
INS
CD38
CD24
CD1c
CD19
IgD
CXCR5
CD27
CD20
IgM
CD21
M0
M1
M2
M3
M4
M5
M6
M7
M8
M9
M10
M11
M12
M13
b
gMFI
800
700
600
500
400
300
200
CD27
CD1c
CD24
CD38
CD20
CD19
IgM
IgD
CXCR5
CD21
c
Naïve
cMBC
CD21low
ASC
% of B cells
0.08
d
HC B
INS B
Total B
CD21
CXCR5
Frequency of max
Ki-67
e
% CD21low
% CXCR5+
% Ki-67+
0.057
0.061

**Figure 3: CD21$^{low}$ CXCR5$^{-}$ B cells and ASCs are actively expanding in active INS.**

**a.** Minimal spanning trees (MST) of HC (*left*) and INS (*right*) B cells generated by FlowSOM clustering. The 14 metaclusters (M0-M13) are labelled on both MSTs. Arrowheads indicate key cell clusters expanded in INS **b.** Heatmap showing the geometric mean fluorescence intensities (gMFI) of the markers used for clustering in each metacluster. **c.** Proportions of each metacluster in HC and INS PBMC. **d., e.** Histograms of CD21, CXCR5, and Ki-67 in the six metaclusters enriched in INS (**d**) with quantification of the proportions of CD21$^{low}$, CXCR5$^{+}$, and Ki-67$^{+}$ cells in each metacluster (**e**); in **d** and **e**, *p* values were determined by Mann-Whitney tests (**p*<0.05, ***p*<0.01, ****p*<0.001, *****p*<0.0001). Each data point corresponds to a single donor. The yellow data point represents the child with glucocorticoid-resistant membranous nephropathy.

## Figure 4

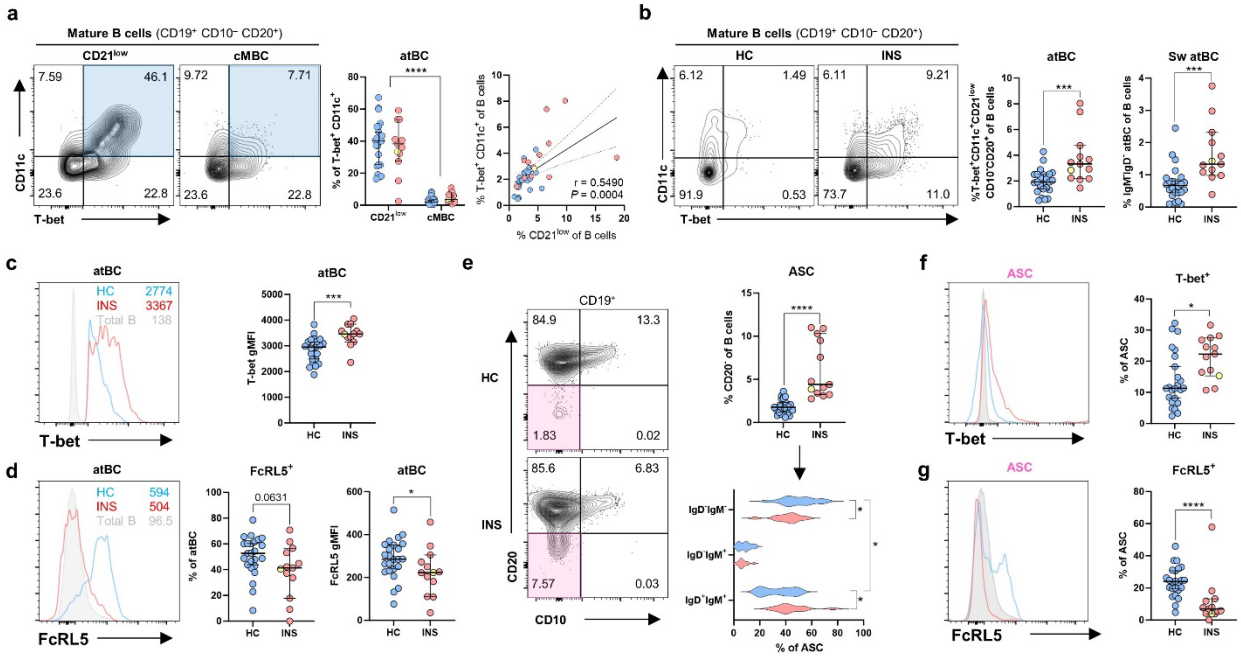
a
Mature B cells (CD19+ CD10− CD20+)
CD21low
cMBC
7.59
46.1
9.72
7.71
23.6
22.8
23.6
22.8
CD11c
T-bet
atBC
****
% of T-bet+ CD11c+
CD21low
cMBC
% T-bet+ CD11c+ of B cells
r = 0.5490
P = 0.0004
% CD21low of B cells
b
Mature B cells (CD19+ CD10− CD20+)
HC
INS
6.12
1.49
6.11
9.21
91.9
0.53
73.7
11.0
CD11c
T-bet
atBC
***
%T-bet+CD11c+CD21low CD10−CD20+ of B cells
HC
INS
Sw atBC
***
% IgM−IgD− atBC of B cells
HC
INS
c
atBC
HC 2774
INS 3367
Total B 138
T-bet
atBC
***
T-bet gMFI
HC
INS
d
atBC
HC 594
INS 504
Total B 96.5
FcRL5
FcRL5+
0.0631
% of atBC
HC
INS
atBC
*
FcRL5 gMFI
HC
INS
e
CD19+
84.9
13.3
1.83
0.02
85.6
6.83
7.57
0.03
HC
INS
CD20
CD10
ASC
****
% CD20− of B cells
HC
INS
IgD−IgM−
IgD−IgM+
IgD+IgM+
*
*
*
0
20
40
60
80
100
% of ASC
f
ASC
T-bet
T-bet+
*
% of ASC
HC
INS
g
ASC
FcRL5
FcRL5+
****
% of ASC
HC
INS

**Figure 4: CD21$^{low}$ T-bet$^{+}$ atBCs and ASCs are a hallmark of childhood INS.**

**a.** Representative flow plots highlighting T-bet$^{+}$CD11c$^{+}$ cells (*aquamarine*) in the CD21$^{low}$ (CD21$^{low}$ CD19$^{+}$ CD10$^{-}$ CD20$^{+}$ CD38$^{-/low}$) and cMBC (CD27$^{+}$ CD21$^{+}$ CD19$^{+}$ CD10$^{-}$ CD20$^{+}$ CD38$^{-/low}$) mature B cell compartments. Proportions of T-bet$^{+}$ CD11c$^{+}$ among CD21$^{low}$ and cMBC mature B cells (*left graph*) are shown along with linear regression analysis between the proportions of T-bet$^{+}$ CD11c$^{+}$ and CD21$^{low}$ mature B cells (*right graph*). **b.** Representative flow plots of atBCs (CD11c$^{+}$ T-bet$^{+}$ mature B cells) in HC and INS. Quantification of the proportion of atBCs (*left graph*) and isotype-switched (IgM$^{-}$ IgD$^{-}$) atBCs (*right graph*) in HC and INS B cells are shown. **c., d.** Histograms showing T-bet (**c**) and FcRL5 (**d**) expression in HC and INS atBC with quantification of MFIs and cell frequencies. **e.** Representative flow plots highlighting ASCs (*pink*) in total B cells. Quantification of the proportions of ASCs in HC and INS B cells (*top right graph*) and their isotype distributions (*bottom right graph*). **f., g.** Histograms showing T-bet (**c**) and FcRL5 (**d**) expression in HC and INS ASCs with quantification of cell frequencies. *p* values were determined by Mann-Whitney tests (**b**, **c**, **d, e**, **f**, **g**), two-way ANOVA with Tukey's multiple testing (**b, e**), or Pearson's correlation (**b**) (*$p$<0.05, **$p$<0.01, ***$p$<0.001, ****$p$<0.0001). Each data point corresponds to a single donor. The yellow data point represents the child with glucocorticoid-resistant membranous nephropathy.

## Figure 5

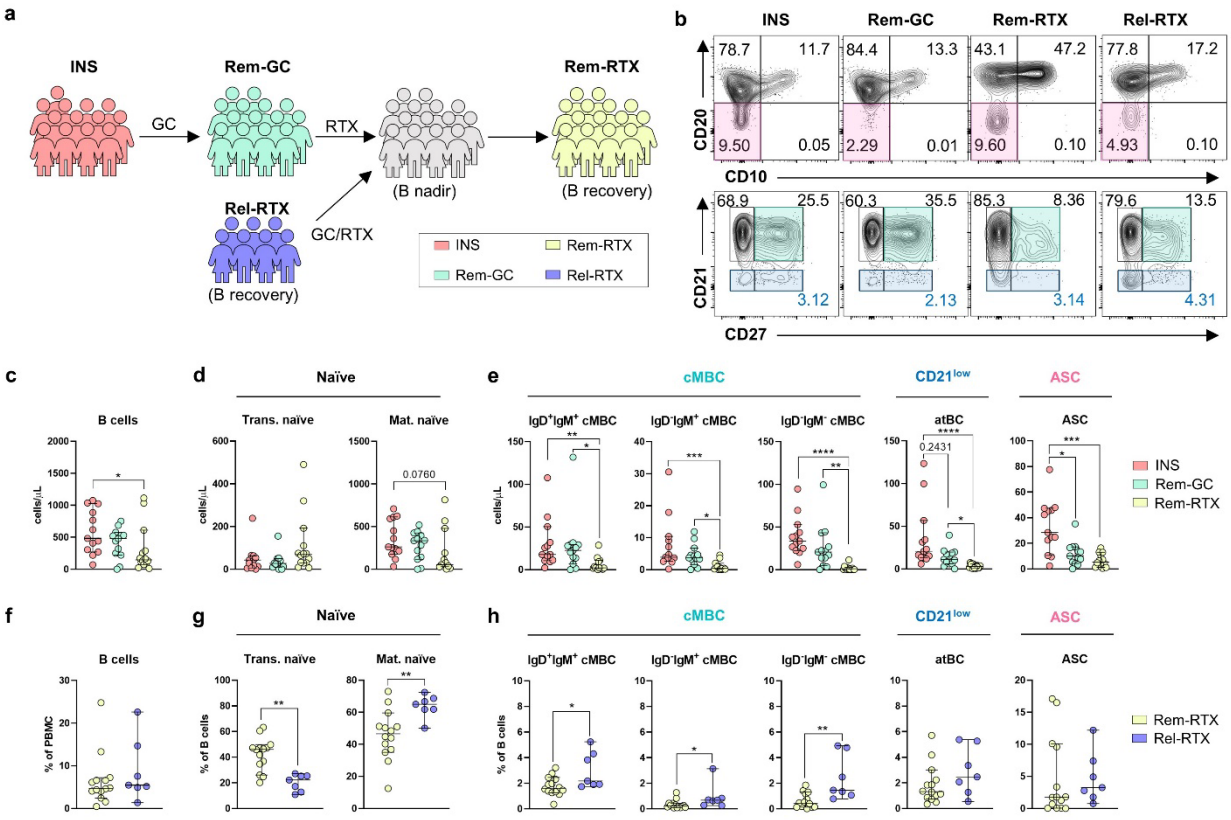
a
INS
Rem-GC
Rem-RTX
GC
RTX
(B nadir)
(B recovery)
Rel-RTX
GC/RTX
(B recovery)
INS
Rem-GC
Rem-RTX
Rel-RTX
b
INS
Rem-GC
Rem-RTX
Rel-RTX
78.7
11.7
9.50
0.05
84.4
13.3
2.29
0.01
43.1
47.2
9.60
0.10
77.8
17.2
4.93
0.10
CD20
CD10
68.9
25.5
3.12
60.3
35.5
2.13
85.3
8.36
3.14
79.6
13.5
4.31
CD21
CD27
c
B cells
cells/μL
d
Naïve
Trans. naïve
Mat. naïve
0.0760
e
cMBC
CD21low
ASC
IgD+IgM+ cMBC
IgD-IgM+ cMBC
IgD-IgM- cMBC
atBC
ASC
0.2431
INS
Rem-GC
Rem-RTX
f
B cells
% of PBMC
g
Naïve
Trans. naïve
Mat. naïve
% of B cells
h
cMBC
CD21low
ASC
IgD+IgM+ cMBC
IgD-IgM+ cMBC
IgD-IgM- cMBC
atBC
ASC
% of B cells
Rem-RTX
Rel-RTX

**Figure 5: atBCs and ASCs are effectively targeted by RTX.**

**a.** Schematic representing the patient groups from which PBMC were obtained in the observational longitudinal cohort. **b.** Representative flow plots from each patient group showing total B cells ($CD19^+$, *top*), and mature B cells ($CD19^+$ $CD10^-$ $CD20^+$, *bottom*). Coloured boxes denote ASCs (*pink*), cMBC (*teal*), and $CD21^{low}$ atBCs (*aquamarine*). **c.-e.** Absolute numbers of total (**c**), naïve (**d**), and memory (**e**) B cell populations in the blood of INS, Rem-GC, and Rem-RTX individuals; *p* values were determined by Kruskal-Wallis tests with Dunn's test for multiple comparisons (**p*<0.05, ***p*<0.01, ****p*<0.001, *****p*<0.0001). **f.-h.** Proportions of total (**f**), naïve (**g**), and memory (**h**) B cells in the blood of Rem-RTX and Rel-RTX individuals; *p* values were determined by Mann-Whitney tests (**p*<0.05, ***p*<0.01, ****p*<0.001, *****p*<0.0001). Each data point corresponds to a single donor.

## Figure 6

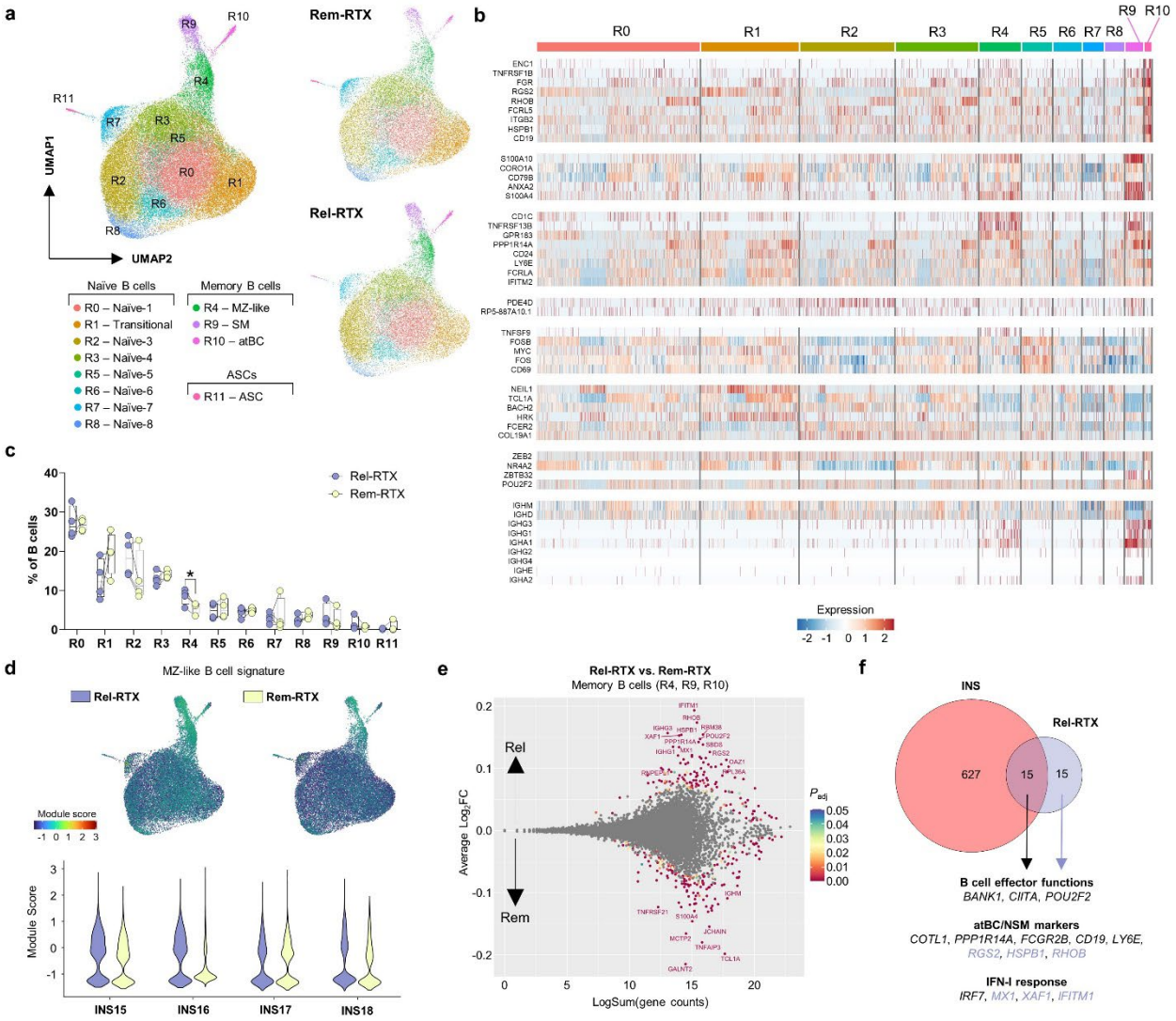
a
Rem-RTX
Rel-RTX
UMAP1
UMAP2
Naïve B cells
R0 – Naïve-1
R1 – Transitional
R2 – Naïve-3
R3 – Naïve-4
R5 – Naïve-5
R6 – Naïve-6
R7 – Naïve-7
R8 – Naïve-8
Memory B cells
R4 – MZ-like
R9 – SM
R10 – atBC
ASCs
R11 – ASC
b
Expression
c
Rel-RTX
Rem-RTX
% of B cells
d
MZ-like B cell signature
Module score
Module Score
INS15
INS16
INS17
INS18
e
Rel-RTX vs. Rem-RTX
Memory B cells (R4, R9, R10)
Rel
Rem
Average Log2FC
LogSum(gene counts)
f
INS
Rel-RTX
627
15
15
B cell effector functions
BANK1, CIITA, POU2F2
atBC/NSM markers
COTL1, PPP1R14A, FCGR2B, CD19, LY6E, RGS2, HSPB1, RHOB
IFN-I response
IRF7, MX1, XAF1, IFITM1

**Figure 6: Post-RTX relapses are associated with a nascent resurgence in extrafollicular B cells.**

**a.** Integrated UMAP of total B cells (*left*) obtained during B cell recovery from four individuals who relapsed following RTX treatment (Rel-RTX, *top right*) and were subsequently treated with GC and RTX to maintain long-term remission (Rem-RTX, *bottom right*). **b.** Heatmap showing expression of B cell subcluster genes identified in Fig. 2c. **c.** Proportions of B cell clusters; *p* values were determined using a paired t-test (*$p < 0.05$). **d.** Feature and violin plots showing the module score for the MZ-like B cell signature in total B cells. **e.** MA plot showing the differential expression of genes between Rel-RTX and Rem-RTX memory B cells. **f.** A Venn diagram showing the overlap between the nephrotic B cell signature and the most enriched genes in Rel-RTX B cells ($|\log_2(\text{Fold Change})|>0.1$, $P_{adj} < 0.01$, minimum percent expression of 15%).

## 2.8 Supplementary Tables and Figures

## Supplementary Figure 1

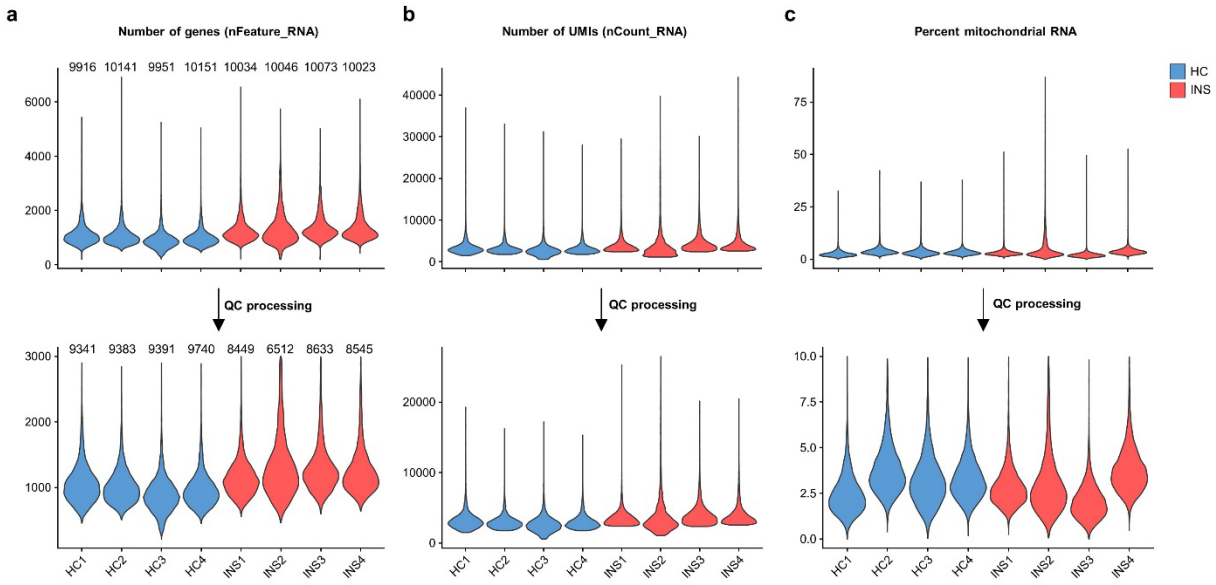

**Supplementary Figure 1. Quality control processing of INS and HC PBMC for scRNA-seq. a.-c.** The number of genes (nFeature_RNA) (**a**), UMIs (nCount_RNA) (**b**), frequencies of mitochondrial RNA (**c**) in each sample before (*top row*) and after (*bottom row*) quality control (QC) processing. QC steps are outlined in the methodology. This Supplementary Figure is associated with Figure 1.

## Supplementary Figure 2

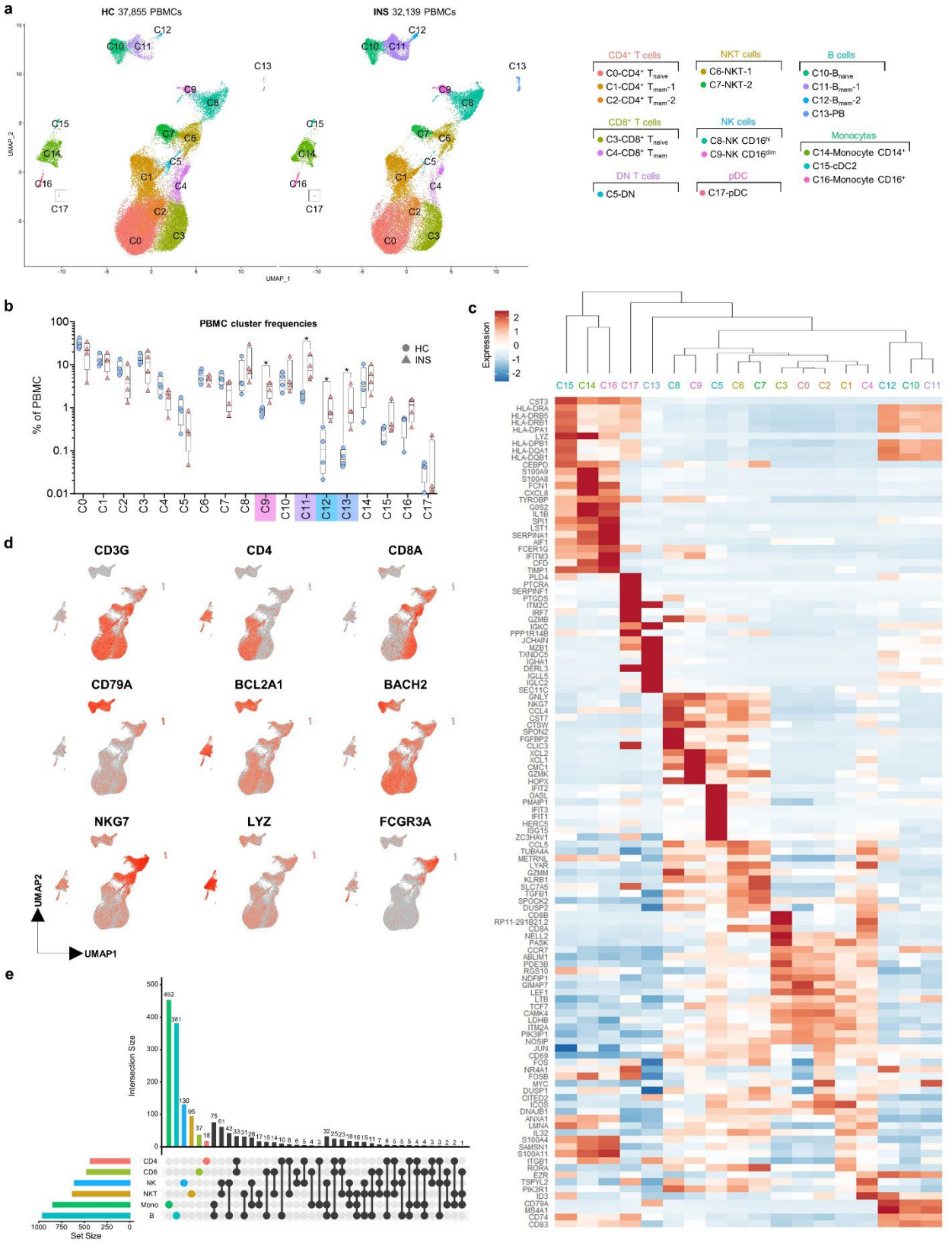

**Supplementary Figure 2: Annotation of PBMC populations by scRNA-seq. a.** Integrated Uniform Manifold Approximation and Projection (UMAP) of the 18 clusters of PBMC from HC (*n = 4*, left) and INS (*n = 4*, right) children. **b.** Frequencies of each PBMC cluster in HC and INS individuals; *p* values were determined using Mann-Whitney tests (*$p<0.05$). **c.** Heatmap showing the expression of the top ten genes in each PBMC cluster. **d.** Feature plots showing the expression of several major lineage defining genes in PBMC. **e.** Upset plot showing the number of differentially expressed genes (set sizes) between INS and HC within each broad cell lineage along with intersection sizes between gene lists following pseudobulk differential gene expression analysis using MUSCAT. This Supplementary Figure is associated with Figure 1.

## Supplementary Figure 3

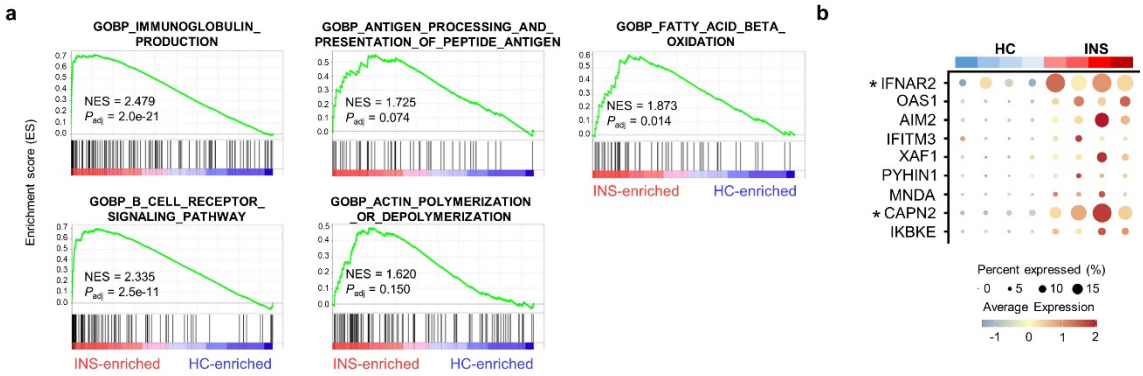

**Supplementary Figure 3: Gene set enrichment analysis (GSEA) on the nephrotic B cell signature. a** Results of GSEA from $\log_2$(Fold Change)-ranked genes following pseudobulk-level differential gene expression analysis between INS and HC B cells. **b** Bubble plot of highly enriched type-I interferon genes. This Supplementary Figure is associated with Figure 1.

## Supplementary Figure 4

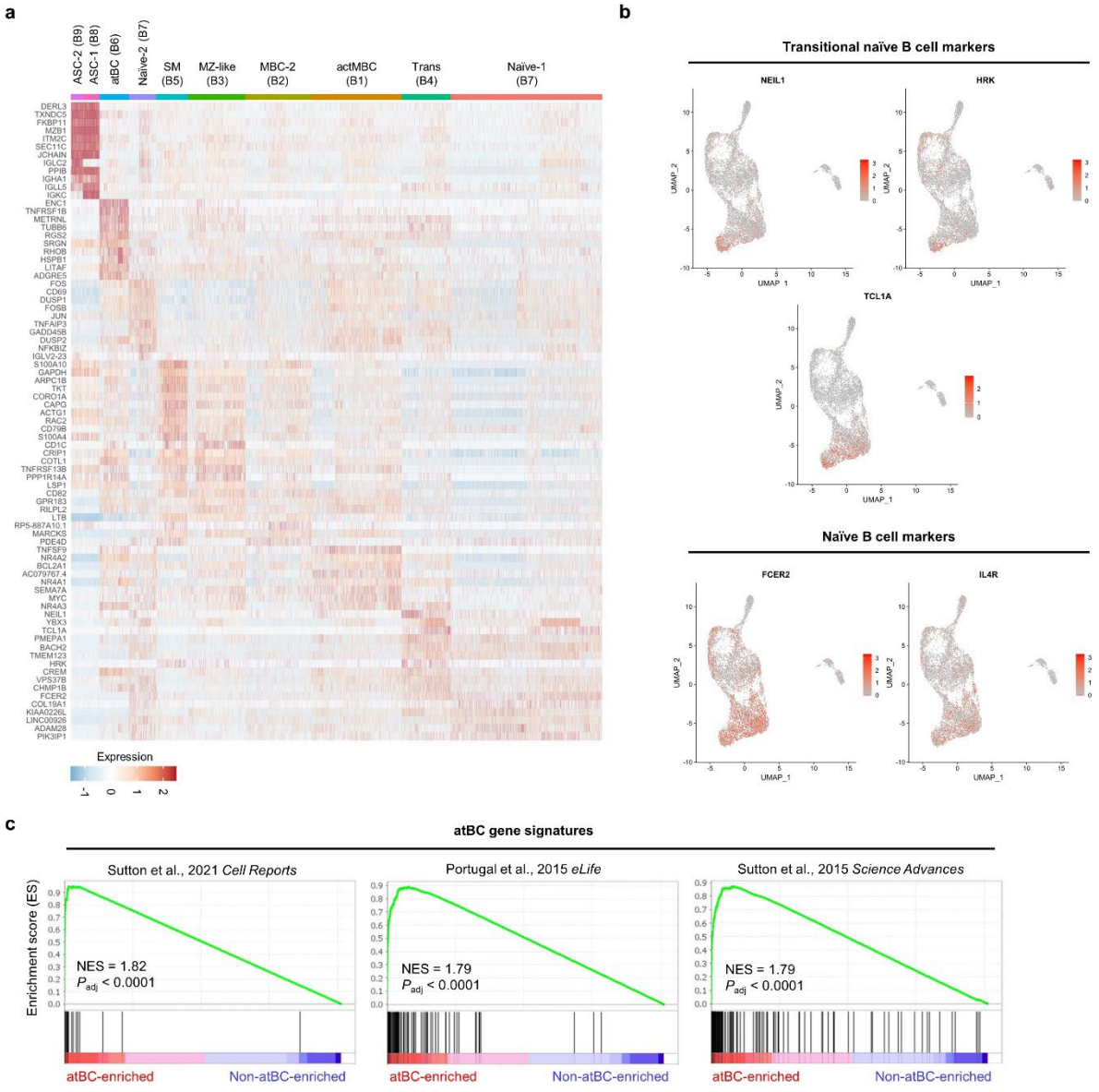

**Supplementary Figure 4: Annotation of B cell subclusters. a.** Heatmap showing the expression of the top ten genes in each of the B cell subclusters. **b.** Feature plots showing the expression of transitional naïve-associated (*NEIL1*, *HRK*, *TCL1A*) and general naïve-associated (*FCER2*, *IL4R*). **c.** GSEA plots showing the enrichment of atBC genes from three independent studies with the atBCs identified herein. This Supplementary Figure is associated with Figure 2.

## Supplementary Figure 5

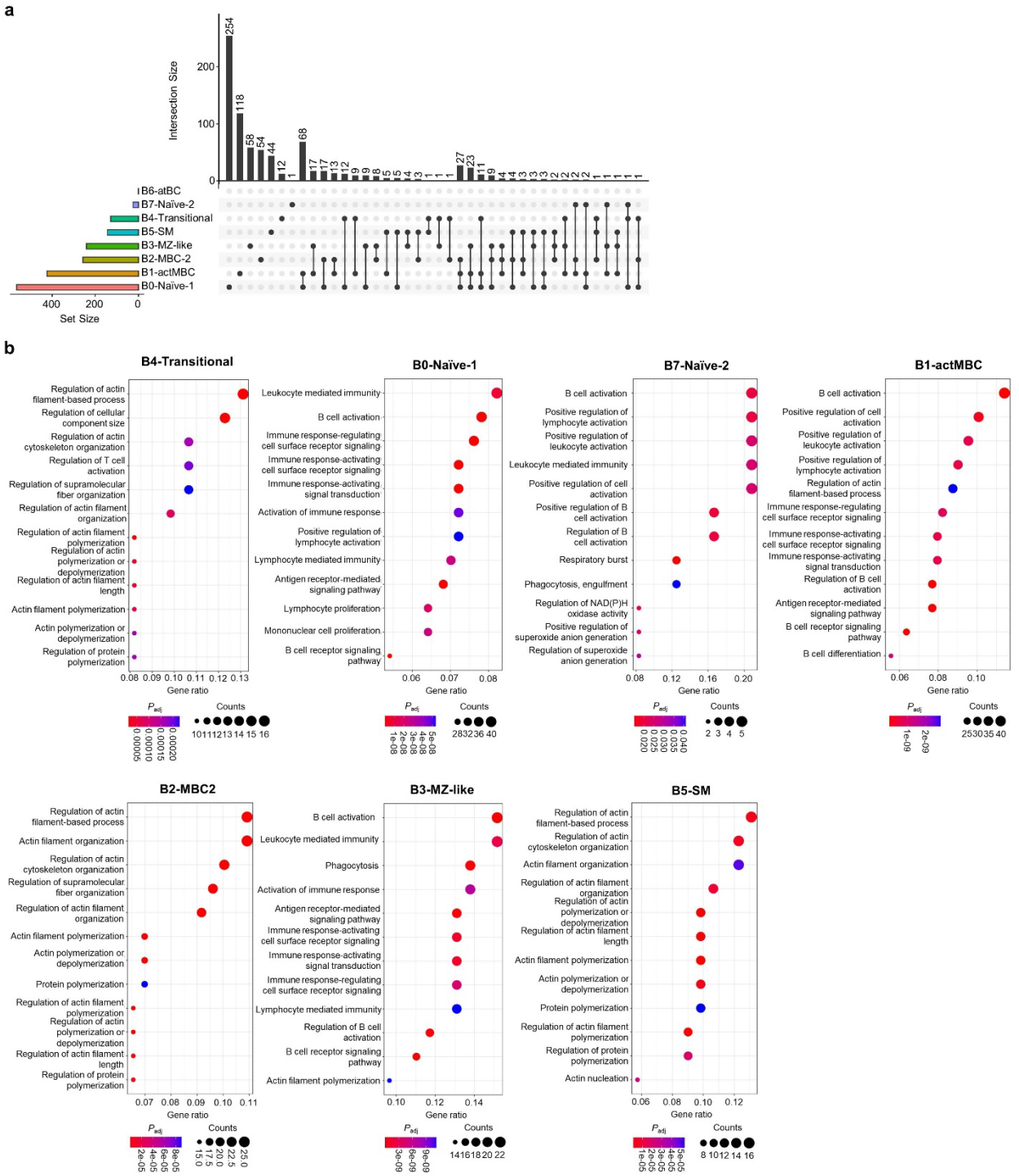

**Supplementary Figure 5: Pathway analysis of INS-associated genes in B cell subclusters. a.** Upset plot showing the set sizes and intersection sizes of pseudobulk-level differentially expressed genes between INS and HC B cell subclusters using the Muscat R package. **b.** Gene Ontology pathways enriched in INS B cell subclusters over HC B cell subclusters. Genes used for pathway analysis were significantly upregulated ($P_{adj}$<0.05 and $|\log_2(\text{Fold Change})|$>0.65) in INS versus HC B cell subclusters; $P_{adj}$ values were determined using the Benjamini-Hochberg correction. This Supplementary Figure is associated with Figure 2.

## Supplementary Figure 6

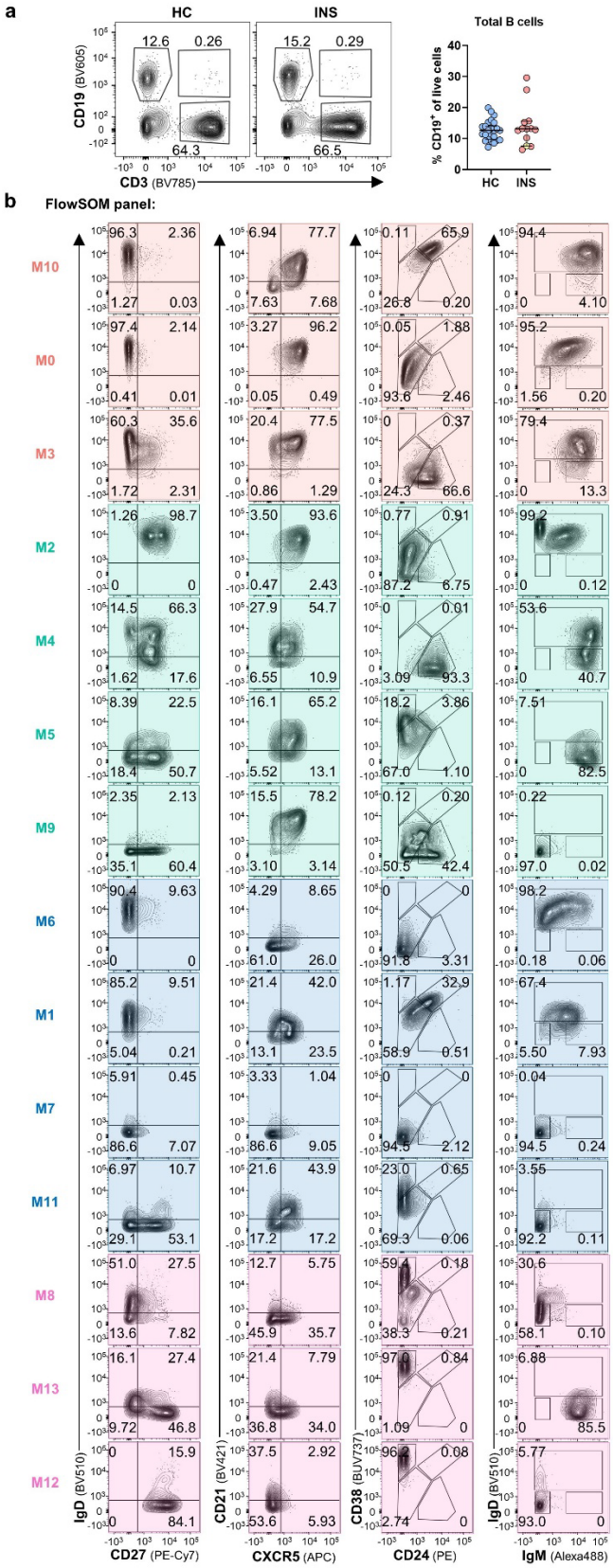

**Supplementary Figure 6: Characterization of B cells in HC and INS children using FlowSOM. a.** Representative flow plots of live PBMC showing total ($CD19^+$) B cells along with the quantification in HC (*n* = 24) and INS (*n* = 13). **b.** Equivalent numbers of randomly selected B cells from HC (*n* = 24; 195,000 B cells) and INS (*n* = 13; 195,000 B cells) children were concatenated and used for FlowSOM clustering on the following markers: CD19, CD20, CD21, IgD, IgM, CD27, CD38, CXCR5, CD1c, and CD24. FlowSOM generated 14 metaclusters (M0-M12). The phenotypes of each cluster using traditional gating strategies for B cells are shown. This Supplementary Figure is associated with Figure 3.

## Supplementary Figure 7

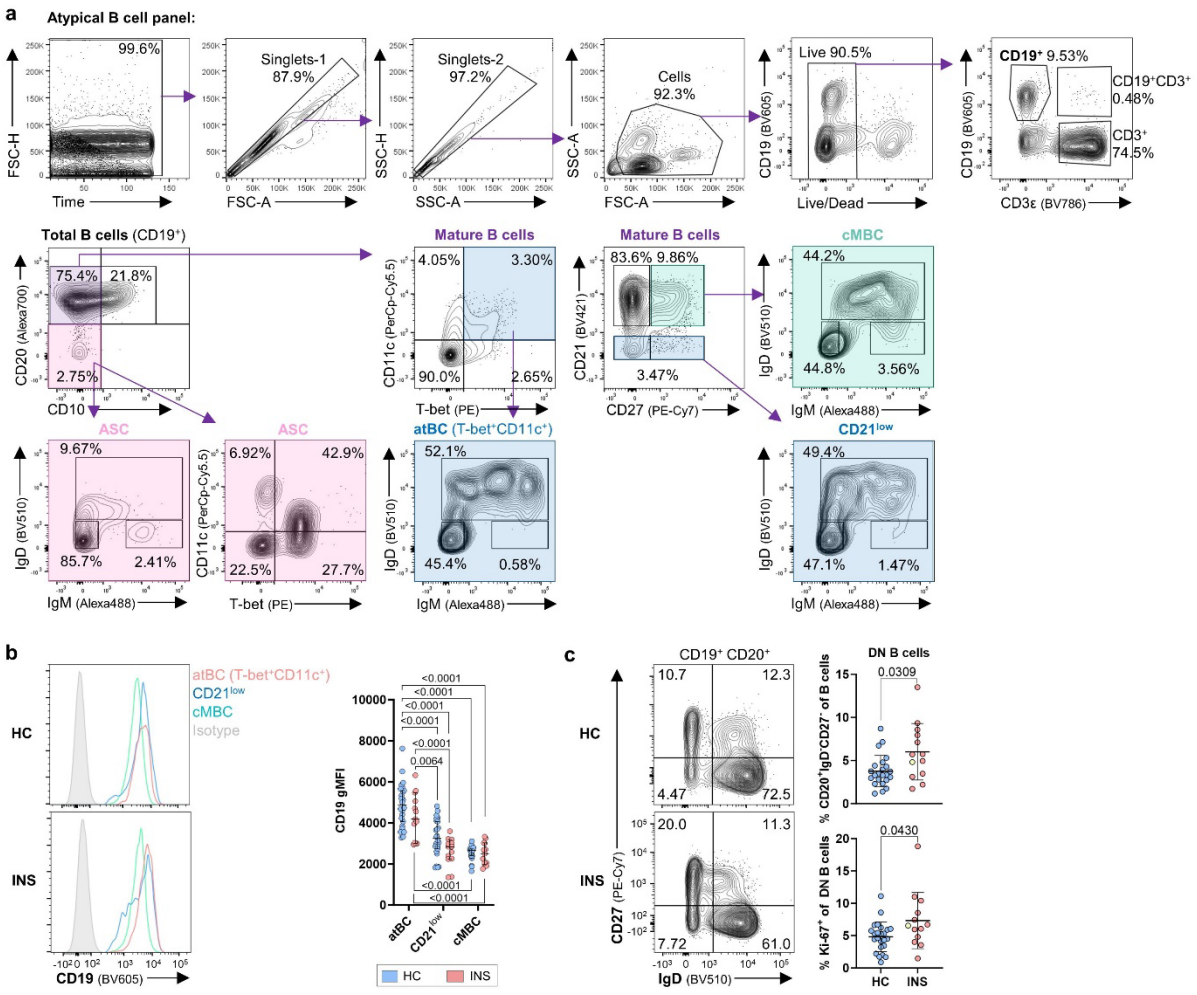

**Supplementary Figure 7: Characterization of atypical B cells in HC and INS PBMC. a.** Gating strategy for atBCs, cMBCs and ASCs. **b.** Representative histograms and quantification of the expression of CD19 in atBC (T-bet$^{+}$ CD11c$^{+}$ CD21$^{low}$ CD19$^{+}$ CD20$^{+}$ CD10$^{-}$), CD21$^{low}$ (CD21$^{low}$ CD19$^{+}$ CD20$^{+}$ CD10$^{-}$), and cMBCs (CD27$^{+}$ CD21$^{+}$ CD19$^{+}$ CD20$^{+}$ CD10$^{-}$) in HC (*n* = 24) and INS (*n* = 13) children. **c.** Representative flow plots and quantification DN B cells (IgD$^{-}$ CD27$^{-}$ CD19$^{+}$ CD20$^{+}$ CD10$^{-}$) in HC (*n* = 24) and INS (*n* = 13) children. Data are shown as median with 95% confidence intervals and *P* values were determined by two-way ANOVA with Tukey's multiple testing (**b**), or two-sided Mann-Whitney U tests (**c**). Each data point corresponds to a single donor. The yellow data point represents the child with glucocorticoid-resistant membranous nephropathy. atBC, atypical B cells; cMBC, classical memory B cells; ASC, antibody-secreting cells. This Supplementary Figure is associated with Figure 4.

## Supplementary Figure 8

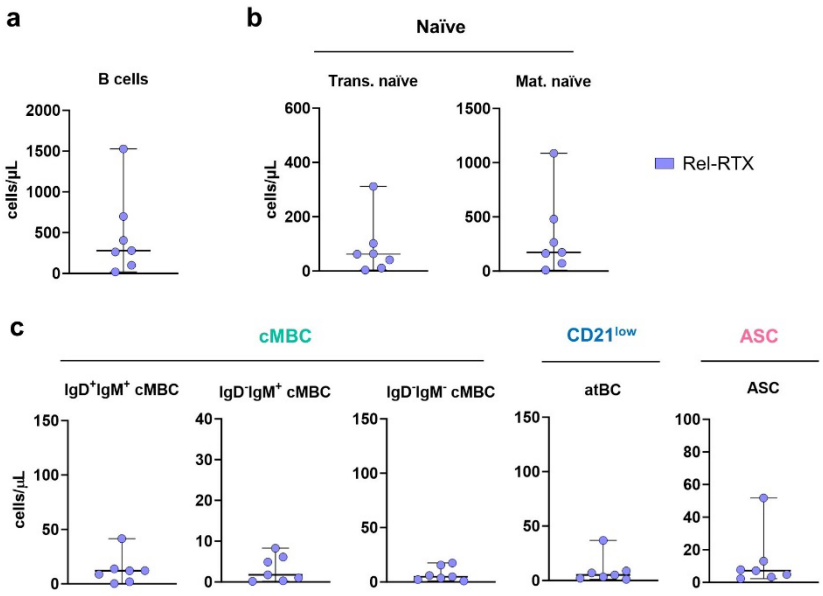

**Supplementary Figure 8: Numbers of B cell subsets in relapses following rituximab therapy. a.-c.** Absolute numbers of total (**a**), naïve (**b**), and memory (**c**) B cell populations in the PBMC of children in post-rituximab relapse (*n* = 7). Rel-RTX, relapse following rituximab. This Supplementary Figure is associated with Figure 5.

## Supplementary Figure 9

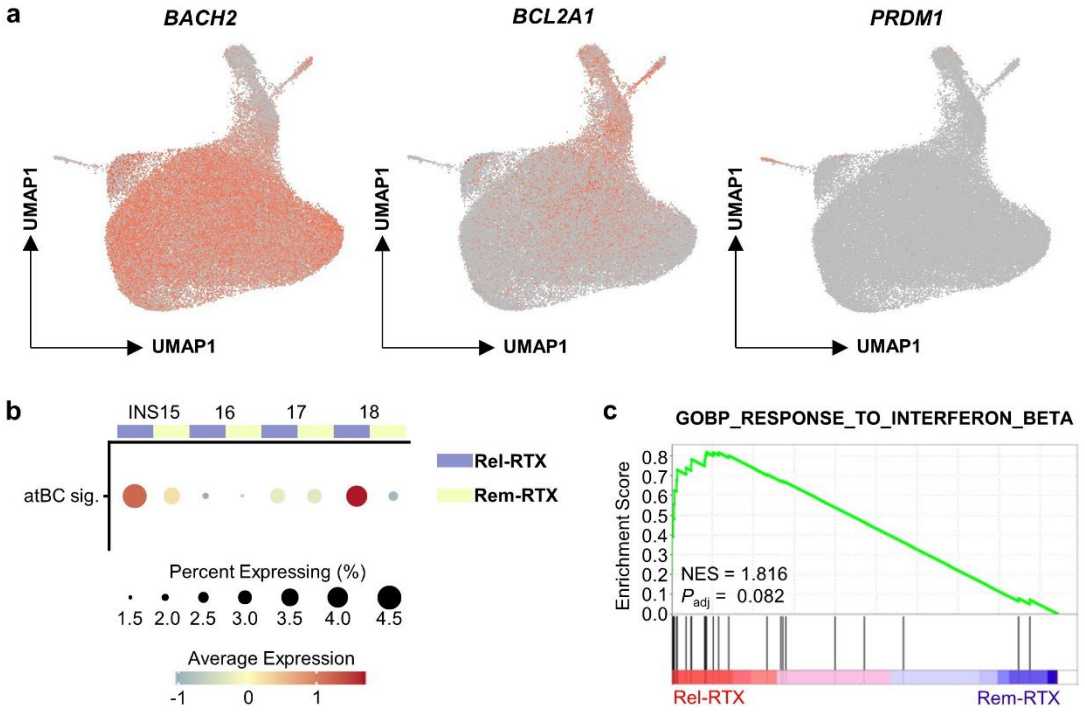

**Supplementary Figure 9: scRNA-seq characterization of memory B cells during relapse or remission following rituximab therapy. a.** Feature plots showing the expression of *BACH2*, *BCL2A1*, and *PRDM1* on the integrated UMAP clusters of post-rituximab relapse and remission B cells. Rel-RTX, relapse following rituximab; Rem-RTX, remission maintained by rituximab. **b.** Bubble plot showing the module score of the atBC signature in total B cells from each donor during post-RTX relapse and remission. **c.** Gene set enrichment analysis (GSEA) of the Gene Ontology term "Response to Interferon Beta" (GO:0035456) in Rel-RTX memory B cells. $P_{adj}$ value was determined using the Benjamini-Hochberg correction for multiple comparisons. NES, normalized enrichment score. This Supplementary Figure is associated with Figure 6.

## Supplementary Figure 10

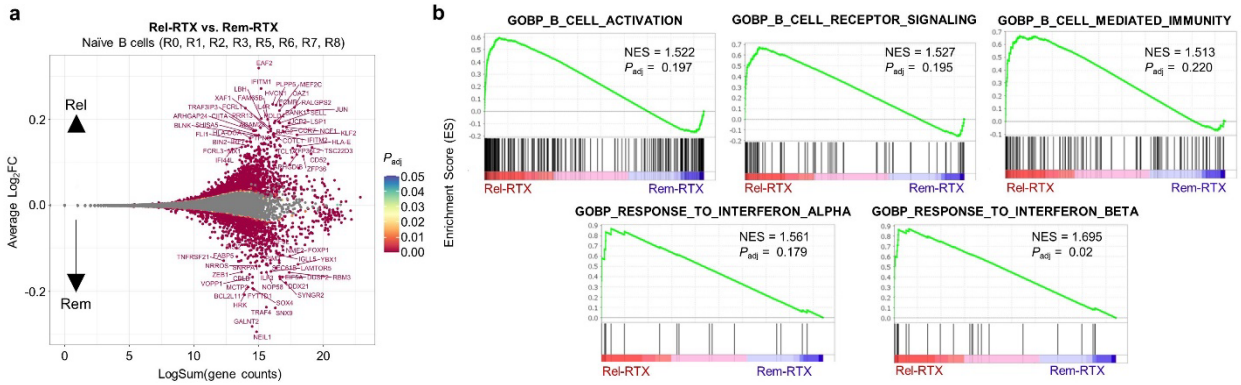

**Supplementary Figure 10: scRNA-seq characterization of naïve B cells during relapse or remission following RTX therapy. a.** MA plot showing the differential expression of genes within all naïve B cells (subclusters R0, R1, R2, R3, R5, R6, R7, and R8) between Rel-RTX and Rem-RTX. Rel-RTX, relapse following rituximab; Rem-RTX, remission maintained by rituximab. **b.** Gene set enrichment analysis (GSEA) showing the enrichment of various Gene Ontology Biological Processes (GOBP) pathway within the relapse-associated naïve B cells. $P_{adj}$ values were determined using the Benjamini-Hochberg correction for multiple comparisons. NES, normalized enrichment score. This Supplementary Figure is associated with Figure 7.

**Supplementary Table 1 – Patient characteristics**

| | INS | Rel-RTX | Rem-GC | Rem-RTX |
|---|---|---|---|---|
| Number (M/F) | 14 (7/7) | 7 (2/5) | 13 (6/7) | 14 (5/9) |
| Median age (years, IQR) | 8.1 (6.2-10.6) | 9.7 (9.1-10.5) | 9.9 (7.0-11.9) | 9.2 (7.2-10.7) |
| Median uPCR (g/mmol, IQR) | 1.02 (0.47-1.58) | 0.75 (0.67-0.79) | 0.01 (0.01-0.02) | 0.01 (0.01-0.01) |
| Stage of disease | | | | |
| First onset | 3 | 0 | N/A | N/A |
| Relapse | 11 | 7 | N/A | N/A |
| Remission | N/A | N/A | 13 | 14 |
| Diagnosis | | | | |
| SSNS | 13 | 7 | 13 | 14 |
| SRNS | 1 | 0 | 0 | 0 |
| Biopsy | | | | |
| MCD | 0 | 2 | 1 | 3 |
| FSGS | 1 | 1 | 0 | 1 |
| MN | 1 | 0 | 0 | 0 |
| Not done | 12 | 4 | 12 | 10 |
| Current medication | | | | |
| Prednisone | 3 | 1 | 0 | 0 |
| Tacrolimus | 1 | 1 | 0 | 1 |
| MMF | 0 | 0 | 2 | 0 |
| Leflunomide | 2 | 0 | 2 | 0 |
| Previous medication | | | | |
| Prednisone | 7 | 0 | 13 | 11 |
| Tacrolimus | 1 | 0 | 0 | 0 |
| MMF | 1 | 0 | 1 | 1 |
| Rituximab | 0 | 7 | 0 | 14 |
| Median time since RTX infusion (months, IQR) | N/A | 9 (8.5-13.5) | N/A | 5.5 (4-7.25) |
| Comorbidities | | | | |
| *Infectious* | | | | |
| URTI | 5 | 2 | 0 | 0 |
| Skin | 2 | 0 | 0 | 0 |
| Gastrointestinal | 0 | 1 | 0 | 0 |
| *Inflammatory* | | | | |
| Airway (e.g. asthma) | 1 | 1 | 0 | 0 |
| Skin (e.g. eczema) | 1 | 2 | 0 | 0 |

uPCR = urinary protein-to-creatinine ratio; SSNS = steroid-sensitive nephrotic syndrome; SRNS = steroid-resistant nephrotic syndrome; MCD = minimal change disease; FSGS = focal segmental glomerulosclerosis; MN = membranous nephropathy; MMF = mycophenolate mofetil; URTI = upper respiratory tract infection.

## 2.10 References


1 Noone, D. G., Iijima, K. & Parekh, R. Idiopathic nephrotic syndrome in children. *The Lancet* **392**, 61-74 (2018). https://doi.org:https://doi.org/10.1016/S0140-6736(18)30536-1

2 Eddy, A. A. & Symons, J. M. Nephrotic syndrome in childhood. *The Lancet* **362**, 629-639 (2003). https://doi.org:10.1016/S0140-6736(03)14184-0

3 Samuel, S. M. *et al.* Setting New Directions for Research in Childhood Nephrotic Syndrome: Results From a National Workshop. *Can J Kidney Health Dis* **4**, 2054358117703386 (2017). https://doi.org:10.1177/2054358117703386

4 Liu, J. & Guan, F. B cell phenotype, activity, and function in idiopathic nephrotic syndrome. *Pediatric Research* (2022). https://doi.org:10.1038/s41390-022-02336-w

5 Takei, T. *et al.* Effect of single-dose rituximab on steroid-dependent minimal-change nephrotic syndrome in adults. *Nephrol Dial Transplant* **28**, 1225-1232 (2013). https://doi.org:10.1093/ndt/gfs515

6 Iijima, K. *et al.* Rituximab for childhood-onset, complicated, frequently relapsing nephrotic syndrome or steroid-dependent nephrotic syndrome: a multicentre, double-blind, randomised, placebo-controlled trial. *The Lancet* **384**, 1273-1281 (2014). https://doi.org:10.1016/S0140-6736(14)60541-9

7 Gauckler, P. *et al.* Rituximab in adult minimal change disease and focal segmental glomerulosclerosis - What is known and what is still unknown? *Autoimmunity Reviews* **19**, 102671 (2020). https://doi.org:https://doi.org/10.1016/j.autrev.2020.102671

8 Printza, N., Papachristou, F., Tzimouli, V., Taparkou, A. & Kanakoudi-Tsakalidou, F. Peripheral CD19+ B cells are increased in children with active steroid-sensitive nephrotic syndrome. *NDT Plus* **2**, 435-436 (2009). https://doi.org:10.1093/ndtplus/sfp087

9 Colucci, M. *et al.* B cell phenotype in pediatric idiopathic nephrotic syndrome. *Pediatric Nephrology* **34**, 177-181 (2019). https://doi.org:10.1007/s00467-018-4095-z

10 Ling, C. *et al.* Altered B-Lymphocyte Homeostasis in Idiopathic Nephrotic Syndrome. *Front Pediatr* **7**, 377 (2019). https://doi.org:10.3389/fped.2019.00377

11 Ling, C. *et al.* Decreased Circulating Transitional B-Cell to Memory B-Cell Ratio Is a Risk Factor for Relapse in Children with Steroid-Sensitive Nephrotic Syndrome. *Nephron* **145**, 107-112 (2021). https://doi.org:10.1159/000511319

12 Akkaya, M., Kwak, K. & Pierce, S. K. B cell memory: building two walls of protection against pathogens. *Nature Reviews Immunology* **20**, 229-238 (2020). https://doi.org:10.1038/s41577-019-0244-2

13 Oniszczuk, J. *et al.* Circulating plasmablasts and high level of BAFF are hallmarks of minimal change nephrotic syndrome in adults. *Nephrol Dial Transplant* **36**, 609-617 (2021). https://doi.org:10.1093/ndt/gfaa279

14 Yang, X. *et al.* Circulating follicular T helper cells are possibly associated with low levels of serum immunoglobulin G due to impaired immunoglobulin class-switch recombination of B cells in children with primary nephrotic syndrome. *Molecular Immunology* **114**, 162-170 (2019). https://doi.org:https://doi.org/10.1016/j.molimm.2019.07.001

15 Watts, A. J. B. *et al.* Discovery of Autoantibodies Targeting Nephrin in Minimal Change Disease Supports a Novel Autoimmune Etiology. *Journal of the American Society of Nephrology* **33**, 238 (2022). https://doi.org:10.1681/ASN.2021060794

16 Ye, Q. *et al.* Seven novel podocyte autoantibodies were identified to diagnosis a new disease subgroup-autoimmune Podocytopathies. *Clin Immunol* **232**, 108869 (2021). https://doi.org:10.1016/j.clim.2021.108869

17 Ye, Q. *et al.* The important roles and molecular mechanisms of annexin A(2) autoantibody in children with nephrotic syndrome. *Ann Transl Med* **9**, 1452 (2021). https://doi.org:10.21037/atm-21-3988

18 Ravani, P. *et al.* Short-term effects of rituximab in children with steroid- and calcineurin-dependent nephrotic syndrome: a randomized controlled trial. *Clin J Am Soc Nephrol* **6**, 1308-1315 (2011). https://doi.org:10.2215/CJN.09421010

19 Sellier-Leclerc, A. L. *et al.* Rituximab in steroid-dependent idiopathic nephrotic syndrome in childhood--follow-up after CD19 recovery. *Nephrol Dial Transplant* **27**, 1083-1089 (2012). https://doi.org:10.1093/ndt/gfr405

20 Colucci, M. *et al.* B Cell Reconstitution after Rituximab Treatment in Idiopathic Nephrotic Syndrome. *J Am Soc Nephrol* **27**, 1811-1822 (2016). https://doi.org:10.1681/ASN.2015050523

21 Lee, D. S. W., Rojas, O. L. & Gommerman, J. L. B cell depletion therapies in autoimmune disease: advances and mechanistic insights. *Nature Reviews Drug Discovery* **20**, 179-199 (2021). https://doi.org:10.1038/s41573-020-00092-2

22 Elsner, R. A. & Shlomchik, M. J. Germinal Center and Extrafollicular B Cell Responses in Vaccination, Immunity, and Autoimmunity. *Immunity* **53**, 1136-1150 (2020). https://doi.org:10.1016/j.immuni.2020.11.006

23 Lam, J. H., Smith, F. L. & Baumgarth, N. B Cell Activation and Response Regulation During Viral Infections. *Viral Immunol* **33**, 294-306 (2020). https://doi.org:10.1089/vim.2019.0207

24 Jenks, S. A. *et al.* Distinct Effector B Cells Induced by Unregulated Toll-like Receptor 7 Contribute to Pathogenic Responses in Systemic Lupus Erythematosus. *Immunity* **49**, 725-739.e726 (2018). https://doi.org:10.1016/j.immuni.2018.08.015

25 Woodruff, M. C. *et al.* Extrafollicular B cell responses correlate with neutralizing antibodies and morbidity in COVID-19. *Nat Immunol* **21**, 1506-1516 (2020). https://doi.org:10.1038/s41590-020-00814-z

26 Ambegaonkar, A. A., Holla, P., Dizon, B. L. P., Sohn, H. & Pierce, S. K. Atypical B cells in chronic infectious diseases and systemic autoimmunity: puzzles with many

missing pieces. *Current Opinion in Immunology* **77**, 102227 (2022). https://doi.org:https://doi.org/10.1016/j.coi.2022.102227

27 Holla, P. *et al.* Shared transcriptional profiles of atypical B cells suggest common drivers of expansion and function in malaria, HIV, and autoimmunity. *Sci Adv* **7** (2021). https://doi.org:10.1126/sciadv.abg8384

28 Sutton, H. J. *et al.* Atypical B cells are part of an alternative lineage of B cells that participates in responses to vaccination and infection in humans. *Cell Rep* **34**, 108684 (2021). https://doi.org:10.1016/j.celrep.2020.108684

29 Malle, L. *et al.* Autoimmunity in Down's syndrome via cytokines, CD4 T cells and CD11c+ B cells. *Nature* **615**, 305-314 (2023). https://doi.org:10.1038/s41586-023-05736-y

30 Wang, S. *et al.* IL-21 drives expansion and plasma cell differentiation of autoreactive CD11c(hi)T-bet(+) B cells in SLE. *Nat Commun* **9**, 1758 (2018). https://doi.org:10.1038/s41467-018-03750-7

31 Claes, N. *et al.* Age-Associated B Cells with Proinflammatory Characteristics Are Expanded in a Proportion of Multiple Sclerosis Patients. *J Immunol* **197**, 4576-4583 (2016). https://doi.org:10.4049/jimmunol.1502448

32 Csomos, K. *et al.* Partial RAG deficiency in humans induces dysregulated peripheral lymphocyte development and humoral tolerance defect with accumulation of T-bet(+) B cells. *Nat Immunol* **23**, 1256-1272 (2022). https://doi.org:10.1038/s41590-022-01271-6

33 Portugal, S. *et al.* Malaria-associated atypical memory B cells exhibit markedly reduced B cell receptor signaling and effector function. *Elife* **4** (2015). https://doi.org:10.7554/eLife.07218

34 MacDonald, N. E., Wolfish, N., McLaine, P., Phipps, P. & Rossier, E. Role of respiratory viruses in exacerbations of primary nephrotic syndrome. *J Pediatr* **108**, 378-382 (1986). https://doi.org:10.1016/s0022-3476(86)80876-9

35 Alwadhi, R. K., Mathew, J. L. & Rath, B. Clinical profile of children with nephrotic syndrome not on glucorticoid therapy, but presenting with infection. *J Paediatr Child Health* **40**, 28-32 (2004). https://doi.org:10.1111/j.1440-1754.2004.00285.x

36 Christian, M. T. *et al.* Evaluation of Daily Low-Dose Prednisolone During Upper Respiratory Tract Infection to Prevent Relapse in Children With Relapsing Steroid-Sensitive Nephrotic Syndrome: The PREDNOS 2 Randomized Clinical Trial. *JAMA Pediatr* **176**, 236-243 (2022). https://doi.org:10.1001/jamapediatrics.2021.5189

37 Crowell, H. L. *et al.* muscat detects subpopulation-specific state transitions from multi-sample multi-condition single-cell transcriptomics data. *Nature Communications* **11**, 6077 (2020). https://doi.org:10.1038/s41467-020-19894-4

38 Price, M. J., Patterson, D. G., Scharer, C. D. & Boss, J. M. Progressive Upregulation of Oxidative Metabolism Facilitates Plasmablast Differentiation to a T-Independent Antigen. *Cell Rep* **23**, 3152-3159 (2018). https://doi.org:10.1016/j.celrep.2018.05.053

39 Urbanczyk, S. *et al.* Mitochondrial respiration in B lymphocytes is essential for humoral immunity by controlling the flux of the TCA cycle. *Cell Reports* **39**, 110912 (2022). https://doi.org:https://doi.org/10.1016/j.celrep.2022.110912

40 Kwak, K. *et al.* Intrinsic properties of human germinal center B cells set antigen affinity thresholds. *Sci Immunol* **3** (2018). https://doi.org:10.1126/sciimmunol.aau6598

41 Keenan, A. B. *et al.* ChEA3: transcription factor enrichment analysis by orthogonal omics integration. *Nucleic Acids Research* **47**, W212-W224 (2019). https://doi.org:10.1093/nar/gkz446

42 Laidlaw, B. J. & Cyster, J. G. Transcriptional regulation of memory B cell differentiation. *Nature Reviews Immunology* **21**, 209-220 (2021). https://doi.org:10.1038/s41577-020-00446-2

43 Fraschilla, I. & Jeffrey, K. L. The Speckled Protein (SP) Family: Immunity's Chromatin Readers. *Trends Immunol* **41**, 572-585 (2020). https://doi.org:10.1016/j.it.2020.04.007

44 Hafler, D. *et al.* Type I Interferon Transcriptional Network Regulates Expression of Coinhibitory Receptors in Human T cells. *Res Sq* (2021). https://doi.org:10.21203/rs.3.rs-133494/v1

45 Tull, T. J. *et al.* Human marginal zone B cell development from early T2 progenitors. *J Exp Med* **218** (2021). https://doi.org:10.1084/jem.20202001

46 Siu, J. H. Y. *et al.* Two subsets of human marginal zone B cells resolved by global analysis of lymphoid tissues and blood. *Science Immunology* **7**, eabm9060 (2022). https://doi.org:doi:10.1126/sciimmunol.abm9060

47 Gatto, D. & Brink, R. B cell localization: regulation by EBI2 and its oxysterol ligand. *Trends in Immunology* **34**, 336-341 (2013). https://doi.org:10.1016/j.it.2013.01.007

48 Trapnell, C. *et al.* The dynamics and regulators of cell fate decisions are revealed by pseudotemporal ordering of single cells. *Nature Biotechnology* **32**, 381-386 (2014). https://doi.org:10.1038/nbt.2859

49 MacLennan, I. C. M. & Vinuesa, C. G. Dendritic Cells, BAFF, and APRIL: Innate Players in Adaptive Antibody Responses. *Immunity* **17**, 235-238 (2002). https://doi.org:10.1016/S1074-7613(02)00398-9

50 Mohr, E. *et al.* Dendritic cells and monocyte/macrophages that create the IL-6/APRIL-rich lymph node microenvironments where plasmablasts mature. *J Immunol* **182**, 2113-2123 (2009). https://doi.org:10.4049/jimmunol.0802771

51 Jin, S. *et al.* Inference and analysis of cell-cell communication using CellChat. *Nature Communications* **12**, 1088 (2021). https://doi.org:10.1038/s41467-021-21246-9

52 Jenks, S. A., Cashman, K. S., Woodruff, M. C., Lee, F. E. & Sanz, I. Extrafollicular responses in humans and SLE. *Immunol Rev* **288**, 136-148 (2019). https://doi.org:10.1111/imr.12741

53 Fribourg, M. *et al.* CyTOF-Enabled Analysis Identifies Class-Switched B Cells as the Main Lymphocyte Subset Associated With Disease Relapse in Children With Idiopathic Nephrotic Syndrome. *Front Immunol* **12**, 726428 (2021). https://doi.org:10.3389/fimmu.2021.726428

54 Warnatz, K. *et al.* Expansion of CD19(hi)CD21(lo/neg) B cells in common variable immunodeficiency (CVID) patients with autoimmune cytopenia. *Immunobiology* **206**, 502-513 (2002). https://doi.org:10.1078/0171-2985-00198

55 Wehr, C. *et al.* A new CD21low B cell population in the peripheral blood of patients with SLE. *Clin Immunol* **113**, 161-171 (2004). https://doi.org:10.1016/j.clim.2004.05.010

56 Isnardi, I. *et al.* Complement receptor 2/CD21− human naive B cells contain mostly autoreactive unresponsive clones. *Blood* **115**, 5026-5036 (2010). https://doi.org:10.1182/blood-2009-09-243071

57 Wildner, N. H. *et al.* B cell analysis in SARS-CoV-2 versus malaria: Increased frequencies of plasmablasts and atypical memory B cells in COVID-19. *J Leukoc Biol* **109**, 77-90 (2021). https://doi.org:10.1002/jlb.5cova0620-370rr

58 Keller, B. *et al.* The expansion of human T-bet(high)CD21(low) B cells is T cell dependent. *Sci Immunol* **6**, eabh0891 (2021). https://doi.org:10.1126/sciimmunol.abh0891

59 Haga, C. L., Ehrhardt, G. R. A., Boohaker, R. J., Davis, R. S. & Cooper, M. D. Fc receptor-like 5 inhibits B cell activation via SHP-1 tyrosine phosphatase recruitment. *Proceedings of the National Academy of Sciences* **104**, 9770-9775 (2007). https://doi.org:doi:10.1073/pnas.0703354104

60 Chappell, C. P., Draves, K. E., Giltiay, N. V. & Clark, E. A. Extrafollicular B cell activation by marginal zone dendritic cells drives T cell-dependent antibody responses. *J Exp Med* **209**, 1825-1840 (2012). https://doi.org:10.1084/jem.20120774

61 Palm, A.-K. E. & Kleinau, S. Marginal zone B cells: From housekeeping function to autoimmunity? *Journal of Autoimmunity* **119**, 102627 (2021). https://doi.org:https://doi.org/10.1016/j.jaut.2021.102627

62 Ye, Q., Liu, H., Wang, D. & Mao, J. Comprehensive mapping of B lymphocyte immune dysfunction in idiopathic nephrotic syndrome children. *Clin Transl Med* **13**, e1177 (2023). https://doi.org:10.1002/ctm2.1177

63 Stone, S. L. *et al.* T-bet Transcription Factor Promotes Antibody-Secreting Cell Differentiation by Limiting the Inflammatory Effects of IFN-γ on B Cells. *Immunity* **50**, 1172-1187.e1177 (2019). https://doi.org:10.1016/j.immuni.2019.04.004

64 Dossier, C., Jamin, A. & Deschênes, G. Idiopathic nephrotic syndrome: the EBV hypothesis. *Pediatric Research* **81**, 233-239 (2017). https://doi.org:10.1038/pr.2016.200

65 Smatti, M. K. *et al.* Viruses and Autoimmunity: A Review on the Potential Interaction and Molecular Mechanisms. *Viruses* **11** (2019). https://doi.org:10.3390/v11080762

66 Bashford-Rogers, R. J. M. *et al.* Analysis of the B cell receptor repertoire in six immune-mediated diseases. *Nature* **574**, 122-126 (2019). https://doi.org:10.1038/s41586-019-1595-3

67 Crickx, E. *et al.* Rituximab-resistant splenic memory B cells and newly engaged naive B cells fuel relapses in patients with immune thrombocytopenia. *Sci Transl Med* **13** (2021). https://doi.org:10.1126/scitranslmed.abc3961

68 Wallin, E. F. *et al.* Human T-follicular helper and T-follicular regulatory cell maintenance is independent of germinal centers. *Blood* **124**, 2666-2674 (2014). https://doi.org:10.1182/blood-2014-07-585976

69 Samuel, S. *et al.* The Canadian Childhood Nephrotic Syndrome (CHILDNEPH) Project: overview of design and methods. *Canadian Journal of Kidney Health and Disease* **1**, 17 (2014). https://doi.org:10.1186/2054-3581-1-17

70 Hao, Y. *et al.* Integrated analysis of multimodal single-cell data. *Cell* **184**, 3573-3587.e3529 (2021). https://doi.org:10.1016/j.cell.2021.04.048

71 Rosain, J. *et al.* Human IRF1 governs macrophagic IFN-γ immunity to mycobacteria. *Cell* **186**, 621-645.e633 (2023). https://doi.org:https://doi.org/10.1016/j.cell.2022.12.038

72 McGinnis, C. S., Murrow, L. M. & Gartner, Z. J. DoubletFinder: Doublet Detection in Single-Cell RNA Sequencing Data Using Artificial Nearest Neighbors. *Cell Systems* **8**, 329-337.e324 (2019). https://doi.org:10.1016/j.cels.2019.03.003

73 Raudvere, U. *et al.* g:Profiler: a web server for functional enrichment analysis and conversions of gene lists (2019 update). *Nucleic Acids Research* **47**, W191-W198 (2019). https://doi.org:10.1093/nar/gkz369

74 Merico, D., Isserlin, R., Stueker, O., Emili, A. & Bader, G. D. Enrichment Map: A Network-Based Method for Gene-Set Enrichment Visualization and Interpretation. *PLOS ONE* **5**, e13984 (2010). https://doi.org:10.1371/journal.pone.0013984

75 Jin, S. *et al.* Inference and analysis of cell-cell communication using CellChat. *Nat Commun* **12**, 1088 (2021). https://doi.org:10.1038/s41467-021-21246-9

76 Quintelier, K. *et al.* Analyzing high-dimensional cytometry data using FlowSOM. *Nature Protocols* **16**, 3775-3801 (2021). https://doi.org:10.1038/s41596-021-00550-0

# CHAPTER 3: Memory B cells are clonally expanded in anti-CRB2-positive children with idiopathic nephrotic syndrome

**Memory B cells are clonally expanded in anti-CRB2-positive children with idiopathic nephrotic syndrome**

Tho-Alfakar Al-Aubodah[1,2,3,4], Simon Leclerc[2,3,4,5], Lamine Aoudjit[3,4], Roman Istomine[1,2], Giuseppe Pascale[4], Maneka A. Perinpanayagam[6], Susan M. Samuel[6], Ciriaco A. Piccirillo[1,2,5,*], Tomoko Takano[3,4,5,*]

[1] Department of Microbiology & Immunology, Faculty of Medicine and Health Sciences, McGill University, Montréal, Québec
[2] Infectious Diseases and Immunity in Global Health Program, Research Institute of the McGill University Health Centre, Montréal, Québec
[3] Metabolic Disorders and Complications Program, Research Institute of the McGill University Health Centre, Montréal, Québec
[4] Division of Nephrology, Faculty of Medicine and Health Sciences, McGill University, Montréal, Québec
[5] Department of Experimental Medicine, Faculty of Medicine and Health Sciences, McGill University, Montréal, Québec
[6] Section of Nephrology, Department of Pediatrics, Cumming School of Medicine, University of Calgary, Calgary, Alberta

*Correspondence should be addressed to:
**Dr. Tomoko Takano, M.D., Ph.D.**
Research Institute of the McGill University Health Centre (RI-MUHC),
Metabolic Disorders and Complications Program, Division of Nephrology
1001 Boulevard Décarie, Bloc E, Room EM1.3244
Montréal, Québec H4A 3J1, Canada
E-mail: tomoko.takano@mcgill.ca

**Dr. Ciriaco A. Piccirillo, Ph.D.**
Research Institute of the McGill University Health Centre (RI-MUHC),
Infectious Diseases and Immunity in Global Health Program
1001 Boulevard Décarie, Bloc E, Room EM2.3248
Montréal, Québec H4A 3J1, Canada
E-mail: ciro.piccirillo@mcgill.ca

**Manuscript in preparation.**

### 3.1 Bridging Statement

In *Chapter 2*, we showed that active INS is associated with the expansion of eMBCs and plasmablasts/SLPCs, thereby implicating extrafollicular B cell responses in INS pathogenesis. These were namely $CD21^{low}$ T-$bet^{+}$ $CD11c^{+}$ atBCs and MZ-like B cells, both of which have been previously implicated in several autoimmune diseases (39, 95). The induction of extrafollicular responses following viral infection and their capacity to rapidly output $IgM^{+}$ plasmablasts/SLPCs provides an immunological basis for understanding two salient features of childhood INS: that relapses tend to occur alongside a viral infection and that long-lasting remission is achieved with RTX therapy (412, 434). Nevertheless, we also observed an expansion in isotype-switched cMBCs ($CD21^{+}$ $CD27^{+}$ $IgD^{-}$ $IgM^{-}$) during active INS and that their resurgence was associated with relapses following RTX treatment, as had been previously reported (425). It remained to be determined whether the expansion of eMBCs, cMBCs, and ASCs constituted a *bona fide* B cell response and, importantly, whether these responses support the production of APAs. In *Chapter 3*, we address this research gap by performing scRNA-seq on eight children with active INS pairing both gene expression and V(D)J sequencing data. Four of these children were seropositive for antibodies targeting CRB2, a type-I transmembrane glycoprotein present at the slit diaphragm that regulates the podocyte actin cytoskeleton, APAs that were recently described by our group in 24% of MCD cases and 52% of FSGS (*data unpublished*). *We hypothesized that the expansion of MBCs and ASCs in childhood INS was antigen-driven (i.e. oligoclonal) and contributed to the production of APAs*.

### 3.2 Abstract

The expansion of memory B cells (MBC) in idiopathic nephrotic syndrome (INS) and its sensitivity to B cell depletion with rituximab is strongly indicative of a humoral autoimmune origin of disease. Whether this expansion of MBCs constitutes an autoantigen-driven B cell response remains unknown. Here, we conducted single-cell RNA-sequencing paired with BCR-sequencing on B cells from eight children with INS, four of whom were seropositive for podocytopathic anti-CRB2 autoantibodies. We identified highly clonal MBC responses in all anti-CRB2+ individuals but only two of the anti-CRB2– donors. These included antibody-secreting cells and two TACI-expressing MBC subsets, one that resembled marginal zone B cells and another isotype-switched classical MBC. High rates of somatic hypermutation indicated a mature B cell response. Altogether, we propose that the expansion of MBCs in INS is antigen-driven and is associated with the production of anti-podocyte autoantibodies.

### 3.3 Introduction

Podocyte injury underlies the pathogenesis of idiopathic nephrotic syndrome (INS), the most prevalent glomerular disease in children, resulting in recurrent episodes of massive proteinuria and edema[1,2]. Minimal change disease (MCD) – where the podocyte lesion is the only histopathological feature – accounts for 80-90% of childhood cases, while more extensive focal segmental glomerulosclerosis (FSGS) is the major manifestation of INS in adults[2]. In all cases, the cause of podocyte injury remains completely unknown. A B cell etiology is suspected given the efficacy of B cell depletion with rituximab at maintaining long-term remission[3,4]. Nevertheless, many patients continue to relapse, often requiring prolonged states of B cell deficiency to prevent proteinuria. Moreover, immunosuppression with glucocorticoids remains to be the most common treatment for childhood INS, despite their unfavorable safety profile[5]. To develop safer, more targeted, and durable drugs, a better understanding of disease pathogenesis is needed.

The expansion of memory B cells (MBCs) in childhood and adult INS supports a B cell origin for podocyte injury[3,6-8]. Notably, isotype-switched classical MBCs (cMBCs, $CD21^{+}$ $CD27^{+}$ $IgD^{-}$ $IgM^{-}$) are particularly abundant during active disease and their resurgence is associated with relapses following rituximab therapy, thereby implicating follicular B cell responses in INS pathogenesis[7,9]. Here, activated B cells undergo class-switch recombination (CSR) and somatic hypermutation (SHM) in germinal centers to augment the affinity of their BCRs, resulting in the generation of highly mature isotype-switched cMBCs and long-lived antibody-secreting cells (ASCs) [10]. Recently, we showed that extrafollicular MBCs (eMBCs), namely $CD21^{low}$ T-$bet^{+}$ $CD11c^{+}$ atypical B cells (atBCs) and TACI (*TNFRSF13B*)-expressing marginal zone (MZ)-like B cells, are also expanded in childhood INS, thereby implicating extrafollicular B cell responses in pathogenesis[7]. Unlike follicular responses, extrafollicular responses primarily yield short-lived ASCs that are sensitive to rituximab treatment and undergo lower rates of CSR and SHM driven by TACI signaling[11-14]. Accordingly, we also observed a significant expansion of rituximab-sensitive short-lived ASCs in childhood INS and the engagement of the APRIL (*TNFSF13*)/BAFF (*TNFSF13B*)-TACI signaling network[7]. Since these eMBCs are enriched with autoreactive clones and are

implicated in the pathogenesis of several autoimmune diseases, the extrafollicular response may represent a route for autoreactivity in childhood INS[12,15-20]. Nevertheless, whether the expansion of eMBCs and isotype-switched cMBCs in INS constitutes a *bona fide* B cell response remains unknown.

The recent description of anti-podocyte autoantibodies (APAs) against several podocyte autoantigens in INS further supports a humoral autoimmune etiology. Autoantibodies against Nephrin, a major component of the podocyte slit diaphragm, were recently described in the blood of approximately 22% of children and 43% of adults with active MCD and were further associated with the recurrence of FSGS in children who received kidney transplants[21,22]. Furthermore, we recently showed that autoantibodies against CRB2, another slit diaphragm protein, were present in 24% of MCD cases and 52% of FSGS[23,24]. In mouse models, both anti-Nephrin and anti-CRB2 induce podocyte injury and proteinuria thereby establishing their podocytopathic potential[25,26]. We hypothesized that the expansion of MBCs and ASCs in INS may be associated with the production of APAs.

In this study, we characterize the clonality of B cells in anti-CRB2+ and anti-CRB2– children during active INS. Using single-cell RNA-sequencing (scRNA-seq), we demonstrate that MZ-like B cells are expanded in both anti-CRB2+ and anti-CRB2– children alongside a population of isotype-switched cMBC that also expresses high levels of *TNFRSF13B*. While highly clonal MBCs were observed in all four anti-CRB2+ individuals analyzed, only two of the four anti-CRB2– children showed high clonality. These clonal MBCs were predominantly composed of MZ-like B cells, *TNFRSF13B*-expressing isotype-switched cMBCs, and ASCs, thereby supporting their involvement in INS pathogenesis. Finally, we show that clonal MBCs underwent significant SHM denoting a mature B cell response. In total, we propose that the expansion of MBCs and ASCs observed in childhood INS is antigen-driven and is associated with APA production.

## 3.4 Results

### *3.4.1. ASCs and TNFRSF13B-expressing MBCs are expanded in childhood INS.*

We previously showed that ASCs are highly expanded in children during active INS[7]. Here, we sought to correlate ASC expansion with the production of APAs. To this end, we immunophenotyped peripheral blood B cells in 18 children with active INS, five of whom were anti-CRB2+ and all were anti-Nephrin– (**Supplemental Data 1**). ASCs ($CD19^+$ $CD38^{high}$ $CD27^+$) were expanded similarly in both anti-CRB2+ and anti-CRB2– INS children and the frequencies of cycling ASCs were significantly elevated over healthy children denoting their participation in an underlying B cell response (**Fig.1A, B**).

To identify the B cell response driving ASC expansion, we evaluated the clonality of total B cells ($CD19^+$) in four anti-CRB2+ (BCS1, BCS2, BCS5, BCS8) and four anti-CRB2– (BCS3, BCS4, BCS6, BCS7) children using scRNA-seq pairing both gene expression and V(D)J data (**Fig. 1C**). Following quality control, we obtained 11 clusters of 93,910 B cells that were uniformly present across all eight donors (**Fig. 1D, S1A, B**). We acquired V(D)J sequences from 69,879 of these cells. Four of the clusters (B0, B1, B3, and B4) corresponded with naïve B cells as was denoted by elevated *BACH2*, *TCL1A*, *IL4R*, and *FCER2* expression, lack of *BCL2A1*, and a non-switched isotype (**Fig. 1E-G, S1C**). An activated population (B3) amongst the naïve B cells was identified based on *FOS* and *FOSB* expression, and transitional naïve B cells by *NEIL1* (**Fig. S1C**). The remaining B cell clusters corresponded with MBCs (B2, B5, B6, B7, B8, and B9) expressing *BCL2A1*, and ASCs (B10) expressing *JCHAIN* (**Fig. 1E**).

MBCs in clusters B2 and B6 were predominantly isotype non-switched, while the remaining clusters had greater degrees of class-switching (**Fig. 1F, G, S1D**). Both non-switched clusters expressed *TNFRSF13B* (TACI) and *GPR183* (EBI2), genes critical for the formation of extrafollicular B cell responses[13,27], while B6 further expressed the MZ B cell-associated genes *CD1C*, *CD24*, *PLD4*, and *MZB1* (**Fig. 1E, S1C**). As such B2 and B6 were termed non-switched memory (NSM) and MZ-like B cells, respectively. Approximately a third of the B cells in cluster B8 were isotype-switched and expressed genes associated with B cell activation, including *TNFSF9*, *FOS*, *FOSB*, and *CD69*, and were thus termed activated MBCs (actMBC) (**Fig. 1E-G, S1C, D**). Clusters B5 and B7 were termed isotype-switched

cMBCs (SM) as they showed the greatest degree of isotype switching and expressed genes associated with a cMBC phenotype like *S100A10* and *S100A4* (**Fig. 1E-G, S1C, D**). However, class-switching in B5 cells was largely towards IgG isotypes whereas B7 cells were predominantly IgA and, accordingly, expressed high levels of *JCHAIN* (**Fig. 1E-G**). B7 cells also preferentially expressed *TNFRSF13B*, clustering adjacent to the *TNFRSF13B*-expressing MZ-like B cells, and were hence termed SM-TACI B cells. Finally, cluster B9 corresponded with atypical B cells (atBCs) given their high expression of genes associated with this subset including *FCRL5*, *ITGAX*, *HSPB1*, *TNFRSF1B*, and *ZBTB32* (**Fig. 1E, S1C**). We verified that these definitions were consistent with what we defined in our prior scRNA-seq assessment of childhood INS[7] using gene set enrichment analysis (**Fig. S1D**). MZ-like B cells and atBCs, which we previously showed were expanded in INS, had low SHM rates consistent with an extrafollicular origin, whereas the SM and SM-TACI B cells had higher SHM rates highlighting a possible follicular origin (**Fig. 1H**). Only atBCs were significantly expanded in anti-CRB2+ over anti-CRB2– children, with no differences observed in the total MBC compartment (**Fig. 1I, J**).

To verify our previous finding that eMBCs are expanded in childhood INS, we obtained transcriptomic data from scRNA-seq experiments conducted on healthy children from two independent studies (14,861 B cells) [28,29] as well as data from children with childhood SLE (7,153 B cells) [29] and reference mapped them onto the B cell clusters generated herein. We also included B cells from the healthy (2,299 B cells from HC1, HC2, HC3, and HC4) and INS (5,210 B cells from INS1, INS2, and INS4) children from our prior study[7] but excluded INS3 as this individual is the same as BCS1. As we previously showed, the frequency of naïve B cells was significantly reduced in INS, whereas the MZ-like B cells and atBCs were expanded (**Fig. 1K, L**). The degree of expansion of atBC, however, was much higher in children with SLE. We also observed a significant increase in the proportions of the *TNFRSF13B*-expressing SM-TACI and NSM B cells but not SM B cells consistent with the possible involvement of TACI signaling in INS pathogenesis (**Fig. 1K, L**). The actMBC cluster was also expanded in childhood INS. These results confirm our previous findings that eMBCs are expanded in INS

and implicate a group of *TNFRSF13B*-expressing isotype-switched cMBCs in the nephrotic B cell response.

### *3.4.2. MBCs and ASCs are clonally expanded in anti-CRB2+ children.*

While the expansion of MBCs and ASCs is highly indicative of an active B cell response, there is no evidence that it is antigen-driven. To this end, we compared the clonality of B cells from our previous dataset of healthy and INS children and observed that B cell clonality was greater in childhood INS supporting an antigen-driven B cell response (**Fig. S2A, B**). The clonality of B cells from INS2, an anti-CRB2+ individual, was particularly elevated with 2.3% of B cells demonstrating high clonal expansion, which we defined as clones containing at least five B cells (**Fig. S2A, C**).

Next, we assessed the clonality of B cells in childhood INS from our current dataset. Of the eight children, highly clonal responses were present in six, including all four anti-CRB2+ donors (BCS1, BCS2, BCS5, BCS8) and only two of the anti-CRB2– individuals (BCS6, BCS7) (**Fig. 2A, S3A, B**). In these six children, clonal cells were spread across B cell clusters incorporating naïve, memory and ASC populations, as would be expected during an active B cell response (**Fig. 2B**). This clonal sharing between clusters was also observed amongst the clonally expanded B cells from INS2 (**Fig. S3D**). In contrast, clonal sharing was negligible amongst clonally expanded B cells from individuals that lacked highly clonal responses (BCS2 and BCS3) (**Fig. S3C**). To identify the B cell populations participating in these clonal responses, we compared the frequencies of each B cell cluster within non-expanded (singleton) and expanded (≥2 B cells/clone) clonal groups from individuals with highly clonal responses (BCS1, BCS2, BCS4, BCS5, BCS6, BCS7, BCS8, and INS2) (**Fig. 3C-E**). Expectedly, we observed a decrease in the frequencies of all naïve clusters between singleton and expanded clonal groups (**Fig. 3D, E**). Conversely, we saw an increase in the prevalence of the INS-associated *TNFRSF13B*-expressing MBCs, namely the MZ-like and SM-TACI B cells (**Fig. 3D, E**). Accordingly, ASCs, whose extrafollicular development is dependent on TACI signaling, were also more prevalent in expanded clones (**Fig. 3D, E**). Altogether, our data indicate the expansion of INS-associated MBCs and ASCs is antigen-driven.

We next compared the clonality between anti-CRB2+ (BCS1, BCS2, BCS5, BCS8, INS2) and anti-CRB2– (BCS3, BCS4, BCS6, BCS7, INS1, INS4) individuals. Regardless of whether we looked at total or exclusively MBC clonality, anti-CRB2+ individuals tended to have greater levels of highly clonal (≥5 B cells/clone) responses (**Fig. 3F, G**). Nevertheless, the anti-CRB2– individual BCS7 had the greatest degree of clonality in the study (**Fig. 3A**). To ensure that our assessment of clonality was not driven by the number of cells captured during scRNA-seq, we correlated the degree of clonality with the number of total or MBCs captured. None of the correlations were significant, although the number of MBCs captured was the most correlated with clonality (**Fig. 3H, I**). In summary, we show that MBC responses in childhood INS are antigen-driven and that clonal responses are associated with the presence of anti-CRB2 autoantibodies.

### *3.4.3. Clonal MBCs and ASCs exhibit high SHM.*

The involvement of extrafollicular responses would indicate the preferential accumulation of non-switched MBCs and ASCs with diminished SHM, events that primarily occur in germinal centers[11]. Thus, we next characterized the degree of CSR and SHM in the expanded MBC repertoire. Of the clonal MBCs, anti-CRB2+ individuals showed lower class-switching than anti-CRB2– individuals, with cells preferentially using the IgM or IgD isotype in three (BCS2, BCS5, INS2) of five individuals, consistent with the expansion of extrafollicular B cells (**Fig. 3A, B**). In contrast, anti-CRB2– individuals showed increased accumulation of IgG isotypes within their clonal memory repertoire (**Fig. 3A**). Nevertheless, SHM rates within the *IGHV* locus were elevated in highly clonal MBCs in all individuals with no major differences between anti-CRB2+ and anti-CRB2– individuals (**Fig. 3C, D**). Notably, the degree of SHM was like that observed in antigen-specific ASCs following vaccination denoting a potential antigen recall response in childhood INS[30]. Thus, while the diminished CSR supports an extrafollicular origin for B cell responses in anti-CRB2+ individuals, the clonally expanded MBCs have undergone significant maturation.

### *3.4.4. The clonal repertoire following rituximab treatment is dominated by naïve B cells.*

Rituximab is effective at maintaining long-term remission from proteinuria. Nevertheless, many children do eventually relapse denoting a degree of rituximab resistance[31,32]. This is often associated with a resurgence of MBCs[9]. To this end, we aimed to characterize B cell clonality in post-rituximab relapses. We obtained paired V(D)J sequences for our previously published scRNA-seq dataset of four anti-CRB2– children at relapse and remission following rituximab treatment[7]. We did not observe any differences in total B cell clonality (≥2 B cells) at either time point, and the degree of clonality was much lower than observed in anti-CRB2+ children in active INS (**Fig. 4A-C**). While the frequencies of highly clonal B cells (≥5 B cells) were like those observed in anti-CRB2+ children, these highly clonal cells were almost exclusively composed of naïve B cells (**Fig. 4C, D**). Indeed, very few MBCs and ASCs were present in the clonally expanded repertoire following rituximab treatment consistent with ongoing B cell reconstitution (**Fig. 4B, D**). Moreover, clonal sharing between relapse and remission time points was minimal (**Fig. 4E**). In summary, we show that peripheral B cell clonality following rituximab treatment is largely restricted to the naïve compartment.

### 3.5 Discussion

The expansion of MBCs and ASCs in the peripheral blood is a robust feature of INS that strongly supports an autoimmune humoral etiology. Whether the expansion of these MBCs constitutes an autoantigen-driven response has so far remained unknown. In this study, we used scRNA-seq pairing gene expression data with V(D)J sequences to assess the clonality of B cell responses in childhood INS. Highly expanded MBC clones were present in six of the eight children studied including all four anti-CRB2+ individuals. MZ-like B cells, *TNFRSF13B*-expressing isotype-switched cMBCs, and ASCs were the primary clonally expanded populations. Clonally expanded MBCs underwent high rates of SHM denoting their participation in a mature B cell response, whereas the low degree of isotype class-switching in anti-CRB2+ individuals supported an extrafollicular origin. Altogether, our study demonstrates that MBC expansion in childhood INS is antigen-driven and is associated with the production of APAs.

We previously conducted scRNA-seq of total PBMC from four children with INS and four age- and sex-matched healthy controls showing that eMBCs are expanded in active INS[7]. Due to the small number of B cells (5,210 cells) and patients obtained, we were unable to meaningfully evaluate whether the extensive changes in the B cell compartment constituted a *bona fide* B cell response. To address this question here, we generated a larger scRNA-seq gene expression dataset of 93,910 childhood INS B cells, of which 69,879 have paired V(D)J sequences, from eight affected children. We also reference mapped B cells from 21 healthy children from three other scRNA-seq studies and the INS-affected children from our previous study to our current dataset to allow comparisons between HC and INS B cells[7,28,29]. With this larger dataset, we confirmed that *TNFRSF13B*-expressing MZ-like B cells and atBCs were expanded in childhood INS, but also observed an increased proportion of a population of isotype-switched cMBCs. Like the MZ-like B cells, these isotype-switched cMBCs expressed high levels of *TNFRSF13B* and were therefore termed SM-TACI B cells. Rates of CSR and SHM in SM-TACI B cells were only slightly under those observed in ASCs. While this may suggest a follicular origin for SM-TACI B cells, extrafollicular responses are also capable of supporting significant CSR and SHM[14,33]. Indeed, the elevated expression of

*TNFRSF13B* by SM-TACI B cells would support an extrafollicular origin since TACI signaling is intimately linked with the extrafollicular generation of ASCs. This increased proportion of SM-TACI B cells is consistent with the frequent observation of increased isotype-switched cMBCs ($CD21^+$ $CD27^+$ $IgD^-$ $IgM^-$) in childhood and adult INS in previous immunophenotyping studies[3,6]. Future work will explore using $TACI^+$ MBCs as a prognostic marker for disease relapse in INS. Indeed, $TACI^+$ eMBCs have been recently implicated in alloimmunity during chronic graft-versus-host disease[20].

The INS-associated MZ-like B cells, SM-TACI B cells, and ASCs were the most clonally expanded populations, denoting their involvement in an ongoing B cell response. These clones had high rates of SHM, like those observed following vaccination[30], suggesting their participation in a recall response to previously encountered antigen. These observations are highly consistent with the relapsing-remitting course of INS and further suggest chronic antigen exposure as a component of pathogenesis. Indeed, chronicity is likely an important factor in the generation of eMBCs in autoimmune disease[34]. Moreover, while we cannot conclude that these clonally expanded B cells are targeting podocyte antigen, highly clonal responses were present in all anti-CRB2+ individuals studied (BCS1, BCS2, BCS5, BCS8, and INS1) and in only two of the anti-CRB2– children (BCS6 and BCS7) and so are at least associated with the presence of APAs. Indeed, eMBCs like MZ B cells are enriched in autoreactive clones and have been implicated in the pathogenesis of several autoimmune diseases including SLE and multiple sclerosis[12,15]. Therefore, it is possible that the clonally expanded MZ-like B cells that we identified here harbor CRB2-reactive B cells and participate in the generation of anti-CRB2-producing ASCs in a TACI-dependent manner.

Nonetheless, the greatest clonality was observed in B cells from BCS7, an anti-CRB2– donor. All children in our cohort were seronegative for anti-Nephrin–, but seropositivity for other APAs was not tested[35-37]. Anti-Annexin $A_2$ antibodies, for example, were previously reported in the sera of 18% of childhood INS cases and anti-UCHL1 in 36%[35,37]. Thus, the clonal responses observed in anti-CRB2– donors may still be associated with APAs. To further explore this, CDR3 sequences from clonally expanded BCRs from both anti-CRB2+ and anti-CRB2– individuals will be cloned into IgG expression vectors for *in vitro*

antibody generation and these antibodies will be tested for their podocytopathic potential *in vitro*. Importantly, we failed to identify significant clonal expansion in two anti-CRB2– individuals, despite the presence of significant ASC expansion. While this may suggest a non-humoral etiology for certain cases of INS, this could have been affected by the highly variable timing for sample procurement during relapse.

We also assessed the clonality of B cell responses in paired post-rituximab relapse and remission samples. However, we did not find any significant change in the clonality between time points and were unable to identify clonally expanded MBCs. Unsurprisingly, most clonal B cells were naïve consistent with B cell reconstitution following rituximab treatment. Our inability to identify clonal MBC responses were hindered by two obstacles: the low numbers of MBCs present following rituximab treatment, and our assessment of solely B cells in circulation. It is possible that the nephrotic MBC clones persist within tissues following rituximab treatment but are ablated from circulation. Indeed, the persistence of clonally expanded MBCs following rituximab treatment has been observed in the spleen during relapses of idiopathic thrombocytopenia, an autoantibody-mediated autoimmune disease[38].

In summary, we demonstrate that the peripheral expansion of MBCs in childhood INS is antigen-driven and is associated with the production of APAs. We propose a mechanism wherein eMBCs, namely MZ B cells, are activated by an exogeneous insult (e.g., respiratory viral infection) recruiting podocyte-reactive clones. Some clones will convert into $CD21^{low}$ $CD11c^{+}$ $T\text{-}bet^{+}$ atBCs for the rapid generation of ASCs in a TACI-dependent manner while others will undergo CSR and SHM to generate high affinity isotype-switched cMBCs, akin to the SM-TACI B cells identified here. These high affinity mature cMBCs will be recalled in subsequent relapses and may contribute to disease progression into more severe FSGS. This study provides a rationale for the investigation of B cell therapeutics that target the extrafollicular B cell response like the TACI inhibitor atacicept and the anti-BAFF monoclonal antibody belimumab.

### 3.6 Materials and Methods

#### *Human participants*

This study includes data from 23 children that were enrolled according to protocols approved by Research Ethics Boards (REBs) at the Research Institute of the McGill University Health Centre (MUHC-14-466, T.T.) and the Alberta Children's Hospital (CHREB-16-2186, S.S.) [39]. Parents or legal guardians were informed of the study and provided written consent for blood collection and use in the study. Children between the ages of 7 and 18 years were also informed of the study and signed an assent form. Blood samples were collected during proteinuric relapses, defined as a urinary protein-to-creatinine ratio of ≥2 g/mmol, serum albumin ≤ 25 g/L, and edema, that necessitated hospital visits. Of the 23 children, 19 were never treated with B cell depleting therapies. For the remaining four children, blood was collected off therapy during relapses that took place in the B cell reconstitution phase following rituximab treatment, and paired remission samples were obtained following a subsequent round of rituximab treatment, off therapy and during B cell reconstitution, at scheduled follow-up visits for treatment. For healthy controls, 24 children undergoing minor day surgery or volunteers from the community were enrolled in the study (11.6 years, IQR of 8.4-14.6 years; 13 females). All samples were used in accordance with our standard operating protocol (MUHC-15-341, T.T.). We previously reported on data obtained from the same blood draws for 18 of the 23 children with active INS and all 24 healthy controls[7]. The data presented here is unique to this study.

#### *Recombinant human CRB2 generation and purification*

*Escherichia coli* transformed with a pET-28a (+) vector containing the gene corresponding to residues 597-943 (extracellular domain) of human CRB2 with an N-terminal $His_6$-tag were generously gifted from Dr. Kunimasa Yan (Kyorin University, Tokyo, Japan) [40]. Transformed *E. coli* were cultured with shaking in LB broth containing 100 µg/ml ampicillin (Millipore Sigma) at 37 °C overnight before inducing $hCRB2_{597-943}$ expression with 0.1 mM IPTG (Millipore Sigma). After 3 h incubation, bacteria were pelleted by centrifugation for 20 minutes at 20,000 ×g and 4 °C. Supernatants were discarded, pellets washed thrice

with PBS, and bacteria were lysed with TNE buffer (50 mM Tris-HCl, 100 mM NaCl, 0.1 mM EDTA, pH 7.4). Purification of rhCRB2$_{597-943}$ was performed using HisPur Ni-NTA Resin (ThermoFisher Scientific) following the manufacturer instructions for denaturing conditions. Dialysis was performed to obtain the purified recombinant protein.

***Anti-hCRB2$_{597-943}$ ELISA***

The wells of ELISA plates (MaxiSorp, ThermoFisher Scientific) were coated with 10 µg of rhCRB2$_{597-943}$ in 0.2 M carbonate-bicarbonate solution overnight at 4 °C. Wells were then washed with PBS+0.05% Tween 20 and subsequently blocked with 200 µl of blocking solution (PBS+2% BSA+0.05% Tween 20) for 2 h at room temperature. Following a second wash, 100 µl of serum samples or anti-CRB2 IgG standard diluted in blocking solution were added to the wells and were incubated for 3 h at room temperature. Wells were washed again and 100 µl of HRP-conjugated goat anti-human IgG1/2/3/4 diluted in blocking solution was added to the plate. After 1 h at room temperature, wells were washed, and 100 µl of TMB substrate was added and allowed to develop for 5 minutes at room temperature. The reaction was stopped using 100 µl of 2 N $H_2SO_4$ and absorbance was measured immediately at 450 nm and 570 nm. Titres were calculated using a four-parameter logistic curve. Individuals were considered positive for anti-CRB2 if titers were above the maximal titer obtained from healthy controls.

***Flow cytometry***

Cryopreserved PBMC from children with active INS (*N* = 19) and age-matched healthy controls (*N* = 24) were thawed, washed in complete RPMI 1640 media (Wisent) (completed with 10% FBS (Wisent), 1% 1M HEPES (Wisent), 1% MEM nonessential amino acids (Wisent) and 1% 10,000 U/ml Penicillin-Streptomycin (Gibco)) and rested for 2 h at 37°C in 5% $CO_2$. Over 90% viability was ensured via a hemocytometer using trypan blue exclusion, and no more than $1\times10^6$ cells used for flow cytometry. Cells were washed with PBS + 2% FBS and incubated with Fixable Viability eFluor 780 Dye (ThermoFisher Scientific, 1:1000) and Fc receptor block (BD Biosciences) at 4°C for 15 min. After washing, extracellular proteins were

stained by incubating cells with a fluorochrome-conjugated antibody cocktail prepared in PBS + 2% FBS and Brilliant Stain Buffer (50 µl/100 µl of cocktail, BD Biosciences) at 4°C for 20 min. The following antibodies detecting extracellular proteins were used: BV711 anti-human CD1c (L161, BioLegend, 1:20), BV785 anti-human CD3ε (OKT3, BioLegend, 1:50), BV605 anti-human CD19 (SJ25C1, BD Biosciences, 1:20), Alexa Fluor 700 anti-human CD20 (2H7, BioLegend, 1:50), BV421 anti-human CD21 (B-ly5, BD Biosciences, 1:20), PE anti-human CD24 (ML5, BD Biosciences, 1:20), PE-Cy7 anti-human CD27 (M-T271, BD Biosciences, 1:20), BUV737 anti-human CD38 (HB7, 1:20, BD Biosciences), BV510 anti-human IgD (IA6-2, BioLegend, 1:20), Alexa Fluor 488 anti-human IgM (MHM-488. BioLegend, 1:40), and APC anti-human CXCR5 (J252D4, BioLegend, 1:20). Cells were then washed with PBS + 2% FBS and fixed/permeabilized using the eBioscience Foxp3/Transcription Factor Staining Buffer Set (eBioscience). Following washing with 1X permeabilization buffer (eBioscience), cells were incubated at 4°C for 45 min with BUV395 anti-human Ki-67 (B56, 1:50, BD Biosciences) prepared in permeabilization buffer. Two final washes were performed in 1X permeabilization buffer and PBS + 2% FBS before cells were acquired on the BD LSRFortessa X-20. Data were analyzed using FlowJo v10.8 software (FlowJo, LLC).

***scRNA-seq library preparation and sequencing***

Cryopreserved PBMC from anti-CRB2+ (*N* = 4) and anti-CRB2– (*N* = 4) were thawed and rested as described in the flow cytometry section. Cells were washed with PBS + 2% FBS and incubated with a cocktail containing Fixable Viability eFluor 780 dye (ThermoFisher Scientific, 1:1000), BV605 anti-human CD19 (SJ25C1, BD Biosciences, 1:20), BV785 anti-human CD3ε (OKT3, BioLegend, 1:50), Alexa Fluor 700 anti-human CD20 (2H7, BioLegend, 1:50), and BUV737 anti-human CD10 (HI10a, BD Biosciences, 1:20) prepared in PBS + 2% FBS at 4°C for 15 min. After another wash in PBS + 2% FBS, cells were filtered through 70 µm mesh and total live B cells (live $CD19^+$ $CD3^-$) were isolated via fluorescence activated cell sorting using the BD FACSAria Fusion. The B cells were washed in PBS + 0.04% BSA, brought to a concentration of 1000 cells/µl, and processed using the Chromium Next GEM Single Cell 5' v2 (PN-1000263) and Chromium Single Cell Human BCR Amplification (PN-1000253)

kits in two batches. We targeted 10,000 and 15,000 captured cells in the first (samples BCS1, BCS2, BCS3, and BCS4) and second (samples BCS5, BCS6, BCS7, and BCS8) batches, respectively. After complementary DNA was synthesized, Chromium Single Cell 5' Gene Expression and V(D)J libraries were prepared according to the manufacturer's instructions. Libraries were sequenced on a NovaSeq6000 (Illumina) to a median sequencing depth of approximately 30,000 reads/cell for the gene expression libraries and 5,000 reads/cell for the V(D)J libraries. We also prepared and sequenced V(D)J libraries for two datasets for which we previously generated gene expression data (GEO accessions GSE233275 and GSE233276).

***Preprocessing and quality control of scRNA-seq gene expression data***

For gene expression data, FASTQ reads were aligned to the GRCh38 reference genome v1.2.0 (refdata-cellranger-GRCh38-1.2.0) and count matrices were generated using CellRanger v7.1.0. All preprocessing and quality control steps were performed using the Seurat v5.0.0 R package[41]. Briefly, contaminating non-B cells expressing *CD3G*, *CD14*, *LILRA4* or hemoglobin genes were removed, and cells with <200 or >2700 features, mitochondrial content >8% of all transcripts, or <14% transcripts corresponding to ribosomal protein genes were filtered out as doublets or nonviable cells. Mitochondrial and ribosomal genes, as well as *MALAT1* and *XIST* were regressed from the dataset to prevent their impact on downstream clustering. Similar quality control was carried out on gene expression data of healthy children PBMC and childhood SLE PBMC from two independent studies (GEO accessions GSE166489 and GSE135779) [28,29]. For the childhood SLE, we limited assessments to those with a disease activity index of ≥4.

***Generating B cell clusters and reference mapping***

The reciprocal PCA method in Seurat v5.0.0 was used to generate B cell clusters that were uniformly present in all individuals and between batches[41]. Data for each sample was normalized and variable features were identified separately. Features that were consistently variable across samples were then selected (SelectIntegrationFeatures), scaled, and used

to perform an initial PCA. The resulting principal components (PCs) were used to identify integration anchors (FindIntegrationAnchors) and integrate the data (IntegrateData). The integrated data was scaled and PCA was performed again. A uniform manifold approximation and projection (UMAP) was generated on KNN values calculated with 10 PCs, and Louvain clusters were generated at a resolution of 0.5. A single cluster of cells with low number of transcripts as removed and a new UMAP was generated using 9 PCs and a resolution of 0.5.

Marker sets for each cluster were generated by running differential gene expression analysis between the query cluster and all other B cells using the FindAllMarkers function in Seurat v5.0.0 (**Supplemental Data 2**). The resulting gene lists were filtered to only include genes expressed in at least 10% of cells and were subsequently used to assign cluster identities (**Fig. S1c**). Broadly, naïve B cells were identified based on the expression of *BACH2*, *TCL1A*, *FCER2*, and *IL4R*; MBCs using *BCL2A1*; ASCs using *PRDM1* and *JCHAIN*.

We reference mapped B cells from healthy, SLE, and INS children from three independent studies (GEO accessions GSE166489, GSE135779, GSE233275, and GSE233276) onto our B cell clusters using the Seurat v.5.0.0[42]. Cells from the query data were projected onto the PCA structure of the integrated B cell clusters of our reference to identify mutual nearest neighbors between datasets (FindTransferAnchors). Query cell cluster identities were assigned using the TransferData function, and integrated embeddings were transferred using the IntegrateEmbeddings function.

***V(D)J processing and gene annotation***

Demultiplexed pair-end FASTQ reads were processed via CellRanger v7.1.0 and aligned to the GRCh38 human reference genome (refdata-cellranger-vdj-GRCh38-alts-ensembl-5.0.0). The resulting outputs were then processed using the Immcantation pipeline. The initial germline annotations were performed using IgBLAST v1.22.0[43] with the IMGT/V-Quest reference[44], and the outputs were converted to the adaptive immune receptor repertoire (AIRR) format using MakeDb.py from Change-O v1.3.0[45]. Only sequences with productive rearrangement, a CDR3 nucleotide sequence length that is a multiple of 3 were

retained. Moreover, cells with no or multiple heavy chains were removed. If a cell had multiple light chains, the most abundant transcript was kept (or the first transcript listed in the case of a tie). Finally, only cells present in the gene expression dataset following processing, quality control, and clustering steps were retained in the V(D)J data.

***Clonal lineage inference***

Clonal lineages were inferred for each donor on productive heavy chain sequences with hierarchical clustering using SCOPer v1.3.0[46-48]. Heavy chains with equivalent V and J genotypes and CDR3 lengths were parsed into partitions, and CDR3 nucleotide sequences within a 0.15 normalized Hamming distance from each other within each partition were defined as clones. Full-length consensus germline sequences were reconstructed for each clone from the IMGT/V-Quest reference using Dowser v2.1.0[49]. Clone networks[50] were then generated using the Dandelion v0.3.5[51] python package on the inferred clones and these were visualized through Scanpy v1.9.8[52].

***Calculating SHM and CSR***

SHM was calculated as the frequency of nucleotide mismatches from the germline sequence of the CDR1, CDR2, FWR1, FWR2, and FWR3 segments of the variable heavy chain using SHazaM v1.2.0[45]. CSR was calculated as the frequency of cells with a constant heavy chain genotype that was not *IGHM* or *IGHD*. The constant heavy chain genotype was obtained from the 'c_call' column of the CellRanger output.

***Clonal sharing analysis***

To visualize the clonal sharing across B cell clusters or samples within the same individual, we used circlize v0.4.15[53].

***Statistical analysis***

Statistical analyses were performed on R v4.4.0 or GraphPad Prism v10.2.2 software. Two-sided analyses between two unpaired groups were done using Mann-Whitney *U*-tests

and a Wilcoxon signed-rank test for paired groups. Comparisons between more than two groups were performed using a Kruskal-Wallis test followed by a Dunn's test for multiple comparisons. Data are shown as median with 95% confidence intervals with each point representing a single participant or box plots with the center at the median, edges at the interquartile range, and whiskers at the minima and maxima. For differential gene expression to obtain markers for cell clusters, $P_{adj}$ values were determined using Wilcoxon rank-sum tests with Bonferroni correction. *P*-values < 0.05 were considered significant and all significant *P*-values were depicted on the graphs. No sample size calculations were conducted *a priori*, and no samples obtained were excluded from the study.

**Online supplemental material**

Four figures and two data sets are provided. Fig. S1 shows the annotation of the B cell clusters from the dataset of eight children with INS that we present in this paper. Fig S2 depicts the V(D)J data for B cells from four healthy and four INS children paired to gene expression data from our previously published dataset (GSE233275). Fig. S3 shows the V(D)J data for two anti-CRB2– children (BCS3 and BCS4) that did not have highly clonal B cells. Supplemental Data 1 provides clinical information for all the INS children who donated samples used in this study. Supplemental Data 2 provides gene lists for each B cell cluster generated by differential gene expression analysis between the cluster and all other B cells in the dataset.

**Data availability**

Sequencing data have been deposited to the Gene Expression Omnibus (GEO) and a temporary access token is generated for reviewers. In this study, the following datasets from the GEO were also used GSE233275, GSE233276, GSE135779, and GSE166489.

**Acknowledgements**

We are grateful to all study participants, their families, and the medical teams involved in their care. We especially thank the Canadian Childhood Nephrotic Syndrome

Study (CHILDNEPH) for supplying PBMC, D.Muruve and the Biobank for the Molecular Classification of Kidney Disease (BMCKD) for processing and storing PBMC, and B.Mazer and B.Foster for supplying healthy children PBMC. We thank I.Ragoussis at the McGill Genome Centre for their 10x Genomics services and M-H. Lacombe, E. Iourtchenko, and H.Pagé-Veillette at the Research Institute of the McGill University Health Centre Immunophenotyping Core for their sorting services. This work was supported by a Canadian Institute of Health Research (CIHR) project grant (PJT-16006 to T.T., C.P., S.S. and PJT-192017 to T.T. and C.P.) and a Kidney Foundation of Canada Kidney Health Research grant (KHRG-190010 to T.T., C.P., S.S.). T.A. was also supported by a CIHR Doctoral Award. The authors declare no competing interests.

**Author contributions**

T.A., C.A.P. and T.T. conceptualized the study and designed all the experiments. T.A. conducted the flow cytometry and scRNA-seq experiments and performed all the data analysis. T.A., L.A., M.A.P. processed all the blood samples. T.A. and R.I. thawed the PBMC and prepared them for cell sorting. L.A. generated the rhCRB2 and S.L. conducted the ELISAs to determine anti-CRB2 serostatus. G.P. and M.A.P. obtained consent from the parents/legal guardians of all participating children and further obtained assent from subjects between 7 and 18 years of age. T.A., L.A., G.P., M.A.P., S.M.S. and T.T. coordinated sample collection and biobanking at the McGill University Health Centre and the Alberta Children's Hospital. T.A., C.A.P and T.T. wrote the initial draft of the manuscript. All authors critically reviewed the manuscript, discussed the results, interpreted the data, and contributed to its formulation.

## 3.7 Figures

## Figure 1

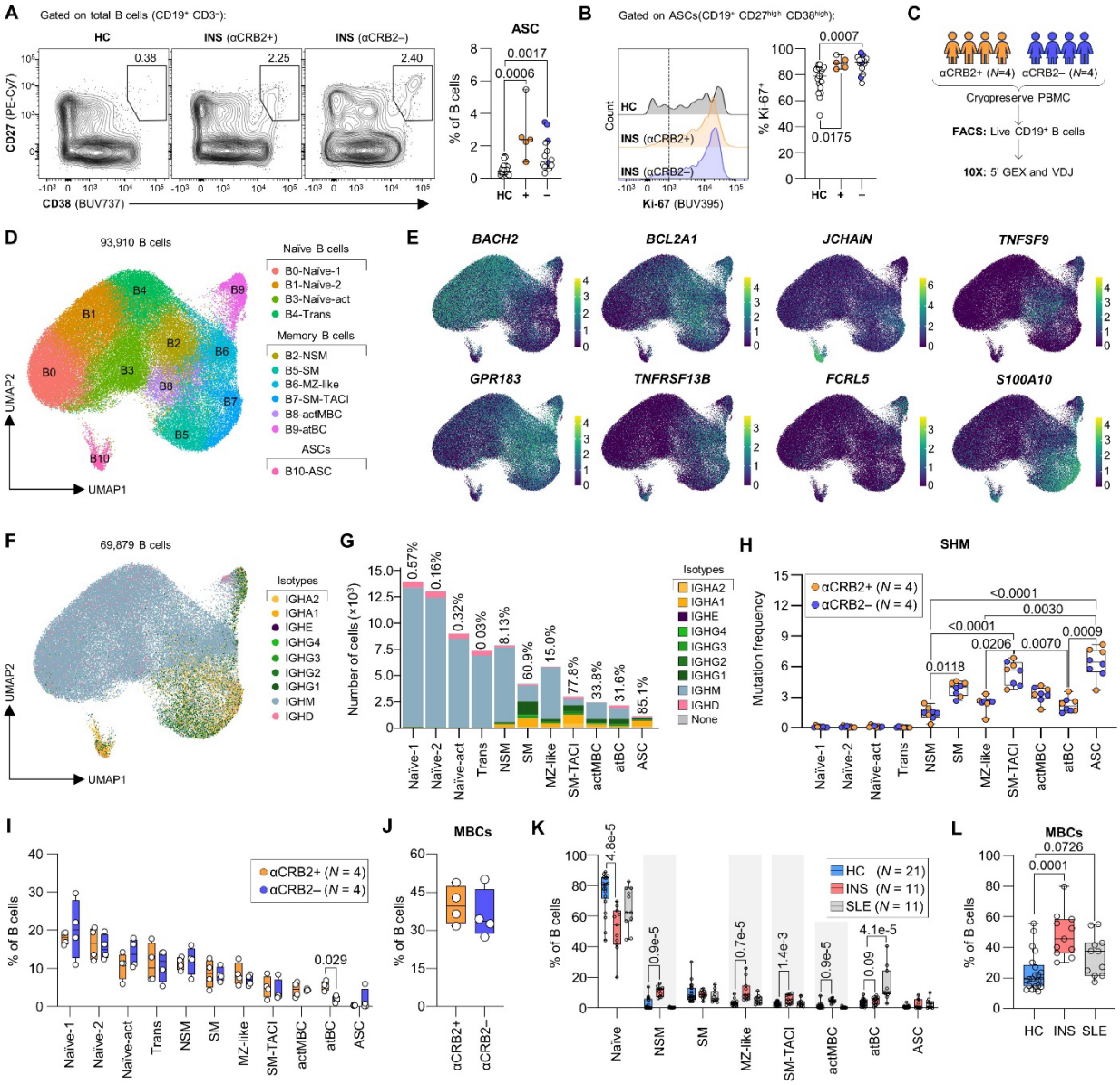

**Figure 1: *TNFRSF13B*-expressing memory B cells and ASCs are expanded in childhood INS.**

(**A**) Representative flow plots and quantification showing the frequency of antibody-secreting cells (ASCs, $CD27^{high}$ $CD38^{high}$) in peripheral blood B cells from healthy (HC, *N* = 24), anti-CRB2+ INS (*N* = 5), and anti-CRB2– INS (*N* = 14) children. (**B**) Histograms showing Ki-67 expression in ASCs and quantification of the frequency of Ki-$67^{+}$ cells. In A and B, each dot represents a single individual. Data are shown as median with 95% confidence intervals. *P*-values were determined using a Kruskal-Wallis test with Dunn's post-hoc testing with multiple comparisons between all groups. (**C**) Set up for scRNA-seq. Live B cells ($CD19^{+}$ $CD3^{-}$) were FACS-isolated from cryopreserved PBMC of anti-CRB2+ INS (*N* = 4) and anti-CRB2– INS (*N* = 4) children (depicted by the orange and violet data points in A and B) for 5' gene expression and V(D)J sequencing. (**D**) Uniform manifold approximation and projection (UMAP) of 93,910 B cells from the eight childhood INS donors. (**E**) Feature plots showing the expression of genes associated with distinct B cell populations. (**F**) UMAP of the 69,879 B cells with paired V(D)J sequences delineating the genotype of the constant heavy chain (isotype usage). (**G**) Bar graph showing the number cells per cluster for each isotype. The percentage at the top of the bar represents the frequency of cells in that cluster that have undergone class-switching (i.e. not *IGHM*, *IGHD*, or none). (**H**) Somatic hypermutation (SHM) measures for each B cluster. Each dot represents a single individual. Data are shown as boxplots with median (center), interquartile range (bounds), and min-max range (whiskers). *P*-values were determined using a Kruskal-Wallis test with Dunn's post-hoc testing for multiple comparisons between memory B cell clusters. (**I and J**) B cell cluster (I) or total memory B cell (J) frequencies for each donor. (**K and L**) B cell cluster (I) or total memory B cell (J) frequencies of B cells obtained from HC (*N* = 4 from GSE233275, 11 from GSE135779, 6 from GSE166489), childhood systemic lupus erythematosus (SLE, *N* = 11 from GSE135779), and childhood INS donors (GSE233275) that were reference mapped onto our current dataset. In I-L, each dot represents a single individual. Data are shown as boxplots with median (center), interquartile range (bounds), and min-max range (whiskers). *P*-values were determined using Mann-Whitney *U*-tests between anti-CRB2+ and anti-CRB2– (I and J) or a Kruskal-Wallis test with Dunn's post-hoc testing for multiple comparisons between INS or SLE to HC (K and L).

## Figure 2

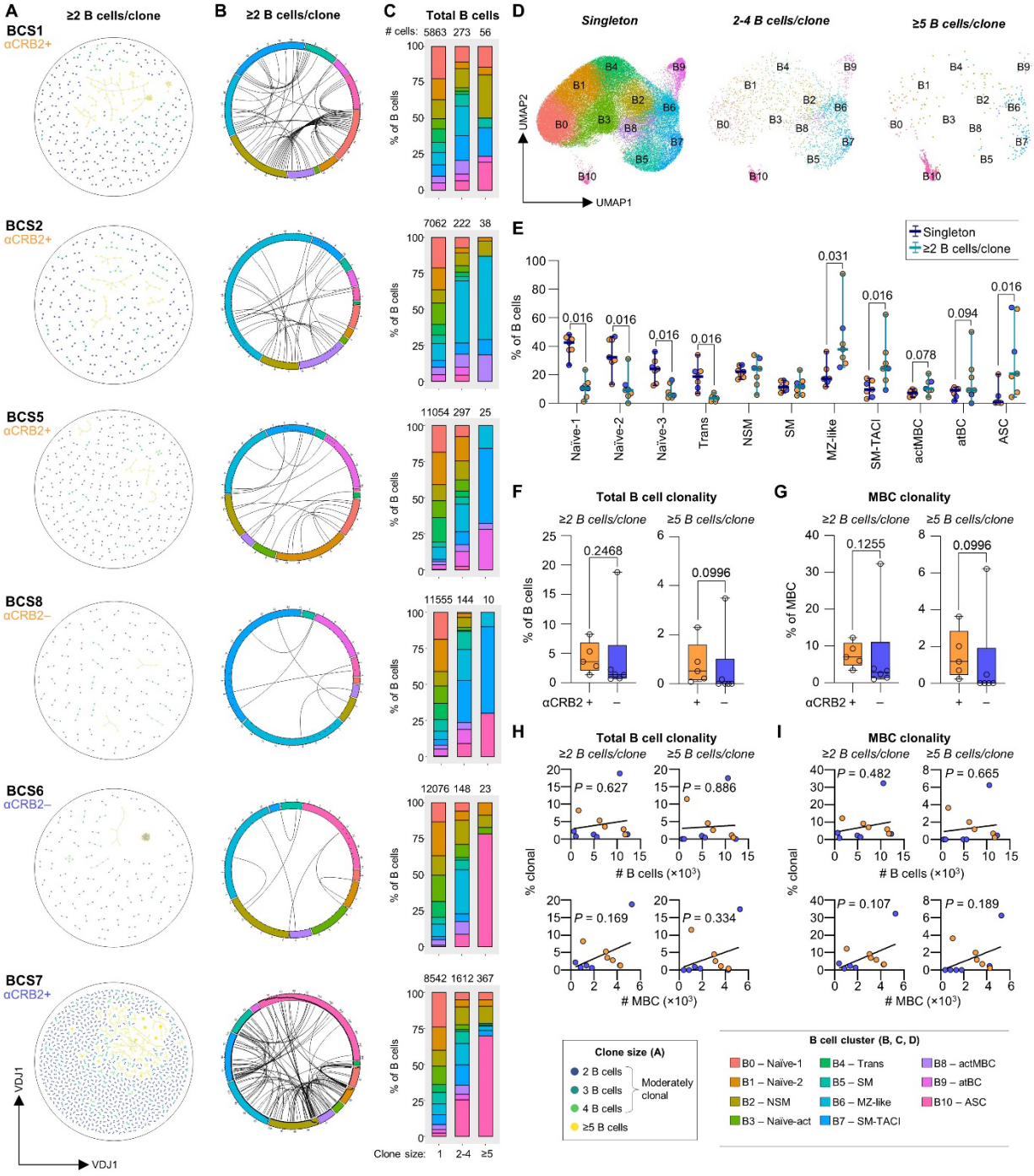
A
≥2 B cells/clone
BCS1
αCRB2+
BCS2
αCRB2+
BCS5
αCRB2+
BCS8
αCRB2–
BCS6
αCRB2–
BCS7
αCRB2+
VDJ1
VDJ1
B
≥2 B cells/clone
C
Total B cells
# cells: 5863 273 56
7062 222 38
11054 297 25
11555 144 10
12076 148 23
8542 1612 367
% of B cells
Clone size: 1 2-4 ≥5
D
Singleton
2-4 B cells/clone
≥5 B cells/clone
UMAP2
UMAP1
B0
B1
B2
B3
B4
B5
B6
B7
B8
B9
B10
E
Singleton
≥2 B cells/clone
% of B cells
0.016
0.016
0.016
0.016
0.031
0.016
0.078
0.094
0.016
Naïve-1
Naïve-2
Naïve-3
Trans
NSM
SM
MZ-like
SM-TACI
actMBC
atBC
ASC
F
Total B cell clonality
≥2 B cells/clone
≥5 B cells/clone
% of B cells
0.2468
0.0996
αCRB2 +
–
+
–
G
MBC clonality
≥2 B cells/clone
≥5 B cells/clone
% of MBC
0.1255
0.0996
αCRB2 +
–
+
–
H
Total B cell clonality
≥2 B cells/clone
≥5 B cells/clone
% clonal
P = 0.627
P = 0.886
P = 0.169
P = 0.334
# B cells (×10³)
# MBC (×10³)
I
MBC clonality
≥2 B cells/clone
≥5 B cells/clone
% clonal
P = 0.482
P = 0.665
P = 0.107
P = 0.189
# B cells (×10³)
# MBC (×10³)
Clone size (A)
2 B cells
3 B cells
4 B cells
≥5 B cells
Moderately clonal
B cell cluster (B, C, D)
B0 – Naïve-1
B1 – Naïve-2
B2 – NSM
B3 – Naïve-act
B4 – Trans
B5 – SM
B6 – MZ-like
B7 – SM-TACI
B8 – actMBC
B9 – atBC
B10 – ASC

**Figure 2: Clonally expanded memory B cells and ASCs are prevalent in anti-CRB2+ children.**

(**A**) Clone networks showing clonal B cells (≥2 B cells/clone) generated using Dandelion for the six donors (BCS1, BCS2, BCS5, BCS6, BCS7, and BCS8) that carried highly clonal B cells (≥5 B cells/clone). Each dot represents a single B cell. Cells of the same clone are connected by a line with CDR3 nucleotide sequence dissimilarity determining the length of the line. (**B**) Circos plots of clonal B cells showing clonal sharing across clusters. B cell clusters are the sectors and cells are arranged in the clockwise direction by decreasing clone size. Lines are drawn connecting B cells with the same clonotype in different B cell clusters. (**C**) Frequencies of each B cell cluster within the singleton (1 B cell/clone), moderately clonal (2-4 B cells/clone), and highly clonal (≥5 B cells/clone) clone size groups with the absolute number of B cells in each group at the top of the bars. (**D**) UMAP of B cells stratified by clone size groups. (**E**) Frequencies of B cell clusters in singleton and clonal (≥2 B cells/clone) groups of INS children with highly clonal B cells (BCS1, BCS2, BCS5, BCS6, BCS7, BCS8, and INS2). Each dot represents a single anti-CRB2+ (orange) or anti-CRB2– (violet) individual. Data are shown as median with 95% confidence intervals. *P*-values were determined using Mann-Whitney *U*-tests. (**F and G**) Total (F) or memory (G) B cell clonality compared between all anti-CRB2+ (*N* = 5) and anti-CRB2– (*N* = 6) INS children. Each dot represents a single individual. Data are depicted as boxplots with median (center), interquartile range (bounds), and min-max range (whiskers). *P*-values were determined using Mann-Whitney *U*-tests. (**H and I**) Correlations of total (H) or memory (B) cell clonality measures against the number of total (top) or memory (bottom) B cells for which V(D)J sequences were obtained. *P*-values were determined using a simple linear regression analysis.

## Figure 3

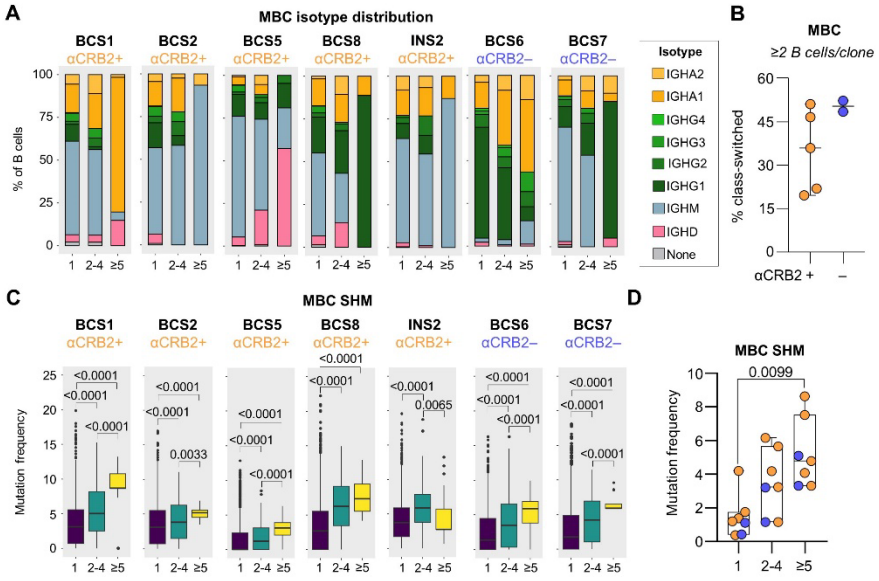
A
MBC isotype distribution
BCS1
αCRB2+
BCS2
αCRB2+
BCS5
αCRB2+
BCS8
αCRB2+
INS2
αCRB2+
BCS6
αCRB2–
BCS7
αCRB2–
% of B cells
100
75
50
25
0
1
2-4
≥5
Isotype
IGHA2
IGHA1
IGHG4
IGHG3
IGHG2
IGHG1
IGHM
IGHD
None
B
MBC
≥2 B cells/clone
% class-switched
60
45
30
15
0
αCRB2 +
–
C
MBC SHM
Mutation frequency
25
20
15
10
5
0
<0.0001
0.0033
0.0065
D
MBC SHM
0.0099
Mutation frequency
10
8
6
4
2
0

**Figure 3: Clonal memory B cells from anti-CRB2+ individuals are largely non-switched.** (**A**) Frequencies of each constant heavy chain genotype in memory B cells for each clone size group in individuals with highly clonal B cell responses. (**B**) Class-switch recombination in clonal memory B cells measured as the frequency of memory B cells with a constant heavy chain genotype that is not *IGHM*, *IGHD* or none. (**C**) Somatic hypermutation (SHM) measures, calculated as the frequency of nucleotide mismatches from the germline in the variable heavy chain locus prior to the CDR3 segment, for each clone size group. Data are represented as boxplots with the median (center), interquartile range (bounds), 95% confidence intervals (whiskers), and outliers (dots). *P*-values were determined using a Kruskal-Wallis test with Dunn's testing for multiple comparisons. (**D**) Compiled SHM measures for each clone size group. Each dot represents a single anti-CRB2+ (orange) or anti-CRB2– (violet) individual. Data are presented as boxplots with median (center), interquartile range (bounds), and min-max range (whiskers). *P*-values were determined using Kruskal-Wallis tests with Dunn's testing for multiple comparisons.

## Figure 4

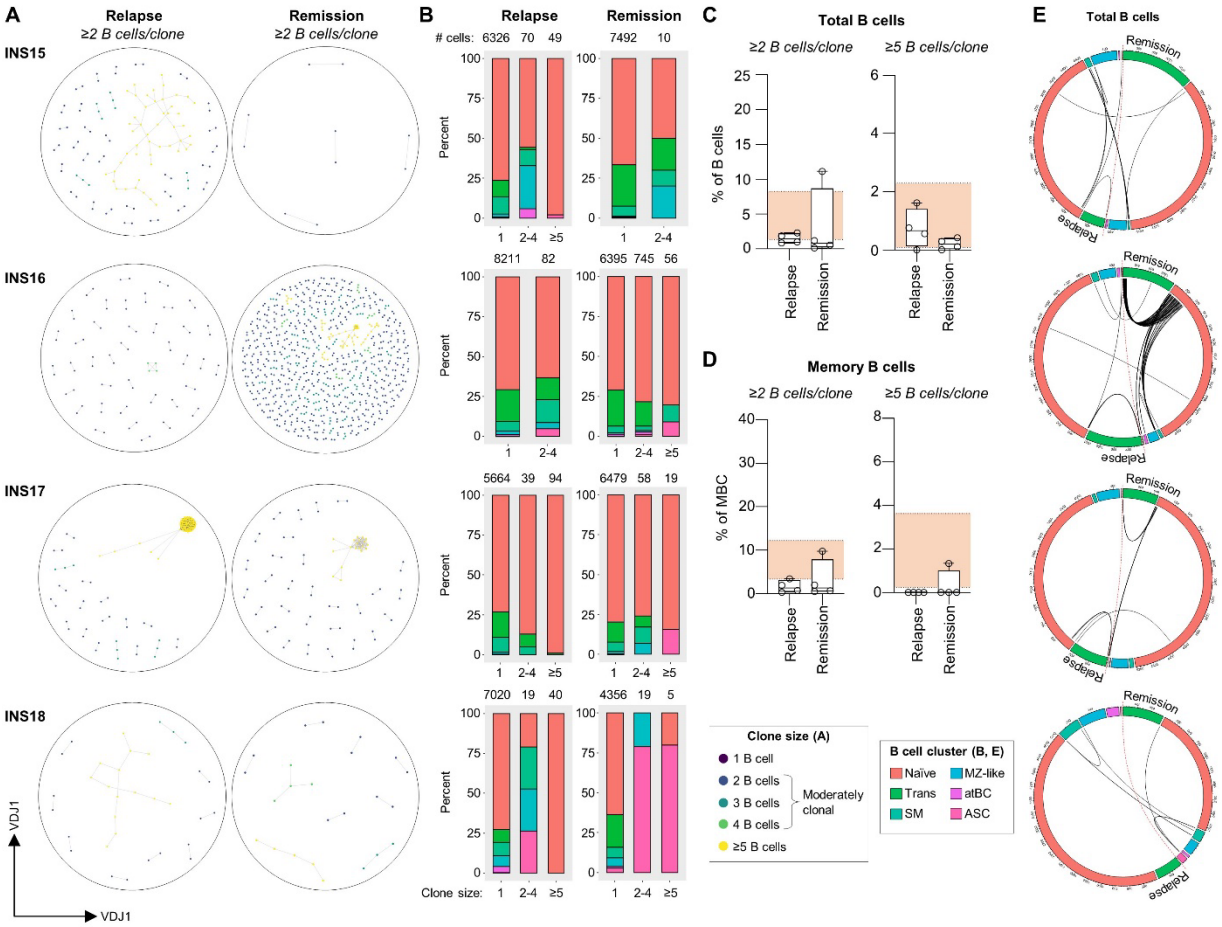
A
Relapse
≥2 B cells/clone
Remission
≥2 B cells/clone
INS15
INS16
INS17
INS18
VDJ1
VDJ1
B
Relapse
Remission
# cells: 6326 70 49
7492 10
8211 82
6395 745 56
5664 39 94
6479 58 19
7020 19 40
4356 19 5
Percent
Clone size: 1 2-4 ≥5
C
Total B cells
≥2 B cells/clone
≥5 B cells/clone
% of B cells
Relapse
Remission
D
Memory B cells
≥2 B cells/clone
≥5 B cells/clone
% of MBC
Clone size (A)
1 B cell
2 B cells
3 B cells
4 B cells
Moderately clonal
≥5 B cells
B cell cluster (B, E)
Naïve
MZ-like
Trans
atBC
SM
ASC
E
Total B cells
Remission
Relapse

**Figure 4: Clonal B cells following rituximab treatment are largely naïve.**

V(D)J libraries were prepared and sequenced from the cDNA of four children from whom we obtained relapse and remission samples following rituximab treatment during the B cell recovery phase. We previously reported on the gene expression data from these same samples, and the data is accessible in the Gene Expression Omnibus under the accession number GSE233276. The gene expression data was reference mapped onto the B cell clusters shown in Figure 1D. (**A**) Clone networks of clonal B cells from remission and relapse samples from each donor. (**B**) Frequencies of each B cell cluster within the singleton (1 B cell/clone), moderately clonal (2-4 B cells/clone), and highly clonal (≥5 B cells/clone) clone size groups with the absolute number of B cells in each group at the top of the bars. (**C and D**) Total (C) and memory (D) B cell clonality measures. Each dot represents a single individual, and the orange background refers to the range of data observed in anti-CRB2+ individuals in Fig. 2F and G. (**E**) Circos plots of clonal B cells showing clonal sharing between clusters. B cell clusters are the sectors and cells are arranged in the clockwise direction by decreasing clone size. Lines are drawn connecting B cells with the same clonotype in different B cell clusters. The dotted red line separates remission and relapse samples.

## Supplemental Figure 1

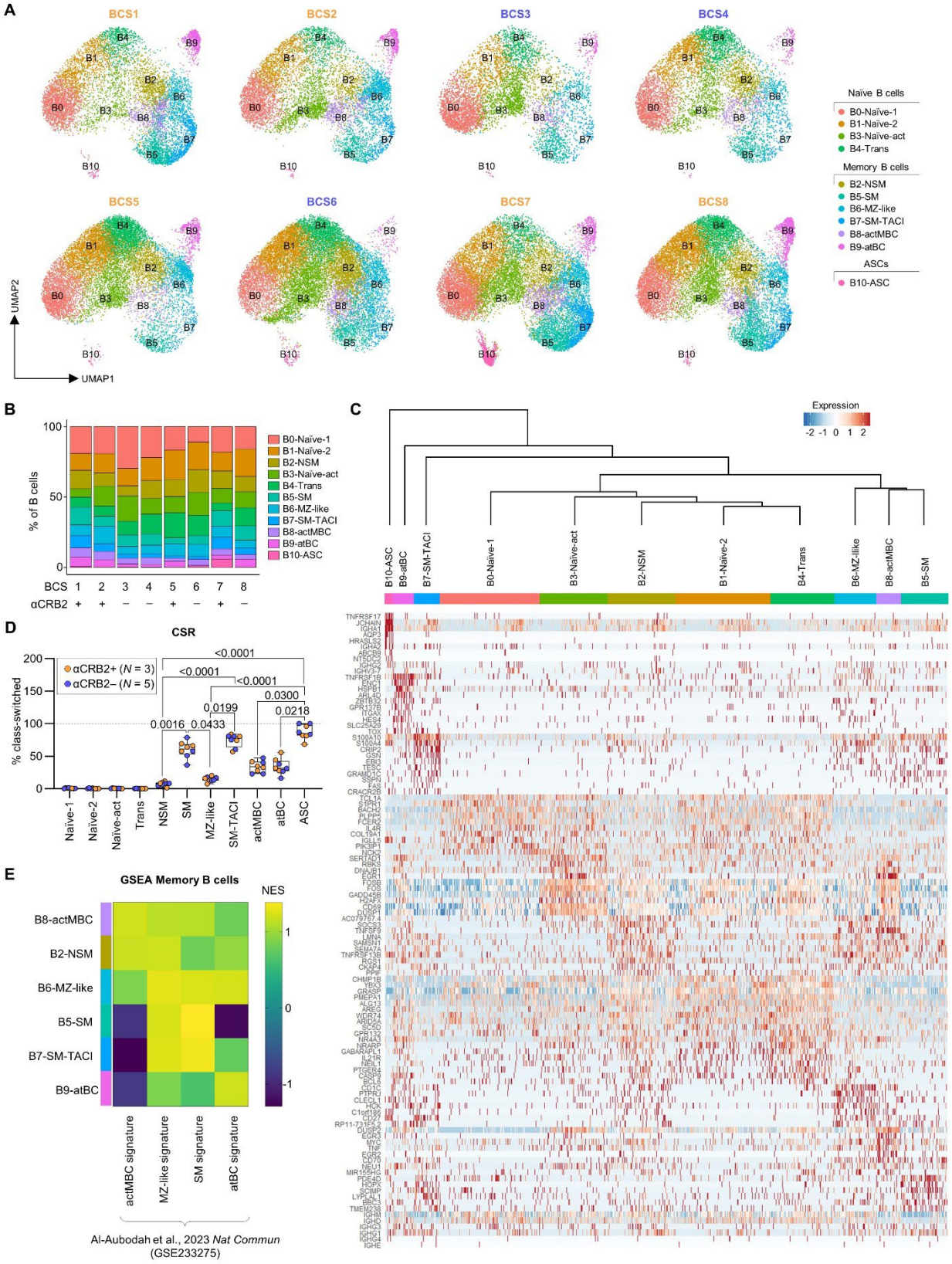

**Supplemental Figure 1: Annotation of B cell clusters from the scRNA-seq gene expression data.**

(**A**) Uniform manifold approximation and projection (UMAPs) of B cells stratified for each of the anti-CRB2+ (*orange*) and anti-CRB2– (*violet*) INS children. (**B**) Frequencies of each B cell cluster by donor. (**C**) Heatmap showing the normalized expression of the top ten genes in each B cell cluster at the single cell level with hierarchical clustering of the B cell clusters. (**D**) Class-switch recombination (CSR) for each B cell cluster measured as the frequency of cells with a constant heavy chain genotype that is not *IGHM*, *IGHD*, or none. Each dot represents a single individual. Data are shown as boxplots with median (center), interquartile range (bounds), and min-max range (whiskers). *P*-values were determined using a Kruskal-Wallis test with Dunn's post-hoc testing for multiple comparisons between memory B cell clusters. (**E**) Gene set enrichment analysis (GSEA) of the actMBC, MZ-like, SM, and atBC signatures from GSE233275 to our memory B cell clusters B2, B5, B6, B7, B8, and B9. This Supplemental Figure is associated with Figure 1.

## Supplemental Figure 2

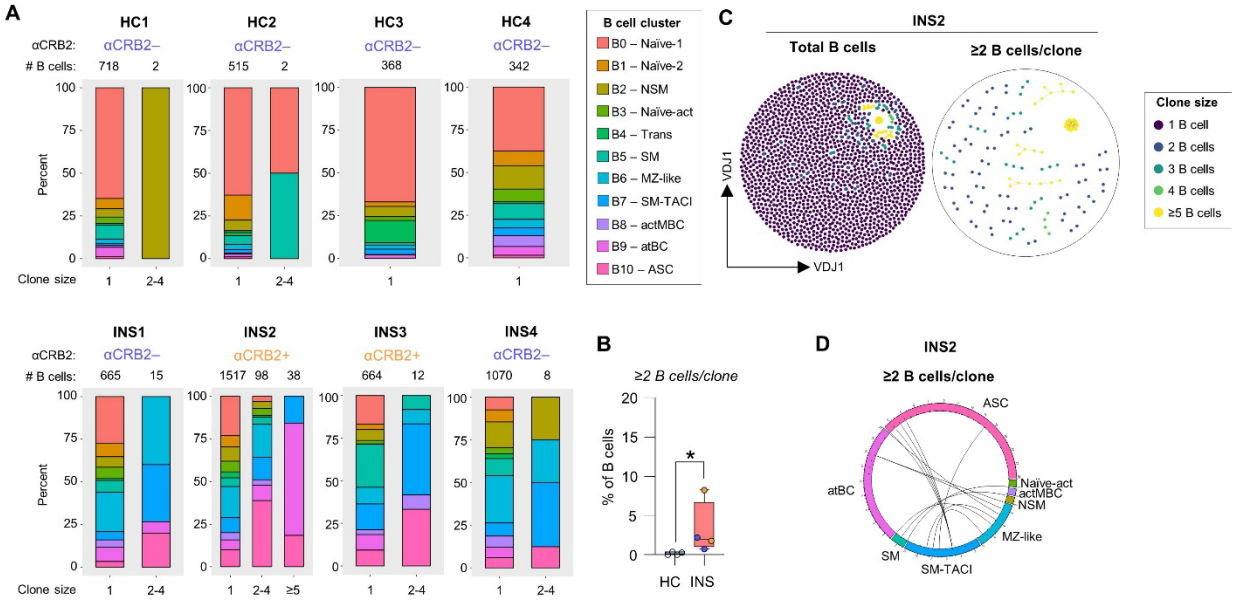

**Supplemental Figure 2: B cells are clonally expanded in childhood INS.**

V(D)J libraries were prepared and sequenced from the cDNA of healthy (HC, *N* = 4) and INS (*N* = 4) children whose gene expression data we previously reported on and is accessible in the Gene Expression Omnibus under the accession number GSE233275. The gene expression data was reference mapped onto the B cell clusters shown in Figure 1D. (**A**) Frequencies of each B cell cluster within the singleton (1 B cell/clone), moderately clonal (2-4 B cells/clone), and highly clonal (≥5 B cells/clone) clone size groups with the absolute number of B cells in each group at the top of the bars. (**B**) Frequencies of clonal B cells in HC and INS children. Each dot represents a single donor. In the INS group, anti-CRB2+ (orange) and anti-CRB2– (violet) donors are shown. (**C**) Clone networks of all B cells (left) or clonal B cells (right) generated using Dandelion for INS2. Each dot represents a single B cell. Cells of the same clone are connected by a line with CDR3 nucleotide sequence dissimilarity determining the length of the line. (**D**) Circos plot of clonal B cells showing clonal sharing across clusters. B cell clusters are the sectors and cells are arranged in the clockwise direction by decreasing clone size. Lines are drawn connecting B cells with the same clonotype in different B cell clusters. This Supplemental Figure is associated with Figure 2.

## Supplemental Figure 3

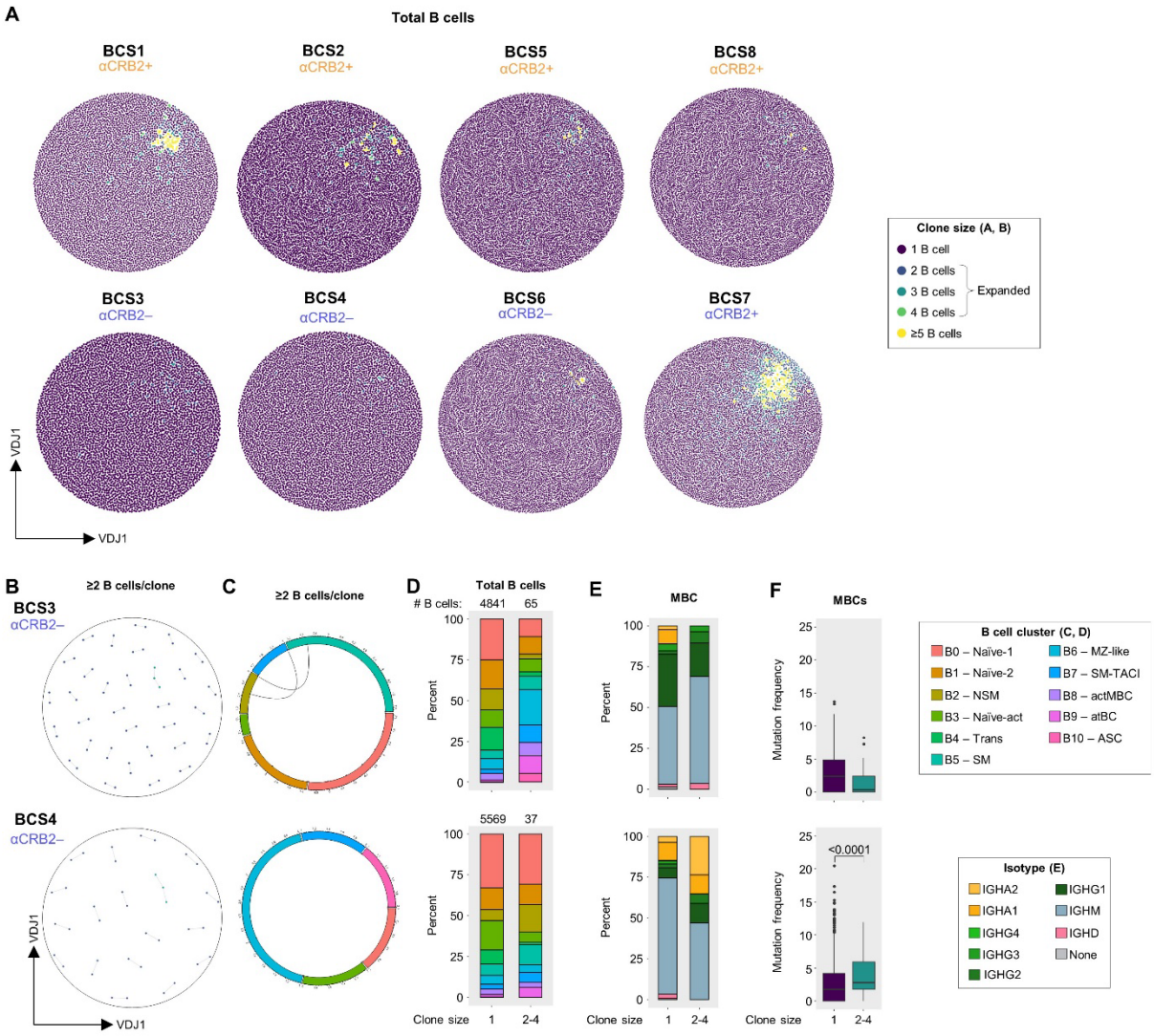

**Supplemental Figure 3: Negligible clonality in two anti-CRB2– INS children.**

(**A**) Clone networks of all B cells for all eight donors in the current study. (**B**) Clone networks of clonal B cells from the two donors that lacked highly clonal B cells. (**C**) Circos plots of clonal B cells showing clonal sharing across B cell clusters. BCS4 lacked any clonal sharing. Frequencies of each B cell cluster within the singleton (1 B cell/clone), moderately clonal (2-4 B cells/clone), and highly clonal (≥5 B cells/clone) clone size groups with the absolute number of B cells in each group at the top of the bars. (**E**) Frequencies of each constant heavy chain genotype by memory B cells in each clone size group. (**F**) Somatic hypermutation (SHM) measures, calculated as the frequency of nucleotide mismatches from the germline in the variable heavy chain locus prior to the CDR3 segment, for each clone size group. Data are represented as boxplots with the median (center), interquartile range (bounds), 95% confidence intervals (whiskers), and outliers (dots). *P*-values were determined using a Mann-Whitney *U*-test. This Supplemental Figure is associated with Figure 2.

### 3.8 References


1 Eddy, A. A. & Symons, J. M. Nephrotic syndrome in childhood. *The Lancet* **362**, 629-639 (2003). https://doi.org:10.1016/S0140-6736(03)14184-0

2 Vivarelli, M., Gibson, K., Sinha, A. & Boyer, O. Childhood nephrotic syndrome. *The Lancet* **402**, 809-824 (2023). https://doi.org:https://doi.org/10.1016/S0140-6736(23)01051-6

3 Colucci, M., Oniszczuk, J., Vivarelli, M. & Audard, V. B-Cell Dysregulation in Idiopathic Nephrotic Syndrome: What We Know and What We Need to Discover. *Frontiers in immunology* **13**, 823204-823204 (2022). https://doi.org:10.3389/fimmu.2022.823204

4 Chan, E. Y.-h. *et al.* Use of Rituximab in Childhood Idiopathic Nephrotic Syndrome. *Clinical Journal of the American Society of Nephrology* **18** (2023).

5 Samuel, S. M. *et al.* Setting New Directions for Research in Childhood Nephrotic Syndrome: Results From a National Workshop. *Can J Kidney Health Dis* **4**, 2054358117703386 (2017). https://doi.org:10.1177/2054358117703386

6 Colucci, M. *et al.* B cell phenotype in pediatric idiopathic nephrotic syndrome. *Pediatric Nephrology* **34**, 177-181 (2019). https://doi.org:10.1007/s00467-018-4095-z

7 Al-Aubodah, T.-A. *et al.* The extrafollicular B cell response is a hallmark of childhood idiopathic nephrotic syndrome. *Nature Communications* **14**, 7682 (2023). https://doi.org:10.1038/s41467-023-43504-8

8 Ling, C. *et al.* Decreased Circulating Transitional B-Cell to Memory B-Cell Ratio Is a Risk Factor for Relapse in Children with Steroid-Sensitive Nephrotic Syndrome. *Nephron* **145**, 107-112 (2021). https://doi.org:10.1159/000511319

9 Colucci, M. *et al.* B Cell Reconstitution after Rituximab Treatment in Idiopathic Nephrotic Syndrome. *J Am Soc Nephrol* **27**, 1811-1822 (2016). https://doi.org:10.1681/ASN.2015050523

10 Akkaya, M., Kwak, K. & Pierce, S. K. B cell memory: building two walls of protection against pathogens. *Nature Reviews Immunology* **20**, 229-238 (2020). https://doi.org:10.1038/s41577-019-0244-2

11 Elsner, R. A. & Shlomchik, M. J. Germinal Center and Extrafollicular B Cell Responses in Vaccination, Immunity, and Autoimmunity. *Immunity* **53**, 1136-1150 (2020). https://doi.org:10.1016/j.immuni.2020.11.006

12 Palm, A.-K. E. & Kleinau, S. Marginal zone B cells: From housekeeping function to autoimmunity? *Journal of Autoimmunity* **119**, 102627 (2021). https://doi.org:https://doi.org/10.1016/j.jaut.2021.102627

13 MacLennan, I. C. M. & Vinuesa, C. G. Dendritic Cells, BAFF, and APRIL: Innate Players in Adaptive Antibody Responses. *Immunity* **17**, 235-238 (2002). https://doi.org:10.1016/S1074-7613(02)00398-9

14 He, B. *et al.* The transmembrane activator TACI triggers immunoglobulin class switching by activating B cells through the adaptor MyD88. *Nat Immunol* **11**, 836-845 (2010). https://doi.org:10.1038/ni.1914

15 Jenks, S. A., Cashman, K. S., Woodruff, M. C., Lee, F. E. & Sanz, I. Extrafollicular responses in humans and SLE. *Immunol Rev* **288**, 136-148 (2019). https://doi.org:10.1111/imr.12741

16 Ambegaonkar, A. A., Holla, P., Dizon, B. L. P., Sohn, H. & Pierce, S. K. Atypical B cells in chronic infectious diseases and systemic autoimmunity: puzzles with many missing pieces. *Current Opinion in Immunology* **77**, 102227 (2022). https://doi.org:https://doi.org/10.1016/j.coi.2022.102227

17 Holla, P. *et al.* Shared transcriptional profiles of atypical B cells suggest common drivers of expansion and function in malaria, HIV, and autoimmunity. *Sci Adv* **7** (2021). https://doi.org:10.1126/sciadv.abg8384

18 Claes, N. *et al.* Age-Associated B Cells with Proinflammatory Characteristics Are Expanded in a Proportion of Multiple Sclerosis Patients. *J Immunol* **197**, 4576-4583 (2016). https://doi.org:10.4049/jimmunol.1502448

19 Wang, S. *et al.* IL-21 drives expansion and plasma cell differentiation of autoreactive CD11c(hi)T-bet(+) B cells in SLE. *Nat Commun* **9**, 1758 (2018). https://doi.org:10.1038/s41467-018-03750-7

20 Poe, J. C. *et al.* Single-cell landscape analysis unravels molecular programming of the human B cell compartment in chronic GVHD. *JCI Insight* **8** (2024). https://doi.org:10.1172/jci.insight.169732

21 Watts, A. J. B. *et al.* Discovery of Autoantibodies Targeting Nephrin in Minimal Change Disease Supports a Novel Autoimmune Etiology. *Journal of the American Society of Nephrology* **33**, 238 (2022). https://doi.org:10.1681/ASN.2021060794

22 Shirai, Y. *et al.* A multi-institutional study found a possible role of anti-nephrin antibodies in post-transplant focal segmental glomerulosclerosis recurrence. *Kidney International* **105**, 608-617 (2024). https://doi.org:10.1016/j.kint.2023.11.022

23 Slavotinek, A. M. The Family of Crumbs Genes and Human Disease. *Molecular Syndromology* **7**, 274-281 (2016). https://doi.org:10.1159/000448109

24 Tanoue, A. *et al.* Podocyte-specific Crb2 knockout mice develop focal segmental glomerulosclerosis. *Scientific Reports* **11**, 20556 (2021). https://doi.org:10.1038/s41598-021-00159-z

25 Takeuchi, K. *et al.* New Anti-Nephrin Antibody Mediated Podocyte Injury Model Using a C57BL/6 Mouse Strain. *Nephron* **138**, 71-87 (2017). https://doi.org:10.1159/000479935

26 Hada, I. *et al.* A Novel Mouse Model of Idiopathic Nephrotic Syndrome Induced by Immunization with the Podocyte Protein Crb2. *Journal of the American Society of Nephrology* **33** (2022).

27 Gatto, D. & Brink, R. B cell localization: regulation by EBI2 and its oxysterol ligand. *Trends in Immunology* **34**, 336-341 (2013). https://doi.org:10.1016/j.it.2013.01.007

28 Ramaswamy, A. *et al.* Immune dysregulation and autoreactivity correlate with disease severity in SARS-CoV-2-associated multisystem inflammatory syndrome in children. *Immunity* **54**, 1083-1095.e1087 (2021). https://doi.org:https://doi.org/10.1016/j.immuni.2021.04.003

29 Nehar-Belaid, D. *et al.* Mapping systemic lupus erythematosus heterogeneity at the single-cell level. *Nat Immunol* **21**, 1094-1106 (2020). https://doi.org:10.1038/s41590-020-0743-0

30 Alsoussi, W. B. *et al.* SARS-CoV-2 Omicron boosting induces de novo B cell response in humans. *Nature* **617**, 592-598 (2023). https://doi.org:10.1038/s41586-023-06025-4

31 Ravani, P. *et al.* Short-term effects of rituximab in children with steroid- and calcineurin-dependent nephrotic syndrome: a randomized controlled trial. *Clin J Am Soc Nephrol* **6**, 1308-1315 (2011). https://doi.org:10.2215/CJN.09421010

32 Sellier-Leclerc, A. L. *et al.* Rituximab in steroid-dependent idiopathic nephrotic syndrome in childhood--follow-up after CD19 recovery. *Nephrol Dial Transplant* **27**, 1083-1089 (2012). https://doi.org:10.1093/ndt/gfr405

33 Di Niro, R. *et al.* Salmonella Infection Drives Promiscuous B Cell Activation Followed by Extrafollicular Affinity Maturation. *Immunity* **43**, 120-131 (2015). https://doi.org:10.1016/j.immuni.2015.06.013

34 Sutton, H. J. *et al.* Atypical B cells are part of an alternative lineage of B cells that participates in responses to vaccination and infection in humans. *Cell Rep* **34**, 108684 (2021). https://doi.org:10.1016/j.celrep.2020.108684

35 Jamin, A. *et al.* Autoantibodies against podocytic UCHL1 are associated with idiopathic nephrotic syndrome relapses and induce proteinuria in mice. *Journal of Autoimmunity* **89**, 149-161 (2018). https://doi.org:https://doi.org/10.1016/j.jaut.2017.12.014

36 Ye, Q. *et al.* Seven novel podocyte autoantibodies were identified to diagnosis a new disease subgroup-autoimmune Podocytopathies. *Clin Immunol* **232**, 108869 (2021). https://doi.org:10.1016/j.clim.2021.108869

37 Ye, Q. *et al.* The important roles and molecular mechanisms of annexin A(2) autoantibody in children with nephrotic syndrome. *Ann Transl Med* **9**, 1452 (2021). https://doi.org:10.21037/atm-21-3988

38 Crickx, E. *et al.* Rituximab-resistant splenic memory B cells and newly engaged naive B cells fuel relapses in patients with immune thrombocytopenia. *Sci Transl Med* **13** (2021). https://doi.org:10.1126/scitranslmed.abc3961

39 Samuel, S. *et al.* The Canadian Childhood Nephrotic Syndrome (CHILDNEPH) Project: overview of design and methods. *Canadian Journal of Kidney Health and Disease* **1**, 17 (2014). https://doi.org:10.1186/2054-3581-1-17

40 Hamano, S. *et al.* Association of crumbs homolog-2 with mTORC1 in developing podocyte. *PLoS One* **13**, e0202400 (2018). https://doi.org:10.1371/journal.pone.0202400

41 Hao, Y. *et al.* Integrated analysis of multimodal single-cell data. *Cell* **184**, 3573-3587.e3529 (2021). https://doi.org:10.1016/j.cell.2021.04.048

42 Stuart, T. *et al.* Comprehensive Integration of Single-Cell Data. *Cell* **177**, 1888-1902.e1821 (2019). https://doi.org:https://doi.org/10.1016/j.cell.2019.05.031

43 Ye, J., Ma, N., Madden, T. L. & Ostell, J. M. IgBLAST: an immunoglobulin variable domain sequence analysis tool. *Nucleic Acids Research* **41**, W34-W40 (2013). https://doi.org:10.1093/nar/gkt382

44 Giudicelli, V., Chaume, D. & Lefranc, M.-P. IMGT/GENE-DB: a comprehensive database for human and mouse immunoglobulin and T cell receptor genes. *Nucleic Acids Research* **33**, D256-D261 (2005). https://doi.org:10.1093/nar/gki010

45 Gupta, N. T. *et al.* Change-O: a toolkit for analyzing large-scale B cell immunoglobulin repertoire sequencing data. *Bioinformatics* **31**, 3356-3358 (2015). https://doi.org:10.1093/bioinformatics/btv359

46 Gupta, N. T. *et al.* Hierarchical Clustering Can Identify B Cell Clones with High Confidence in Ig Repertoire Sequencing Data. *The Journal of Immunology* **198**, 2489-2499 (2017). https://doi.org:10.4049/jimmunol.1601850

47 Zhou, J. Q. & Kleinstein, S. H. Cutting Edge: Ig H Chains Are Sufficient to Determine Most B Cell Clonal Relationships. *The Journal of Immunology* **203**, 1687-1692 (2019). https://doi.org:10.4049/jimmunol.1900666

48 Nouri, N. & Kleinstein, S. H. A spectral clustering-based method for identifying clones from high-throughput B cell repertoire sequencing data. *Bioinformatics* **34**, i341-i349 (2018). https://doi.org:10.1093/bioinformatics/bty235

49 Hoehn, K. B., Pybus, O. G. & Kleinstein, S. H. Phylogenetic analysis of migration, differentiation, and class switching in B cells. *PLOS Computational Biology* **18**, e1009885 (2022). https://doi.org:10.1371/journal.pcbi.1009885

50 Bashford-Rogers, R. J. M. *et al.* Network properties derived from deep sequencing of human B-cell receptor repertoires delineate B-cell populations. *Genome Research* **23**, 1874-1884 (2013). https://doi.org:10.1101/gr.154815.113

51 Suo, C. *et al.* Dandelion uses the single-cell adaptive immune receptor repertoire to explore lymphocyte developmental origins. *Nature Biotechnology* **42**, 40-51 (2024). https://doi.org:10.1038/s41587-023-01734-7

52 Wolf, F. A., Angerer, P. & Theis, F. J. SCANPY: large-scale single-cell gene expression data analysis. *Genome Biology* **19**, 15 (2018). https://doi.org:10.1186/s13059-017-1382-0

53 Gu, Z., Gu, L., Eils, R., Schlesner, M. & Brors, B. circlize implements and enhances circular visualization in R. *Bioinformatics* **30**, 2811-2812 (2014). https://doi.org:10.1093/bioinformatics/btu393

# CHAPTER 4: Susceptibility to Crb2-induced experimental autoimmune nephrotic syndrome is mouse strain-dependent.

**Susceptibility to Crb2-induced experimental autoimmune nephrotic syndrome is mouse strain-dependent.**

Tho-Alfakar Al-Aubodah[1,2,3,4], Lamine Aoudjit[3,4], Sebastian Grocott[1,2], Simon Leclerc[2,3,4,5], Soichiro Suzuki[3,4,5], Ciriaco A. Piccirillo[1,2,5,*], Tomoko Takano[3,4,5,*]

[1] Department of Microbiology & Immunology, Faculty of Medicine and Health Sciences, McGill University, Montréal, Québec
[2] Infectious Diseases and Immunity in Global Health Program, Research Institute of the McGill University Health Centre, Montréal, Québec
[3] Metabolic Disorders and Complications Program, Research Institute of the McGill University Health Centre, Montréal, Québec
[4] Division of Nephrology, Faculty of Medicine and Health Sciences, McGill University, Montréal, Québec
[5] Department of Experimental Medicine, Faculty of Medicine and Health Sciences, McGill University, Montréal, Québec

*Correspondence should be addressed to:
**Dr. Ciriaco A. Piccirillo, Ph.D.**
Research Institute of the McGill University Health Centre (RI-MUHC),
Infectious Diseases and Immunity in Global Health Program
1001 Boulevard Décarie, Bloc E, Room EM2.3248
Montréal, Québec H4A 3J1, Canada
E-mail: ciro.piccirillo@mcgill.ca

**Dr. Tomoko Takano, M.D., Ph.D.**
Research Institute of the McGill University Health Centre (RI-MUHC),
Metabolic Disorders and Complications Program, Division of Nephrology
1001 Boulevard Décarie, Bloc E, Room EM1.3244
Montréal, Québec H4A 3J1, Canada
E-mail: tomoko.takano@mcgill.ca

**Manuscript in preparation.**

**4.1 Bridging Statement**

In *Chapter 3*, we demonstrated that the expansion of eMBCs, cMBCs, and ASCs during active INS was oligoclonal, denoting a *bona fide* B cell response. Moreover, we further implicated APRIL/BAFF-TACI signaling, which we first identified in *Chapter 2*, as a potential driver of MBC and ASC generation. *However, the underlying immunological factors predisposing individuals to develop these potentially autoreactive responses remains unknown*.

GWAS have identified several genetic polymorphisms associated with INS but their contribution to disease pathogenesis is not understood. As with other autoimmune diseases, polymorphisms in the HLA-II locus – specifically *HLA-DQA1**02, *HLA-DQB1**02, and *HLA-DRB1**07/08 – consistently confer the greatest risk (404-411). HLA-II polymorphisms can act through multiple mechanisms, as outlined in *Chapter 1.2.1*, but ultimately shape the nature of the autoreactive T cell response. Thus, through the T-B cell crosstalk, these polymorphisms can also impact the quality of autoantibody production. Whether these HLA-II polymorphisms are involved in INS pathogenesis by promoting the generation of APAs is not known. Since the breadth and prevalence of APAs in INS and the identities of immunodominant epitopes of target autoantigens remain ill-defined, addressing this research gap using human samples is currently difficult. Here, mouse models are advantageous since we can limit the heterogeneity associated with human disease and directly assess pathogenesis. The newly developed *experimental autoimmune nephrotic syndrome (EANS)* is currently the only immune-mediated mouse model of INS (436). It is induced by immunizing C3H/HeN mice with the extracellular domain of Crb2 resulting in the generation of podocytopathic anti-Crb2 antibodies. In *Chapter 4*, we test the capacity for MHC-II haplotypes to impact APA generation by inducing EANS in mouse strains with completely distinct MHC-II allele usage – though other underlying strain differences also exist. *We hypothesized that MHC-II haplotype impacts the generation of podocytopathic APAs thereby contributing to disease susceptibility.*

## 4.2 Abstract

### Background

Polymorphisms within the HLA-II locus are associated with childhood idiopathic nephrotic syndrome (INS) but the mechanism by which they promote disease remains elusive. Recently, anti-podocyte antibodies (APAs) raised against key slit diaphragm proteins like Nephrin and Crb2 have been described in subsets of affected children and are hypothesized to mediate the podocyte lesion observed in INS. Nevertheless, the factors dictating the development of these autoantibodies are unknown. We hypothesized that distinct major histocompatibility complex (MHC)-II alleles have varying capacities to induce podocytopathic APAs.

### Methods

First, the HLA locus was typed for 22 children with INS to validate the presence of risk-associated alleles. Next, MHC-II distinct mouse strains were immunized and re-challenged with the extracellular domain of Crb2 ($rmCrb2_{601-940}$) to induce experimental autoimmune nephrotic syndrome (EANS). Urinary albumin and serum anti-Crb2 IgG concentrations were measured along with antibody deposition within the glomerulus of these mice, and B cell responses in the draining lymph nodes were assessed by flow cytometry.

### Results

Childhood INS was associated with previously established HLA-II risk alleles, namely *HLA-DQA1**02:01, *DQB1**02:02, and *DRB1**07:01. In the EANS model, C3H/HeN and BALB/c mice were susceptible to proteinuria while C57BL/6 mice were completely protected. Nevertheless, C57BL/6 mice developed high titers of anti-Crb2 antibodies, but these antibodies failed to bind podocytes within the glomerulus. Unlike the susceptible strains which formed robust germinal centers upon re-challenge with $rmCrb2_{601-940}$, germinal centers in C57BL/6 mice were not reestablished.

### Conclusions

The results provide strong evidence that the MHC-II haplotype dictates the podocytopathic potential of APAs.

### 4.3 Introduction

Idiopathic nephrotic syndrome (INS) is the most common chronic glomerular disorder in children featuring recurrent episodes of heavy proteinuria and edema[1,2]. A cytoskeletal defect in the podocytes of the glomerulus, termed podocyte foot process effacement, is central to disease pathogenesis though the etiology remains unknown. While 90% of affected children will respond to glucocorticoids, denoting an immune origin for disease, more than 80% of steroid-sensitive cases will relapse requiring repetitive immunosuppressive treatments to maintain remission[3]. This highly immunosuppressive regimen is associated with significant side effects, warranting the development of safer, more specific glucocorticoid-sparing therapies[4].

B cell depleting therapies, especially using the CD20-targeting monoclonal antibody rituximab, can maintain longer periods of remission than glucocorticoids alone suggesting an autoimmune humoral origin for INS pathogenesis[5]. This implication of B cells in INS is supported by numerous studies showing that circulating memory B cells and follicular helper T ($T_{FH}$) cells are more abundant during active disease than in healthy controls, and the resurgence of isotype-switched memory B cells are associated with relapses following B cell depletion[6-10]. Moreover, we recently demonstrated that childhood INS is associated with the peripheral expansion of autoimmune-associated extrafollicular memory B cells[11]. These were namely $CD21^{low}$ T-$bet^{+}$ $CD11c^{+}$ atypical B cells (atBC) and marginal zone (MZ) B cells, populations that are enriched with autoreactive BCRs and are capable of rapidly converting into plasmablasts, which were themselves strongly expanded in childhood INS[10,11].

Accordingly, anti-podocyte antibodies (APAs) have also been recently identified in some children with INS, further underscoring a humoral autoimmune etiology[12-14]. These include autoantibodies against major proteins of the slit diaphragm, the structure that confers podocytes with their selective filtering capacity, like Nephrin and Crb2. The podocytopathic potential of these antibodies have been demonstrated in murine models[15]. Specifically, immunization of C3H/HeN mice with just the extracellular proportion of Crb2 ($Crb2_{601-940}$) closely recapitulates renal pathology of human INS, mediating experimental

autoimmune nephrotic syndrome (EANS)[16]. The factors mediating the breach of tolerance to these podocyte antigens, thereby enabling the development of APAs, remain elusive.

Susceptibility to and protection from human autoimmune diseases is intimately linked with polymorphisms in the human leukocyte antigen (HLA) locus, which contains the genes encoding the human major histocompatibility complex (MHC). By affecting the geometry of autoantigen presentation to T cells, these polymorphisms can dictate the outcome of autoreactive T cell responses[17,18]. As B cell responses are reliant on the formation of the $T_{FH}$-B cell crosstalk, HLA-II polymorphisms can also impact the development of autoantibodies. Indeed, autoreactive B cell responses have been linked to HLA-II polymorphisms in several autoimmune settings[19,20]. Several HLA-II loci are associated with increased risk in childhood INS including *HLA-DQA1* (DQA1*02), *HLA-DQB1* (DQB1*02), and *HLA-DRB1* (DRB1*07 and DRB1*08), though the mechanism remains unknown[21-27].

We hypothesized that polymorphisms in the genes encoding MHC-II impact the capacity for APA generation in INS. In this study, we use the Crb2 immunization-based EANS model in mice with distinct MHC-II haplotypes and demonstrate that disease induction is tightly dependent on mouse strain. Unlike C3H/HeN and BALB/c mice, which develop significant proteinuria following EANS induction, C57BL/6 mice are fully protected despite developing high titers of anti-Crb2 antibody. In the C57BL/6 strain, anti-Crb2 antibodies do not bind podocytes and germinal center responses fail to regenerate in subsequent challenges with autoantigen, denoting an antigen-specific defect in humoral immunity or the development of tolerance. In total, we propose that the production of APAs capable of inducing podocyte injury is linked with the MHC-II haplotype.

## 4.4 Methods

### *Human Subjects and HLA-typing*

Blood samples were obtained from 22 children with INS participating in an observational longitudinal study as previously described[11]. Children were enrolled according to protocols approved by institutional Research Ethics Boards (REBs) at the Research Institute of the McGill University Health Centre (MUHC-14-466, T.T.) or the Alberta Children's Hospital (CHREB-16-2186, S.S.). Samples were collected at disease remission (urinary protein-to-creatinine ratio < 0.02 g/mmol or negative/trace dipstick) during scheduled hospital visits for follow-up or treatment. Of the 22 children, 20 received were steroid-sensitive (SSNS), four of which had biopsy-proven minimal change disease (MCD). The remaining two children were steroid-resistant (SRNS) with biopsies showing focal segmental glomerulosclerosis (FSGS). Peripheral blood mononuclear cells (PBMC) were isolated from the blood by Ficoll-paque centrifugation and were cryopreserved in FBS containing 10% DMSO. Genomic DNA was isolated from $1\times10^6$ PBMC and HLA-I and HLA-II sequences were obtained via next generation sequencing on the Illumina MiSeq (Illumina). Sequence alignment and HLA genotyping up to eight digits was completed using the TruSight HLA Assign software (Illumina).

### *Mice*

Wildtype C57BL/6, BALB/c, and C3H/HeN (Charles River Laboratories, Wilmington, MA) were bred at the Research Institute of the McGill University Health Centre (RI-MUHC, Montréal, QC). All mice were raised in specific pathogen-free conditions and male 8-week-old mice were used in all experiments. Experiments were performed according to the Canadian Council on Animal Care and to institutional guidelines at McGill University, and ethical guidelines approved by local committees at the RI-MUHC.

### *Recombinant mouse Crb2 generation and purification*

*Escherichia coli* transformed with a pET22b (+) vector containing the gene corresponding to the amino acids 601-940 of mouse Crb2 with N-terminal fusions of the

Factor Xa recognition sequence, Strep-tag, FLAG-tag, and $His_6$-tag were generously gifted by Dr. Kunimasa Yan (Kyorin University, Tokyo, Japan)[16]. Transformed *E. coli* were cultured with shaking in LB broth containing 100 µg/ml ampicillin (Millipore Sigma, St. Louis, MO) at 37 °C overnight before inducing $mCrb2_{601-940}$ production with 0.1 mM isopropyl β-D-thiogalactopyranoside (Millipore Sigma). After 3 h incubation, bacteria were pelleted (20,000 ×g, 4 °C, 20 minutes), supernatant discarded, and washed thrice with PBS before lysing with TNE buffer (50 mM Tris-HCl, 100 mM NaCl, 0.1 mM EDTA, pH 7.4). $rmCrb2_{601-940}$ production was confirmed via Coomassie blue. Purification was completed using HisPur Ni-NTA Resin (ThermoFisher Scientific) following the manufacturer's instructions under denaturing conditions. First, pellet lysates were equilibrated in equilibration buffer (PBS, 6 M guanidine-HCl, 10 mM imidazole, pH 7.4), applied to the resin bed, and rotated for 30 minutes. After centrifugation (700 ×g, room temperature, 2 minutes), the resin was washed twice with wash buffer (PBS, 6 M guanidine-HCl, 25 mM imidazole, pH 5.0) and eluted with elution buffer (PBS, 6 M guanidine-HCl, 250 mM imidazole). Dialysis was performed to obtain purified $rmCrb2_{601-940}$.

***EANS induction***

For the initial immunization, 1 mg/ml $rmCrb2_{601-940}$ in PBS solution (or only PBS for control mice) was emulsified 1:1 with Complete Freund's Adjuvant (CFA, Millipore Sigma) and 100 µl was injected bilaterally at the base of the tail for a total dose of 100 µg $rmCrb2_{601-940}$. Mice were re-challenged after 2, 4, and 6 weeks with the subcutaneous administration of 100 µl of 1mg/ml $rmCrb2_{601-940}$ in PBS (or only PBS for control mice) emulsified 1:1 with Incomplete Freund's Adjuvant (IFA, Millipore Sigma) at both flanks. Urine was collected manually, and urinary albumin (Bethyl Laboratories) and creatinine (Cayman Chemical) concentrations were measured by ELISAs. The former was normalized to the latter to obtain urinary albumin-to-creatinine ratios (uACR). Serum was collected from the saphenous vein prior to sacrifice.

***Anti-Crb2 ELISA***

Wells of ELISA plates (MaxiSorp, ThermoFisher Scientific) were coated with 100 µl $rmCrb2_{601-940}$ (1 µg in 0.2 M sodium carbonate-bicarbonate solution) and incubated at 4 °C for 16 h. After washing with washing buffer (PBS, 0.05% Tween 20), wells were blocked with 200 µl blocking buffer (PBS, 2% BSA, 0.05% Tween 20) for 2 h at room temperature. Wells were washed and 100 µl of diluted serum samples and standards were added; serum samples were diluted 1:5000 and 1:25,000 in blocking buffer and standards were prepared using purified polyclonal mouse anti-mouse Crb2 IgG. After 3 h of incubation at room temperature, wells were washed and 100 µl of HRP-conjugated goat anti-mouse IgG1/IgG2a/IgG2b/IgG3 (1:1000 in blocking buffer) was added for 1 h at room temperature. After washing, 100 µl of 3,3',5,5'-tetramethylbenzidine substrate solution was added to each well and allowed to develop for 5 minutes at room temperature before quenching with 100 µl of 2 N $H_2SO_4$. Absorbance was measured at 450 nm and 570 nm. Titres were calculated using a four-parameter logistic curve.

***Immunofluorescence***

Kidneys were harvested from mice, frozen in O.C.T., and 4 µm sections were mounted onto glass slides. After airdrying, slides were washed in ice-cold acetone and fixed with 4% paraformaldehyde for 15 minutes at room temperature. Slides were then washed with PBS and blocked for 30 minutes with blocking buffer (3% BSA in PBS) at room temperature. To reduce background mouse IgG staining, slides were incubated with donkey anti-mouse IgG in blocking buffer for another 30 minutes at room temperature. Slides were then stained with goat anti-Nephrin IgG for 16 h at 4 °C, washed, and incubated with anti-goat IgG-Alexa Fluor 488 and anti-mouse IgG-Alexa Fluor 555 for 1 h at room temperature. Nuclei were stained with DAPI dye and mounted using Aqua-Mount mounting medium (ThermoFisher Scientific). Confocal images were captured with Zeiss LSM 780 confocal microscope and processed via Zen v8.1.0.484 software (Zeiss). Fluorescence intensity was averaged across 40-60 glomeruli across each section.

***Cell isolation***

Draining (inguinal) and non-draining (cervical) lymph nodes were mechanically dissociated between the frosted ends of two sterile glass slides and washed with complete medium (RPMI-1640, 10% fetal bovine serum, 1% HEPES, 1% penicillin/streptomycin). Cells were centrifuged (400 ×g, 4 °C, 5 minutes), resuspended in complete medium and filtered through a 70 µm cell strainer. Spleens were dissociated similarly, but red blood cells were lysed using ammonium-chloride-potassium solution before the washing and filtering steps. Single cell suspensions were counted on the hemocytometer using Trypan blue exclusion dye.

***Crb2-specific T cell quantification***

To quantify Crb2-specific T cell responses, $1\times10^6$ unfractionated cells from inguinal lymph nodes of rmCrb2$_{601\text{-}940}$ immunized or vehicle-treated mice were cultured in complete media with 4 µg of rmCrb2$_{601\text{-}940}$. For each sample, another well receiving equimolar quantities of PBS diluted in complete media were used as the negative control. After incubating for 12 h at 37 °C and 5% $CO_2$, cells were treated with GolgiStop (1:1000, BD Biosciences) and GolgiPlug (1:1000, BD Biosciences) and left in culture for an additional six hours before staining for flow cytometry. The quantity of Crb2-specific T cells producing TNF-α, IFN-γ, and IL-17A in each sample were determined by subtracting the proportion of cytokine-producing T cells in the negative control well from those in the rmCrb2$_{601\text{-}940}$ stimulated well.

***Flow cytometry***

From the single cell suspension, no more than $1\times10^6$ cells were stained for each flow cytometry panel. Cells were incubated with Fixable Viability eFluor 780 dye (ThermoFisher Scientific) at 4 °C for 15 minutes, washed with ice-cold PBS+2% FBS, and then incubated for another 15 minutes with rat anti-mouse CD16/32 (BD Biosciences). After another wash, extracellular staining was performed using cocktails of antibodies targeting extracellular proteins prepared in PBS+2% FBS: BUV737 anti-mouse CD3ε (17A2, BD Biosciences, 1:100),

Alexa700 anti-mouse CD4 (RM4-5, BioLegend, 1:100), PE anti-mouse CD8α (53-6.7, BioLegend, 1:100), BV510 anti-mouse CD8β (H35-17.2, BD Biosciences, 1:100), PerCp-Cy5.5 anti-mouse CD62L (MEL-14, ThermoFisher Scientific, 1:100), APC anti-mouse CD44 (IM7, ThermoFisher Scientific, 1:100), Super Bright 436 anti-mouse PD-1 (eBioJ105, ThermoFisher Scientific, 1:100), BUV737 anti-mouse CD19 (1D3, BD Biosciences, 1:100), PE anti-mouse CD138 (281-2, BioLegend, 1:100), PE-CF594 anti-mouse CD95 (Jo2, BD Biosciences, 1:100), PerCp-Cy5.5 anti-mouse GL7 (GL7, BioLegend, 1:100), FITC anti-mouse IgM (RMM-1, BioLegend, 1:100), BUV395 anti-mouse IgD (11-26c.2a, BD Biosciences, 1:100), and APC anti-mouse polyIgG (Poly4053, BioLegend, 1:100). Cells were then washed in ice-cold PBS, fixed using the eBioscience Foxp3/Transcription Factor buffer set (eBioscience), and incubated with antibody cocktails targeting intracellular proteins prepared in 1X permeabilization buffer (eBioscience): BUV395 anti-Ki-67 (B56, BD Biosciences, 1:50), FITC anti-mouse Foxp3 (FJK-16s, ThermoFisher Scientific, 1:100), PE-Cy7 anti-mouse/human Helios (22F6, BioLegend, 1:100), APC-Cy7 anti-mouse/human Bcl-6 (K112-91, BD Biosciences, 1:40), APC anti-mouse TNF (MP6-XT22, BioLegend, 1:100), PE-Cy7 anti-mouse IFN-γ (XMG1.2, BioLegend, 1:100), PE anti-mouse IL-4 (11B11, ThermoFisher Scientific, 1:100), and V450 anti-mouse IL-17A (TC11-18H10, BD Biosciences, 1:100). Cells were washed twice more, once in 1X permeabilization buffer and once in PBS, before acquisition on the BD LSRFortessa X-20. Data were analyzed on FlowJo v10.8 (FlowJo, LLC).

***Statistics***

Statistical analyses were performed on GraphPad Prism v10 (GraphPad). Odds ratios are displayed as forest plots with the mean (point) and 95% confidence intervals (whiskers). All other data are displayed as mean ± standard deviation with an individual dot representing a single mouse. Multivariate analyses were done using a two-way ANOVA with Tukey's post-hoc testing for multiple comparisons. *P*-values <0.05 were considered significant and significant *P*-values were depicted on the graph as *$P \leq 0.05$, **$P \leq 0.01$, ***$P \leq 0.001$, and

****$P \leq 0.0001$. No data were excluded unless the material (e.g. urine, kidney tissue, cells) were not sufficient for the experiment.

## 4.5 Results

### *4.5.1. DRB1, DQA1, and DQB1 alleles are associated with childhood INS.*

Genome wide association studies (GWAS) have identified several HLA alleles associated with increased risk for childhood INS. We sought to evaluate the presence of these risk alleles in a Canadian multi-ethnic cohort of 22 children with INS by typing 11 distinct HLA loci using next-generation sequencing (**Supplemental Data 1**). Hierarchical clustering was performed, and the six most prevalent alleles were clustered together: *HLA-DPB1**04:01, *HLA-DPA1**01:03, *HLA-DRB4**01:03, *HLA-DRB1**07:01, *HLA-DQA1**02:01, and *HLA-DQB1**02:02 (**Figure 1A**). The first three are highly abundant alleles within the general population, while the last three have been previously associated with increased risk of childhood INS[26,28]. Of the 22 individuals evaluated, 14 were heterozygous carriers of the risk-associated alleles with one individual being homozygous for all three (**Figure 1A**). Carriers included all three children with biopsy-proven MCD and one of the two children with biopsy-proven FSGS (**Figure 1A**). We next calculated the risk associated with each of these alleles at the allelic (i.e. allelic frequency) and carrier (i.e. incidence) levels utilizing a dataset of 496 healthy individuals from San Diego, California with *HLA-DPB1*, *HLA-DRB1*, *HLA-DQA1*, and *HLA-DQB1* genotypes completed as control. Risk for childhood INS was strongly associated with *DRB1**07:01, *DQA1**02:01, and *DQB1**02:02 (**Figure 1B and C**).

### *4.5.2. C57BL/6 mice are protected from EANS1 despite producing anti-Crb2 antibody.*

The clear association of INS with HLA-II alleles and the recent discovery of APAs in subsets of affected individuals encouraged us to evaluate the impact of MHC-II on the generation of podocytopathic antibodies. To this end, we made use of the recently developed Crb2 immunization-based EANS mouse model wherein an initial immunization with $rmCrb2_{601\text{-}940}$ followed by two boosts generates anti-Crb2 antibodies capable of inducing podocyte injury and significant proteinuria[16]. In lieu of HLA transgenic mice, mice with completely distinct MHC-II allele usage, namely C57BL/6, BALB/c, and C3H/HeN, were immunized with $rmCrb2_{601\text{-}940}$ or vehicle and were subsequently re-challenged every two weeks for a total of three boosts (**Figure 2A**). As expected, 7/9 C3H/HeN mice, the

background in which the model was originally established, developed substantial proteinuria following the second boost while this was only the case for approximately half of the BALB/c mice (**Figure 2B**). Notably, C57BL/6 mice were completely protected from proteinuria, despite developing anti-Crb2 IgG at levels comparable to C3H/HeN mice and significantly higher than those in BALB/c mice (**Figure 2B and C**).

Next, to test the podocytopathic potential of these anti-Crb2 antibodies, we investigated if autoantibodies were binding podocytes within the glomeruli of each strain. Control mice that received only vehicle showed no glomerular deposition of mouse IgG and served as our reference for quantifying signal (**Figure 2D and E**). In contrast, Crb2-immunized C3H/HeN and BALB/c mice had significant IgG deposition that overlapped with Nephrin$^+$ podocytes (**Figure 2D and 2E**). Crb2-immunized C57BL/6 mice, however, showed no glomerular IgG deposition (**Figure 2D and E**). These data demonstrate that Crb2 immunization robustly induces anti-Crb2 antibody generation, but the podocytopathic potential of these antibodies is dependent on mouse strain.

### *4.5.3. Germinal centres fail to persist with repeated Crb2 immunization in C57BL/6 mice.*

Since the podocyte-binding capacity of anti-Crb2 antibodies was impaired in C57BL/6 mice while their production remained intact, we sought to compare the dynamics of the B cell response between mouse strains. B cell frequencies and numbers within inguinal lymph nodes did not change significantly over the course of the experiment and remained comparable to control mice (**Figure 3A**). Nevertheless, germinal centers (CD95$^+$ GL7$^+$ B cells), the primary sites of antibody maturation, were induced in all mouse strains following the first boost, and this was particularly pronounced in the fully susceptible C3H/HeN mice (**Fig. 3B and C**). Following the final boost, however, only C3H/HeN and BALB/c mice mounted robust germinal center responses; germinal centers in C57BL/6 mice were significantly diminished (**Fig. 3B and C**). Accordingly, isotype-switched memory B cells were significantly reduced in C57BL/6 mice as well (**Fig. 3D**). Together, our data indicates

that C57BL/6 mice are not capable of mounting robust humoral responses following repeated rmCrb2$_{601\text{-}940}$ challenge.

### *4.5.4. Crb2-specific T cell responses were present in all strains.*

A possible explanation for the lack of persistence of germinal center responses in C57BL/6 mice is the development of tolerance with repeated immunization. To test this, we evaluated the presence of Crb2-specific T cell responses in each strain, which we hypothesized would also be dampened by the same tolerance mechanisms. Cells from inguinal lymph nodes taken four days following the final boost from Crb2-immunized and control mice were cultured alongside rmCrb2$_{601\text{-}940}$ for 18 h, with Golgi transport inhibitors added in the last 6 h before assessing cytokine production by flow cytometry. Within the CD4$^+$ T cell compartment, Crb2-specific TNF-α$^+$ and IL-17A$^+$ cells were observed in all immunized mice (**Figure 4A and B**). While IFN-γ$^+$ CD4$^+$ T cells were also present in both C57BL/6 and C3H/HeN strains, they were absent from BALB/c mice, which was expected since the BALB/c background possesses a $T_H2$ bias (**Figure 4A and B**). Equivalent results were obtained within the CD8$^+$ T cell compartment with the induction of Crb2-specific TNF-α$^+$ and IL-17A$^+$ cells in all strains and IFN-γ$^+$ cells solely in C57BL/6 and C3H/HeN strains (**Figure 4C and D**). Thus, despite the lack of persistence of germinal centers in C57BL/6 mice, intact recall responses were evident in the T cell compartment regardless of mouse background.

### 4.6 Discussion

The factors regulating the generation of autoantibodies capable of mediating podocyte injury in childhood INS remain unknown[12]. Given the frequent association of HLA-II alleles with childhood INS, we sought to investigate the impact of MHC-II on the production of APAs[21-27]. Using the Crb2 immunization-based EANS model in MHC-II distinct C57BL/6, BALB/c, and C3H/HeN strains, we show that C57BL/6 mice were completely protected from disease induction while C3H/HeN and BALB/c mice were susceptible. Despite all strains developing high titers of anti-Crb2 antibodies, antibodies from C57BL/6 mice failed to bind to podocytes in the glomerulus. Moreover, germinal center responses in C57BL/6 mice failed to be recalled with subsequent rmCrb2$_{601\text{-}940}$ challenge despite an intact recall response taking place within the T cell compartment. Altogether, our study provides strong evidence that MHC-II polymorphisms impact the podocytopathic potential of APAs.

GWAS have identified several distinct genetic loci associated with increased risk in childhood INS. These include possibly immune-related genes like *TNFSF15*, *CD28*, *CALHM6*, *MICA*, *CLEC16A*, and *ELMO1* and the gene encoding Nephrin (*NPHS1*)[26]. In all studies, however, the HLA-II locus consistently confers the greatest risk. In our study, we HLA typed 22 children with INS and found that *HLA-DQA1**02:01, *HLA-DQB1**02:02, and *HLA-DRB1**07:01 were associated with increased risk. Indeed, the *DQA1**02:01 and *DQB1**02:02 alleles are the most consistently identified INS-associated polymorphisms by GWAS. These alleles are in linkage disequilibrium explaining their shared inheritance within our cohort. *DRB1**07 was also previously implicated in INS, though the *HLA-DRB1**08 allele that was also identified by GWAS was not particularly enriched in our cohort[23,28]. Polymorphisms in the HLA-II locus can impact the nature of autoreactive T cell responses and can thus, through $T_{FH}$-B cell interactions, impact the outcome of autoantibody-production[18].

With no immunodominant T or B cell epitope established for either Nephrin or Crb2, it is difficult to explore the impact of MHC-II on the generation of APAs in humans. As such, we opted to use the EANS mouse model, an experimental setting where APAs are generated against a single podocyte antigen with established podocytopathic capacity, and MHC-II haplotypes are easily changed. Using C57BL/6, BALB/c and C3H/HeN mice, strains with

completely distinct MHC-II usage, we showed that C57BL/6 mice are resistant to developing proteinuria following EANS induction while C3H/HeN and BALB/c mice were susceptible. Despite C57BL/6 mice developing high anti-Crb2 titers, these antibodies did not bind to podocytes in the glomerulus. The impaired podocytopathic potential of C57BL/6 antibodies could be explained by the preferential utilisation of Crb2 epitopes in the $T_{FH}$-B cell crosstalk that do not support strong germinal center responses, resulting in the generation of lower affinity anti-Crb2 antibodies[29]. Indeed, while C57BL/6 mice initially developed modest germinal centers following the first boost, they failed to regenerate after the final challenge. This was in complete contrast to the fully susceptible C3H/HeN mice, which generated strong germinal center responses even following the initial boost. A reduced affinity for C57BL/6 anti-Crb2 antibodies would hinder their ability to bind Crb2 within the slit diaphragm and mediate podocytopathy. To evaluate this, we are currently testing the affinity and avidity of anti-Crb2 antibodies raised in different strains by ELISA.

Moreover, it is possible that repeated challenges with $rmCrb2_{601\text{-}940}$ in the C57BL/6 strain resulted in tolerance thereby suppressing the Crb2-directed B cell response, for example through the induction of Crb2-specific regulatory T ($T_{REG}$) cells. The engagement of $T_{REG}$ or inflammatory T cell responses through a MHC-II haplotype-dependent mechanism was previously demonstrated using the experimental autoimmune glomerulonephritis model for Goodpasture's syndrome[30]. Nevertheless, we observed strong pro-inflammatory Crb2-specific T cell responses denoted by TNF-α, IFN-γ, and IL-17A production in protected and susceptible strains, suggesting that tolerance had not developed. In BALB/c mice, which were variable in disease induction, we did not observe significant Crb2-specific IFN-$\gamma^+$ T cell induction consistent with their bias against $T_H1$ cell responses. Thus, the immune biases of these unique strains may also play a role in susceptibility to disease induction. To better assess both $T_{REG}$ and conventional T cell responses in EANS, we are currently identifying immunodominant epitopes of $rmCrb2_{601\text{-}940}$ with the eventual goal of generating MHC-II tetramers for *in vivo* use.

Finally, susceptibility to EANS may have been conferred by podocyte-intrinsic differences between strains. To better elucidate the mechanisms for susceptibility in EANS,

we are actively generating bone marrow chimeras between the fully protected C57BL/6 and fully susceptible C3H/HeN strain. Immune origins for susceptibility would be conferred by the donor bone marrow, whereas podocyte origins would be conferred by the host strain.

In summary, our study provides evidence that MHC-II haplotype determines the pathogenic potential of APAs. With a clear HLA-II association and the identification of several APAs in childhood INS, the utilization of transgenic mice introgressed with HLA-II susceptibility alleles would be crucial to understanding disease pathogenesis[30,31]. We envision that this work can lead to the development of antigen-specific methods for disease prognostication in humans.

**Acknowledgements**

We are grateful to all study participants, their families, and the medical teams involved in their care. We thank C. Saw and A. Maryunich from the HLA Lab of the McGill University Health Centre for their HLA typing services. This work was supported by Canadian Institute of Health Research (CIHR) project grants (PJT-16006 to T.T., C.P., S.S., and PJT-192017 to T.T., C.P.). T.A. was also supported by a CIHR Doctoral Award. The authors declare no competing interests.

**Author contributions**

T.A., C.A.P. and T.T. conceptualized the study and designed all the experiments. T.A. completed all the data analysis. T.A. and L.A. processed the blood samples for HLA typing. T.A., S.G., S.L., and S.S. performed all immunizations. T.A. and S.G. collected urine and blood. T.A. performed urine and serum ELISAs, sacrificed the mice and harvested the organs, performed flow cytometry, and ran the *in vitro* Crb2-specific T cell culture. L.A. performed the immunofluorescence experiments. T.A., C.A.P and T.T. wrote the initial draft of the manuscript.

## 4.7 Figures

## Figure 1

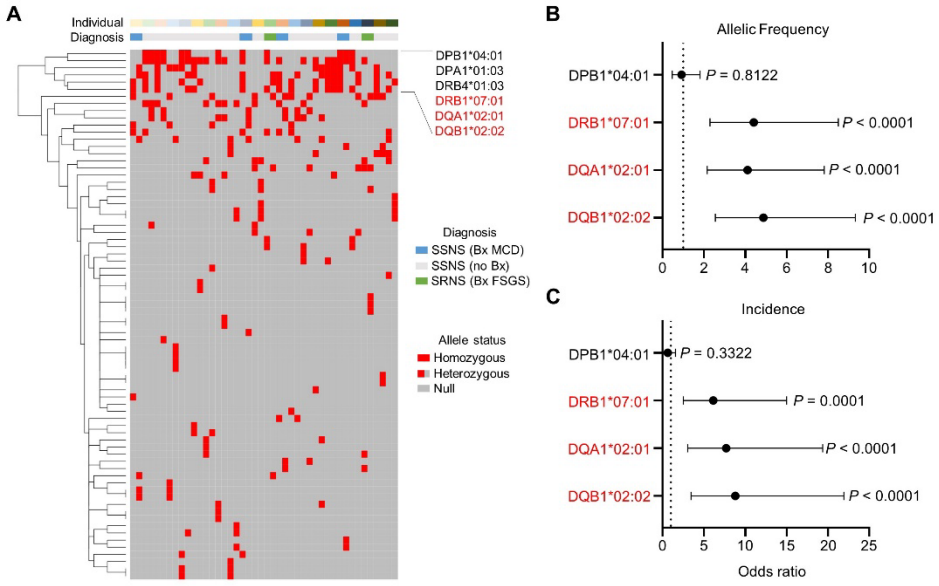

**Figure 1: Childhood INS is associated with DQA1*02:01, DQB1*02:02, and DRB1*07:01 alleles.** (**A**) Heatmap with hierarchical clustering of HLA class II alleles in rows and children with INS (*N* = 22) on top. Only HLA class II alleles present in the cohort are shown. There are two columns for every individual each corresponding with one allele. (**B and C**) Odds ratios with 95% confidence intervals calculated based on the allelic frequency (B) and incidence (C) of HLA alleles in the cohort. A reference cohort of healthy individuals from San Diego, California (*N* = 496) was used as control.

## Figure 2

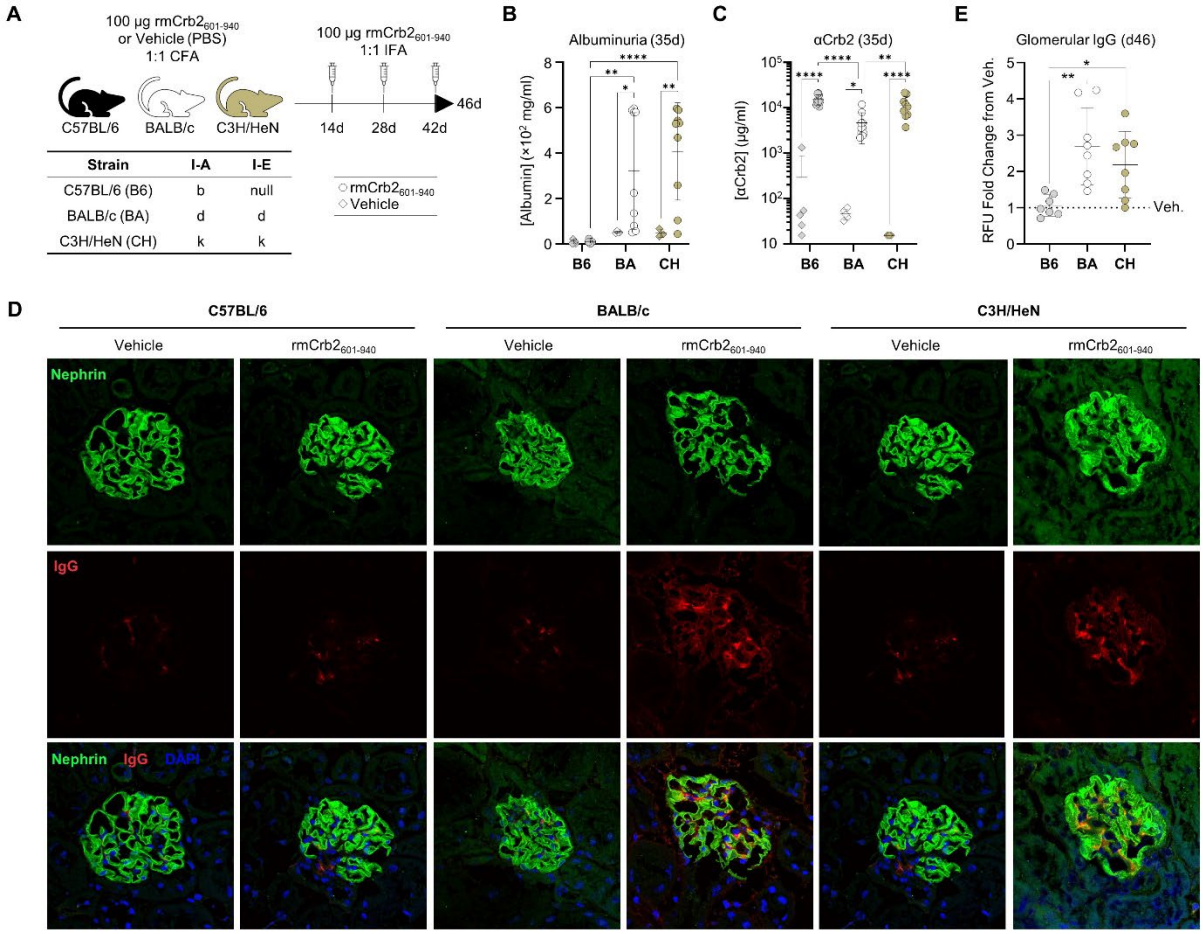
A
100 µg rmCrb2601-940
or Vehicle (PBS)
1:1 CFA
C57BL/6
BALB/c
C3H/HeN
100 µg rmCrb2601-940
1:1 IFA
14d
28d
42d
46d
rmCrb2601-940
Vehicle
Strain | I-A | I-E
C57BL/6 (B6) | b | null
BALB/c (BA) | d | d
C3H/HeN (CH) | k | k
B
Albuminuria (35d)
[Albumin] (×10² mg/ml)
B6
BA
CH
C
αCrb2 (35d)
[αCrb2] (µg/ml)
E
Glomerular IgG (d46)
RFU Fold Change from Veh.
Veh.
D
C57BL/6
BALB/c
C3H/HeN
Vehicle
rmCrb2601-940
Nephrin
IgG
Nephrin IgG DAPI

**Figure 2: MHC-II distinct mice are differentially susceptible to EANS induction.** (**A**) Schematic for EANS induction in the MHC-II distinct C57BL/6, BALB/c, and C3H/HeN strains. The MHC-II haplotypes are shown in the table. (**B**) Urinary albumin concentrations one week following the second challenge (day 35) in rmCrb2$_{601\text{-}940}$-immunized or PBS (vehicle)-treated C57BL/6 (B6, $n_{Crb2}$ = 9, $n_{Veh}$ = 5), BALB/c (BA, $n_{Crb2}$ = 9, $n_{Veh}$ = 4), and C3H/HeN (CH, $n_{Crb2}$ = 9, $n_{Veh}$ = 3) mice. (**C**) Serum anti-rmCrb2$_{601\text{-}940}$ concentrations one week following the second challenge (day 35) in B6 ($n_{Crb2}$ = 9, $n_{Veh}$ = 5), BA ($n_{Crb2}$ = 10, $n_{Veh}$ = 5), and CH ($n_{Crb2}$ = 9, $n_{Veh}$ = 3) mice. (**D and E**) Representative confocal images showing Nephrin and mouse IgG in glomeruli from Crb2-immunized or vehicle control B6 ($n_{Crb2}$ = 7, $n_{Veh}$ = 3), BA ($n_{Crb2}$ = 8, $n_{Veh}$ = 3), and CH ($n_{Crb2}$ = 8, $n_{Veh}$ = 3) mice (D) with quantification (E) following the final challenge (day 46). Relative fluorescent units (RFU) from the immunized are shown as fold change from the vehicle controls. Data were compiled across two independent experiments ($n$ = 4-5 in Crb2-immunized groups, 1-3 in vehicle control groups) and are shown as mean ± standard deviation with each dot representing an individual mouse. *P*-values were determined using a two-way ANOVA with Tukey's post-hoc testing for multiple comparisons (B and C) or one-way ANOVA with Tukey's post-hoc testing (D) (*$P$≤0.05, **$P$≤0.01, ***$P$≤0.001, and ****$P$≤0.0001).

## Figure 3

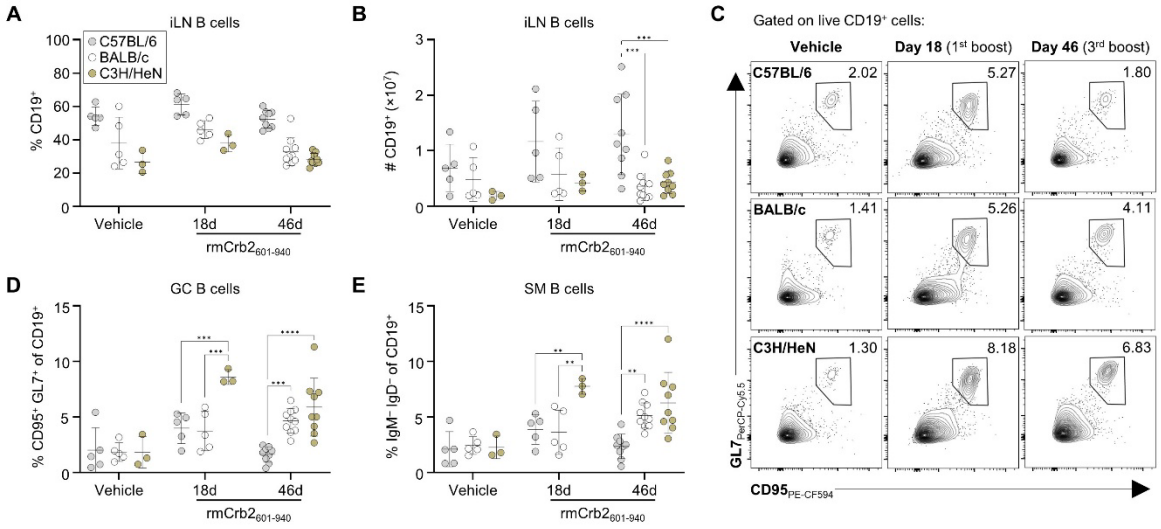
A
iLN B cells
C57BL/6
BALB/c
C3H/HeN
% CD19+
Vehicle
18d
46d
rmCrb2601-940
B
iLN B cells
# CD19+ (×10⁷)
C
Gated on live CD19+ cells:
Vehicle
Day 18 (1st boost)
Day 46 (3rd boost)
C57BL/6
2.02
5.27
1.80
BALB/c
1.41
5.26
4.11
C3H/HeN
1.30
8.18
6.83
GL7PerCP-Cy5.5
CD95PE-CF594
D
GC B cells
% CD95+ GL7+ of CD19+
E
SM B cells
% IgM− IgD− of CD19+

**Figure 3: Germinal centers are not recalled after re-challenge with rmCrb2$_{601\text{-}940}$ in C57BL/6 mice.** (**A and B**) Frequencies (A) and absolute (B) numbers of B cells in the draining inguinal lymph nodes of rmCrb2$_{601\text{-}940}$-immunized or PBS (vehicle)-treated C57BL/6 ($n_{18d}$ = 5, $n_{46d}$ = 9, $n_{Veh}$ = 5), BALB/c ($n_{18d}$ = 5, $n_{46d}$ = 10, $n_{Veh}$ = 5), and C3H/HeN ($n_{18d}$ = 3, $n_{46d}$ = 9, $n_{Veh}$ = 3) mice. (**C and D**) Representative flow plots showing germinal center B cells (GL7$^+$ CD95$^+$) in draining inguinal lymph nodes (C) and quantification of the frequencies (D). (**E**) Frequencies of isotype-switched memory (IgM$^-$ IgD$^-$) B cells in draining inguinal lymph nodes. Data were compiled across two independent experiments ($n$ = 4-5 in rmCrb2$_{601\text{-}940}$-immunized groups, 1-3 in vehicle control groups) except for the 18d time point which is from a single experiment. Data are shown as mean ± standard deviation with each dot representing an individual mouse. *P*-values were determined using a two-way ANOVA with Tukey's post-hoc testing for multiple comparisons (*$P$≤0.05, **$P$≤0.01, ***$P$≤0.001, and ****$P$≤0.0001).

## Figure 4

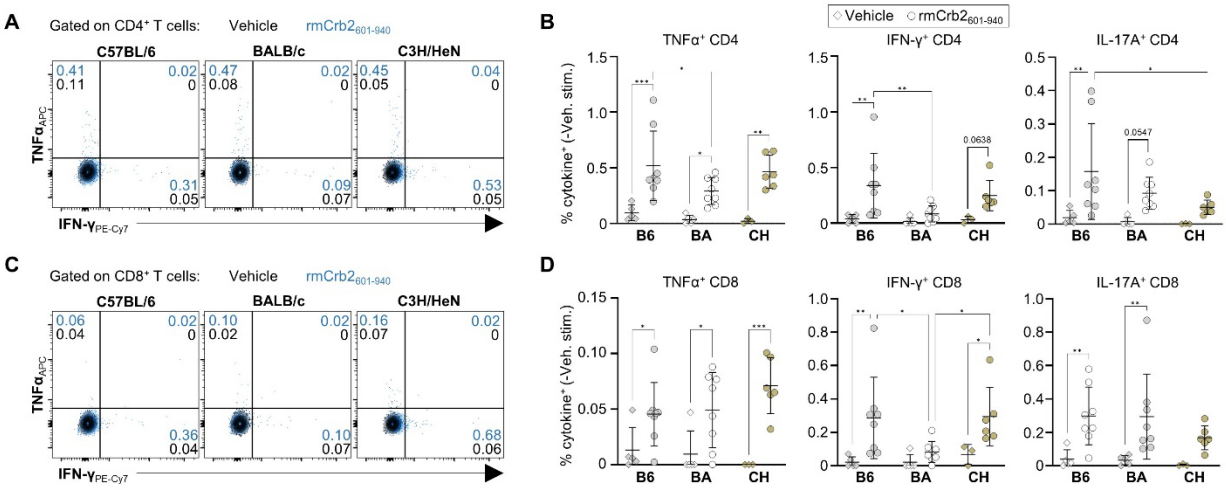
A
Gated on CD4⁺ T cells:
Vehicle
rmCrb2601-940
C57BL/6
BALB/c
C3H/HeN
TNFαAPC
IFN-γPE-Cy7
0.41
0.11
0.02
0
0.47
0.08
0.02
0
0.45
0.05
0.04
0
0.31
0.05
0.09
0.07
0.53
0.05
B
Vehicle
rmCrb2601-940
TNFα⁺ CD4
IFN-γ⁺ CD4
IL-17A⁺ CD4
% cytokine⁺ (-Veh. stim.)
B6
BA
CH
0.0638
0.0547
C
Gated on CD8⁺ T cells:
Vehicle
rmCrb2601-940
C57BL/6
BALB/c
C3H/HeN
TNFαAPC
IFN-γPE-Cy7
0.06
0.04
0.02
0
0.10
0.02
0.02
0
0.16
0.07
0.02
0
0.36
0.04
0.10
0.07
0.68
0.06
D
TNFα⁺ CD8
IFN-γ⁺ CD8
IL-17A⁺ CD8
% cytokine⁺ (-Veh. stim.)
B6
BA
CH

**Figure 4: Crb2-specific T cell responses develop in all strains.** (**A and C**) Representative flow plots showing TNF-α and IFN-γ production by $CD4^+$ (A) and $CD8^+$ T cells from inguinal lymph nodes of $rmCrb2_{601\text{-}940}$-immunized mice harvested four days following the final challenge and stimulated *in vitro* with $rmCrb2_{601\text{-}940}$ (*blue*) or vehicle (*black*). (**B and D**) Quantification of Crb2-specific cytokine production in $CD4^+$ (B) and $CD8^+$ (D) T cells from $rmCrb2_{601\text{-}940}$-immunized or PBS (vehicle)-treated mice. Values were obtained by subtracting the proportion of $cytokine^+$ cells in the $rmCrb2_{601\text{-}940}$-stimulated condition from the proportion of $cytokine^+$ cells in the vehicle-stimulated condition. Data were obtained from two independent experiments ($n$ = 4-5 in $rmCrb2_{601\text{-}940}$-immunized groups, 1-3 in vehicle control groups) and are shown as mean ± standard deviation with each dot representing an individual mouse. $P$-values were determined using two-way ANOVA with Tukey's post-hoc testing for multiple comparisons (*$P$≤0.05, **$P$≤0.01, ***$P$≤0.001, and ****$P$≤0.0001).

### 4.8 References


1 Eddy, A. A. & Symons, J. M. Nephrotic syndrome in childhood. *The Lancet* **362**, 629-639 (2003). https://doi.org:10.1016/S0140-6736(03)14184-0

2 Vivarelli, M., Gibson, K., Sinha, A. & Boyer, O. Childhood nephrotic syndrome. *The Lancet* **402**, 809-824 (2023). https://doi.org:https://doi.org/10.1016/S0140-6736(23)01051-6

3 Noone, D. G., Iijima, K. & Parekh, R. Idiopathic nephrotic syndrome in children. *The Lancet* **392**, 61-74 (2018). https://doi.org:https://doi.org/10.1016/S0140-6736(18)30536-1

4 Samuel, S. M. *et al.* Setting New Directions for Research in Childhood Nephrotic Syndrome: Results From a National Workshop. *Can J Kidney Health Dis* **4**, 2054358117703386 (2017). https://doi.org:10.1177/2054358117703386

5 Chan, E. Y.-h. *et al.* Use of Rituximab in Childhood Idiopathic Nephrotic Syndrome. *Clinical Journal of the American Society of Nephrology* **18** (2023).

6 Colucci, M., Oniszczuk, J., Vivarelli, M. & Audard, V. B-Cell Dysregulation in Idiopathic Nephrotic Syndrome: What We Know and What We Need to Discover. *Frontiers in immunology* **13**, 823204-823204 (2022). https://doi.org:10.3389/fimmu.2022.823204

7 Printza, N., Papachristou, F., Tzimouli, V., Taparkou, A. & Kanakoudi-Tsakalidou, F. Peripheral CD19+ B cells are increased in children with active steroid-sensitive nephrotic syndrome. *NDT Plus* **2**, 435-436 (2009). https://doi.org:10.1093/ndtplus/sfp087

8 Colucci, M. *et al.* B cell phenotype in pediatric idiopathic nephrotic syndrome. *Pediatric Nephrology* **34**, 177-181 (2019). https://doi.org:10.1007/s00467-018-4095-z

9 Ling, C. *et al.* Decreased Circulating Transitional B-Cell to Memory B-Cell Ratio Is a Risk Factor for Relapse in Children with Steroid-Sensitive Nephrotic Syndrome. *Nephron* **145**, 107-112 (2021). https://doi.org:10.1159/000511319

10 Yang, X. *et al.* Circulating follicular T helper cells are possibly associated with low levels of serum immunoglobulin G due to impaired immunoglobulin class-switch recombination of B cells in children with primary nephrotic syndrome. *Molecular Immunology* **114**, 162-170 (2019). https://doi.org:https://doi.org/10.1016/j.molimm.2019.07.001

11 Al-Aubodah, T.-A. *et al.* The extrafollicular B cell response is a hallmark of childhood idiopathic nephrotic syndrome. *Nature Communications* **14**, 7682 (2023). https://doi.org:10.1038/s41467-023-43504-8

12 Watts, A. J. B. *et al.* Discovery of Autoantibodies Targeting Nephrin in Minimal Change Disease Supports a Novel Autoimmune Etiology. *Journal of the American Society of Nephrology* **33**, 238 (2022). https://doi.org:10.1681/ASN.2021060794

13 Ye, Q. *et al.* The important roles and molecular mechanisms of annexin A(2) autoantibody in children with nephrotic syndrome. *Ann Transl Med* **9**, 1452 (2021). https://doi.org:10.21037/atm-21-3988

14 Ye, Q. *et al.* Seven novel podocyte autoantibodies were identified to diagnosis a new disease subgroup-autoimmune Podocytopathies. *Clin Immunol* **232**, 108869 (2021). https://doi.org:10.1016/j.clim.2021.108869

15 Takeuchi, K. *et al.* New Anti-Nephrin Antibody Mediated Podocyte Injury Model Using a C57BL/6 Mouse Strain. *Nephron* **138**, 71-87 (2017). https://doi.org:10.1159/000479935

16 Hada, I. *et al.* A Novel Mouse Model of Idiopathic Nephrotic Syndrome Induced by Immunization with the Podocyte Protein Crb2. *Journal of the American Society of Nephrology* **33** (2022).

17 Cho, J. H. & Gregersen, P. K. Genomics and the Multifactorial Nature of Human Autoimmune Disease. *New England Journal of Medicine* **365**, 1612-1623 (2011). https://doi.org:doi:10.1056/NEJMra1100030

18 Robson, K. J., Ooi, J. D., Holdsworth, S. R., Rossjohn, J. & Kitching, A. R. HLA and kidney disease: from associations to mechanisms. *Nature Reviews Nephrology* **14**, 636-655 (2018). https://doi.org:10.1038/s41581-018-0057-8

19 Miyadera, H. & Tokunaga, K. Associations of human leukocyte antigens with autoimmune diseases: challenges in identifying the mechanism. *Journal of Human Genetics* **60**, 697-702 (2015). https://doi.org:10.1038/jhg.2015.100

20 Paisansinsup, T. *et al.* HLA Class II Influences the Immune Response and Antibody Diversification to Ro60/Sjögren's Syndrome-A: Heightened Antibody Responses and Epitope Spreading in Mice Expressing HLA-DR molecules1. *The Journal of Immunology* **168**, 5876-5884 (2002). https://doi.org:10.4049/jimmunol.168.11.5876

21 Gbadegesin, R. A. *et al.* HLA-DQA1 and PLCG2 Are Candidate Risk Loci for Childhood-Onset Steroid-Sensitive Nephrotic Syndrome. *Journal of the American Society of Nephrology* **26** (2015).

22 Debiec, H. *et al.* Transethnic, Genome-Wide Analysis Reveals Immune-Related Risk Alleles and Phenotypic Correlates in Pediatric Steroid-Sensitive Nephrotic Syndrome. *Journal of the American Society of Nephrology* **29** (2018).

23 Jia, X. *et al.* Strong Association of the HLA-DR/DQ Locus with Childhood Steroid-Sensitive Nephrotic Syndrome in the Japanese Population. *Journal of the American Society of Nephrology* **29** (2018).

24 Jia, X. *et al.* Common risk variants in NPHS1 and TNFSF15 are associated with childhood steroid-sensitive nephrotic syndrome. *Kidney International* **98**, 1308-1322 (2020). https://doi.org:10.1016/j.kint.2020.05.029

25 Dufek, S. *et al.* Genetic Identification of Two Novel Loci Associated with Steroid-Sensitive Nephrotic Syndrome. *Journal of the American Society of Nephrology* **30** (2019).

26 Barry, A. *et al.* Multi-population genome-wide association study implicates immune and non-immune factors in pediatric steroid-sensitive nephrotic syndrome. *Nature Communications* **14**, 2481 (2023). https://doi.org:10.1038/s41467-023-37985-w

27 Downie, M. L. *et al.* Common Risk Variants in AHI1 Are Associated With Childhood Steroid Sensitive Nephrotic Syndrome. *Kidney Int Rep* **8**, 1562-1574 (2023). https://doi.org:10.1016/j.ekir.2023.05.018

28 Ramanathan, A. S. K. *et al.* Association of HLA-DR/DQ alleles and haplotypes with nephrotic syndrome. *Nephrology* **21**, 745-752 (2016). https://doi.org:https://doi.org/10.1111/nep.12669

29 Walker, L. S. K. The link between circulating follicular helper T cells and autoimmunity. *Nature Reviews Immunology* **22**, 567-575 (2022). https://doi.org:10.1038/s41577-022-00693-5

30 Ooi, J. D. *et al.* Dominant protection from HLA-linked autoimmunity by antigen-specific regulatory T cells. *Nature* **545**, 243-247 (2017). https://doi.org:10.1038/nature22329

31 Forsthuber, T. G. *et al.* T cell epitopes of human myelin oligodendrocyte glycoprotein identified in HLA-DR4 (DRB1*0401) transgenic mice are encephalitogenic and are presented by human B cells. *J Immunol* **167**, 7119-7125 (2001). https://doi.org:10.4049/jimmunol.167.12.7119

# CHAPTER 5: IL-1 and IL-33 limit $T_{REG}$ cell control of autologous responses in rapidly-progressive glomerulonephritis.

**IL-1 and IL-33 limit $T_{REG}$ cell control of autologous responses in rapidly-progressive glomerulonephritis.**

Tho-Alfakar Al-Aubodah[1,2,3], Roman Istomine[1,2], Fernando Alvarez[1,2], Tomoko Takano[3,4*], Ciriaco A. Piccirillo[1,2*]

[1] Department of Microbiology & Immunology, Faculty of Medicine and Health Sciences, McGill University, Montréal, Québec
[2] Infectious Diseases and Immunity in Global Health Program, Research Institute of the McGill University Health Centre, Montréal, Québec
[3] Metabolic Disorders and Complications Program, Research Institute of the McGill University Health Centre, Montréal, Québec
[4] Division of Nephrology, Faculty of Medicine and Health Sciences, McGill University, Montréal, Québec

*Correspondence should be addressed to:
**Dr. Ciriaco A. Piccirillo, Ph.D.**
Research Institute of the McGill University Health Centre (RI-MUHC),
Infectious Diseases and Immunity in Global Health Program
1001 Boulevard Décarie, Bloc E, Room EM2.3248
Montréal, Québec H4A 3J1, Canada
E-mail: ciro.piccirillo@mcgill.ca

**Dr. Tomoko Takano, M.D., Ph.D.**
Research Institute of the McGill University Health Centre (RI-MUHC),
Metabolic Disorders and Complications Program, Division of Nephrology
1001 Boulevard Décarie, Bloc E, Room EM1.3244
Montréal, Québec H4A 3J1, Canada
E-mail: tomoko.takano@mcgill.ca

**Manuscript in preparation.**

**5.1 Bridging Statement**

*Chapters 2* and *3* provide strong support for an autoimmune humoral origin for INS, positioning this disorder alongside MN as a non-inflammatory glomerulopathy with an APA-dependent etiology. However, in *Chapter 4*, we show that at least some APAs are in themselves not sufficient to mediate podocytopathy, but rely on underlying factors (e.g., HLA) to become pathogenetic. Another well-established feature of INS is a defect in the number of circulating $T_{REG}$ cells (414-421). Indeed, we also identified this defect in our cohort of children with INS (*unpublished data*) but were unable to qualify the nature of this defect due to the paucity of $T_{REG}$ cells in the PBMC of affected individuals. Whether this defect in $T_{REG}$ cells promotes the development of podocytopathic APAs remains unknown.

The importance of $T_{REG}$ cells in preventing kidney-directed autoimmunity is best established in inflammatory glomerulonephritis that lead to RPGN (e.g., IgAN, lupus nephritis, ANCA GN, and anti-GBM nephritis). Here, $T_{REG}$ cells provide protection from both the onset of disease by preventing autoantibody generation and chronicity by limiting the nephritogenic T cell responses that occur within the kidney (437). As such, the use of $T_{REG}$ cells in the treatment of glomerular disorders is becoming an attractive therapeutic option (438). Nevertheless, little is known about $T_{REG}$ cell development and function within the kidney, in both homeostasis and during inflammatory injury. In other autoimmune settings, the presence of pro-inflammatory cytokines is thought to counteract $T_{REG}$ cell suppression either by directly destabilizing $T_{REG}$ cells or by promoting $T_{EFF}$ cell resistance (210, 439-441). *Whether inflammation induced by kidney injury restricts $T_{REG}$ cell suppressive function thereby provoking glomerulonephritis remains unknown*. In *Chapter 5*, we explore this research gap by using a mouse model of RPGN wherein heterologous anti-GBM antibodies leads to largescale tissue destruction and the release of pro-inflammatory mediators. *We hypothesized that pro-inflammatory cytokines produced during acute kidney injury impair $T_{REG}$ cell control of nephritogenic T cell responses*.

## 5.2 Abstract

### Background

Regulatory T ($T_{REG}$) cells are critical at limiting pro-inflammatory T cell responses during rapidly-progressive glomerulonephritis (RPGN). While the therapeutic potential of $T_{REG}$ cells is clear, the factors controlling their development and function within the kidney remain poorly defined. Here, we investigated the impact of IL-1 and IL-33, alarmins released upon glomerular injury, on renal $T_{REG}$ cell control of nephritogenic T cell responses.

### Method

The nephrotoxic nephritis (NTN) model of RPGN was used to characterize renal $T_{REG}$ cell dynamics following kidney injury. Mouse models wherein $T_{REG}$ cells lack the capacity for IL-33 signaling and IL-1 signaling were used to evaluate the impact of IL-1 and IL-33 on renal $T_{REG}$ cells.

### Results

$T_{REG}$ cells accumulated in kidneys during the chronic (autologous) phase of NTN alongside $T_H1$ cells. These $T_{REG}$ arose as GATA-3$^+$ cells in renal lymph nodes (rLNs) independently of IL-33 signaling. Indeed, IL-33 signaling was detrimental to their control of autologous $T_H1$ cell responses in both the kidneys and rLNs. Similarly, IL-1 signaling diminished $T_{REG}$ cell capacity to limit renal $T_H1$ cell responses and promoted the loss of Foxp3 expression.

### Conclusions

IL-1 and IL-33 curtail $T_{REG}$ cell control of kidney-directed T cell responses. Thus, targeting these signals may augment immunoregulation within the kidney.

## 5.3 Introduction

Glomerulonephritis (GN) is the most frequent consequence of pathological immunity in the kidney, resulting in a progressive loss of kidney function and the eventual development of end-stage kidney disease[1, 2]. Autoimmune responses raised against renal or systemic autoantigens are the predominant causes of GN, with autoimmune GNs being the third largest contributors to chronic kidney disease globally[3]. The most aggressive forms are mediated by autoantibodies that precipitate a rapidly-progressive necrotizing injury hallmarked by the proliferation of glomerular parietal epithelial cells giving rise to crescentic lesions[4]. Intense immunosuppression is warranted for the treatment of rapidly-progressive GN (RPGN), but its efficacy is hampered by the non-specificity of therapeutic regimens, delayed diagnosis, and the incidence of severe treatment-associated side effects.

Though autoantibodies are the primary mediators of the inciting injury in RPGN, $CD4^+$ effector T ($T_{EFF}$) cells play an important role in orchestrating the immune responses responsible for disease progression[5, 6]. IL-17A-producing $T_H17$ and IFN-γ-producing $T_H1$ cells recruit and activate neutrophils and macrophages, which subsequently lead to the destruction of kidney tissue. $CD8^+$ cytotoxic T lymphocytes (CTLs) are also involved in perpetuating tissue injury. The dynamics of nephritogenic T cell responses in RPGN have been largely studied using the nephrotoxic nephritis (NTN) model[5, 7]. Here, $T_H17$ cells raised against heterologous anti-GBM antibodies coordinate the initial wave of inflammation (heterologous phase, 1-4 days) during which largescale tissue damage liberates kidney antigens[7]. The presentation of these autoantigens in the renal lymph node (rLN) induces autologous $T_H1$ cells that will mediate disease chronicity (autologous phase, >4 days) [8-10]. Targeting renal $T_{EFF}$ cells is becoming an attractive therapeutic option for RPGN[1, 7, 11].

Regulatory T ($T_{REG}$) cells, a class of immunosuppressive $CD4^+$ T cells, are pivotal at both preventing the onset of autoimmune GNs and limiting renal tissue destruction[12]. Diminished $T_{REG}$ cell abundance in peripheral blood is described in most forms of RPGN, and compromising $T_{REG}$ cells in mouse models aggravates RPGN pathology[12, 13]. In the NTN model, $T_{REG}$ cells tailor their suppressive capacity by adopting the expression of $T_{EFF}$-defining transcription factors, thereby enabling them to localize to the target $T_{EFF}$ cell. Notably, $T_H17$-

like $T_{REG}$ cells upregulate CCR6 in a STAT3-dependent manner and control nephritogenic $T_H17$ cell responses while T-bet$^+$ $T_H1$-like $T_{REG}$ cells express CXCR3 and specifically curtail $T_H1$ cell responses[14, 15]. GATA-3$^+$ $T_{REG}$ cells, known to reside in the gut, lungs, skin, and visceral adipose tissue under homeostatic settings and exert potent immunosuppressive functions[16-18], were recently shown to accumulate in the kidneys in NTN, though their functions in the renal environment remains unknown[19]. While the immunoregulatory potential of renal $T_{REG}$ cells is clear, the factors controlling their differentiation and function in the kidney remain poorly defined.

The rampant cell death in RPGN results in the release of pro-inflammatory mediators, termed alarmins, that can exert control over T cell responses[20]. Amongst these alarmins, the IL-1 family cytokines IL-1α/β (IL-1) and IL-33 are known to impact $T_{REG}$ cell suppressive function and stability[16, 18, 21, 22]. In the gut and lungs, IL-33, signaling through its receptor ST2, promotes the expansion of GATA-3$^+$ $T_{REG}$ cells while IL-1, signaling through IL-1R1, counteracts this and promotes the expansion of $T_H17$-like $T_{REG}$ cells[16]. Unlike GATA-3$^+$ $T_{REG}$ cells, which show robust suppressive functions, we showed that $T_H17$-like $T_{REG}$ cells were prone to losing Foxp3 expression, denoting that IL-1 and IL-33 may play opposing roles dictating $T_{REG}$ cell suppressive function during inflammation[16]. Indeed, blocking IL-1 in NTN ameliorates disease, though its impact on the $T_{EFF}$ and $T_{REG}$ cell response remains unknown[23, 24].

Here, we investigated the impact of IL-1 and IL-33 on renal $T_{REG}$ cell control of nephritogenic $T_{EFF}$ cell responses. Using the NTN model, we show that GATA-3$^+$ $T_{REG}$ cells arise in both the kidneys and rLNs during the autologous phase, acquiring ST2 expression only upon entry into the kidneys. Conditional removal of ST2 on $T_{REG}$ cells did not impact renal GATA-3$^+$ $T_{REG}$ cell accumulation, but strongly improved their capacity to control autologous $T_H1$ and B cell responses, indicating that IL-33 is detrimental for renal $T_{REG}$ cell suppressive functions. Similarly, $T_{REG}$ cells deficient in IL-1R1 were better able to control $T_H1$ cell responses. Thus, IL-1 and IL-33 limit $T_{REG}$ cell control of kidney-directed adaptive immunity suggesting that modulating IL-1 signals could be beneficial for augmenting $T_{REG}$ cell suppressive functions in RPGN.

## 5.4 Methods

### *Mice*

Wildtype C57BL/6J mice (The Jackson Laboratory, Bar Harbor, ME) were bred at the Research Institute of the McGill University Health Centre (RI-MUHC, Montréal, QC). The *Foxp3*$^{\text{GFP-CreERT2}}$ mice were generated by crossing B6.*Foxp3*$^{tm9(EGFP/cre/ERT2)Ayr}$/J mice from Dr. Woong-Kyung Suh (RI-MUHC, Montréal, QC) with *Rosa26*-RFP$^{\text{loxP-stop-loxP}}$ mice from Dr. Jeffrey Bluestone (University of California, San Francisco, CA). These mice were then crossed to B6.129-*Il1rl1*$^{loxP/loxP}$ mice from Dr. Stephen McSorley (University of California, Davis, CA) to generate *Foxp3*$^{\text{GFP-CreERT2}}$ *Il1rl1*$^{\text{fl/fl}}$ (ST2$^{\text{i}\Delta\text{TREG}}$ mice), which have a tamoxifen-inducible defect in ST2 expression in all *Foxp3*-expressing cells. Mice with a Foxp3 and eGFP fusion, B6.*Foxp3*$^{\text{GFPki}}$, were obtained from Dr. Alexander Rudensky (Memorial Sloan Kettering Cancer Center, New York City, NY) and were bred with congenic Ly5.1$^{+}$ mice for over ten generations to generate congenic *Foxp3*$^{\text{GFPki}}$ mice and with B6.129S1-*Il1r1*$^{tm1roml}$/J (The Jackson Laboratory, Bar Harbor, ME) to generate *Foxp3*$^{\text{GFPki}}$ *Il1r1*$^{-/-}$ mice. Finally, B6.129P2-*Tcrb*$^{tm1Mom}$/J mice (The Jackson Laboratory, Bar Harbor, ME) were bred at the RI-MUHC. All mice were raised in specific pathogen-free conditions and male 8–10-week-old mice were used in all experiments. Experiments were performed according to the Canadian Council on Animal Care and to institutional guidelines at McGill University, and ethical guidelines were approved by local committees at the RI-MUHC.

### *NTN induction*

Mice were injected intraperitoneally with 1-2 µl/g of body weight, depending on the batch, nephrotoxic sheep serum (NTS, PTX-001S-Ms from Probetex) or control pre-immunized sheep serum (PTX-000S from Probetex). In experiments using *Foxp3*$^{\text{CreERT2-GFP}}$ mice, tamoxifen (Millipore Sigma, St. Louis, MO) diluted in corn oil (Millipore Sigma) was injected intraperitoneally at 20 µg/mouse seven and five days prior to NTS injection since tamoxifen is renoprotective. Urine was collected manually and ELISAs were used to measure albumin (Bethyl Laboratories) and creatinine (Cayman Chemical) concentrations, and the former was normalized to the latter to obtain urinary albumin-to-creatinine ratios (uACR).

Urine was not collected from mice that were profoundly anuric and were excluded from uACR measurements.

***Histology***

A slice from the apical portion of the left kidney was taken for histological assessment from every mouse. Kidneys were fixed in 10% formalin for 24 hours before transfer into 70% ethanol for two days. Hematoxylin and eosin (H&E) and periodic acid-Schiff (PAS) staining was performed by the Histology Core at the RI-MUHC.

***Cell isolation***

Kidneys were mechanically dissociated with scissors and were transferred into digestion buffer containing 0.1 mg/ml collagenase D (Millipore Sigma) and 100 µg/ml DNase I (Millipore Sigma) in complete medium (RPMI-1640, 10% fetal bovine serum, 1% HEPES, 1% penicillin/streptomycin). Kidneys were digested for 45 minutes at 37 °C and 5% $CO_2$ before filtering through a 70 µm strainer. Red blood cells were lysed using ammonium-chloride-potassium (ACK) solution. The cells were finally resuspended in complete medium. Renal, brachial, axillary, and inguinal lymph nodes were mechanically dissociated between the frosted ends of two sterile glass slides and washed with complete medium. After spinning, the cells were resuspended in complete medium and filtered through a 70 µm strainer. Spleens were dissociated like the lymph nodes but red blood cell lysis in ACK solution was performed before the wash and filtering steps. Single cell suspensions were then counted on the hemocytometer using Trypan Blue exclusion dye.

***Flow cytometry***

From the single cell suspensions, no more than $1\times10^6$ cells for each flow cytometry panel. Cells were incubated with Fixable Viability eFluor 780 Dye (ThermoFisher Scientific) or Fixable Viability eFluor 506 Dye (ThermoFisher Scientific) at 4 °C for 15 minutes, washed with ice-cold PBS+2% FBS, and then incubated for another 15 minutes with rat anti-mouse CD16/32 (BD Biosciences). Cells were then washed with ice-cold PBS and incubated at 4 °C

for 20 minutes in cocktails containing the following antibodies against extracellular proteins: CD45.2 APC-Cy7 (104, Invitrogen, 1:100), CD45.2 PerCp-Cy5.5 (104, BioLegend, 1:100), CD45.2 BV786 (104, BD Biosciences, 1:100), CD45.1 PerCp-Cy5.5 (A20, Invitrogen, 1:100), CD3 BUV737 (17A2, BD Biosciences, 1:100), CD4 Alexa700 (RM4-5, BD Biosciences, 1:100), CD8β BV510 (H35-17.2, BD Biosciences, 1:100), ST2 PerCp-eFluor710 (RMST2-2, Invitrogen, 1:100), CD19 BUV737 (1D3, BD Biosciences, 1:100), CD95 PE-CF594 (Jo2, BD Biosciences, 1:100), GL7 PerCp-Cy5.5 (GL7, BioLegend, 1:100), IgM FITC (RMM-1, BioLegend, 1:100), IgD BUV395 (11-26c.2a, BD Biosciences, 1:100), IgG APC (Poly4053, BioLegend, 1:100), PD-1 BV421 (29F.1A12, BioLegend, 1:100), and ICOS PE (C398.4A, Invitrogen, 1:100). Cells were then washed in ice-cold PBS and fixed using the eBioscience Foxp3/Transcription Factor buffer set (eBioscience). Cells were washed with ice-cold 1X permeabilization buffer (eBioscience) and incubated at 4 °C for 45 minutes in cocktails prepared in the same permeabilization buffer containing the following antibodies against intracellular proteins: Foxp3 FITC (FJK-16s, Invitrogen, 1:100), RORγt PE (AFKJS-9, Invitrogen, 1:50), GATA-3 BUV395 (L50-823, BD Biosciences, 1:50), Helios Pacific Blue (22F6, BioLegend, 1:100), T-bet PE-Cy7 (4B10, BioLegend, 1:50), Bcl-6 APC-Cy7 (K112-91, BD Biosciences, 1:100), IFN-γ PE-Cy7 (XMG1.2, Invitrogen, 1:200), IL-17A APC (eBio17B7, Invitrogen, 1:100), and IL-4 PE (11B11, Invitrogen, 1:100). Two final washes were performed, the first in ice-cold 1X permeabilization buffer and the second in ice-cold PBS, before acquisition on the BD LSRFortessa X-20. Data were analyzed on FlowJo v10.8 Software (FlowJo, LLC).

***Adoptive transfer experiments***

Single cell suspensions from spleens and brachial, axillary, and inguinal lymph nodes of Foxp3 reporter mice were pooled and labeled with anti-mouse CD4 microbeads (Miltenyi Biotec). $CD4^+$ T cells were enriched using the deplete sensitive program on the autoMACS (Miltenyi Biotec) and the positive fraction was labeled with Alexa700 anti-mouse CD4 (1:40, GK1.5, ThermoFisher Scientific) for flow-based sorting on the BD FACSAria Fusion cell sorter. $T_{EFF}$ cells ($CD4^+$ Foxp3-$GFP^-$) from $Ly5.1^+$ *Foxp3*$^{GFPki}$ and $T_{REG}$ cells ($CD4^+$ Foxp3-$GFP^+$)

from Ly5.2 *Foxp3*$^{GFPki}$ mice were sorted to >99% purity. Approximately $5.0\times10^5$ of each cell type was transferred intravenously into *Tcrb*$^{-/-}$ mice five days prior to NTS induction.

***Statistics***

Statistical analyses were performed on GraphPad Prism v10 software (GraphPad). All data are displayed as mean ± standard deviation or as box plots depicting the mean (centre), interquartile range (bounds), and min-max range (whiskers). Where individual points are shown, each point represents a single mouse. Analyses between two groups were done using an unpaired two-sided student's *t*-test while analyses between more than two groups were done using a one-way ANOVA with Tukey's post-hoc testing for multiple comparisons. Any multivariate analyses were done using a two-way ANOVA with Bonferroni's post-hoc testing. *P*-values <0.05 were considered significant and significant *P*-values were depicted on the graph as **P*≤0.05, ***P*≤0.01, ****P*≤0.001, and *****P*≤0.0001.

## 5.5 Results

### *5.5.1. GATA-3$^+$ $T_{REG}$ accumulate alongside $T_H1$ cells in the autologous phase of disease.*

We first sought to characterize renal $T_{REG}$ cell dynamics during RPGN. To this end, we induced the NTN model in C57BL/6J mice and followed them for 4, 10, and 18 days, the latter two time points corresponding with the autologous phase of NTN. Hyaline casts were evident as early as day 4, coinciding with the onset of proteinuria, and extensive crescent formation was observed by day 10, consistent with the development of RPGN (**Supplemental Figure 1A, B**). Transient weight loss was also observed in NTN mice during the early autologous phase (**Supplemental Figure 1C**). Largescale immune cell infiltration was evident by day 10 and was sustained until the end of the experiment (**Supplemental Figure 1D**). The accumulation of $CD4^+$ and CTLs was most pronounced during the autologous phase of disease, denoting the development of a kidney-directed T cell response (**Supplemental Figure 2A-C**).

$T_H17$ cells infiltrated rapidly following NTN induction but subsided by day 18, being replaced by $T_H1$ cells and IFN-$\gamma^+$ CTLs (**Figure 1A, Supplemental Figure 2D**). This is consistent with the biphasic $T_H17$-$T_H1$ response noted by other groups. Notably, $T_{REG}$ cell accumulation in the kidney occurred predominantly during the late autologous phase (**Figure 1B**). These $T_{REG}$ cells were principally Helios$^+$ GATA-3$^+$ cells, a phenotype associated with potent suppressive function (**Figure 1B, C**). Like GATA-3$^+$ $T_{REG}$ cells in other organs, approximately half of the renal GATA-3$^+$ $T_{REG}$ cells expressed the IL-33 receptor ST2[16, 21, 25]. Nevertheless, the majority of ST2$^+$ $T_{REG}$ cells present in the autologous phase lacked GATA-3 expression, suggesting the presence of at least two distinct renal $T_{REG}$ cell populations (**Figure 1C**). The accumulation of $T_{REG}$ cells in the kidney strongly correlated with the generation of $T_H1$ and CTL responses but not $T_H17$ cell responses (**Figure 1D, E**). Altogether, these data demonstrate that GATA-3$^+$ $T_{REG}$ cells preferentially accumulate in the autologous phase, likely in response to kidney-directed $T_H1$ cell responses.

### *5.5.2. GATA-3$^+$ $T_{REG}$ cells arise in rLNs alongside autologous T and B cells.*

We rationalized that the accumulation of GATA-3$^+$ $T_{REG}$ cells alongside $T_H1$ cells in the autologous phase was driven by antigen presentation in the rLN. To this end, we examined adaptive responses in the rLNs following NTN induction. Lymph node cellularity nearly tripled by day 4 of NTN and remained elevated for the course of the experiment, indicating the presence of an active immune response (**Supplemental Figure 3A**). While the proportions of T cells in the rLN diminished slightly, possibly due to T cell egress, they were nevertheless highly expanded at all time points (**Supplemental Figure 3B-D**). $T_H1$ cells and CTLs were induced in rLNs at day 10 of NTN, but there was no evidence of $T_H17$ cells at any timepoint (**Figure 2A, B**). Notably, GATA-3$^+$ $T_{REG}$ cells arose in rLNs alongside $T_H1$ cells and were completely devoid of surface ST2 expression (**Figure 2C**). As such, the differentiation of $T_{REG}$ cells in GATA-3$^+$ cells likely occurs in rLNs, with ST2 upregulation taking place within the kidney.

The autologous responses supporting $T_{REG}$ and $T_H1$ generation in rLN likely also support the development of B cells, whose contribution to the chronicity of RPGN is currently not known. Indeed, both B cell proportions and numbers increased significantly by day 4 of NTN (**Figure 2D**). This corresponded with the formation of germinal centers during the autologous phase of NTN, kinetics consistent with a primary adaptive immune response (**Figure 2E**). Accordingly, we also observed the development of Bcl-6$^{high}$ ICOS$^+$ follicular helper T ($T_{FH}$) cells alongside germinal center formation (**Figure 2F**).

### *5.5.3. IL-33 diminishes $T_{REG}$ cell control of autologous T and B cell responses.*

ST2$^+$ GATA-3$^+$ $T_{REG}$ cells are a highly suppressive $T_{REG}$ subset present in various tissues and expand readily upon exposure to IL-33[18, 26]. Since ST2$^+$ GATA-3$^+$ $T_{REG}$ cells were accumulating in the kidney specifically during the autologous phase, we hypothesized that these $T_{REG}$ cells played an essential role at limiting autologous NTN responses in an IL-33-dependent manner. To this end, we utilized *Foxp3*$^{CreERT2\text{-}GFP}$ *Il1rl1*$^{fl/fl}$ (ST2$^{i\Delta TREG}$) mice, in which all *Foxp3*-expressing cells lose ST2 (*Il1rl1*) expression following tamoxifen treatment, and *Foxp3*$^{CreERT2\text{-}GFP}$ *Il1rl1*$^{wt/wt}$ (WT) controls. Mice were injected with tamoxifen at seven and five

days prior to NTN induction and were followed up to day 18 of NTN (**Figure 3A**). While the proportions of ST2-expressing $T_{REG}$ cells were substantially reduced in the kidneys of $ST2^{i\Delta TREG}$ mice, we found minimal effect on the proportions of GATA-$3^+$ $T_{REG}$ cells, denoting that GATA-$3^+$ $T_{REG}$ cell accumulation in the kidney is independent of IL-33 (**Figure 3B**). Nevertheless, the proportions of total renal $T_{REG}$ cells were slightly reduced in $ST2^{i\Delta TREG}$ mice (**Supplemental Figure 3A, B**). Surprisingly, while kidneys from both WT and $ST2^{i\Delta TREG}$ developed hyaline casts, kidney inflammation was strongly diminished in $ST2^{i\Delta TREG}$ mice (**Figure 3C, D**). Likewise, proteinuria and weight loss were also reduced (**Figure 3E, F**). This decreased kidney pathology in $ST2^{i\Delta TREG}$ mice was consistent with lower T cell infiltration (**Figure 3G**) and $T_H1$ and CTL responses (**Figure 3H, I**). There were no differences observed in $T_H17$ cells (**Figure 3H**). In all, these data suggest that IL-33 curtails $T_{REG}$ cell control of autologous responses within the kidney.

The evaluate whether IL-33 also impacts $T_{REG}$-mediated suppression of autologous responses within rLN, we also examined the adaptive responses therein. Lymph node cellularity was strongly diminished in $ST2^{i\Delta TREG}$ mice, corresponding with decreases in the number of T and B cells (**Figure 4A-C**). Accordingly, $T_H1$ and CTL responses were also significantly reduced (**Figure 4D, E**). Consistent with the decrease in B cells, we observed a strong reduction in $T_{FH}$ cell frequencies within rLN (**Figure 4F**). Thus, IL-33 restricts $T_{REG}$ cell control of autologous responses both within the kidney and in the rLN.

### *5.5.4. IL-1R1 signaling reduces $T_{REG}$ cell control of renal $T_H1$ responses.*

We previously showed that IL-1 signaling through IL-1R1 restricts GATA-$3^+$ $T_{REG}$ cell differentiation in the gut and lungs thereby augmenting $T_{EFF}$ cell responses[16]. Hence, we rationalized that IL-1R1 would also be detrimental to $T_{REG}$ cell control of kidney-directed T cell responses. In the absence of mice carrying a $T_{REG}$-specific deletion of IL-1R1, we transferred CD45.$1^+$ $T_{EFF}$ ($CD4^+$ $Foxp3^-$) cells from Ly5.1 *Foxp3*$^{GFP}$ reporter mice intravenously into congenic Ly5.2 *Tcrb*$^{-/-}$ mice alongside CD45.$2^+$ $T_{REG}$ ($CD4^+$ $Foxp3^+$) from either Ly5.2 *Foxp3*$^{GFPki}$ *Il1r1*$^{+/+}$ (*Il1r1*$^{WT}$) or Ly5.2 *Foxp3*$^{GFPki}$ *Il1r1*$^{-/-}$ (*Il1r1*$^{-/-}$) mice. After five days of expansion, mice were injected with NTS and were sacrificed at 8 days (early autologous phase) (**Figure 5A**).

An earlier time point and a high ratio of $T_{REG}$ to $T_{EFF}$ cells (1:1) were used to prevent the development of colitis, which usually takes place 21 days following transfer[16]. Mice that received $T_{EFF}$ alone or with *Il1r1*$^{-/-}$ $T_{REG}$ showed moderate weight loss following NTN induction, while weight was maintained in mice that received *Il1r1*$^{WT}$ $T_{REG}$ (**Figure 5B**). Nevertheless, all mice developed proteinuria (**Figure 5C**). Mice that received either *Il1r1*$^{WT}$ or *Il1r1*$^{-/-}$ $T_{REG}$ cells were better protected from kidney inflammation, corresponding with decreased T cell infiltration (**Figure 5D,E**). Notably, mice that received *Il1r1*$^{-/-}$ $T_{REG}$ showed lower $T_H1$ cell responses in the kidneys but had worse control of renal $T_H17$ cells (**Figure 5F**). These results indicate that, much like IL-33, IL-1 also restricts $T_{REG}$ cell control of renal $T_H1$ cells.

We hypothesized that IL-1 signaling might curtail renal $T_{REG}$ cell suppressive capacity by destabilizing the $T_{REG}$ cell phenotype, as we have previously observed in a colitis model[16]. Mice that received *Il1r1*$^{-/-}$ $T_{REG}$ cells had greater $T_{REG}$ cell accumulation in the kidney compared to mice that received *Il1r1*$^{WT}$ $T_{REG}$ (**Figure 5G**). Indeed, *Il1r1*$^{-/-}$ $T_{REG}$ cells retained Foxp3 expression to a greater extent than *Il1r1*$^{WT}$ $T_{REG}$ (**Figure 5I**). Thus, IL-1 may dampen renal $T_{REG}$ cell suppressive function by driving their lineage instability.

## 5.6 Discussion

Renal $T_{REG}$ cells are critical at limiting the kidney-directed T cell responses that mediate the chronicity of RPGN. Hence, augmenting their functions is becoming an increasingly attractive therapeutic option[27,28]. To do so, a better understanding of the factors impacting their development and function is necessary. Utilizing the NTN model of RPGN, we showed that renal GATA-3$^+$ $T_{REG}$ cells originate in the rLNs generated alongside $T_H1$ cells, CTLs, $T_{FH}$ cells, and germinal center B cells during the autologous phase. The development of these $T_{REG}$ cells was independent of ST2, and IL-33 was detrimental to $T_{REG}$ cell control of autologous adaptive responses. Similarly, intact IL-1 signaling diminished $T_{REG}$ cell control of $T_H1$ cell responses, possibly by destabilizing the $T_{REG}$ cell phenotype.

The T cell response in NTN is biphasic characterized by $T_H17$ cells in the heterologous phase followed by a $T_H1$ response consisting of both $T_H1$ cells and CTLs[5]. The development of $T_H1$ cells in the autologous phase was previously shown to rely on CX3CR1$^+$ dendritic cells[29]. Accordingly, we showed that $T_H1$ cell responses develop in rLNs, possibly in response to autoantigens liberated by glomerular injury. The identities of the antigens driving the autologous response have not yet been characterized, and it remains possible that resident T cells contribute to the pool of infiltrating $T_H1$ cells and CTLs. We also demonstrate that germinal centers are generated specifically within the autologous phase, supporting the notion of autoantigen release following glomerular injury. The role of these B cells in NTN pathogenesis has not yet been evaluated.

ST2$^+$ GATA-3$^+$ $T_{REG}$ cells are a highly suppressive $T_{REG}$ cell subset that have been described in numerous tissues including the gut, lungs, skin, and adipose[16,18,21]. Here, we demonstrated that GATA-3$^+$ $T_{REG}$ cells arise in both the kidneys and rLNs during the autologous phase of NTN, suggesting that GATA-3$^+$ $T_{REG}$ cells, like $T_H1$ cells, are developing in response to autoantigens. Likewise, we cannot rule out the contribution of tissue resident $T_{REG}$ cells to this population. Notably, while almost half of the GATA-3$^+$ $T_{REG}$ cells in the kidney expressed ST2, ST2 expression was completely absent in rLNs. This upregulation of ST2 as $T_{REG}$ cells transitioned into the kidney was likely driven by tissue-specific signals including IL-33, which is known to promote ST2 expression in the presence of a STAT5 signal (e.g., IL-2)[21].

The specific accumulation of GATA-3$^+$ $T_{REG}$ cells during the autologous phase suggests they are critical for the regulation of autologous responses, which we aim to test directly using mice with a tamoxifen-inducible $T_{REG}$-specific deletion of *Gata3*. Using a T cell transfer model like the one we present in Figure 5, GATA-3$^+$ $T_{REG}$ cells were recently shown to be protective from NTN, but their control of T cell responses was not evaluated[19].

Interestingly, we observed that IL-33 signaling in $T_{REG}$ cells was detrimental to their control of autologous renal $T_H1$ cell responses and enhanced NTN pathology. While IL-33 is known to promote GATA-3$^+$ $T_{REG}$ cell expansion and suppressive function within mucosal tissues, it is possible that its effects are context-dependent[16,21]. For example, it was recently reported that IL-33 administration worsened the pathology observed in a mouse model of type-1 diabetes[30]. We also showed that IL-33 limited $T_{REG}$ cell control of autologous responses within the rLN. Since IL-33 is likely released locally within the kidney upon tissue injury, we predict that IL-33 may dampen $T_{REG}$ cell control of the dendritic cells that trigger rLN responses. Unfortunately, our study was limited by the unavailability of littermate *Foxp3*$^{CreERT2\text{-}GFP}$ mice as controls for the ST2$^{i\Delta TREG}$ mice. Thus, to be certain of this surprising finding, we aim to repeat these experiments with appropriate littermate controls.

Since we previously showed that IL-1R1 signaling counteracted GATA-3$^+$ $T_{REG}$ cell differentiation in the lungs and gut, we sought to investigate the effects of IL-1R1 signaling on renal $T_{REG}$ cells[16]. Indeed, IL-1α and IL-1β are released upon glomerular injury and are highly nephritogenic[20,23,24,31]. In the absence of mice with a $T_{REG}$-specific deletion of *Il1r1*, we used the adoptive transfer model for NTN. Despite the limitations of this model, we showed that IL-1R1 signaling, like ST2 signaling, also curtailed renal $T_{REG}$ cell control of $T_H1$ responses. We also observed that IL-1R1 signaling promoted lineage instability in renal $T_{REG}$ cells, though this could be a consequence of the adoptive transfer model where the proliferation of $T_{REG}$ cells in a lymphopenic environment promotes the loss of Foxp3 expression. Nonetheless, our work highlights the potential of targeting IL-1 family cytokines to augment immunoregulation within the kidney during RPGN.

Finally, there is a growing appreciation that $T_{REG}$ cell suppressive function *in vivo* is antigen-specific[32-36]. While both ST2 and IL-1R1 signaling negatively impacted $T_{REG}$ cell

suppression of $T_{EFF}$ cell responses, this was specific to $T_H1$ cell responses. As both renal GATA-3$^+$ $T_{REG}$ cells and $T_H1$ cells were raised in rLN, likely in response to renal antigens released by glomerular injury, the specificity of $T_{REG}$ cell suppression towards $T_H1$ cells was possibly antigen driven. Likewise, we also observed that ST2 signaling limited $T_{REG}$ cell control of $T_{FH}$-B cell responses in rLN. Future work is aimed at defining the antigen-specificity of nephritogenic and immunoregulatory T cell responses during RPGN.

**Acknowledgements**

We would like to thank A. Rudensky, S. McSorley, and J. Bluestone for the mice used in this study and the RI-MUHC Immunophenotyping Platform for their sorting services. This work was supported by Canadian Institute of Health Research project grants (PJT-159678 to T.T., and PJT-166006 to T.T. and C.A.P.). T.A. was supported by a CIHR Doctoral Award and a FRQS Doctoral Award.

**Author Contributions**

T.A., T.T., and C.A.P. conceptualized the study and designed all the experiments. T.A., R.I., and F.A. conducted all the investigations. Formal analysis was completed by T.A.. T.A., T.T., and C.A.P. wrote the initial draft of this manuscript.

## 5.7 Figures

## Figure 1

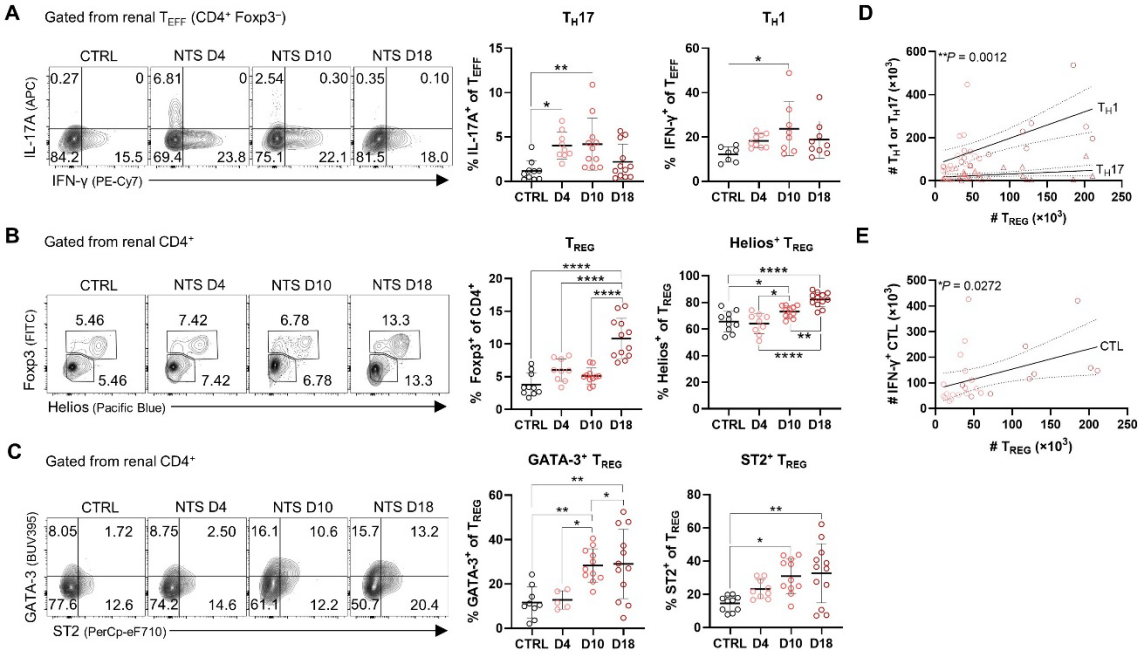

**Figure 1: GATA-3$^+$ $T_{REG}$ cells accumulate in the kidney during the $T_H1$ dominated autologous phase.** (**A**) Representative flow plots showing renal IL-17A-producing ($T_H17$) and IFN-γ-producing ($T_H1$) $T_{EFF}$ cells and quantification of their proportions from total $T_{EFF}$ cells (CD4$^+$ Foxp3$^-$ T cells). (**B**) Representative flow plots showing renal $T_{REG}$ cells (CD4$^+$ Foxp3$^+$) alongside quantification of their frequencies in the CD4$^+$ T cell compartment. The proportions of Helios$^+$ cells within the $T_{REG}$ cell compartment are also graphed. (**C**) Representative flow plots showing GATA-3 and ST2 expression within renal $T_{REG}$ cells alongside quantification of the frequencies of GATA-3$^+$ and ST2$^+$ cells within the $T_{REG}$ cell compartment. (**D, E**) Correlations between the number of $T_{REG}$ cells and the number of $T_H1$, $T_H17$ (**D**), and IFN-γ-producing CTLs (**E**) in the kidneys. Data are shown as mean ± SD (**A-C**) or scatter plots with a line-of-best-fit ± SD (**D, E**) compiled from three independent experiments. Each dot represents a single mouse. *P*-values were determined using one-way ANOVA with Tukey's post-hoc test for multiple comparisons (**A-C**) or a simple linear regression (**D, E**) (*$P$≤0.05, **$P$≤0.01, ***$P$≤0.001, and ****$P$≤0.0001).

## Figure 2

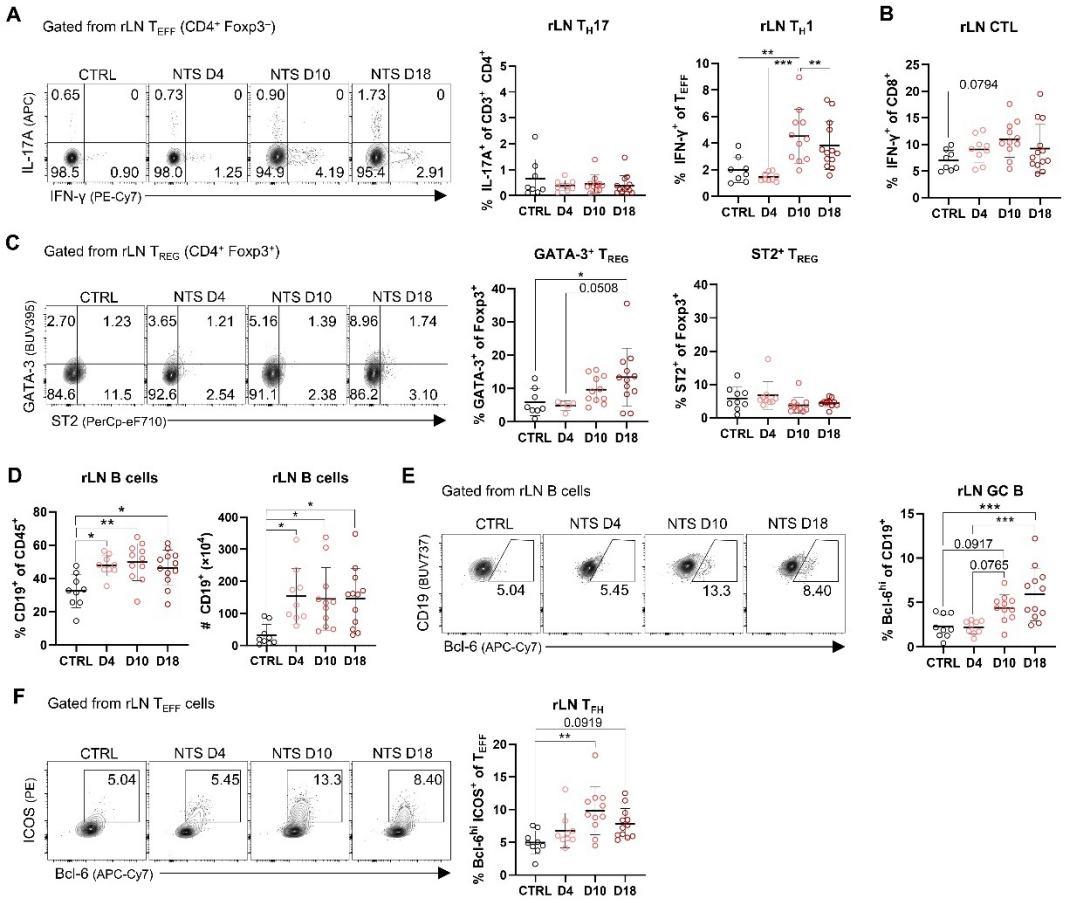
A
Gated from rLN T_EFF (CD4+ Foxp3−)
CTRL
NTS D4
NTS D10
NTS D18
IL-17A (APC)
IFN-γ (PE-Cy7)
rLN T_H17
rLN T_H1
B
rLN CTL
0.0794
C
Gated from rLN T_REG (CD4+ Foxp3+)
GATA-3 (BUV395)
ST2 (PerCp-eF710)
GATA-3+ T_REG
ST2+ T_REG
0.0508
D
rLN B cells
E
Gated from rLN B cells
CD19 (BUV737)
Bcl-6 (APC-Cy7)
rLN GC B
0.0917
0.0765
F
Gated from rLN T_EFF cells
ICOS (PE)
rLN T_FH
0.0919

**Figure 2: GATA-3$^+$ $T_{REG}$ cells arise in renal lymph nodes alongside autologous T and B cells.** (**A**) Representative flow plots of rLN $T_H17$ and $T_H1$ cells and quantification of their frequencies amongst total $T_{EFF}$ cells (CD4$^+$ Foxp3$^-$). (**B**) Frequencies of IFN-γ-producing CTLs in rLN. (**C**) Representative flow plots showing GATA-3 and ST2 expression in rLN $T_{REG}$ cells alongside the frequencies of GATA-3$^+$ and ST2$^+$ $T_{REG}$ cells (CD4$^+$ Foxp3$^+$). (**D**) Quantification of the frequencies and absolute numbers of rLN B cells. (**E**) Representative flow plots and quantification of germinal Center B cells (GC B: CD19$^+$ Bcl-6$^{high}$) within rLN. (**F**) Representative flow plots and quantification of $T_{FH}$ cells (CD4$^+$ Bcl-6$^{hi}$ ICOS$^+$) in the $T_{EFF}$ cell compartment. Data are shown as mean ± SD from three independent experiments. Each dot represents a single mouse. *P*-values were determined using a one-way ANOVA with Tukey's post-hoc test for multiple comparisons (*$P$≤0.05, **$P$≤0.01, ***$P$≤0.001, and ****$P$≤0.0001).

## Figure 3

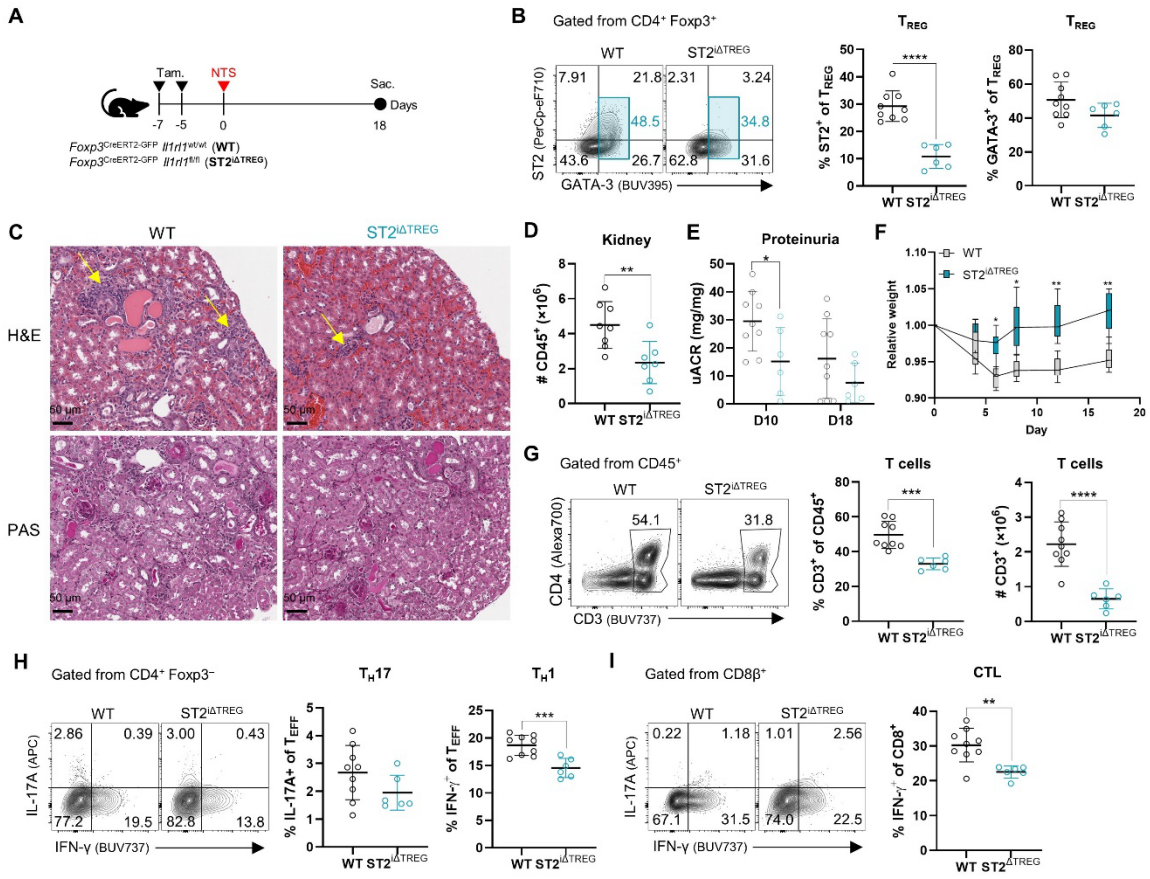
A
Tam.
NTS
Sac.
-7
-5
0
Days
18
Foxp3CreERT2-GFP Il1rl1wt/wt (WT)
Foxp3CreERT2-GFP Il1rl1fl/fl (ST2iΔTREG)
B
Gated from CD4+ Foxp3+
WT
ST2iΔTREG
ST2 (PerCp-eF710)
GATA-3 (BUV395)
7.91
21.8
48.5
43.6
26.7
2.31
3.24
34.8
62.8
31.6
TREG
% ST2+ of TREG
% GATA-3+ of TREG
****
C
WT
ST2iΔTREG
H&E
PAS
50 µm
D
Kidney
# CD45+ (×10^6)
**
E
Proteinuria
uACR (mg/mg)
*
D10
D18
F
WT
ST2iΔTREG
Relative weight
Day
G
Gated from CD45+
CD4 (Alexa700)
CD3 (BUV737)
54.1
31.8
T cells
% CD3+ of CD45+
# CD3+ (×10^6)
***
****
H
Gated from CD4+ Foxp3−
TH17
TH1
IL-17A (APC)
IFN-γ (BUV737)
2.86
0.39
77.2
19.5
3.00
0.43
82.8
13.8
% IL-17A+ of TEFF
% IFN-γ+ of TEFF
I
Gated from CD8β+
CTL
0.22
1.18
67.1
31.5
1.01
2.56
74.0
22.5
% IFN-γ+ of CD8+
WT ST2iΔTREG

**Figure 3: IL-33 signaling in $T_{REG}$ cells diminishes control of autologous $T_H1$ responses.** (**A**) Schematic showing the experimental design. *Foxp3*$^{CreERT2\text{-}GFP}$ *Il1rl1*$^{WT}$ (WT) and *Foxp3*$^{CreERT2\text{-}GFP}$ *Il1rl1*$^{fl/fl}$ (ST2$^{i\Delta TREG}$) mice were treated with tamoxifen at 7 and 5 days before NTN induction. Mice were followed until day 18. (**B**) Representative flow plots showing ST2 and GATA-3 expression in WT and ST2$^{i\Delta TREG}$ in renal $T_{REG}$ at day 18 of NTN. (**C**) Representative photographs of H&E and PAS kidney sections at day 18 of NTN. The yellow arrow indicates immune cell infiltration. (**D**) Number of immune cells in the kidneys of WT and ST2$^{i\Delta TREG}$ mice. (**E**) Quantification of uACR at days 10 and 18 of NTN. (**F**) Time course of weight loss relative to the day of NTS injection. (**G**) Representative flow plots showing renal T cell gating alongside quantification of their frequencies and absolute numbers. (**H**) Representative flow plots showing renal $T_H17$ and $T_H1$ cells alongside the quantification of their frequencies. (**I**) Representative flow plots showing renal CTL production of IFN-γ alongside quantification of their frequencies. Data are shown as mean ± SD (**B**, **D**, **E, G-I**) or boxplots showing the mean (center), interquartile range (bounds), and min-max range (whiskers) (**F**) from a compilation of two independent experiments. *P*-values were determined using an unpaired two-sided student's *t* test (**B, D, E, G-I**) or two-way ANOVA with Bonferroni's post-hoc test for multiple comparisons (**F**) (*$P \leq 0.05$, **$P \leq 0.01$, ***$P \leq 0.001$, and ****$P \leq 0.0001$).

## Figure 4

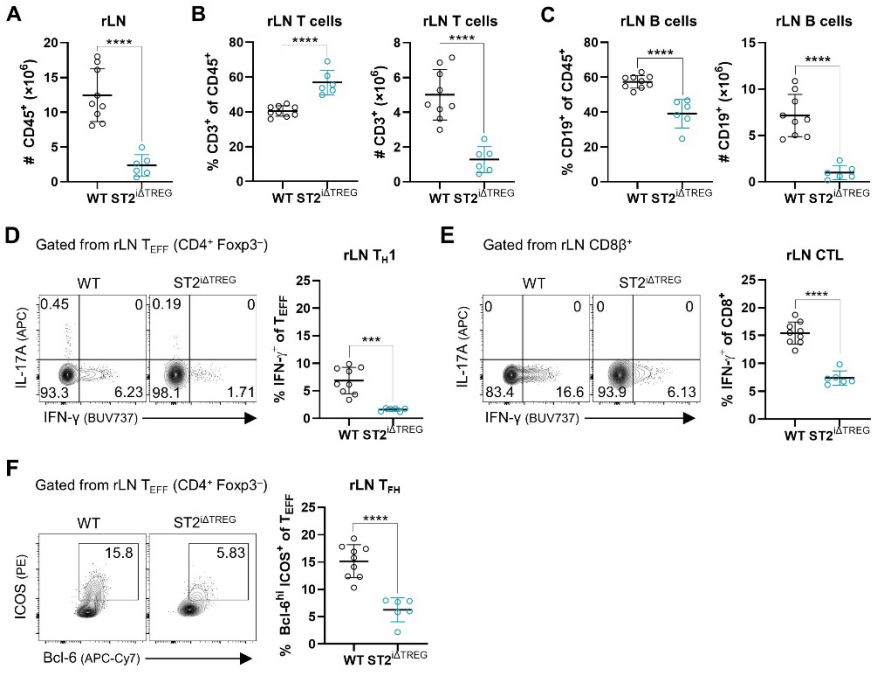
A
rLN
# CD45+ (×10^6)
B
rLN T cells
% CD3+ of CD45+
rLN T cells
# CD3+ (×10^6)
C
rLN B cells
% CD19+ of CD45+
rLN B cells
# CD19+ (×10^6)
WT
ST2ΔTREG
D
Gated from rLN TEFF (CD4+ Foxp3−)
WT
ST2ΔTREG
0.45
0
93.3
6.23
0.19
0
98.1
1.71
IL-17A (APC)
IFN-γ (BUV737)
rLN TH1
% IFN-γ+ of TEFF
E
Gated from rLN CD8β+
WT
ST2ΔTREG
0
0
83.4
16.6
0
0
93.9
6.13
IL-17A (APC)
IFN-γ (BUV737)
rLN CTL
% IFN-γ+ of CD8+
F
Gated from rLN TEFF (CD4+ Foxp3−)
WT
ST2ΔTREG
15.8
5.83
ICOS (PE)
Bcl-6 (APC-Cy7)
rLN TFH
% Bcl-6hi ICOS+ of TEFF

**Figure 4: IL-33 signaling in $T_{REG}$ cells limits control of autologous responses in lymph nodes.** (**A**) Numbers of immune cells in rLN of WT and $ST2^{i\Delta TREG}$ mice. (**B**) Quantification of the frequencies and absolute numbers of rLN T cells. (**C**) Quantification of the frequencies and absolute numbers of rLN B cells. (**D**) Representative flow plots showing rLN $T_H1$ cells alongside quantification of their frequencies. (**E**) Representative flow plots showing IFN-γ production by rLN CTLs alongside quantification of their frequencies. (**F**) Representative flow plots showing $T_{FH}$ cells (Bcl-$6^{hi}$ $ICOS^+$) and the quantification of their frequencies. Data are shown as mean ± SD from a compilation of two independent experiments. *P*-values were determined using an unpaired student's *t* test (**P*≤0.05, ***P*≤0.01, ****P*≤0.001, and *****P*≤0.0001).

## Figure 5

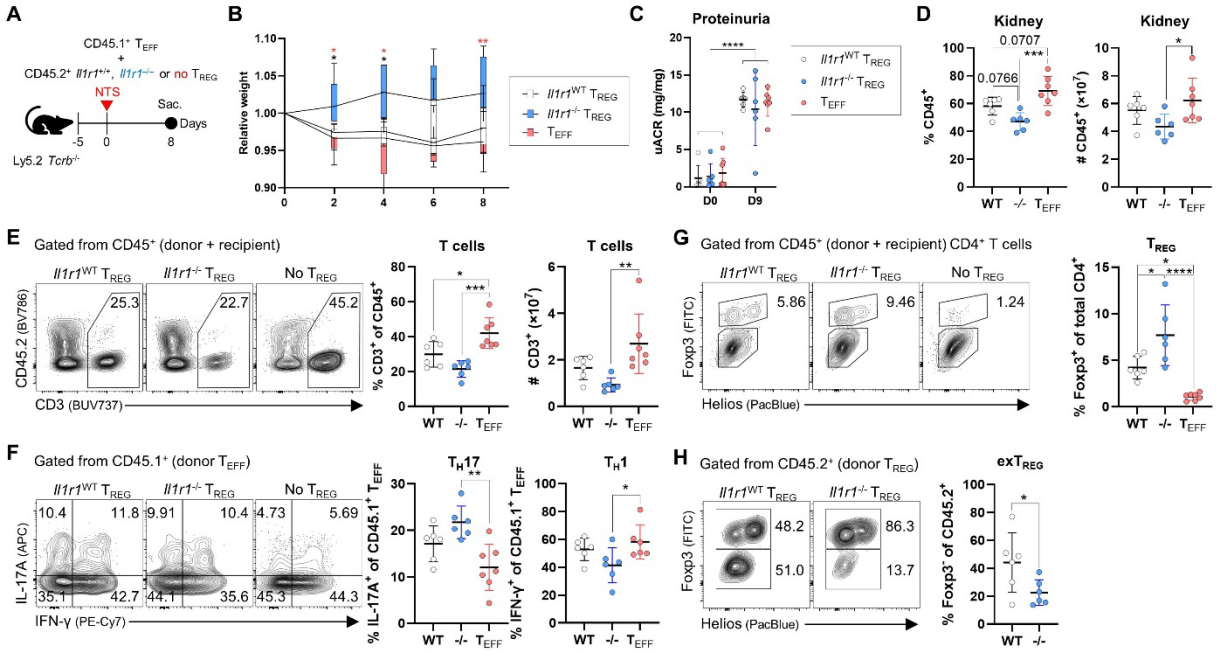
A
CD45.1+ TEFF
+
CD45.2+ Il1r1+/+, Il1r1-/- or no TREG
NTS
Sac.
Days
-5
0
8
Ly5.2 Tcrb-/-
B
Relative weight
Il1r1WT TREG
Il1r1-/- TREG
TEFF
C
Proteinuria
uACR (mg/mg)
D0
D9
D
Kidney
% CD45+
0.0766
0.0707
Kidney
# CD45+ (×10^7)
WT
-/-
TEFF
E
Gated from CD45+ (donor + recipient)
Il1r1WT TREG
Il1r1-/- TREG
No TREG
25.3
22.7
45.2
CD45.2 (BV786)
CD3 (BUV737)
T cells
% CD3+ of CD45+
T cells
# CD3+ (×10^7)
G
Gated from CD45+ (donor + recipient) CD4+ T cells
5.86
9.46
1.24
Foxp3 (FITC)
Helios (PacBlue)
TREG
% Foxp3+ of total CD4+
F
Gated from CD45.1+ (donor TEFF)
10.4
11.8
9.91
10.4
4.73
5.69
35.1
42.7
44.1
35.6
45.3
44.3
IL-17A (APC)
IFN-γ (PE-Cy7)
TH17
% IL-17A+ of CD45.1+ TEFF
TH1
% IFN-γ+ of CD45.1+ TEFF
H
Gated from CD45.2+ (donor TREG)
48.2
51.0
86.3
13.7
Foxp3 (FITC)
Helios (PacBlue)
exTREG
% Foxp3- of CD45.2+

**Figure 5: IL-1 signaling in $T_{REG}$ restricts control of renal $T_H1$ responses in NTN.** (**A**) Schematic showing the experimental design. $T_{EFF}$ cells (Foxp3-GFP$^-$ CD4$^+$) were isolated from Ly5.1 *Foxp3*$^{GFP}$ reporter mice and were transferred alongside $T_{REG}$ cells (Foxp3-GFP$^+$ CD4$^+$) cells from Ly5.2 *Foxp3*$^{GFP}$ *Il1r1*$^{+/+}$ or Ly5.2 *Foxp3*$^{GFP}$ *Il1r1*$^{-/-}$ at a 1:1 ratio or on their own into Ly5.2 *Tcrb*$^{-/-}$ mice five days prior to NTS injection. Mice were followed for eight days following NTN induction. (**B**) Time course of weight loss relative to the day of NTS injection. (**C**) Quantification of uACR prior to NTN induction and at day 8 of NTN. (**D**) Quantification of the frequencies and absolute numbers of renal immune cells. (**E**) Representative flow plots showing the gating of total renal T cells (donor CD45.1$^+$, donor CD45.2$^+$, recipient CD45.2$^+$) alongside quantification of the frequencies and absolute numbers. (**F**) Representative flow plots showing renal $T_H17$ and $T_H1$ cells from the donor (CD45.1$^+$) alongside quantification of their frequencies. Cells were gated from CD45.1$^+$ Foxp3$^-$ cells. (**G**) Representative flow plots showing total renal $T_{REG}$ cells alongside their quantification. (**H**) Representative flow plots showing ex$T_{REG}$ formation from donor-derived n$T_{REG}$ alongside quantification. Data are shown as mean ± SD (**C-H**) or boxplots showing the mean (center), interquartile range (bounds), and min-max range (whiskers) (**B**) from a compilation of two independent experiments. *P*-values were determined using a one-way ANOVA with Tukey's post-hoc testing for multiple comparisons (*$P$≤0.05, **$P$≤0.01, ***$P$≤0.001, and ****$P$≤0.0001).

## Supplemental Figure 1

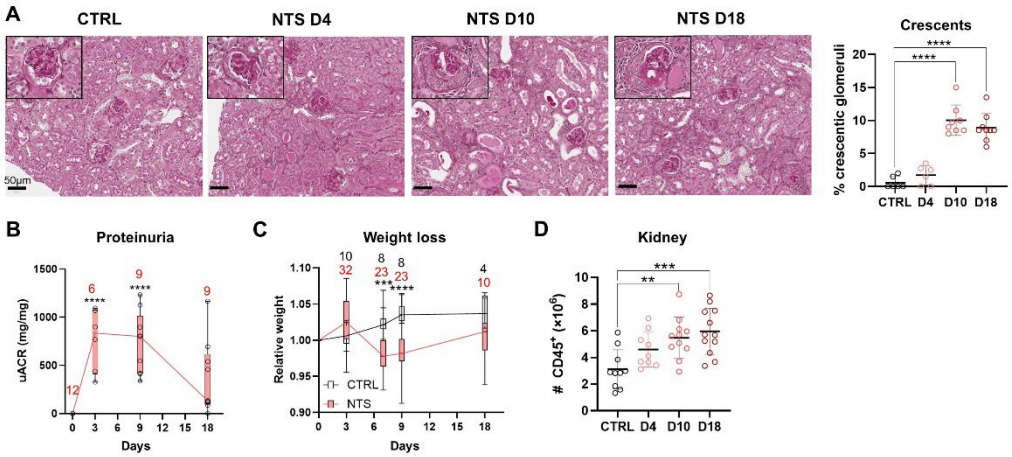

**Supplemental Figure 1: Characterization of NTN pathology.**

(**A**) Representative photographs of H&E kidney sections from control serum-injected mice (CTRL, *n*=6) or mice at 4 (*n*=6), 10 (*n*=8), and 18 (*n*=9) days following NTS injection alongside quantification of the frequencies of crescentic glomeruli in each section. (**B**) Time course of urinary albumin-to-creatinine ratios (uACR). uACR was measured at days 0, 3, 9, and 18 following NTS-injection from mice that were sacrificed at day 18 (*n*=12) across three independent experiments. Mice that were severely anuric following NTN induction were not included. The numbers above the boxes represent the number of mice. (**C**) Time course of weight change relative to the day of NTS or control serum injection. Numbers above the boxes represent the number of mice in the CTRL (black) and NTS-injected (red) groups. (**D**) Numbers of immune ($CD45^+$) cells in the kidneys. Data are shown as mean ± SD (**A**, **D**) or box plots showing the mean (center), quartiles (bounds), and min-max range (whiskers) (**B**, **C**) compiled from three independent experiments. Each dot represents a single mouse. *P*-values were determined using a one-way ANOVA with Tukey's post-hoc test for multiple comparisons (**A, B, D**) or two-way ANOVA with Bonferroni's post-hoc test for multiple comparisons (**C**) (*$P \leq 0.05$, **$P \leq 0.01$, ***$P \leq 0.001$, and ****$P \leq 0.0001$). This supplemental figure is associated with Figure 1.

## Supplemental Figure 2

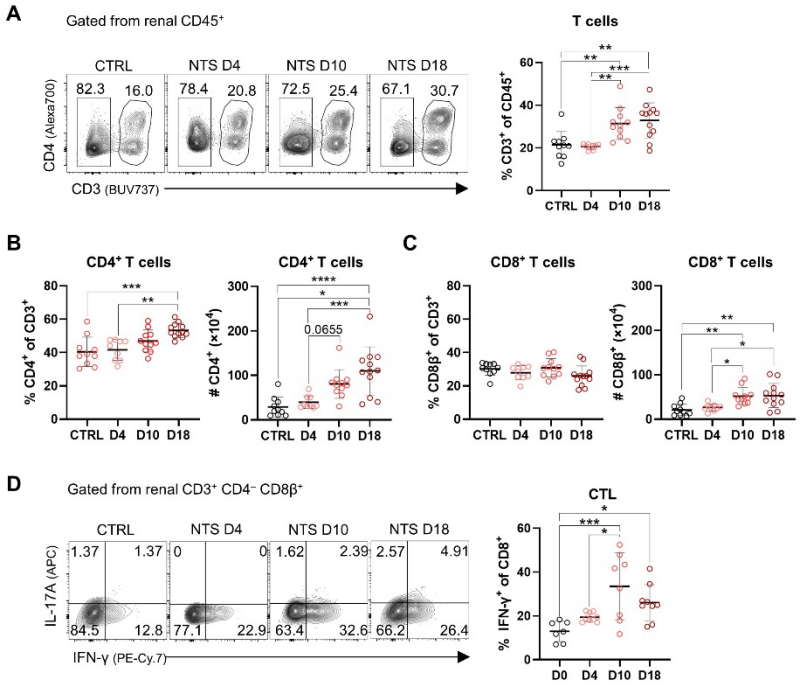

**Supplemental Figure 2: Characterization of renal T cell populations.**

(**A**) Representative flow plots showing renal T cells from CTRL and NTS-injected mice alongside quantification of their frequencies. (**B, C**) Frequencies and absolute numbers of $CD4^+$ (**B**) and $CD8^+$ T cells (**C**) in the kidneys of CTRL and NTN mice. (**D**) Representative flow plots and quantification of IFN-γ-producing cytotoxic T lymphocytes (CTLs) in the kidneys. Data are shown as mean ± SD compiled from three independent experiments. Each dot represents a single mouse. *P*-values were determined using a one-way ANOVA with Tukey's post-hoc test for multiple comparisons (**P*≤0.05, ***P*≤0.01, ****P*≤0.001, and *****P*≤0.0001). This supplemental figure is associated with Figure 1.

## Supplemental Figure 3

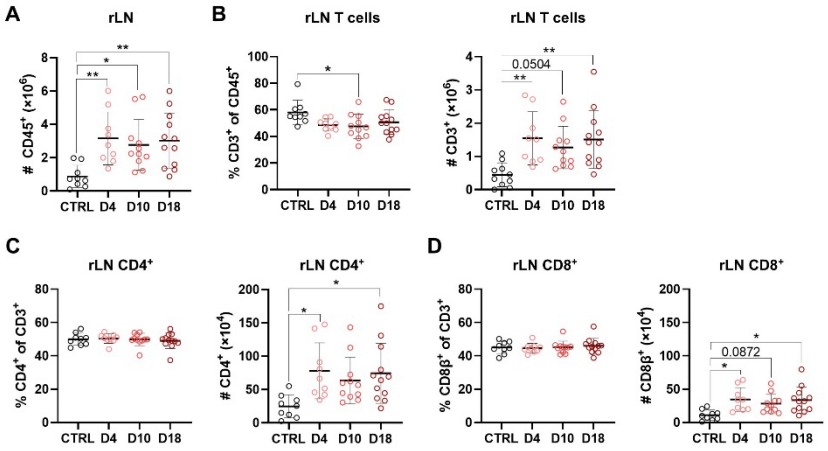

**Supplemental Figure 3: Characterization of T cells in renal lymph nodes.**

(**A**) Numbers of immune cells in the renal lymph nodes (rLN). (**B**) Quantification of the frequencies and absolute numbers of T cells in the renLN. (**C, D**) Frequencies and absolute numbers of $CD4^+$ (**C**) and $CD8^+$ T cells (**D**) in rLNs of CTRL and NTS-injected mice. Data are shown as mean ± SD compiled from three independent experiments. Each dot represents a single mouse. *P*-values were determined using a one-way ANOVA with Tukey's post-hoc test for multiple comparisons (*$P \leq 0.05$, **$P \leq 0.01$, ***$P \leq 0.001$, and ****$P \leq 0.0001$). This supplemental figure is associated with Figure 2.

## Supplemental Figure 4

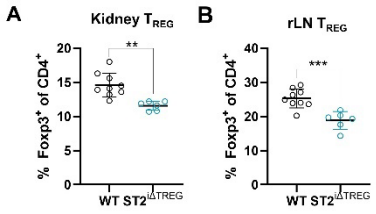

**Supplemental Figure 4: Characterization of $T_{REG}$ cells in $ST2^{i\Delta TREG}$ mice.**

(**A, B**) Quantification of the frequencies of $T_{REG}$ cells in the kidneys (**A**) and rLNs (**B**) of *Foxp3*$^{CreERT2\text{-}GFP}$ *Il1rl1*$^{WT}$ (WT) and *Foxp3*$^{CreERT2\text{-}GFP}$ *Il1rl1*$^{fl/fl}$ ($ST2^{i\Delta TREG}$) mice. Data are shown as mean ± SD compiled from three independent experiments. Each dot represents a single mouse. *P*-values were determined using a one-way ANOVA with Tukey's post-hoc test for multiple comparisons (**P*≤0.05, ***P*≤0.01, ****P*≤0.001, and *****P*≤0.0001). This supplemental figure is associated with Figure 3.

### 5.8 References


1 Anders, H.-J., Kitching, A. R., Leung, N. & Romagnani, P. Glomerulonephritis: immunopathogenesis and immunotherapy. *Nature Reviews Immunology* **23**, 453-471 (2023). https://doi.org:10.1038/s41577-022-00816-y

2 Chadban, S. J. & Atkins, R. C. Glomerulonephritis. *The Lancet* **365**, 1797-1806 (2005). https://doi.org:10.1016/S0140-6736(05)66583-X

3 Jha, V. *et al.* Chronic kidney disease: global dimension and perspectives. *The Lancet* **382**, 260-272 (2013). https://doi.org:10.1016/S0140-6736(13)60687-X

4 Moroni, G. & Ponticelli, C. Rapidly progressive crescentic glomerulonephritis: Early treatment is a must. *Autoimmunity Reviews* **13**, 723-729 (2014). https://doi.org:https://doi.org/10.1016/j.autrev.2014.02.007

5 Kurts, C., Panzer, U., Anders, H.-J. & Rees, A. J. The immune system and kidney disease: basic concepts and clinical implications. *Nature Reviews Immunology* **13**, 738-753 (2013). https://doi.org:10.1038/nri3523

6 Krebs, C. F. *et al.* Plasticity of Th17 Cells in Autoimmune Kidney Diseases. *J Immunol* **197**, 449-457 (2016). https://doi.org:10.4049/jimmunol.1501831

7 Krebs, C. F., Schmidt, T., Riedel, J.-H. & Panzer, U. T helper type 17 cells in immune-mediated glomerular disease. *Nature Reviews Nephrology* **13**, 647 (2017). https://doi.org:10.1038/nrneph.2017.112

8 Sung, S.-S. & Bolton, W. K. T cells and dendritic cells in glomerular disease: the new glomerulotubular feedback loop. *Kidney International* **77**, 393-399 (2010). https://doi.org:10.1038/ki.2009.489

9 Hochheiser, K. *et al.* Exclusive CX3CR1 dependence of kidney DCs impacts glomerulonephritis progression. *The Journal of Clinical Investigation* **123**, 4242-4254 (2013). https://doi.org:10.1172/JCI70143

10 Lukacs-Kornek, V. *et al.* The kidney-renal lymph node-system contributes to cross-tolerance against innocuous circulating antigen. *J Immunol* **180**, 706-715 (2008). https://doi.org:10.4049/jimmunol.180.2.706

11 Uriol-Rivera, M. G. *et al.* Sequential administration of paricalcitol followed by IL-17 blockade for progressive refractory IgA nephropathy patients. *Scientific Reports* **14**, 4866 (2024). https://doi.org:10.1038/s41598-024-55425-7

12 Alikhan, M. A., Huynh, M., Kitching, A. R. & Ooi, J. D. Regulatory T cells in renal disease. *Clin Transl Immunology* **7**, e1004 (2018). https://doi.org:10.1002/cti2.1004

13 Paust, H. J. *et al.* Regulatory T cells control the Th1 immune response in murine crescentic glomerulonephritis. *Kidney Int* **80**, 154-164 (2011). https://doi.org:10.1038/ki.2011.108

14 Kluger, M. A. *et al.* Stat3 Programs Th17-Specific Regulatory T Cells to Control GN. *Journal of the American Society of Nephrology* **25**, 1291-1302 (2014). https://doi.org:10.1681/asn.2013080904

15 Nosko, A. *et al.* T-Bet Enhances Regulatory T Cell Fitness and Directs Control of Th1 Responses in Crescentic GN. *Journal of the American Society of Nephrology* **28**, 185-196 (2017). https://doi.org:10.1681/asn.2015070820

16 Alvarez, F. *et al.* The alarmins IL-1 and IL-33 differentially regulate the functional specialisation of Foxp3+ regulatory T cells during mucosal inflammation. *Mucosal Immunology* **12**, 746-760 (2019). https://doi.org:10.1038/s41385-019-0153-5

17 Wang, Y., Su, Maureen A. & Wan, Yisong Y. An Essential Role of the Transcription Factor GATA-3 for the Function of Regulatory T Cells. *Immunity* **35**, 337-348 (2011). https://doi.org:https://doi.org/10.1016/j.immuni.2011.08.012

18 Whibley, N., Tucci, A. & Powrie, F. Regulatory T cell adaptation in the intestine and skin. *Nature Immunology* **20**, 386-396 (2019). https://doi.org:10.1038/s41590-019-0351-z

19 Sakai, R. *et al.* Kidney GATA3(+) regulatory T cells play roles in the convalescence stage after antibody-mediated renal injury. *Cell Mol Immunol* (2020). https://doi.org:10.1038/s41423-020-00547-x

20 Anders, H.-J. Of Inflammasomes and Alarmins: IL-1β and IL-1α in Kidney Disease. *Journal of the American Society of Nephrology : JASN* **27**, 2564-2575 (2016). https://doi.org:10.1681/ASN.2016020177

21 Schiering, C. *et al.* The alarmin IL-33 promotes regulatory T-cell function in the intestine. *Nature* **513**, 564-568 (2014). https://doi.org:10.1038/nature13577

22 Schenten, D. *et al.* Signaling through the Adaptor Molecule MyD88 in CD4<sup>+</sup> T Cells Is Required to Overcome Suppression by Regulatory T Cells. *Immunity* **40**, 78-90 (2014). https://doi.org:10.1016/j.immuni.2013.10.023

23 Timoshanko, J. R., Kitching, A. R., Iwakura, Y., Holdsworth, S. R. & Tipping, P. G. Contributions of IL-1β and IL-1α to Crescentic Glomerulonephritis in Mice. *Journal of the American Society of Nephrology* **15** (2004).

24 Timoshanko, J. R., Kitching, A. R., Iwakura, Y., Holdsworth, S. R. & Tipping, P. G. Leukocyte-derived interleukin-1beta interacts with renal interleukin-1 receptor I to promote renal tumor necrosis factor and glomerular injury in murine crescentic glomerulonephritis. *Am J Pathol* **164**, 1967-1977 (2004). https://doi.org:10.1016/s0002-9440(10)63757-1

25 Wohlfert, E. A. *et al.* GATA3 controls Foxp3$^+$ regulatory T cell fate during inflammation in mice. *J Clin Invest* **121**, 4503-4515 (2011). https://doi.org:10.1172/jci57456

26 Alvarez, F., Al-Aubodah, T. A., Yang, Y. H. & Piccirillo, C. A. Mechanisms of T(REG) cell adaptation to inflammation. *J Leukoc Biol* **108**, 559-571 (2020). https://doi.org:10.1002/jlb.1mr0120-196r

27 Li, Y., Liu, H., Yan, H. & Xiong, J. *Autoimmunity Reviews* **22**, 103257 (2023). https://doi.org:https://doi.org/10.1016/j.autrev.2022.103257

28 Eggenhuizen, P. J. *et al.* Smith-specific regulatory T cells halt the progression of lupus nephritis. *Nature Communications* **15**, 899 (2024). https://doi.org:10.1038/s41467-024-45056-x

29 Heymann, F. *et al.* Kidney dendritic cell activation is required for progression of renal disease in a mouse model of glomerular injury. *J Clin Invest* **119**, 1286-1297 (2009). https://doi.org:10.1172/jci38399

30 Kiaf, B., Bode, K., Schuster, C. & Kissler, S. Gata3 is detrimental to regulatory T cell function in autoimmune diabetes. *bioRxiv* (2023). https://doi.org:10.1101/2023.03.18.533297

31 Lichtnekert, J. *et al.* Anti-GBM glomerulonephritis involves IL-1 but is independent of NLRP3/ASC inflammasome-mediated activation of caspase-1. *PLoS One* **6**, e26778 (2011). https://doi.org:10.1371/journal.pone.0026778

32 Levine, A. G., Arvey, A., Jin, W. & Rudensky, A. Y. Continuous requirement for the TCR in regulatory T cell function. *Nature Immunology* **15**, 1070-1078 (2014). https://doi.org:10.1038/ni.3004

33 Hori, S., Haury, M., Coutinho, A. & Demengeot, J. Specificity requirements for selection and effector functions of CD25+4+ regulatory T cells in anti-myelin basic protein T cell receptor transgenic mice. *Proc Natl Acad Sci U S A* **99**, 8213-8218 (2002). https://doi.org:10.1073/pnas.122224799

34 Ooi, J. D. *et al.* Dominant protection from HLA-linked autoimmunity by antigen-specific regulatory T cells. *Nature* **545**, 243-247 (2017). https://doi.org:10.1038/nature22329

35 Tarbell, K. V., Yamazaki, S., Olson, K., Toy, P. & Steinman, R. M. CD25+ CD4+ T cells, expanded with dendritic cells presenting a single autoantigenic peptide, suppress autoimmune diabetes. *J Exp Med* **199**, 1467-1477 (2004). https://doi.org:10.1084/jem.20040180

36 Tang, Q. *et al.* In vitro-expanded antigen-specific regulatory T cells suppress autoimmune diabetes. *J Exp Med* **199**, 1455-1465 (2004). https://doi.org:10.1084/jem.20040139

## CHAPTER 6: CONCLUSION AND GENERAL DISCUSSION

The study of autoimmune diseases over the past few decades has revealed a common underlying structure for the pathogenesis of highly heterogeneous pathologies. This 'immunogenetic' architecture (reviewed in *Chapter 1.2.1*) posits that genetics is the primary, though often insufficient, underlying factor for the development of autoreactivity (160, 164). Environmental factors, such as infections, dietary components, pollutants, and many others, act on this genetic background to break tolerance and thereby elicit responses from autoreactive T and B cells. Indeed, T-B cell crosstalk is at the heart of autoimmunity – autoreactive T cells provide B cells with assistance in the production of autoantibodies, and autoreactive B cells, highly specialized for autoantigen presentation, induce self-directed T cell responses. The resulting pathology is diverse, varying greatly in both the intensity of organ inflammation and the rate at which the disease progresses. This is particularly evident in autoimmune kidney disease; while autoantibodies cause the initial injury, the disease experienced bifurcates into the rapidly progressing inflammatory glomerulonephritis (e.g., IgAN, lupus nephritis, ANCA GN, anti-GBM nephritis) or the slowly progressing non-inflammatory glomerulopathies (e.g., MN).

The etiologies of MCD and FSGS, which account for all childhood manifestations of INS and up to 70% of adult cases, have long remained unknown (10). An autoimmune origin, particularly for childhood INS, has been predicted based on their responsiveness to immunosuppression with GCs. The recent success of RTX in maintaining long-term remissions in MCD and FSGS, and the even more recent identification of podocyte-targeting autoantibodies has positioned humoral immunity as central to the pathogenesis of INS (435). In the first part of this thesis, consisting of *Chapters 2*, *3*, and *4*, we sought to provide evidence for an autoimmune humoral etiology for childhood INS. In *Chapter 2*, we showed that INS is associated with the expansion of eMBCs and ASCs. Then, in *Chapter 3*, we demonstrated that the expansion of these cells in INS is antigen-driven and was associated with the production of APAs. Finally, in *Chapter 4*, we used an experimental mouse model of INS to demonstrate that the pathogenicity of APAs is influenced by the MHC-II context in

which tolerance to podocyte autoantigens is broken. In this chapter, we will discuss these findings in light of the immunogenetic architecture of autoimmunity (**Figure 5**).

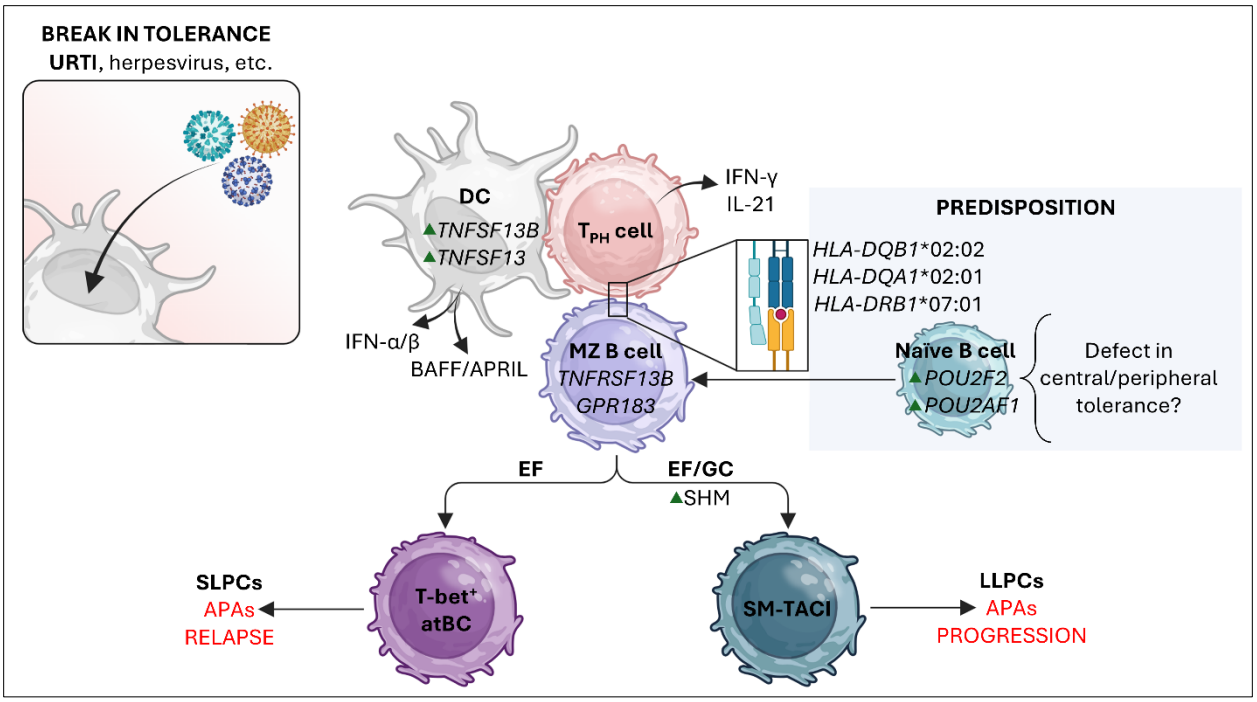


***Figure 5 - Autoimmune architecture of childhood INS.*** Predisposition to INS is mediated by HLA-II polymorphisms that promote the activation of podocytopathic B cells, and defects in central/peripheral tolerance that enable the escape of autoreactive naïve B cells into the periphery. Upper respiratory tract infections (URTI), herpesvirus infection/reactivation, or other immune events result in a break of tolerance and trigger the production of type-I IFNs. Podocyte-targeting extrafollicular memory B cells like marginal zone (MZ) B cells give rise to T-bet$^+$ atypical B cells (atBCs) through extrafollicular (EF) responses supported by BAFF(*TNFSF13B*)/APRIL(*TNFSF13*) signals. Short-lived plasma cells (SLPC) generated from EF responses produce anti-podocyte antibodies (APAs) that mediate INS relapse. Memory B cells may also undergo high degrees of somatic hypermutation (SHM) and class-switching through EF or germinal center (GC) responses to give rise to isotype-switched classical memory B cells in a TACI-dependent manner (SM-TACI). Long-lived PCs (LLPC) generated from these cells may contribute to the progression of some childhood INS cases to more severe, steroid-resistant forms of disease. Created with BioRender.com.

## 6.1 B cell dysregulation

### *6.1.1 A hyperactive B cell pool*

Before RTX was identified as an effective means of controlling relapses in INS, T cells were thought to be the culprit cells driving pathogenesis. This hypothesis stemmed from a seminal 1974 Lancet paper by Robert Shalhoub, in which he argued that several key features of INS suggested a T cell origin: measles infection induces remission (measles disrupts T cell-mediated immunity), remission is effectively achieved with GCs and

cyclophosphamide, and INS can occur secondary to Hodgkin lymphoma (originally thought to be a T cell lymphoma) (11). However, it is now understood that these features may equally, or in the case of Hodkin lymphoma preferentially, implicate B cells in the pathogenesis of the disease (442). Nevertheless, many studies have since attempted to identify a pathogenic T cell signature, but these have often been contradictory (443-450). In *Chapter 2*, we used scRNA-seq on total PBMC from children with active INS and age/sex-matched healthy controls and showed that the major perturbation in PBMC was in the B cell compartment. We defined a nephrotic B cell transcriptional signature that was consistent with an activated B cell state, and this signature was most prevalent among naïve B cells. Indeed, naïve B cells appear to be dysregulated in several autoimmune diseases, where they are highly responsive to even mild BCR stimulation (177, 451-454). Defects in central and peripheral tolerance (checkpoints 3 and 4) likely allow these naïve B cells to enter the mature B cell repertoire.

### *6.1.2 Engagement of autoimmune-prone B cells*

A major finding in *Chapter 2* was the expansion of autoimmune-prone eMBCs, namely $CD21^{low}$ $T\text{-}bet^{+}$ $CD11c^{+}$ atBCs and MZ-like B cells, in childhood INS, hence implicating the extrafollicular response in disease pathogenesis. $T\text{-}bet^{+}$ $CD11c^{+}$ atBCs have been identified in numerous autoimmune settings, both in peripheral blood and affected tissues, with a consistent phenotype (119, 135, 251, 253). While the precise functions of these cells in human autoimmune disease remain an active area of investigation, several lines of evidence suggest that atBCs act as precursors for plasmablasts/SLPCs. Their conversion into antibody-secreting cells (ASCs) is dependent on T-bet, as has been shown for the corresponding ABCs in mice (124). Accordingly, we observed a marked expansion of ASCs in the blood during active INS, and these cells preferentially expressed T-bet. Consistent with an extrafollicular origin, these ASCs were depleted after RTX treatment, indicating a plasmablast/SLPC identity. In addition, the innate viral sensors TLR7 and TLR9 have also been implicated in the expansion of atBCs and their conversion into plasmablasts/SLPCs (134, 135). While, we have not compared the ability of INS and healthy B cells to convert into

atBCs upon TLR7 and TLR9 stimulation, it is well known that that viral infections are a common trigger for INS relapses (412). Therefore, relapses may be elicited by virus-mediated activation of autoreactive atBCs. Furthermore, IL-21 and IFN-γ produced by circulating $T_{FH}$ cells – or $T_{PH}$ cells – are also known to drive atBC responses (96, 131, 270). Indeed, some studies have reported an increase in circulating $T_{FH}$ cells during active INS, though this was not investigated in this thesis (455). Finally, chronic BCR signaling appears to be critical for the development of these cells, at least in conditions like SLE and malaria (113, 119). This is consistent with the relapsing-remitting nature of INS, where constant autoantigen exposure may promote the development of atBCs. Despite strong evidence demonstrating that atBCs function as plasmablast/SLPC precursors, several investigations argue that atBCs represent an exhausted population denoted by high expression of inhibitory FCRL molecules (110, 113). Interestingly, we showed that atBCs in INS children had lower expression of FCRL5 than in healthy individuals, suggesting that these atBCs may be more responsive to BCR stimulation. Nevertheless, this theory needs to be tested *in vitro*.

MZ B cells have also been implicated in autoimmunity, as they are enriched with autoreactive clones even under homeostasis. The majority of $IgM^+$ MBCs in the peripheral blood correspond with recirculating MZ B cells (139, 140). Thus, the expanded MZ-like B cells we observed in INS may represent a recirculating MZ B cell population. The increased expression of T-bet in INS MBCs supports this hypothesis, as it has recently been shown that T-bet expression in MBCs is associated with a splenic program (456). Moreover, as discussed in *Chapter 1.1.3*, MZ B cells participate in extrafollicular responses giving rise to both plasmablasts/SLPCs and MBCs through TD and TI mechanisms. Whether these MZ B cells can develop into atBCs remains to be determined, but two recent studies suggest that this is the case. In the first, trajectory analysis showed that expanded atBCs in the blood of malaria-infected individuals arise from MZ-like MBCs (expressing *GPR183*, *TNFRSF13B*, and *IGHM*) (128). In the second, *IGHV* utilization by atBCs overlapped with both MZ and follicular B cell repertoires, suggesting that a both populations contribute to the atBC pool (457). Similarly, trajectory analysis of B cells in INS supported these findings showing that MZ-like B cells and atBCs comprise a distinct developmental pathway for MBCs, and this is

associated with elevated expression of *GPR183* and *TNFRSF13B*. Both EBI2 (*GPR183*) and TACI (*TNFRSF13B*) are associated with extrafollicular responses.

### *6.1.3 APRIL/BAFF-driven clonal expansion*

In *Chapter 3*, we investigated whether the expansion of MBCs in childhood INS is antigen-specific. Using scRNA-seq pairing both gene expression and V(D)J data, we first confirmed that INS was associated with increases in MZ-like B cells, atBCs, and ASCs. In addition, we found that a population of cMBCs expressing high levels of *TNFRSF13B* and preferentially utilizing an *IGHA1* BCR, which we termed SM-TACI B cells, were also expanded in INS. Accordingly, an increased abundance of isotype-switched cMBCs ($IgM^-$ $IgD^-$ $CD27^+$) in the peripheral blood has been consistently observed in active INS, and their resurgence is associated with relapses after B cell depletion, findings that we confirmed in *Chapter 2* (425, 426). Whether the expansion of SM-TACI B cells in scRNA-seq corresponds to these isotype-switched cMBCs is currently unknown and will be resolved by evaluating TACI expression on INS B cells by flow cytometry. Importantly, we showed that the expansion of MZ-like B cells, SM-TACI B cells, and ASCs was oligoclonal, suggesting their involvement in an active B cell response at the time of relapse. The common expression of *TNFRSF13B* between MZ-like B cells and SM-TACI B cells underscores the possible involvement of APRIL/BAFF-TACI signaling in mediating pathology. Indeed, in *Chapter 2*, we showed that this signaling pathway is actively engaged in childhood INS, with myeloid cells from affected children preferentially expressing *TNFSF13* (APRIL) and *TNFSF13B* (BAFF), and MBCs expressing *TNFRSF13B* (TACI). The induction of CSR and SHM by TACI enables the secondary diversification of BCRs during extrafollicular responses, therefore its high expression on SM-TACI B cells may underlie the high degree of CSR and SHM observed in this population (103). More generally, the clonally expanded MBCs and ASCs in childhood INS exhibited high rates of SHM, which could be supported by TACI signaling.

The BCR-sequencing in *Chapter 3* was performed on B cells from four children seropositive for anti-CRB2 antibodies and four seronegative individuals. All four anti-CRB2+ donors had highly clonal MBCs in the peripheral blood, while this was only the case for two

of the anti-CRB2– donors. These data suggest that the active B cell responses in INS are associated with APAs, but this cannot be definitively concluded at this time. To address this question, we plan to generate antibodies from the most clonally expanded MBC and ASC populations and test their ability to bind podocytes *in vitro* and in kidney tissue. Furthermore, while all the children in our cohort lacked anti-Nephrin, the most recently described APA in INS, we cannot rule out the presence of other APAs in our anti-CRB2– children. Indeed, the most clonal MBC response we observed was in an anti-CRB2– individual, indicating an active B cell response. Questions regarding the diversification of APA species through epitope spreading were not addressed in this thesis but are essential for understanding the autoimmune humoral etiology of MCD/FSGS. Indeed, these APAs may eventually serve as important prognostic biomarkers for the disease, similar to ANAs in SLE.

### *6.1.4 The extrafollicular response as a conserved target for autoimmunity*

As discussed in *Chapter 1.2.3*, the extrafollicular B cell response is emerging as a common pathway for B cell autoreactivity (253). Our work in *Chapters 2* and *3* provides strong evidence that extrafollicular B cell responses are involved in the pathogenesis of childhood INS. We propose that autoreactive B cells escape into the MZ B cell pool, which gives rise to atBCs and isotype-switched cMBCs in a TACI-dependent manner (**Figure 5**). Both populations may serve as SLPC precursors leading to the generation of podocytopathic APAs. Since our assessment of B cell responses were limited to blood, we cannot exclude the possibility that germinal centers contribute to the generation of APAs; the development of LLPCs may lead to steroid resistance and the development of more severe FSGS manifestations. Nevertheless, childhood INS may benefit from therapeutics that target extrafollicular B cell responses. One such example is TACI-Ig (atacicept/telitacicept), which inhibits BAFF and APRIL to eradicate both SLPCs and the eMBCs that give rise to them. TACI-Ig is currently being explored in the treatment of IgAN, where the extrafollicular expansion of B cells has been observed in the associated pharyngitis (292, 328).

## 6.2 Factors predisposing to INS

### *6.2.1 Viral infection, IFN-I and molecular mimicry*

Relapses of INS are usually associated with some immune insult, with 45% of cases being triggered by upper respiratory tract viral infections (e.g., influenza virus, coronavirus, respiratory syncytial virus, etc.) (412). Many other cases are associated with herpes virus reactivation, skin infections, atopic flares, allergic reactions, asthma, gastroenteritis, and even vaccinations. The expansion of atBCs has recently been associated with both acute respiratory viral infections (e.g., influenza virus and SARS-CoV-2) and chronic viral/parasitic infections (e.g., EBV and *P. falciparum*), and in both cases has been attributed to the development of autoimmunity (113, 458, 459). For example, SARS-CoV-2 infection was recently shown to drive the development of autoreactive ASCs from atBCs, resulting in the production of autoantibodies against nuclear antigens, phospholipids, and the GBM in severe COVID-19 (458). Thus, our results in *Chapter 2* suggest that viral infections in childhood INS may also contribute to the production of APAs through the extrafollicular generation of autoreactive ASCs. There are two main mechanisms by which viruses may induce these responses. First, as we mentioned in the previous section, viruses may drive extrafollicular responses in an antigen non-specific manner by interacting with intracellular TLR7 and TLR9, thereby promoting atBC activation. This is a likely scenario in childhood INS, given the breadth of viral insults that can trigger relapses of INS. Accordingly, we observed an elevated IFN-I signature in B cells from INS children compared to HCs, though confirmation with a greater sample number is needed.

The second major mechanism is through molecular mimicry. In *Chapter 1.2.1*, we outlined how the similarity between $EBNA1_{393-399}$ and $GlialCAM_{377-383}$ (SPPR(R/A)P motif) may result in the production of anti-GlialCAM antibodies in MS following EBV infection (192). Interestingly, a large study of 124 children at the onset of INS demonstrated an association with EBV infection (442). Although we did not assess the possibility of mimicry by EBV in this thesis, the same $EBNA1_{394-400}$ motif does overlap with the extracellular domain of $Nephrin_{593-598}$ (PPRR(P/A)P motif), suggesting that this may contribute to autoreactivity. To further

explore the topic of molecular mimicry, we plan to test antibodies generated from clonally expanded MBCs and ASCs for cross-reactivity to a panel of common viral antigens.

### *6.2.2 HLA-II polymorphisms and APA production*

One of the strongest predisposing factors to childhood INS are HLA-II alleles. GWAS have identified several HLA-II hits, but most consistently show that *HLA-DQA1**02, *HLA-DQB1**02, and *HLA-DRB1**07/08 are associated with increased risk (404-411). In *Chapter 3*, we genotyped the children in our cohort for both HLA-I and HLA-II alleles and verified the association of *HLA-DQA1**02:01, *HLA-DQB1**02:02, and *HLA-DRB1**07:01 with INS. These alleles are in linkage disequilibrium, making it difficult to determine which is directly involved in the pathogenesis of INS. HLA polymorphisms in autoimmunity are thought to act by influencing antigen presentation to T cells, thereby shaping the resulting autoreactive T cell response. However, through the T-B cell crosstalk, these HLA polymorphisms may also influence the development of autoantibodies.

In *Chapter 3*, we sought to address this question by using the Crb2 immunization-based EANS model in mice with different MHC-II haplotypes. We showed that susceptibility to EANS induction was strain dependent, with C3H/HeN and BALB/c mice being highly susceptible to disease, whereas C57BL/6 mice were protected. While all strains produced high titers of anti-Crb2 antibodies, these antibodies were not able to bind podocytes in C57BL/6 mice. Thus, we predict that the MHC-II haplotype in C57BL/6 favours the presentation of Crb2 peptides that are either inaccessible to antibodies within the slit diaphragm or that do not favour the generation of strong humoral responses. Accordingly, we observed reduced germinal center responses in the C57BL/6 mice compared to the susceptible C3H/HeN and BALB/c strains. If a similar mechanism holds true in humans, we would expect to find APAs in healthy individuals that are not capable of mediating disease. Indeed, anti-PLA2R, the major APA contributing to disease in MN, is also present in the healthy population, albeit at lower concentrations (460, 461). Nevertheless, *Chapter 3* remains an indirect study of the MHC-II haplotype, as the mouse strains used differ in more than just the MHC-II usage; immune biases are well established for each strain with

C3H/HeN mice favouring the development of humoral responses, BALB/c mice showing a $T_H2$ and $T_H17$ bias, and C57BL/6 mice preferentially adopting $T_H1$ immunity. Therefore, we are currently performing bone marrow chimera experiments between C57BL/6 and C3H/HeN strains to address this issue. In the future, the use of mice introgressed with human susceptibility alleles would be beneficial to our understanding of INS pathogenesis.

To best understand how viral infection and HLA-II polymorphisms may influence INS pathogenesis, effort must be made to identify the precise epitopes that drive autoreactive B and T cell responses in INS. To this end, we can develop tetramers for the flow cytometric isolation of podocytopathic B and T cells for *in vitro* functional assessments. For example, single B cell cloning of podocytopathic MBCs would facilitate the generation of large arrays of antibodies – probably much more than we will get from the V(D)J sequencing in *Chapter 3* – for screening against viral antigens. Moreover, podocytopathic T cells could be screened for reactivity to cell lines carrying HLA-II risk alleles pulsed with podocyte antigen.

### 6.3 Defects in $T_{REG}$ cell function

In the second part of this thesis, consisting of *Chapter 5*, we explored how defects in $T_{REG}$ cells may contribute to autoimmune kidney disease. Most forms of glomerulonephritis, including childhood INS, are associated with a decrease in $T_{REG}$ cell abundance, but the cause of the defect remains largely unknown (199, 437, 462). In *Chapter 1.2.1*, we highlighted how HLA-II haplotypes in anti-GBM nephritis undermine the selection of α3(IV)NC1-specific $T_{REG}$ cells, thereby allowing the development of autoreactive $T_{EFF}$ cells. Whether this occurs in other autoimmune kidney diseases remains unknown. We also discussed that pro-inflammatory cytokines are known to destabilize $T_{REG}$ functions in other autoimmune diseases such as RA, but whether this occurs in autoimmune kidney disease was not known. In *Chapter 5*, we showed that two tissue-derived pro-inflammatory cytokines, IL-1 and IL-33, drive $T_{REG}$ cell instability and promote the development of kidney-directed T cell responses following glomerular injury. Importantly, our data not only support the notion that $T_{REG}$ cells controlled the inflammatory responses within the kidney, but also limit the development of the T-B cell crosstalk within lymph nodes. The findings in *Chapter 5*

highlight the potential therapeutic value of targeting IL-1 family cytokines in RPGN and are relevant to the development of $T_{REG}$-based therapies for the treatment of autoimmune diseases. Enhancing the functions of endogenous $T_{REG}$ cells or engineering autoantigen-specific $T_{REG}$ cells are at the core of $T_{REG}$-based therapies, so preventing their destabilization upon entering an inflammatory environment would be advantageous (463). For example, deletion of IL-1R1 could improve the stability of CAR-$T_{REG}$ cells in the treatment of RPGN.

### 6.4 Conclusion

I began the literature review with a quote on evolution, a paradigm that I believe rationalizes all observed biological phenomena. And I think this is particularly true in the case of autoimmune diseases. Despite the vastly differing pathologies, the underlying mechanisms that support the development of autoreactivity appear to be conserved. As such, by studying one autoimmune disease, important lessons can be learned about the rest. In this thesis, we provide strong support for an autoimmune humoral origin for childhood INS by demonstrating that relapses are associated with the clonal expansion of memory B cells, which have now been linked to several manifestations of autoimmunity – both systemic and organ-specific. It is my hope that this work will eventually be translated into the clinic for the development of prognostic biomarkers and that it will provide an important rationale for the use of emerging B cell-targeting therapeutics in the treatment of childhood INS.

**REFERENCES**


1. Al-Aubodah T-A, Aoudjit L, Pascale G, Perinpanayagam MA, Langlais D, Bitzan M, et al. The extrafollicular B cell response is a hallmark of childhood idiopathic nephrotic syndrome. *Nature Communications*. 2023;14(1):7682.
2. Francis A, Harhay MN, Ong ACM, Tummalapalli SL, Ortiz A, Fogo AB, et al. Chronic kidney disease and the global public health agenda: an international consensus. *Nature Reviews Nephrology*. 2024.
3. Global, regional, and national burden of chronic kidney disease, 1990-2017: a systematic analysis for the Global Burden of Disease Study 2017. *Lancet*. 2020;395(10225):709-33.
4. Anders H-J, Kitching AR, Leung N, and Romagnani P. Glomerulonephritis: immunopathogenesis and immunotherapy. *Nature Reviews Immunology*. 2023;23(7):453-71.
5. Jha V, Garcia-Garcia G, Iseki K, Li Z, Naicker S, Plattner B, et al. Chronic kidney disease: global dimension and perspectives. *The Lancet*. 2013;382(9888):260-72.
6. Wetmore JB, Guo H, Liu J, Collins AJ, and Gilbertson DT. The incidence, prevalence, and outcomes of glomerulonephritis derived from a large retrospective analysis. *Kidney Int*. 2016;90(4):853-60.
7. Oleinika K, Mauri C, and Salama AD. Effector and regulatory B cells in immune-mediated kidney disease. *Nature Reviews Nephrology*. 2019;15(1):11-26.
8. Zhang Z, Xu Q, and Huang L. B cell depletion therapies in autoimmune diseases: Monoclonal antibodies or chimeric antigen receptor-based therapy? *Frontiers in Immunology*. 2023;14.
9. Mathur M, Barratt J, Chacko B, Chan TM, Kooienga L, Oh K-H, et al. A Phase 2 Trial of Sibeprenlimab in Patients with IgA Nephropathy. *New England Journal of Medicine*. 2024;390(1):20-31.
10. Vivarelli M, Gibson K, Sinha A, and Boyer O. Childhood nephrotic syndrome. *The Lancet*. 2023;402(10404):809-24.
11. Shalhoub R. Pathogenesis of lipoid nephrosis: a disorder of T-cell function. *The Lancet*. 1974;304(7880):556-60.
12. Flajnik MF, and Kasahara M. Origin and evolution of the adaptive immune system: genetic events and selective pressures. *Nature Reviews Genetics*. 2010;11(1):47-59.
13. LeBien TW, and Tedder TF. B lymphocytes: how they develop and function. *Blood*. 2008;112(5):1570-80.
14. Pieper K, Grimbacher B, and Eibel H. B-cell biology and development. *Journal of Allergy and Clinical Immunology*. 2013;131(4):959-71.
15. Schatz DG, and Ji Y. Recombination centres and the orchestration of V(D)J recombination. *Nature Reviews Immunology*. 2011;11(4):251-63.
16. Brack C, Hirama M, Lenhard-Schuller R, and Tonegawa S. A complete immunoglobulin gene is created by somatic recombination. *Cell*. 1978;15(1):1-14.
17. Nutt SL, and Kee BL. The Transcriptional Regulation of B Cell Lineage Commitment. *Immunity*. 2007;26(6):715-25.

18. Hagman J, Ramírez J, and Lukin K. B lymphocyte lineage specification, commitment and epigenetic control of transcription by early B cell factor 1. *Curr Top Microbiol Immunol.* 2012;356:17-38.
19. Cordeiro Gomes A, Hara T, Lim VY, Herndler-Brandstetter D, Nevius E, Sugiyama T, et al. Hematopoietic Stem Cell Niches Produce Lineage-Instructive Signals to Control Multipotent Progenitor Differentiation. *Immunity.* 2016;45(6):1219-31.
20. Melchers F. The pre-B-cell receptor: selector of fitting immunoglobulin heavy chains for the B-cell repertoire. *Nature Reviews Immunology.* 2005;5(7):578-84.
21. Galler GR, Mundt C, Parker M, Pelanda R, Mårtensson IL, and Winkler TH. Surface mu heavy chain signals down-regulation of the V(D)J-recombinase machinery in the absence of surrogate light chain components. *J Exp Med.* 2004;199(11):1523-32.
22. Shimizu T, Mundt C, Licence S, Melchers F, and Mårtensson IL. VpreB1/VpreB2/lambda 5 triple-deficient mice show impaired B cell development but functional allelic exclusion of the IgH locus. *J Immunol.* 2002;168(12):6286-93.
23. Melchers F. Checkpoints that control B cell development. *J Clin Invest.* 2015;125(6):2203-10.
24. Parker MJ, Licence S, Erlandsson L, Galler GR, Chakalova L, Osborne CS, et al. The pre-B-cell receptor induces silencing of VpreB and lambda5 transcription. *Embo j.* 2005;24(22):3895-905.
25. Karnowski A, Cao C, Matthias G, Carotta S, Corcoran LM, Martensson IL, et al. Silencing and nuclear repositioning of the lambda5 gene locus at the pre-B cell stage requires Aiolos and OBF-1. *PLoS One.* 2008;3(10):e3568.
26. Doyle CM, Han J, Weigert MG, and Prak ET. Consequences of receptor editing at the lambda locus: multireactivity and light chain secretion. *Proc Natl Acad Sci U S A.* 2006;103(30):11264-9.
27. Wardemann H, Yurasov S, Schaefer A, Young JW, Meffre E, and Nussenzweig MC. Predominant autoantibody production by early human B cell precursors. *Science.* 2003;301(5638):1374-7.
28. Gay D, Saunders T, Camper S, and Weigert M. Receptor editing: an approach by autoreactive B cells to escape tolerance. *J Exp Med.* 1993;177(4):999-1008.
29. Radic MZ, Erikson J, Litwin S, and Weigert M. B lymphocytes may escape tolerance by revising their antigen receptors. *J Exp Med.* 1993;177(4):1165-73.
30. Tiegs SL, Russell DM, and Nemazee D. Receptor editing in self-reactive bone marrow B cells. *J Exp Med.* 1993;177(4):1009-20.
31. Rolink AG, Andersson J, and Melchers F. Characterization of immature B cells by a novel monoclonal antibody, by turnover and by mitogen reactivity. *European Journal of Immunology.* 1998;28(11):3738-48.
32. Chung JB, Silverman M, and Monroe JG. Transitional B cells: step by step towards immune competence. *Trends in Immunology.* 2003;24(6):342-8.
33. Marie-Cardine A, Divay F, Dutot I, Green A, Perdrix A, Boyer O, et al. Transitional B cells in humans: Characterization and insight from B lymphocyte reconstitution after hematopoietic stem cell transplantation. *Clinical Immunology.* 2008;127(1):14-25.

34. Batten M, Groom J, Cachero TG, Qian F, Schneider P, Tschopp J, et al. BAFF mediates survival of peripheral immature B lymphocytes. *J Exp Med*. 2000;192(10):1453-66.
35. Rowland SL, Leahy KF, Halverson R, Torres RM, and Pelanda R. BAFF Receptor Signaling Aids the Differentiation of Immature B Cells into Transitional B Cells following Tonic BCR Signaling. *The Journal of Immunology*. 2010;185(8):4570-81.
36. Pillai S, and Cariappa A. The follicular versus marginal zone B lymphocyte cell fate decision. *Nature Reviews Immunology*. 2009;9(11):767-77.
37. Förster R, Mattis AE, Kremmer E, Wolf E, Brem G, and Lipp M. A putative chemokine receptor, BLR1, directs B cell migration to defined lymphoid organs and specific anatomic compartments of the spleen. *Cell*. 1996;87(6):1037-47.
38. Weller S, Braun MC, Tan BK, Rosenwald A, Cordier C, Conley ME, et al. Human blood IgM "memory" B cells are circulating splenic marginal zone B cells harboring a prediversified immunoglobulin repertoire. *Blood*. 2004;104(12):3647-54.
39. Palm A-KE, and Kleinau S. Marginal zone B cells: From housekeeping function to autoimmunity? *Journal of Autoimmunity*. 2021;119:102627.
40. Weill J-C, Weller S, and Reynaud C-A. Human Marginal Zone B Cells. *Annual Review of Immunology*. 2009;27(Volume 27, 2009):267-85.
41. Allen CD, and Cyster JG. Follicular dendritic cell networks of primary follicles and germinal centers: phenotype and function. *Semin Immunol*. 2008;20(1):14-25.
42. Natkanski E, Lee W-Y, Mistry B, Casal A, Molloy JE, and Tolar P. B Cells Use Mechanical Energy to Discriminate Antigen Affinities. *Science*. 2013;340(6140):1587-90.
43. Cyster JG. B cell follicles and antigen encounters of the third kind. *Nature Immunology*. 2010;11(11):989-96.
44. Reif K, Ekland EH, Ohl L, Nakano H, Lipp M, Förster R, et al. Balanced responsiveness to chemoattractants from adjacent zones determines B-cell position. *Nature*. 2002;416(6876):94-9.
45. Gatto D, Paus D, Basten A, Mackay CR, and Brink R. Guidance of B Cells by the Orphan G Protein-Coupled Receptor EBI2 Shapes Humoral Immune Responses. *Immunity*. 2009;31(2):259-69.
46. Pereira JP, Kelly LM, Xu Y, and Cyster JG. EBI2 mediates B cell segregation between the outer and centre follicle. *Nature*. 2009;460(7259):1122-6.
47. Hannedouche S, Zhang J, Yi T, Shen W, Nguyen D, Pereira JP, et al. Oxysterols direct immune cell migration via EBI2. *Nature*. 2011;475(7357):524-7.
48. Liu C, Yang XV, Wu J, Kuei C, Mani NS, Zhang L, et al. Oxysterols direct B-cell migration through EBI2. *Nature*. 2011;475(7357):519-23.
49. Cyster JG, and Allen CDC. B Cell Responses: Cell Interaction Dynamics and Decisions. *Cell*. 2019;177(3):524-40.
50. Zaretsky I, Atrakchi O, Mazor RD, Stoler-Barak L, Biram A, Feigelson SW, et al. ICAMs support B cell interactions with T follicular helper cells and promote clonal selection. *J Exp Med*. 2017;214(11):3435-48.
51. Liu D, Xu H, Shih C, Wan Z, Ma X, Ma W, et al. T-B-cell entanglement and ICOSL-driven feed-forward regulation of germinal centre reaction. *Nature*. 2015;517(7533):214-8.

52. Ise W, Fujii K, Shiroguchi K, Ito A, Kometani K, Takeda K, et al. T Follicular Helper Cell-Germinal Center B Cell Interaction Strength Regulates Entry into Plasma Cell or Recycling Germinal Center Cell Fate. *Immunity.* 2018;48(4):702-15.e4.
53. Crotty S. T follicular helper cell differentiation, function, and roles in disease. *Immunity.* 2014;41(4):529-42.
54. Victora GD, and Nussenzweig MC. Germinal Centers. *Annual Review of Immunology.* 2012;30(Volume 30, 2012):429-57.
55. Klein U, Tu Y, Stolovitzky GA, Keller JL, Haddad J, Miljkovic V, et al. Transcriptional analysis of the B cell germinal center reaction. *Proceedings of the National Academy of Sciences.* 2003;100(5):2639-44.
56. Linterman MA, Beaton L, Yu D, Ramiscal RR, Srivastava M, Hogan JJ, et al. IL-21 acts directly on B cells to regulate Bcl-6 expression and germinal center responses. *J Exp Med.* 2010;207(2):353-63.
57. Zotos D, Coquet JM, Zhang Y, Light A, D'Costa K, Kallies A, et al. IL-21 regulates germinal center B cell differentiation and proliferation through a B cell-intrinsic mechanism. *J Exp Med.* 2010;207(2):365-78.
58. Chevrier S, Kratina T, Emslie D, Tarlinton DM, and Corcoran LM. IL4 and IL21 cooperate to induce the high Bcl6 protein level required for germinal center formation. *Immunol Cell Biol.* 2017;95(10):925-32.
59. Saito M, Novak U, Piovan E, Basso K, Sumazin P, Schneider C, et al. BCL6 suppression of BCL2 via Miz1 and its disruption in diffuse large B cell lymphoma. *Proc Natl Acad Sci U S A.* 2009;106(27):11294-9.
60. Phan RT, and Dalla-Favera R. The BCL6 proto-oncogene suppresses p53 expression in germinal-centre B cells. *Nature.* 2004;432(7017):635-9.
61. Phan RT, Saito M, Basso K, Niu H, and Dalla-Favera R. BCL6 interacts with the transcription factor Miz-1 to suppress the cyclin-dependent kinase inhibitor p21 and cell cycle arrest in germinal center B cells. *Nature Immunology.* 2005;6(10):1054-60.
62. Ranuncolo SM, Polo JM, Dierov J, Singer M, Kuo T, Greally J, et al. Bcl-6 mediates the germinal center B cell phenotype and lymphomagenesis through transcriptional repression of the DNA-damage sensor ATR. *Nature Immunology.* 2007;8(7):705-14.
63. Tunyaplin C, Shaffer AL, Angelin-Duclos CD, Yu X, Staudt LM, and Calame KL. Direct Repression of prdm1 by Bcl-6 Inhibits Plasmacytic Differentiation1. *The Journal of Immunology.* 2004;173(2):1158-65.
64. Ochiai K, Maienschein-Cline M, Simonetti G, Chen J, Rosenthal R, Brink R, et al. Transcriptional regulation of germinal center B and plasma cell fates by dynamical control of IRF4. *Immunity.* 2013;38(5):918-29.
65. Corcoran L, Emslie D, Kratina T, Shi W, Hirsch S, Taubenheim N, et al. Oct2 and Obf1 as Facilitators of B:T Cell Collaboration during a Humoral Immune Response. *Front Immunol.* 2014;5:108.
66. Allen CDC, Ansel KM, Low C, Lesley R, Tamamura H, Fujii N, et al. Germinal center dark and light zone organization is mediated by CXCR4 and CXCR5. *Nature Immunology.* 2004;5(9):943-52.
67. Klein U, and Dalla-Favera R. Germinal centres: role in B-cell physiology and malignancy. *Nature Reviews Immunology.* 2008;8(1):22-33.

68. Muramatsu M, Kinoshita K, Fagarasan S, Yamada S, Shinkai Y, and Honjo T. Class Switch Recombination and Hypermutation Require Activation-Induced Cytidine Deaminase (AID), a Potential RNA Editing Enzyme. *Cell.* 2000;102(5):553-63.
69. Papavasiliou FN, and Schatz DG. Somatic Hypermutation of Immunoglobulin Genes: Merging Mechanisms for Genetic Diversity. *Cell.* 2002;109(2):S35-S44.
70. McHeyzer-Williams M, Okitsu S, Wang N, and McHeyzer-Williams L. Molecular programming of B cell memory. *Nature Reviews Immunology.* 2012;12(1):24-34.
71. Kepler TB, and Perelson AS. Cyclic re-entry of germinal center B cells and the efficiency of affinity maturation. *Immunol Today.* 1993;14(8):412-5.
72. McAdam AJ, Greenwald RJ, Levin MA, Chernova T, Malenkovich N, Ling V, et al. ICOS is critical for CD40-mediated antibody class switching. *Nature.* 2001;409(6816):102-5.
73. Ehrenstein MR, and Notley CA. The importance of natural IgM: scavenger, protector and regulator. *Nat Rev Immunol.* 2010;10(11):778-86.
74. Vidarsson G, Dekkers G, and Rispens T. IgG subclasses and allotypes: from structure to effector functions. *Front Immunol.* 2014;5:520.
75. Rispens T, and Huijbers MG. The unique properties of IgG4 and its roles in health and disease. *Nature Reviews Immunology.* 2023;23(11):763-78.
76. Gould HJ, and Sutton BJ. IgE in allergy and asthma today. *Nature Reviews Immunology.* 2008;8(3):205-17.
77. Chen K, Magri G, Grasset EK, and Cerutti A. Rethinking mucosal antibody responses: IgM, IgG and IgD join IgA. *Nature Reviews Immunology.* 2020;20(7):427-41.
78. Inoue T, and Kurosaki T. Memory B cells. *Nature Reviews Immunology.* 2024;24(1):5-17.
79. Weisel FJ, Zuccarino-Catania GV, Chikina M, and Shlomchik MJ. A Temporal Switch in the Germinal Center Determines Differential Output of Memory B and Plasma Cells. *Immunity.* 2016;44(1):116-30.
80. Laidlaw BJ, and Cyster JG. Transcriptional regulation of memory B cell differentiation. *Nat Rev Immunol.* 2021;21(4):209-20.
81. Shinnakasu R, Inoue T, Kometani K, Moriyama S, Adachi Y, Nakayama M, et al. Regulated selection of germinal-center cells into the memory B cell compartment. *Nat Immunol.* 2016;17(7):861-9.
82. Miura Y, Morooka M, Sax N, Roychoudhuri R, Itoh-Nakadai A, Brydun A, et al. Bach2 Promotes B Cell Receptor-Induced Proliferation of B Lymphocytes and Represses Cyclin-Dependent Kinase Inhibitors. *J Immunol.* 2018;200(8):2882-93.
83. Laidlaw BJ, Duan L, Xu Y, Vazquez SE, and Cyster JG. The transcription factor Hhex cooperates with the corepressor Tle3 to promote memory B cell development. *Nat Immunol.* 2020;21(9):1082-93.
84. Schiepers A, van 't Wout MFL, Greaney AJ, Zang T, Muramatsu H, Lin PJC, et al. Molecular fate-mapping of serum antibody responses to repeat immunization. *Nature.* 2023;615(7952):482-9.

85. Turner JS, Zhou JQ, Han J, Schmitz AJ, Rizk AA, Alsoussi WB, et al. Human germinal centres engage memory and naive B cells after influenza vaccination. *Nature*. 2020;586(7827):127-32.
86. Saito M, Gao J, Basso K, Kitagawa Y, Smith PM, Bhagat G, et al. A Signaling Pathway Mediating Downregulation of BCL6 in Germinal Center B Cells Is Blocked by BCL6 Gene Alterations in B Cell Lymphoma. *Cancer Cell*. 2007;12(3):280-92.
87. Lin KI, Angelin-Duclos C, Kuo TC, and Calame K. Blimp-1-dependent repression of Pax-5 is required for differentiation of B cells to immunoglobulin M-secreting plasma cells. *Mol Cell Biol*. 2002;22(13):4771-80.
88. Shaffer AL, Lin K-I, Kuo TC, Yu X, Hurt EM, Rosenwald A, et al. Blimp-1 Orchestrates Plasma Cell Differentiation by Extinguishing the Mature B Cell Gene Expression Program. *Immunity*. 2002;17(1):51-62.
89. Shaffer AL, Shapiro-Shelef M, Iwakoshi NN, Lee AH, Qian SB, Zhao H, et al. XBP1, downstream of Blimp-1, expands the secretory apparatus and other organelles, and increases protein synthesis in plasma cell differentiation. *Immunity*. 2004;21(1):81-93.
90. Hargreaves DC, Hyman PL, Lu TT, Ngo VN, Bidgol A, Suzuki G, et al. A coordinated change in chemokine responsiveness guides plasma cell movements. *J Exp Med*. 2001;194(1):45-56.
91. Benson MJ, Dillon SR, Castigli E, Geha RS, Xu S, Lam KP, et al. Cutting edge: the dependence of plasma cells and independence of memory B cells on BAFF and APRIL. *J Immunol*. 2008;180(6):3655-9.
92. O'Connor BP, Raman VS, Erickson LD, Cook WJ, Weaver LK, Ahonen C, et al. BCMA is essential for the survival of long-lived bone marrow plasma cells. *J Exp Med*. 2004;199(1):91-8.
93. Matz HC, McIntire KM, and Ellebedy AH. 'Persistent germinal center responses: slow-growing trees bear the best fruits'. *Current Opinion in Immunology*. 2023;83:102332.
94. Elsner RA, and Shlomchik MJ. Germinal Center and Extrafollicular B Cell Responses in Vaccination, Immunity, and Autoimmunity. *Immunity*. 2020;53(6):1136-50.
95. Jenks SA, Cashman KS, Woodruff MC, Lee FE, and Sanz I. Extrafollicular responses in humans and SLE. *Immunol Rev*. 2019;288(1):136-48.
96. Odegard JM, Marks BR, DiPlacido LD, Poholek AC, Kono DH, Dong C, et al. ICOS-dependent extrafollicular helper T cells elicit IgG production via IL-21 in systemic autoimmunity. *J Exp Med*. 2008;205(12):2873-86.
97. Glaros V, Rauschmeier R, Artemov AV, Reinhardt A, Ols S, Emmanouilidi A, et al. Limited access to antigen drives generation of early B cell memory while restraining the plasmablast response. *Immunity*. 2021;54(9):2005-23.e10.
98. MacLennan ICM, and Vinuesa CG. Dendritic Cells, BAFF, and APRIL: Innate Players in Adaptive Antibody Responses. *Immunity*. 2002;17(3):235-8.
99. Goenka R, Matthews AH, Zhang B, O'Neill PJ, Scholz JL, Migone TS, et al. Local BLyS production by T follicular cells mediates retention of high affinity B cells during affinity maturation. *J Exp Med*. 2014;211(1):45-56.

100. Castigli E, Wilson SA, Garibyan L, Rachid R, Bonilla F, Schneider L, et al. TACI is mutant in common variable immunodeficiency and IgA deficiency. *Nat Genet*. 2005;37(8):829-34.
101. von Bülow GU, van Deursen JM, and Bram RJ. Regulation of the T-independent humoral response by TACI. *Immunity*. 2001;14(5):573-82.
102. Ou X, Xu S, and Lam KP. Deficiency in TNFRSF13B (TACI) expands T-follicular helper and germinal center B cells via increased ICOS-ligand expression but impairs plasma cell survival. *Proc Natl Acad Sci U S A*. 2012;109(38):15401-6.
103. He B, Santamaria R, Xu W, Cols M, Chen K, Puga I, et al. The transmembrane activator TACI triggers immunoglobulin class switching by activating B cells through the adaptor MyD88. *Nat Immunol*. 2010;11(9):836-45.
104. Cattoretti G, Büttner M, Shaknovich R, Kremmer E, Alobeid B, and Niedobitek G. Nuclear and cytoplasmic AID in extrafollicular and germinal center B cells. *Blood*. 2006;107(10):3967-75.
105. Schröder AE, Greiner A, Seyfert C, and Berek C. Differentiation of B cells in the nonlymphoid tissue of the synovial membrane of patients with rheumatoid arthritis. *Proc Natl Acad Sci U S A*. 1996;93(1):221-5.
106. Woodruff MC, Ramonell RP, Nguyen DC, Cashman KS, Saini AS, Haddad NS, et al. Extrafollicular B cell responses correlate with neutralizing antibodies and morbidity in COVID-19. *Nature Immunology*. 2020;21(12):1506-16.
107. Gao X, Shen Q, Roco JA, Dalton B, Frith K, Munier CML, et al. Zeb2 drives the formation of CD11c<sup>+</sup> atypical B cells to sustain germinal centers that control persistent infection. *Science Immunology*. 2024;9(93):eadj4748.
108. Haas KM. Noncanonical B Cells: Characteristics of Uncharacteristic B Cells. *The Journal of Immunology*. 2023;211(9):1257-65.
109. Cancro MP. Age-Associated B Cells. *Annual Review of Immunology*. 2020;38(Volume 38, 2020):315-40.
110. Ehrhardt GtRA, Hsu JT, Gartland L, Leu C-M, Zhang S, Davis RS, et al. Expression of the immunoregulatory molecule FcRH4 defines a distinctive tissue-based population of memory B cells. *Journal of Experimental Medicine*. 2005;202(6):783-91.
111. Ehrhardt GtRA, Hijikata A, Kitamura H, Ohara O, Wang J-Y, and Cooper MD. Discriminating gene expression profiles of memory B cell subpopulations. *Journal of Experimental Medicine*. 2008;205(8):1807-17.
112. Weiss GE, Crompton PD, Li S, Walsh LA, Moir S, Traore B, et al. Atypical memory B cells are greatly expanded in individuals living in a malaria-endemic area. *The Journal of Immunology*. 2009;183(3):2176-82.
113. Portugal S, Tipton CM, Sohn H, Kone Y, Wang J, Li S, et al. Malaria-associated atypical memory B cells exhibit markedly reduced B cell receptor signaling and effector function. *Elife*. 2015;4.
114. Moir S, Ho J, Malaspina A, Wang W, DiPoto AC, O'Shea MA, et al. Evidence for HIV-associated B cell exhaustion in a dysfunctional memory B cell compartment in HIV-infected viremic individuals. *Journal of Experimental Medicine*. 2008;205(8):1797-805.

115. Knox JJ, Buggert M, Kardava L, Seaton KE, Eller MA, Canaday DH, et al. T-bet+ B cells are induced by human viral infections and dominate the HIV gp140 response. *JCI insight*. 2017;2(8).
116. Lau D, Lan LY-L, Andrews SF, Henry C, Rojas KT, Neu KE, et al. Low CD21 expression defines a population of recent germinal center graduates primed for plasma cell differentiation. *Science Immunology*. 2017;2(7):eaai8153.
117. Andrews SF, Chambers MJ, Schramm CA, Plyler J, Raab JE, Kanekiyo M, et al. Activation Dynamics and Immunoglobulin Evolution of Pre-existing and Newly Generated Human Memory B cell Responses to Influenza Hemagglutinin. *Immunity*. 2019;51(2):398-410.e5.
118. Horns F, Dekker CL, and Quake SR. Memory B Cell Activation, Broad Anti-influenza Antibodies, and Bystander Activation Revealed by Single-Cell Transcriptomics. *Cell Reports*. 2020;30(3):905-13.e6.
119. Holla P, Dizon B, Ambegaonkar AA, Rogel N, Goldschmidt E, Boddapati AK, et al. Shared transcriptional profiles of atypical B cells suggest common drivers of expansion and function in malaria, HIV, and autoimmunity. *Sci Adv*. 2021;7(22).
120. Arazi A, Rao DA, Berthier CC, Davidson A, Liu Y, Hoover PJ, et al. The immune cell landscape in kidneys of patients with lupus nephritis. *Nat Immunol*. 2019;20(7):902-14.
121. Zhao J, Zhang S, Liu Y, He X, Qu M, Xu G, et al. Single-cell RNA sequencing reveals the heterogeneity of liver-resident immune cells in human. *Cell Discov*. 2020;6:22.
122. Ramesh A, Schubert RD, Greenfield AL, Dandekar R, Loudermilk R, Sabatino JJ, et al. A pathogenic and clonally expanded B cell transcriptome in active multiple sclerosis. *Proceedings of the National Academy of Sciences*. 2020;117(37):22932-43.
123. Zhang F, Wei K, Slowikowski K, Fonseka CY, Rao DA, Kelly S, et al. Defining inflammatory cell states in rheumatoid arthritis joint synovial tissues by integrating single-cell transcriptomics and mass cytometry. *Nat Immunol*. 2019;20(7):928-42.
124. Rubtsova K, Rubtsov AV, van Dyk LF, Kappler JW, and Marrack P. T-box transcription factor T-bet, a key player in a unique type of B-cell activation essential for effective viral clearance. *Proceedings of the National Academy of Sciences*. 2013;110(34):E3216-E24.
125. Pérez-Mazliah D, Gardner PJ, Schweighoffer E, McLaughlin S, Hosking C, Tumwine I, et al. Plasmodium-specific atypical memory B cells are short-lived activated B cells. *Elife*. 2018;7.
126. Dai D, Gu S, Han X, Ding H, Jiang Y, Zhang X, et al. The transcription factor ZEB2 drives the formation of age-associated B cells. *Science*. 2024;383(6681):413-21.
127. Yang R, Avery DT, Jackson KJ, Ogishi M, Benhsaien I, Du L, et al. Human T-bet governs the generation of a distinct subset of CD11chighCD21low B cells. *Science immunology*. 2022;7(73):eabq3277.
128. Sutton HJ, Aye R, Idris AH, Vistein R, Nduati E, Kai O, et al. Atypical B cells are part of an alternative lineage of B cells that participates in responses to vaccination and infection in humans. *Cell Rep*. 2021;34(6):108684.

129. Obeng-Adjei N, Portugal S, Holla P, Li S, Sohn H, Ambegaonkar A, et al. Malaria-induced interferon-γ drives the expansion of Tbethi atypical memory B cells. *PLOS Pathogens*. 2017;13(9):e1006576.
130. Naradikian MS, Myles A, Beiting DP, Roberts KJ, Dawson L, Herati RS, et al. Cutting Edge: IL-4, IL-21, and IFN-γ Interact To Govern T-bet and CD11c Expression in TLR-Activated B Cells. *The Journal of Immunology*. 2016;197(4):1023-8.
131. Keller B, Strohmeier V, Harder I, Unger S, Payne KJ, Andrieux G, et al. The expansion of human T-bet<sup>high</sup>CD21<sup>low</sup> B cells is T cell dependent. *Science Immunology*. 2021;6(64):eabh0891.
132. Moir S, Malaspina A, Ho J, Wang W, DiPoto AC, O'Shea MA, et al. Normalization of B Cell Counts and Subpopulations after Antiretroviral Therapy in Chronic HIV Disease. *The Journal of Infectious Diseases*. 2008;197(4):572-9.
133. Sundling C, Rönnberg C, Yman V, Asghar M, Jahnmatz P, Lakshmikanth T, et al. B cell profiling in malaria reveals expansion and remodeling of CD11c+ B cell subsets. *JCI Insight*. 2019;4(9).
134. Rubtsov AV, Rubtsova K, Fischer A, Meehan RT, Gillis JZ, Kappler JW, et al. Toll-like receptor 7 (TLR7)-driven accumulation of a novel CD11c$^{+}$ B-cell population is important for the development of autoimmunity. *Blood*. 2011;118(5):1305-15.
135. Jenks SA, Cashman KS, Zumaquero E, Marigorta UM, Patel AV, Wang X, et al. Distinct Effector B Cells Induced by Unregulated Toll-like Receptor 7 Contribute to Pathogenic Responses in Systemic Lupus Erythematosus. *Immunity*. 2018;49(4):725-39.e6.
136. Austin JW, Buckner CM, Kardava L, Wang W, Zhang X, Melson VA, et al. Overexpression of T-bet in HIV infection is associated with accumulation of B cells outside germinal centers and poor affinity maturation. *Science translational medicine*. 2019;11(520):eaax0904.
137. Zhang W, Zhang H, Liu S, Xia F, Kang Z, Zhang Y, et al. Excessive CD11c(+)Tbet(+) B cells promote aberrant T(FH) differentiation and affinity-based germinal center selection in lupus. *Proc Natl Acad Sci U S A*. 2019;116(37):18550-60.
138. Song H, and Cerny J. Functional Heterogeneity of Marginal Zone B Cells Revealed by Their Ability to Generate Both Early Antibody-forming Cells and Germinal Centers with Hypermutation and Memory in Response to a T-dependent Antigen. *Journal of Experimental Medicine*. 2003;198(12):1923-35.
139. Bagnara D, Squillario M, Kipling D, Mora T, Walczak AM, Da Silva L, et al. A Reassessment of IgM Memory Subsets in Humans. *The Journal of Immunology*. 2015;195(8):3716-24.
140. Siu JHY, Pitcher MJ, Tull TJ, Velounias RL, Guesdon W, Montorsi L, et al. Two subsets of human marginal zone B cells resolved by global analysis of lymphoid tissues and blood. *Science Immunology*. 2022;7(69):eabm9060.
141. Sakaguchi S, Mikami N, Wing JB, Tanaka A, Ichiyama K, and Ohkura N. Regulatory T Cells and Human Disease. *Annu Rev Immunol*. 2020;38:541-66.
142. Klein L, Robey EA, and Hsieh C-S. Central CD4+ T cell tolerance: deletion versus regulatory T cell differentiation. *Nature Reviews Immunology*. 2019;19(1):7-18.

143. Tai X, Indart A, Rojano M, Guo J, Apenes N, Kadakia T, et al. How autoreactive thymocytes differentiate into regulatory versus effector CD4+ T cells after avoiding clonal deletion. *Nature Immunology*. 2023;24(4):637-51.
144. Bennett CL, Christie J, Ramsdell F, Brunkow ME, Ferguson PJ, Whitesell L, et al. The immune dysregulation, polyendocrinopathy, enteropathy, X-linked syndrome (IPEX) is caused by mutations of FOXP3. *Nat Genet*. 2001;27(1):20-1.
145. Wildin RS, Ramsdell F, Peake J, Faravelli F, Casanova J-L, Buist N, et al. X-linked neonatal diabetes mellitus, enteropathy and endocrinopathy syndrome is the human equivalent of mouse scurfy. *Nature Genetics*. 2001;27(1):18-20.
146. Kinnunen T, Chamberlain N, Morbach H, Choi J, Kim S, Craft J, et al. Accumulation of peripheral autoreactive B cells in the absence of functional human regulatory T cells. *Blood*. 2013;121(9):1595-603.
147. Lim HW, Hillsamer P, Banham AH, and Kim CH. Cutting Edge: Direct Suppression of B Cells by CD4+CD25+ Regulatory T Cells1. *The Journal of Immunology*. 2005;175(7):4180-3.
148. Lim HW, Hillsamer P, and Kim CH. Regulatory T cells can migrate to follicles upon T cell activation and suppress GC-Th cells and GC-Th cell-driven B cell responses. *J Clin Invest*. 2004;114(11):1640-9.
149. Chung Y, Tanaka S, Chu F, Nurieva RI, Martinez GJ, Rawal S, et al. Follicular regulatory T cells expressing Foxp3 and Bcl-6 suppress germinal center reactions. *Nat Med*. 2011;17(8):983-8.
150. Linterman MA, Pierson W, Lee SK, Kallies A, Kawamoto S, Rayner TF, et al. Foxp3+ follicular regulatory T cells control the germinal center response. *Nat Med*. 2011;17(8):975-82.
151. Wollenberg I, Agua-Doce A, Hernández A, Almeida C, Oliveira VG, Faro J, et al. Regulation of the germinal center reaction by Foxp3+ follicular regulatory T cells. *J Immunol*. 2011;187(9):4553-60.
152. Fu W, Liu X, Lin X, Feng H, Sun L, Li S, et al. Deficiency in T follicular regulatory cells promotes autoimmunity. *J Exp Med*. 2018;215(3):815-25.
153. Gonzalez-Figueroa P, Roco JA, Papa I, Núñez Villacís L, Stanley M, Linterman MA, et al. Follicular regulatory T cells produce neuritin to regulate B cells. *Cell*. 2021;184(7):1775-89.e19.
154. Koch MA, Tucker-Heard Gs, Perdue NR, Killebrew JR, Urdahl KB, and Campbell DJ. The transcription factor T-bet controls regulatory T cell homeostasis and function during type 1 inflammation. *Nature Immunology*. 2009;10(6):595-602.
155. Nosko A, Kluger MA, Diefenhardt P, Melderis S, Wegscheid C, Tiegs G, et al. T-Bet Enhances Regulatory T Cell Fitness and Directs Control of Th1 Responses in Crescentic GN. *Journal of the American Society of Nephrology*. 2017;28(1):185-96.
156. Sefik E, Geva-Zatorsky N, Oh S, Konnikova L, Zemmour D, McGuire AM, et al. MUCOSAL IMMUNOLOGY. Individual intestinal symbionts induce a distinct population of RORγ$^{+}$ regulatory T cells. *Science*. 2015;349(6251):993-7.
157. Yang BH, Hagemann S, Mamareli P, Lauer U, Hoffmann U, Beckstette M, et al. Foxp3<sup>+</sup> T cells expressing RORγt represent a stable regulatory T-

cell effector lineage with enhanced suppressive capacity during intestinal inflammation. *Mucosal Immunology*. 2016;9(2):444-57.
158. Le Coz C, Oldridge DA, Herati RS, De Luna N, Garifallou J, Cruz Cabrera E, et al. Human T follicular helper clones seed the germinal center-resident regulatory pool. *Sci Immunol*. 2023;8(82):eade8162.
159. Kumar S, Fonseca VR, Ribeiro F, Basto AP, Água-Doce A, Monteiro M, et al. Developmental bifurcation of human T follicular regulatory cells. *Science Immunology*. 2021;6(59):eabd8411.
160. Liston A, Humblet-Baron S, Duffy D, and Goris A. Human immune diversity: from evolution to modernity. *Nature Immunology*. 2021;22(12):1479-89.
161. Edwards SV, and Hedrick PW. Evolution and ecology of MHC molecules: from genomics to sexual selection. *Trends in Ecology & Evolution*. 1998;13(8):305-11.
162. Conrad N, Misra S, Verbakel JY, Verbeke G, Molenberghs G, Taylor PN, et al. Incidence, prevalence, and co-occurrence of autoimmune disorders over time and by age, sex, and socioeconomic status: a population-based cohort study of 22 million individuals in the UK. *The Lancet*. 2023;401(10391):1878-90.
163. Pisetsky DS. Pathogenesis of autoimmune disease. *Nature Reviews Nephrology*. 2023;19(8):509-24.
164. Goris A, and Liston A. The immunogenetic architecture of autoimmune disease. *Cold Spring Harb Perspect Biol*. 2012;4(3).
165. Criswell LA, Pfeiffer KA, Lum RF, Gonzales B, Novitzke J, Kern M, et al. Analysis of Families in the Multiple Autoimmune Disease Genetics Consortium (MADGC) Collection: the PTPN22 620W Allele Associates with Multiple Autoimmune Phenotypes. *The American Journal of Human Genetics*. 2005;76(4):561-71.
166. Dendrou CA, Petersen J, Rossjohn J, and Fugger L. HLA variation and disease. *Nature Reviews Immunology*. 2018;18(5):325-39.
167. Raj P, Rai E, Song R, Khan S, Wakeland BE, Viswanathan K, et al. Regulatory polymorphisms modulate the expression of HLA class II molecules and promote autoimmunity. *eLife*. 2016;5:e12089.
168. Ooi JD, Petersen J, Tan YH, Huynh M, Willett ZJ, Ramarathinam SH, et al. Dominant protection from HLA-linked autoimmunity by antigen-specific regulatory T cells. *Nature*. 2017;545(7653):243-7.
169. Scally SW, Petersen J, Law SC, Dudek NL, Nel HJ, Loh KL, et al. A molecular basis for the association of the HLA-DRB1 locus, citrullination, and rheumatoid arthritis. *Journal of Experimental Medicine*. 2013;210(12):2569-82.
170. Hudson BG, Tryggvason K, Sundaramoorthy M, and Neilson EG. Alport's Syndrome, Goodpasture's Syndrome, and Type IV Collagen. *New England Journal of Medicine*. 2003;348(25):2543-56.
171. Robson KJ, Ooi JD, Holdsworth SR, Rossjohn J, and Kitching AR. HLA and kidney disease: from associations to mechanisms. *Nature Reviews Nephrology*. 2018;14(10):636-55.

172. Raychaudhuri S, Sandor C, Stahl EA, Freudenberg J, Lee H-S, Jia X, et al. Five amino acids in three HLA proteins explain most of the association between MHC and seropositive rheumatoid arthritis. *Nature Genetics*. 2012;44(3):291-6.
173. Smolen JS, Aletaha D, Barton A, Burmester GR, Emery P, Firestein GS, et al. Rheumatoid arthritis. *Nature Reviews Disease Primers*. 2018;4(1):18001.
174. Huizinga TWJ, Amos CI, van der Helm-van Mil AHM, Chen W, van Gaalen FA, Jawaheer D, et al. Refining the complex rheumatoid arthritis phenotype based on specificity of the HLA–DRB1 shared epitope for antibodies to citrullinated proteins. *Arthritis & Rheumatism*. 2005;52(11):3433-8.
175. Stanford SM, and Bottini N. PTPN22: the archetypal non-HLA autoimmunity gene. *Nature Reviews Rheumatology*. 2014;10(10):602-11.
176. Arechiga AF, Habib T, He Y, Zhang X, Zhang ZY, Funk A, et al. Cutting edge: the PTPN22 allelic variant associated with autoimmunity impairs B cell signaling. *J Immunol*. 2009;182(6):3343-7.
177. Menard L, Saadoun D, Isnardi I, Ng YS, Meyers G, Massad C, et al. The PTPN22 allele encoding an R620W variant interferes with the removal of developing autoreactive B cells in humans. *J Clin Invest*. 2011;121(9):3635-44.
178. Sinha A, and Bagga A. Rituximab therapy in nephrotic syndrome: implications for patients' management. *Nature Reviews Nephrology*. 2013;9(3):154-69.
179. d'Hennezel E, Bin Dhuban K, Torgerson T, and Piccirillo CA. The immunogenetics of immune dysregulation, polyendocrinopathy, enteropathy, X linked (IPEX) syndrome. *J Med Genet*. 2012;49(5):291-302.
180. Tsuda M, Torgerson TR, Selmi C, Gambineri E, Carneiro-Sampaio M, Mannurita SC, et al. The spectrum of autoantibodies in IPEX syndrome is broad and includes anti-mitochondrial autoantibodies. *J Autoimmun*. 2010;35(3):265-8.
181. Caielli S, Wan Z, and Pascual V. Systemic Lupus Erythematosus Pathogenesis: Interferon and Beyond. *Annual Review of Immunology*. 2023;41(Volume 41, 2023):533-60.
182. Vinuesa CG, Shen N, and Ware T. Genetics of SLE: mechanistic insights from monogenic disease and disease-associated variants. *Nature Reviews Nephrology*. 2023;19(9):558-72.
183. Taylor KE, Chung SA, Graham RR, Ortmann WA, Lee AT, Langefeld CD, et al. Risk Alleles for Systemic Lupus Erythematosus in a Large Case-Control Collection and Associations with Clinical Subphenotypes. *PLOS Genetics*. 2011;7(2):e1001311.
184. Brown GJ, Cañete PF, Wang H, Medhavy A, Bones J, Roco JA, et al. TLR7 gain-of-function genetic variation causes human lupus. *Nature*. 2022;605(7909):349-56.
185. Barrie W, Irving-Pease EK, Willerslev E, Iversen AKN, and Fugger L. Ancient DNA reveals evolutionary origins of autoimmune diseases. *Nature Reviews Immunology*. 2024;24(2):85-6.
186. Rosenblum MD, Remedios KA, and Abbas AK. Mechanisms of human autoimmunity. *J Clin Invest*. 2015;125(6):2228-33.
187. Touil H, Mounts K, and De Jager PL. Differential impact of environmental factors on systemic and localized autoimmunity. *Front Immunol*. 2023;14:1147447.

188. Mills KHG. TLR-dependent T cell activation in autoimmunity. *Nature Reviews Immunology*. 2011;11(12):807-22.
189. Soldan SS, and Lieberman PM. Epstein–Barr virus and multiple sclerosis. *Nature Reviews Microbiology*. 2023;21(1):51-64.
190. Filippi M, Bar-Or A, Piehl F, Preziosa P, Solari A, Vukusic S, et al. Multiple sclerosis. *Nature Reviews Disease Primers*. 2018;4(1):43.
191. Lünemann JD, Jelčić I, Roberts S, Lutterotti A, Tackenberg Br, Martin R, et al. EBNA1-specific T cells from patients with multiple sclerosis cross react with myelin antigens and co-produce IFN-γ and IL-2. *Journal of Experimental Medicine*. 2008;205(8):1763-73.
192. Lanz TV, Brewer RC, Ho PP, Moon J-S, Jude KM, Fernandez D, et al. Clonally expanded B cells in multiple sclerosis bind EBV EBNA1 and GlialCAM. *Nature*. 2022;603(7900):321-7.
193. Cornaby C, Gibbons L, Mayhew V, Sloan CS, Welling A, and Poole BD. B cell epitope spreading: Mechanisms and contribution to autoimmune diseases. *Immunology Letters*. 2015;163(1):56-68.
194. Arbuckle MR, McClain MT, Rubertone MV, Scofield RH, Dennis GJ, James JA, et al. Development of autoantibodies before the clinical onset of systemic lupus erythematosus. *N Engl J Med*. 2003;349(16):1526-33.
195. Deshmukh US, Bagavant H, Sim D, Pidiyar V, and Fu SM. A SmD Peptide Induces Better Antibody Responses to Other Proteins within the Small Nuclear Ribonucleoprotein Complex than to SmD Protein via Intermolecular Epitope Spreading1. *The Journal of Immunology*. 2007;178(4):2565-71.
196. Degn SE, van der Poel CE, Firl DJ, Ayoglu B, Al Qureshah FA, Bajic G, et al. Clonal Evolution of Autoreactive Germinal Centers. *Cell*. 2017;170(5):913-26.e19.
197. Fahlquist-Hagert C, Wittenborn TR, Terczyńska-Dyla E, Kastberg KS, Yang E, Rallistan AN, et al. Antigen presentation by B cells enables epitope spreading across an MHC barrier. *Nature Communications*. 2023;14(1):6941.
198. Elliott SE, Kongpachith S, Lingampalli N, Adamska JZ, Cannon BJ, Mao R, et al. Affinity Maturation Drives Epitope Spreading and Generation of Proinflammatory Anti-Citrullinated Protein Antibodies in Rheumatoid Arthritis. *Arthritis Rheumatol*. 2018;70(12):1946-58.
199. Mikami N, and Sakaguchi S. Regulatory T cells in autoimmune kidney diseases and transplantation. *Nature Reviews Nephrology*. 2023;19(9):544-57.
200. d'Hennezel E, Yurchenko E, Sgouroudis E, Hay V, and Piccirillo CA. Single-cell analysis of the human T regulatory population uncovers functional heterogeneity and instability within FOXP3+ cells. *J Immunol*. 2011;186(12):6788-97.
201. Bin Dhuban K, d'Hennezel E, Nashi E, Bar-Or A, Rieder S, Shevach EM, et al. Coexpression of TIGIT and FCRL3 identifies Helios+ human memory regulatory T cells. *Journal of immunology (Baltimore, Md : 1950)*. 2015;194(8):3687-96.
202. Kim HJ, Barnitz RA, Kreslavsky T, Brown FD, Moffett H, Lemieux ME, et al. Stable inhibitory activity of regulatory T cells requires the transcription factor Helios. *Science*. 2015;350(6258):334-9.

203. Long SA, and Buckner JH. CD4+FOXP3+ T Regulatory Cells in Human Autoimmunity: More Than a Numbers Game. *The Journal of Immunology*. 2011;187(5):2061-6.
204. Attias M, Al-Aubodah T, and Piccirillo CA. Mechanisms of human FoxP3(+) T(reg) cell development and function in health and disease. *Clin Exp Immunol*. 2019;197(1):36-51.
205. Garg G, Tyler JR, Yang JH, Cutler AJ, Downes K, Pekalski M, et al. Type 1 diabetes-associated IL2RA variation lowers IL-2 signaling and contributes to diminished CD4+CD25+ regulatory T cell function. *J Immunol*. 2012;188(9):4644-53.
206. Yang JH, Cutler AJ, Ferreira RC, Reading JL, Cooper NJ, Wallace C, et al. Natural Variation in Interleukin-2 Sensitivity Influences Regulatory T-Cell Frequency and Function in Individuals With Long-standing Type 1 Diabetes. *Diabetes*. 2015;64(11):3891-902.
207. Samson M, Audia S, Janikashvili N, Ciudad M, Trad M, Fraszczak J, et al. Brief report: inhibition of interleukin-6 function corrects Th17/Treg cell imbalance in patients with rheumatoid arthritis. *Arthritis Rheum*. 2012;64(8):2499-503.
208. Pesce B, Soto L, Sabugo F, Wurmann P, Cuchacovich M, López MN, et al. Effect of interleukin-6 receptor blockade on the balance between regulatory T cells and T helper type 17 cells in rheumatoid arthritis patients. *Clin Exp Immunol*. 2013;171(3):237-42.
209. Bin Dhuban K, Bartolucci S, d'Hennezel E, and Piccirillo CA. Signaling Through gp130 Compromises Suppressive Function in Human FOXP3(+) Regulatory T Cells. *Front Immunol*. 2019;10:1532.
210. Valencia X, Stephens G, Goldbach-Mansky R, Wilson M, Shevach EM, and Lipsky PE. TNF downmodulates the function of human CD4+CD25hi T-regulatory cells. *Blood*. 2006;108(1):253-61.
211. Schiering C, Krausgruber T, Chomka A, Fröhlich A, Adelmann K, Wohlfert EA, et al. The alarmin IL-33 promotes regulatory T-cell function in the intestine. *Nature*. 2014;513(7519):564-8.
212. Alvarez F, Istomine R, Shourian M, Pavey N, Al-Aubodah TA-F, Qureshi S, et al. The alarmins IL-1 and IL-33 differentially regulate the functional specialisation of Foxp3+ regulatory T cells during mucosal inflammation. *Mucosal Immunology*. 2019;12(3):746-60.
213. Hemmers S, Schizas M, and Rudensky AY. T reg cell-intrinsic requirements for ST2 signaling in health and neuroinflammation. *J Exp Med*. 2021;218(2).
214. SHARMA R, and SABAPATHY V. “Alarming" T-Regulatory Cells (Tregs) to Protect from Type 1 Diabetes (T1D). *Diabetes*. 2018;67(Supplement_1).
215. Schenten D, Nish Simone A, Yu S, Yan X, Lee Heung K, Brodsky I, et al. Signaling through the Adaptor Molecule MyD88 in CD4<sup>+</sup> T Cells Is Required to Overcome Suppression by Regulatory T Cells. *Immunity*. 2014;40(1):78-90.
216. Harris F, Berdugo YA, and Tree T. IL-2-based approaches to Treg enhancement. *Clinical and Experimental Immunology*. 2022;211(2):149-63.
217. Stremska ME, Dai C, Venkatadri R, Wang H, Sabapathy V, Kumar G, et al. IL233, an IL-2-IL-33 hybrid cytokine induces prolonged remission of mouse lupus nephritis by targeting Treg cells as a single therapeutic agent. *J Autoimmun*. 2019;102:133-41.

218. Lee DSW, Rojas OL, and Gommerman JL. B cell depletion therapies in autoimmune disease: advances and mechanistic insights. *Nature Reviews Drug Discovery*. 2021;20(3):179-99.
219. Smith-Jensen T, Burgoon MP, Anthony J, Kraus H, Gilden DH, and Owens GP. Comparison of immunoglobulin G heavy-chain sequences in MS and SSPE brains reveals an antigen-driven response. *Neurology*. 2000;54(6):1227-32.
220. van Es JH, Gmelig Meyling FH, van de Akker WR, Aanstoot H, Derksen RH, and Logtenberg T. Somatic mutations in the variable regions of a human IgG anti-double-stranded DNA autoantibody suggest a role for antigen in the induction of systemic lupus erythematosus. *J Exp Med*. 1991;173(2):461-70.
221. Volkov M, Coppola M, Huizinga R, Eftimov F, Huizinga TWJ, van der Kooi AJ, et al. Comprehensive overview of autoantibody isotype and subclass distribution. *Journal of Allergy and Clinical Immunology*. 2022;150(5):999-1010.
222. Gilhus NE, Tzartos S, Evoli A, Palace J, Burns TM, and Verschuuren JJGM. Myasthenia gravis. *Nature Reviews Disease Primers*. 2019;5(1):30.
223. Conti-Fine BM, Milani M, and Kaminski HJ. Myasthenia gravis: past, present, and future. *J Clin Invest*. 2006;116(11):2843-54.
224. Brito-Zerón P, Baldini C, Bootsma H, Bowman SJ, Jonsson R, Mariette X, et al. Sjögren syndrome. *Nature Reviews Disease Primers*. 2016;2(1):16047.
225. Chaturvedi S, Braunstein EM, Yuan X, Yu J, Alexander A, Chen H, et al. Complement activity and complement regulatory gene mutations are associated with thrombosis in APS and CAPS. *Blood*. 2020;135(4):239-51.
226. Meroni PL, Borghi MO, Raschi E, and Tedesco F. Pathogenesis of antiphospholipid syndrome: understanding the antibodies. *Nature Reviews Rheumatology*. 2011;7(6):330-9.
227. Spadaro M, Winklmeier S, Beltrán E, Macrini C, Höftberger R, Schuh E, et al. Pathogenicity of human antibodies against myelin oligodendrocyte glycoprotein. *Ann Neurol*. 2018;84(2):315-28.
228. Ramesh S, Morrell CN, Tarango C, Thomas GD, Yuhanna IS, Girardi G, et al. Antiphospholipid antibodies promote leukocyte–endothelial cell adhesion and thrombosis in mice by antagonizing eNOS via β2GPI and apoER2. *The Journal of Clinical Investigation*. 2011;121(1):120-31.
229. Yalavarthi S, Gould TJ, Rao AN, Mazza LF, Morris AE, Núñez-Álvarez C, et al. Release of neutrophil extracellular traps by neutrophils stimulated with antiphospholipid antibodies: a newly identified mechanism of thrombosis in the antiphospholipid syndrome. *Arthritis Rheumatol*. 2015;67(11):2990-3003.
230. Kitching AR, Anders H-J, Basu N, Brouwer E, Gordon J, Jayne DR, et al. ANCA-associated vasculitis. *Nature Reviews Disease Primers*. 2020;6(1):71.
231. Audia S, Mahévas M, Samson M, Godeau B, and Bonnotte B. Pathogenesis of immune thrombocytopenia. *Autoimmunity Reviews*. 2017;16(6):620-32.
232. Pollmann R, Schmidt T, Eming R, and Hertl M. Pemphigus: a Comprehensive Review on Pathogenesis, Clinical Presentation and Novel Therapeutic Approaches. *Clinical Reviews in Allergy & Immunology*. 2018;54(1):1-25.

233. Hoover PJ, and Costenbader KH. Insights into the epidemiology and management of lupus nephritis from the US rheumatologist's perspective. *Kidney Int.* 2016;90(3):487-92.
234. Meta-analysis: Diagnostic Accuracy of Anti–Cyclic Citrullinated Peptide Antibody and Rheumatoid Factor for Rheumatoid Arthritis. *Annals of Internal Medicine.* 2007;146(11):797-808.
235. Harre U, Georgess D, Bang H, Bozec A, Axmann R, Ossipova E, et al. Induction of osteoclastogenesis and bone loss by human autoantibodies against citrullinated vimentin. *The Journal of Clinical Investigation.* 2012;122(5):1791-802.
236. Steffen U, Schett G, and Bozec A. How Autoantibodies Regulate Osteoclast Induced Bone Loss in Rheumatoid Arthritis. *Front Immunol.* 2019;10:1483.
237. Bizzaro N, Bartoloni E, Morozzi G, Manganelli S, Riccieri V, Sabatini P, et al. Anti-cyclic citrullinated peptide antibody titer predicts time to rheumatoid arthritis onset in patients with undifferentiated arthritis: results from a 2-year prospective study. *Arthritis Research & Therapy.* 2013;15(1):R16.
238. Jónsson T, Thorsteinsson J, Kolbeinsson A, Jónasdóttir E, Sigfússon N, and Valdimarsson H. Population study of the importance of rheumatoid factor isotypes in adults. *Annals of the Rheumatic Diseases.* 1992;51(7):863.
239. O'Connor KC, Chitnis T, Griffin DE, Piyasirisilp S, Bar-Or A, Khoury S, et al. Myelin basic protein-reactive autoantibodies in the serum and cerebrospinal fluid of multiple sclerosis patients are characterized by low-affinity interactions. *Journal of Neuroimmunology.* 2003;136(1):140-8.
240. Brennan KM, Galban-Horcajo F, Rinaldi S, O'Leary CP, Goodyear CS, Kalna G, et al. Lipid arrays identify myelin-derived lipids and lipid complexes as prominent targets for oligoclonal band antibodies in multiple sclerosis. *Journal of Neuroimmunology.* 2011;238(1):87-95.
241. Höftberger R, Lassmann H, Berger T, and Reindl M. Pathogenic autoantibodies in multiple sclerosis — from a simple idea to a complex concept. *Nature Reviews Neurology.* 2022;18(11):681-8.
242. Brändle SM, Obermeier B, Senel M, Bruder J, Mentele R, Khademi M, et al. Distinct oligoclonal band antibodies in multiple sclerosis recognize ubiquitous self-proteins. *Proc Natl Acad Sci U S A.* 2016;113(28):7864-9.
243. Reich DS, Lucchinetti CF, and Calabresi PA. Multiple Sclerosis. *N Engl J Med.* 2018;378(2):169-80.
244. Raine CS. The Dale E. McFarlin Memorial Lecture: the immunology of the multiple sclerosis lesion. *Ann Neurol.* 1994;36 Suppl:S61-72.
245. Hauser SL, Waubant E, Arnold DL, Vollmer T, Antel J, Fox RJ, et al. B-cell depletion with rituximab in relapsing-remitting multiple sclerosis. *N Engl J Med.* 2008;358(7):676-88.
246. Kappos L, Li D, Calabresi PA, O'Connor P, Bar-Or A, Barkhof F, et al. Ocrelizumab in relapsing-remitting multiple sclerosis: a phase 2, randomised, placebo-controlled, multicentre trial. *Lancet.* 2011;378(9805):1779-87.

247. Cao Y, Goods BA, Raddassi K, Nepom GT, Kwok WW, Love JC, et al. Functional inflammatory profiles distinguish myelin-reactive T cells from patients with multiple sclerosis. *Sci Transl Med*. 2015;7(287):287ra74.
248. Jelcic I, Al Nimer F, Wang J, Lentsch V, Planas R, Jelcic I, et al. Memory B Cells Activate Brain-Homing, Autoreactive CD4(+) T Cells in Multiple Sclerosis. *Cell*. 2018;175(1):85-100.e23.
249. Wang J, Jelcic I, Mühlenbruch L, Haunerdinger V, Toussaint NC, Zhao Y, et al. HLA-DR15 Molecules Jointly Shape an Autoreactive T Cell Repertoire in Multiple Sclerosis. *Cell*. 2020;183(5):1264-81.e20.
250. Wang S, Wang J, Kumar V, Karnell JL, Naiman B, Gross PS, et al. IL-21 drives expansion and plasma cell differentiation of autoreactive CD11c(hi)T-bet(+) B cells in SLE. *Nat Commun*. 2018;9(1):1758.
251. Claes N, Fraussen J, Vanheusden M, Hellings N, Stinissen P, Van Wijmeersch B, et al. Age-Associated B Cells with Proinflammatory Characteristics Are Expanded in a Proportion of Multiple Sclerosis Patients. *J Immunol*. 2016;197(12):4576-83.
252. Saadoun D, Terrier B, Bannock J, Vazquez T, Massad C, Kang I, et al. Expansion of Autoreactive Unresponsive CD21−/low B Cells in Sjögren's Syndrome–Associated Lymphoproliferation. *Arthritis & Rheumatism*. 2013;65(4):1085-96.
253. Ambegaonkar AA, Holla P, Dizon BLP, Sohn H, and Pierce SK. Atypical B cells in chronic infectious diseases and systemic autoimmunity: puzzles with many missing pieces. *Current Opinion in Immunology*. 2022;77:102227.
254. Kim HJ, Krenn V, Steinhauser G, and Berek C. Plasma cell development in synovial germinal centers in patients with rheumatoid and reactive arthritis. *J Immunol*. 1999;162(5):3053-62.
255. Scheel T, Gursche A, Zacher J, Häupl T, and Berek C. V-region gene analysis of locally defined synovial B and plasma cells reveals selected B cell expansion and accumulation of plasma cell clones in rheumatoid arthritis. *Arthritis & Rheumatism*. 2011;63(1):63-72.
256. Schröder AE, Greiner A, Seyfert C, and Berek C. Differentiation of B cells in the nonlymphoid tissue of the synovial membrane of patients with rheumatoid arthritis. *Proceedings of the National Academy of Sciences*. 1996;93(1):221-5.
257. Stott DI, Hiepe F, Hummel M, Steinhauser G, and Berek C. Antigen-driven clonal proliferation of B cells within the target tissue of an autoimmune disease. The salivary glands of patients with Sjögren's syndrome. *The Journal of Clinical Investigation*. 1998;102(5):938-46.
258. William J, Euler C, Christensen S, and Shlomchik MJ. Evolution of Autoantibody Responses via Somatic Hypermutation Outside of Germinal Centers. *Science*. 2002;297(5589):2066-70.
259. Tipton CM, Fucile CF, Darce J, Chida A, Ichikawa T, Gregoretti I, et al. Diversity, cellular origin and autoreactivity of antibody-secreting cell population expansions in acute systemic lupus erythematosus. *Nature immunology*. 2015;16(7):755-65.
260. Zumaquero E, Stone SL, Scharer CD, Jenks SA, Nellore A, Mousseau B, et al. IFNγ induces epigenetic programming of human T-bethi B cells and promotes TLR7/8 and IL-21 induced differentiation. *Elife*. 2019;8:e41641.

261. Fan H, Ren D, and Hou Y. TLR7, a third signal for the robust generation of spontaneous germinal center B cells in systemic lupus erythematosus. *Cellular & Molecular Immunology*. 2018;15(3):286-8.
262. Ricker E, Manni M, Flores-Castro D, Jenkins D, Gupta S, Rivera-Correa J, et al. Altered function and differentiation of age-associated B cells contribute to the female bias in lupus mice. *Nature Communications*. 2021;12(1):4813.
263. Reyes RA, Batugedara G, Dutta P, Reers AB, Garza R, Ssewanyana I, et al. Atypical B cells consist of subsets with distinct functional profiles. *iScience*. 2023;26(12):108496.
264. Bao W, Xie M, and Ye Y. Age-associated B cells indicate disease activity in rheumatoid arthritis. *Cell Immunol*. 2022;377:104533.
265. Wang Y, Lloyd KA, Melas I, Zhou D, Thyagarajan R, Lindqvist J, et al. Rheumatoid arthritis patients display B-cell dysregulation already in the naïve repertoire consistent with defects in B-cell tolerance. *Scientific Reports*. 2019;9(1):19995.
266. McGrath S, Grimstad K, Thorarinsdottir K, Forslind K, Glinatsi D, Leu Agelii M, et al. Professional antigen-presenting Tbet+CD11c+ B cells correlate with bone destruction in untreated rheumatoid arthritis. *Arthritis & Rheumatology*.n/a(n/a).
267. Kristyanto H, Blomberg NJ, Slot LM, van der Voort EIH, Kerkman PF, Bakker A, et al. Persistently activated, proliferative memory autoreactive B cells promote inflammation in rheumatoid arthritis. *Science Translational Medicine*. 2020;12(570):eaaz5327.
268. Reijm S, Kwekkeboom JC, Blomberg NJ, Suurmond J, van der Woude D, Toes REM, et al. Autoreactive B cells in rheumatoid arthritis include mainly activated CXCR3+ memory B cells and plasmablasts. *JCI Insight*. 2023;8(20).
269. Rao DA, Gurish MF, Marshall JL, Slowikowski K, Fonseka CY, Liu Y, et al. Pathologically expanded peripheral T helper cell subset drives B cells in rheumatoid arthritis. *Nature*. 2017;542(7639):110-4.
270. Bocharnikov AV, Keegan J, Wacleche VS, Cao Y, Fonseka CY, Wang G, et al. PD-1hiCXCR5– T peripheral helper cells promote B cell responses in lupus via MAF and IL-21. *JCI Insight*. 2019;4(20).
271. Cragg MS, and Glennie MJ. Antibody specificity controls in vivo effector mechanisms of anti-CD20 reagents. *Blood*. 2004;103(7):2738-43.
272. Kumar A, Planchais C, Fronzes R, Mouquet H, and Reyes N. Binding mechanisms of therapeutic antibodies to human CD20. *Science*. 2020;369(6505):793-9.
273. Beers SA, French RR, Chan HTC, Lim SH, Jarrett TC, Vidal RM, et al. Antigenic modulation limits the efficacy of anti-CD20 antibodies: implications for antibody selection. *Blood*. 2010;115(25):5191-201.
274. Hauser SL, Waubant E, Arnold DL, Vollmer T, Antel J, Fox RJ, et al. B-Cell Depletion with Rituximab in Relapsing–Remitting Multiple Sclerosis. *New England Journal of Medicine*. 2008;358(7):676-88.
275. Montalban X, Hauser SL, Kappos L, Arnold DL, Bar-Or A, Comi G, et al. Ocrelizumab versus Placebo in Primary Progressive Multiple Sclerosis. *New England Journal of Medicine*. 2017;376(3):209-20.

276. Edwards JCW, Szczepański L, Szechiński J, Filipowicz-Sosnowska A, Emery P, Close DR, et al. Efficacy of B-Cell–Targeted Therapy with Rituximab in Patients with Rheumatoid Arthritis. *New England Journal of Medicine*. 2004;350(25):2572-81.
277. Stasi R, Pagano A, Stipa E, and Amadori S. Rituximab chimeric anti-CD20 monoclonal antibody treatment for adults with chronic idiopathic thrombocytopenic purpura. *Blood*. 2001;98(4):952-7.
278. Crickx E, Chappert P, Sokal A, Weller S, Azzaoui I, Vandenberghe A, et al. Rituximab-resistant splenic memory B cells and newly engaged naive B cells fuel relapses in patients with immune thrombocytopenia. *Sci Transl Med*. 2021;13(589).
279. Stone JH, Merkel PA, Spiera R, Seo P, Langford CA, Hoffman GS, et al. Rituximab versus cyclophosphamide for ANCA-associated vasculitis. *N Engl J Med*. 2010;363(3):221-32.
280. Piehl F, Eriksson-Dufva A, Budzianowska A, Feresiadou A, Hansson W, Hietala MA, et al. Efficacy and Safety of Rituximab for New-Onset Generalized Myasthenia Gravis: The RINOMAX Randomized Clinical Trial. *JAMA Neurology*. 2022;79(11):1105-12.
281. Whittam DH, Cobo-Calvo A, Lopez-Chiriboga AS, Pardo S, Gornall M, Cicconi S, et al. Treatment of MOG-IgG-associated disorder with rituximab: An international study of 121 patients. *Mult Scler Relat Disord*. 2020;44:102251.
282. Cree BA, Lamb S, Morgan K, Chen A, Waubant E, and Genain C. An open label study of the effects of rituximab in neuromyelitis optica. *Neurology*. 2005;64(7):1270-2.
283. Merrill JT, Neuwelt CM, Wallace DJ, Shanahan JC, Latinis KM, Oates JC, et al. Efficacy and safety of rituximab in moderately-to-severely active systemic lupus erythematosus: The randomized, double-blind, phase ii/iii systemic lupus erythematosus evaluation of rituximab trial. *Arthritis & Rheumatism*. 2010;62(1):222-33.
284. Cree BAC, Bennett JL, Kim HJ, Weinshenker BG, Pittock SJ, Wingerchuk DM, et al. Inebilizumab for the treatment of neuromyelitis optica spectrum disorder (N-MOmentum): a double-blind, randomised placebo-controlled phase 2/3 trial. *The Lancet*. 2019;394(10206):1352-63.
285. Agius MA, Klodowska-Duda G, Maciejowski M, Potemkowski A, Li J, Patra K, et al. Safety and tolerability of inebilizumab (MEDI-551), an anti-CD19 monoclonal antibody, in patients with relapsing forms of multiple sclerosis: Results from a phase 1 randomised, placebo-controlled, escalating intravenous and subcutaneous dose study. *Mult Scler*. 2019;25(2):235-45.
286. Vikse J, Jonsdottir K, Kvaløy JT, Wildhagen K, and Omdal R. Tolerability and safety of long-term rituximab treatment in systemic inflammatory and autoimmune diseases. *Rheumatol Int*. 2019;39(6):1083-90.
287. Navarra SV, Guzmán RM, Gallacher AE, Hall S, Levy RA, Jimenez RE, et al. Efficacy and safety of belimumab in patients with active systemic lupus erythematosus: a randomised, placebo-controlled, phase 3 trial. *The Lancet*. 2011;377(9767):721-31.
288. Vincent FB, Morand EF, Schneider P, and Mackay F. The BAFF/APRIL system in SLE pathogenesis. *Nature Reviews Rheumatology*. 2014;10(6):365-73.

289. Stohl W, Hiepe F, Latinis KM, Thomas M, Scheinberg MA, Clarke A, et al. Belimumab reduces autoantibodies, normalizes low complement levels, and reduces select B cell populations in patients with systemic lupus erythematosus. *Arthritis & Rheumatism*. 2012;64(7):2328-37.
290. Facon T, Kumar S, Plesner T, Orlowski RZ, Moreau P, Bahlis N, et al. Daratumumab plus Lenalidomide and Dexamethasone for Untreated Myeloma. *N Engl J Med*. 2019;380(22):2104-15.
291. Roccatello D, Fenoglio R, Caniggia I, Kamgaing J, Naretto C, Cecchi I, et al. Daratumumab monotherapy for refractory lupus nephritis. *Nature Medicine*. 2023;29(8):2041-7.
292. Barratt J, Tumlin J, Suzuki Y, Kao A, Aydemir A, Pudota K, et al. Randomized Phase II JANUS Study of Atacicept in Patients With IgA Nephropathy and Persistent Proteinuria. *Kidney Int Rep*. 2022;7(8):1831-41.
293. Genovese MC, Kinnman N, de La Bourdonnaye G, Pena Rossi C, and Tak PP. Atacicept in patients with rheumatoid arthritis and an inadequate response to tumor necrosis factor antagonist therapy: Results of a phase II, randomized, placebo-controlled, dose-finding trial. *Arthritis & Rheumatism*. 2011;63(7):1793-803.
294. Ginzler EM, Wax S, Rajeswaran A, Copt S, Hillson J, Ramos E, et al. Atacicept in combination with MMF and corticosteroids in lupus nephritis: results of a prematurely terminated trial. *Arthritis Research & Therapy*. 2012;14(1):R33.
295. Kappos L, Hartung H-P, Freedman MS, Boyko A, Radü EW, Mikol DD, et al. Atacicept in multiple sclerosis (ATAMS): a randomised, placebo-controlled, double-blind, phase 2 trial. *The Lancet Neurology*. 2014;13(4):353-63.
296. Mackensen A, Müller F, Mougiakakos D, Böltz S, Wilhelm A, Aigner M, et al. Anti-CD19 CAR T cell therapy for refractory systemic lupus erythematosus. *Nature Medicine*. 2022;28(10):2124-32.
297. Müller F, Taubmann J, Bucci L, Wilhelm A, Bergmann C, Völkl S, et al. CD19 CAR T-Cell Therapy in Autoimmune Disease — A Case Series with Follow-up. *New England Journal of Medicine*. 2024;390(8):687-700.
298. Kerner G, Neehus A-L, Philippot Q, Bohlen J, Rinchai D, Kerrouche N, et al. Genetic adaptation to pathogens and increased risk of inflammatory disorders in post-Neolithic Europe. *Cell Genomics*. 2023;3(2):100248.
299. Fumagalli M, Pozzoli U, Cagliani R, Comi GP, Riva S, Clerici M, et al. Parasites represent a major selective force for interleukin genes and shape the genetic predisposition to autoimmune conditions. *Journal of Experimental Medicine*. 2009;206(6):1395-408.
300. Patrakka J, and Tryggvason K. New insights into the role of podocytes in proteinuria. *Nat Rev Nephrol*. 2009;5(8):463-8.
301. Daehn IS, and Duffield JS. The glomerular filtration barrier: a structural target for novel kidney therapies. *Nature Reviews Drug Discovery*. 2021;20(10):770-88.
302. Grahammer F, Schell C, and Huber TB. The podocyte slit diaphragm—from a thin grey line to a complex signalling hub. *Nature Reviews Nephrology*. 2013;9(10):587-98.

303. Kocylowski MK, Aypek H, Bildl W, Helmstädter M, Trachte P, Dumoulin B, et al. A slit-diaphragm-associated protein network for dynamic control of renal filtration. *Nature Communications*. 2022;13(1):6446.
304. Birtasu AN, Wieland K, Ermel UH, Rahm JV, Scheffer MP, Flottmann B, et al. The molecular architecture of the kidney slit diaphragm. *bioRxiv*. 2023:2023.10.27.564405.
305. Huber TB, Simons M, Hartleben B, Sernetz L, Schmidts M, Gundlach E, et al. Molecular basis of the functional podocin–nephrin complex: mutations in the NPHS2 gene disrupt nephrin targeting to lipid raft microdomains. *Human Molecular Genetics*. 2003;12(24):3397-405.
306. Faul C, Asanuma K, Yanagida-Asanuma E, Kim K, and Mundel P. Actin up: regulation of podocyte structure and function by components of the actin cytoskeleton. *Trends in Cell Biology*. 2007;17(9):428-37.
307. Yaddanapudi S, Altintas MM, Kistler AD, Fernandez I, Möller CC, Wei C, et al. CD2AP in mouse and human podocytes controls a proteolytic program that regulates cytoskeletal structure and cellular survival. *J Clin Invest*. 2011;121(10):3965-80.
308. Huber TB, Hartleben B, Kim J, Schmidts M, Schermer B, Keil A, et al. Nephrin and CD2AP Associate with Phosphoinositide 3-OH Kinase and Stimulate AKT-Dependent Signaling. *Molecular and Cellular Biology*. 2003;23(14):4917-28.
309. Reiser J, Kriz W, Kretzler M, and Mundel P. The glomerular slit diaphragm is a modified adherens junction. *J Am Soc Nephrol*. 2000;11(1):1-8.
310. Kestilä M, Lenkkeri U, Männikkö M, Lamerdin J, McCready P, Putaala H, et al. Positionally cloned gene for a novel glomerular protein--nephrin--is mutated in congenital nephrotic syndrome. *Mol Cell*. 1998;1(4):575-82.
311. Weber S, Gribouval O, Esquivel EL, Morinière V, Tête M-J, Legendre C, et al. NPHS2 mutation analysis shows genetic heterogeneityof steroid-resistant nephrotic syndrome and lowpost-transplant recurrence. *Kidney International*. 2004;66(2):571-9.
312. Chadban SJ, and Atkins RC. Glomerulonephritis. *The Lancet*. 2005;365(9473):1797-806.
313. Noone DG, Iijima K, and Parekh R. Idiopathic nephrotic syndrome in children. *The Lancet*. 2018;392(10141):61-74.
314. Holdsworth SR, Gan P-Y, and Kitching AR. Biologics for the treatment of autoimmune renal diseases. *Nature Reviews Nephrology*. 2016;12(4):217-31.
315. Salama AD, and Pusey CD. Drug Insight: rituximab in renal disease and transplantation. *Nature Clinical Practice Nephrology*. 2006;2(4):221-30.
316. Wu H, and Humphreys BD. The promise of single-cell RNA sequencing for kidney disease investigation. *Kidney International*. 2017;92(6):1334-42.
317. Zhu J, Lu J, and Weng H. Single-cell RNA sequencing for the study of kidney disease. *Molecular Medicine*. 2023;29(1):85.
318. Sethi S, De Vriese AS, and Fervenza FC. Acute glomerulonephritis. *The Lancet*. 2022;399(10335):1646-63.
319. Wyatt RJ, and Julian BA. IgA Nephropathy. *New England Journal of Medicine*. 2013;368(25):2402-14.

320. Galla JH. IgA nephropathy. *Kidney Int.* 1995;47(2):377-87.
321. Lai KN. Pathogenesis of IgA nephropathy. *Nature Reviews Nephrology.* 2012;8(5):275-83.
322. Lafayette Richard A, and Kelepouris E. Immunoglobulin A Nephropathy: Advances in Understanding of Pathogenesis and Treatment. *American Journal of Nephrology.* 2018;47(Suppl. 1):43-52.
323. Lai KN, Leung JC, Chan LY, Saleem MA, Mathieson PW, Tam KY, et al. Podocyte injury induced by mesangial-derived cytokines in IgA nephropathy. *Nephrol Dial Transplant.* 2009;24(1):62-72.
324. Leung JCK, Lai KN, and Tang SCW. Role of Mesangial-Podocytic-Tubular Cross-Talk in IgA Nephropathy. *Semin Nephrol.* 2018;38(5):485-95.
325. Kiryluk K, Moldoveanu Z, Sanders JT, Eison TM, Suzuki H, Julian BA, et al. Aberrant glycosylation of IgA1 is inherited in both pediatric IgA nephropathy and Henoch–Schönlein purpura nephritis. *Kidney International.* 2011;80(1):79-87.
326. Kiryluk K, Sanchez-Rodriguez E, Zhou X-J, Zanoni F, Liu L, Mladkova N, et al. Genome-wide association analyses define pathogenic signaling pathways and prioritize drug targets for IgA nephropathy. *Nature Genetics.* 2023;55(7):1091-105.
327. Li M, Wang L, Shi D-C, Foo J-N, Zhong Z, Khor C-C, et al. Genome-Wide Meta-Analysis Identifies Three Novel Susceptibility Loci and Reveals Ethnic Heterogeneity of Genetic Susceptibility for IgA Nephropathy. *Journal of the American Society of Nephrology.* 2020;31(12).
328. Harper SJ, Allen AC, Béné MC, Pringle JH, Faure G, Lauder I, et al. Increased dimeric IgA-producing B cells in tonsils in IgA nephropathy determined by in situ hybridization for J chain mRNA. *Clin Exp Immunol.* 1995;101(3):442-8.
329. Gleeson PJ, Benech N, Chemouny J, Metallinou E, Berthelot L, da Silva J, et al. The gut microbiota posttranslationally modifies IgA1 in autoimmune glomerulonephritis. *Sci Transl Med.* 2024;16(740):eadl6149.
330. Yu X-Q, Li M, Zhang H, Low H-Q, Wei X, Wang J-Q, et al. A genome-wide association study in Han Chinese identifies multiple susceptibility loci for IgA nephropathy. *Nature Genetics.* 2012;44(2):178-82.
331. Kiryluk K, Li Y, Scolari F, Sanna-Cherchi S, Choi M, Verbitsky M, et al. Discovery of new risk loci for IgA nephropathy implicates genes involved in immunity against intestinal pathogens. *Nature Genetics.* 2014;46(11):1187-96.
332. Zheng N, Xie K, Ye H, Dong Y, Wang B, Luo N, et al. TLR7 in B cells promotes renal inflammation and Gd-IgA1 synthesis in IgA nephropathy. *JCI Insight.* 2020;5(14).
333. Hirano K, Matsuzaki K, Yasuda T, Nishikawa M, Yasuda Y, Koike K, et al. Association Between Tonsillectomy and Outcomes in Patients With Immunoglobulin A Nephropathy. *JAMA Network Open.* 2019;2(5):e194772-e.
334. Feehally J, Farrall M, Boland A, Gale DP, Gut I, Heath S, et al. HLA Has Strongest Association with IgA Nephropathy in Genome-Wide Analysis. *Journal of the American Society of Nephrology.* 2010;21(10).
335. Kiryluk K, Li Y, Sanna-Cherchi S, Rohanizadegan M, Suzuki H, Eitner F, et al. Geographic Differences in Genetic Susceptibility to IgA Nephropathy: GWAS

Replication Study and Geospatial Risk Analysis. *PLOS Genetics*. 2012;8(6):e1002765.
336. Nihei Y, Haniuda K, Higashiyama M, Asami S, Iwasaki H, Fukao Y, et al. Identification of IgA autoantibodies targeting mesangial cells redefines the pathogenesis of IgA nephropathy. *Science Advances*. 2023;9(12):eadd6734.
337. Hocaoğlu M, Valenzuela-Almada MO, Dabit JY, Osei-Onomah S-A, Chevet B, Giblon RE, et al. Incidence, Prevalence, and Mortality of Lupus Nephritis: A Population-Based Study Over Four Decades Using the Lupus Midwest Network. *Arthritis & Rheumatology*. 2023;75(4):567-73.
338. Hakkim A, Fürnrohr BG, Amann K, Laube B, Abed UA, Brinkmann V, et al. Impairment of neutrophil extracellular trap degradation is associated with lupus nephritis. *Proceedings of the National Academy of Sciences*. 2010;107(21):9813-8.
339. Li P, Jiang M, Li K, Li H, Zhou Y, Xiao X, et al. Glutathione peroxidase 4–regulated neutrophil ferroptosis induces systemic autoimmunity. *Nature Immunology*. 2021;22(9):1107-17.
340. Arazi A, Rao DA, Berthier CC, Davidson A, Liu Y, Hoover PJ, et al. The immune cell landscape in kidneys of patients with lupus nephritis. *Nature Immunology*. 2019;20(7):902-14.
341. Schiffer L, Bethunaickan R, Ramanujam M, Huang W, Schiffer M, Tao H, et al. Activated Renal Macrophages Are Markers of Disease Onset and Disease Remission in Lupus Nephritis1. *The Journal of Immunology*. 2008;180(3):1938-47.
342. Villanueva E, Yalavarthi S, Berthier CC, Hodgin JB, Khandpur R, Lin AM, et al. Netting neutrophils induce endothelial damage, infiltrate tissues, and expose immunostimulatory molecules in systemic lupus erythematosus. *The Journal of Immunology*. 2011;187(1):538-52.
343. Camussi G, Cappio FC, Messina M, Coppo R, Stratta P, and Vercellone A. The polymorphonuclear neutrophil (PMN) immunohistological technique: detection of immune complexes bound to the PMN membrane in acute poststreptococcal and lupus nephritis. *Clinical nephrology*. 1980;14(6):280-7.
344. Mesquita D, Jr., Kirsztajn GM, Franco MF, Reis LA, Perazzio SF, Mesquita FV, et al. CD4+ T helper cells and regulatory T cells in active lupus nephritis: an imbalance towards a predominant Th1 response? *Clinical and Experimental Immunology*. 2017;191(1):50-9.
345. Koga T, Ichinose K, and Tsokos GC. T cells and IL-17 in lupus nephritis. *Clinical Immunology*. 2017;185:95-9.
346. Chang A, Henderson SG, Brandt D, Liu N, Guttikonda R, Hsieh C, et al. In Situ B Cell-Mediated Immune Responses and Tubulointerstitial Inflammation in Human Lupus Nephritis. *The Journal of Immunology*. 2011;186(3):1849-60.
347. Jennette JC, and Nachman PH. ANCA Glomerulonephritis and Vasculitis. *Clinical Journal of the American Society of Nephrology*. 2017;12(10).
348. Kessenbrock K, Krumbholz M, Schönermarck U, Back W, Gross WL, Werb Z, et al. Netting neutrophils in autoimmune small-vessel vasculitis. *Nature Medicine*. 2009;15(6):623-5.

349. Dick J, Gan P-Y, Ford SL, Odobasic D, Alikhan MA, Loosen SH, et al. C5a receptor 1 promotes autoimmunity, neutrophil dysfunction and injury in experimental anti-myeloperoxidase glomerulonephritis. *Kidney International*. 2018;93(3):615-25.
350. Krebs CF, Reimers D, Zhao Y, Paust H-J, Bartsch P, Nuñez S, et al. Pathogen-induced tissue-resident memory T<sub>H</sub>17 (T<sub>RM</sub>17) cells amplify autoimmune kidney disease. *Science Immunology*. 2020;5(50):eaba4163.
351. Sharma RK, Yoosuf N, Afonso M, Scheffschick A, Avik A, Bartoletti A, et al. Identification of proteinase 3 autoreactive CD4+T cells and their T-cell receptor repertoires in antineutrophil cytoplasmic antibody–associated vasculitis. *Kidney International*. 2023;103(5):973-85.
352. Free ME, Stember KG, Hess JJ, McInnis EA, Lardinois O, Hogan SL, et al. Restricted myeloperoxidase epitopes drive the adaptive immune response in MPO-ANCA vasculitis. *Journal of Autoimmunity*. 2020;106:102306.
353. Hilhorst M, Arndt F, Joseph Kemna M, Wieczorek S, Donner Y, Wilde B, et al. HLA–DPB1 as a Risk Factor for Relapse in Antineutrophil Cytoplasmic Antibody–Associated Vasculitis: A Cohort Study. *Arthritis & Rheumatology*. 2016;68(7):1721-30.
354. Tsuchiya N. Genetics of ANCA-associated vasculitis in Japan: a role for HLA-DRB1*09:01 haplotype. *Clinical and Experimental Nephrology*. 2013;17(5):628-30.
355. Martorana D, Maritati F, Malerba G, Bonatti F, Alberici F, Oliva E, et al. PTPN22 R620W polymorphism in the ANCA-associated vasculitides. *Rheumatology (Oxford)*. 2012;51(5):805-12.
356. von Borstel A, Abdulahad WH, Sanders JS, Rip J, Neys SFH, Hendriks RW, et al. Evidence for enhanced Bruton's tyrosine kinase activity in transitional and naïve B cells of patients with granulomatosis with polyangiitis. *Rheumatology (Oxford)*. 2019;58(12):2230-9.
357. Lepse N, Abdulahad WH, Rutgers A, Kallenberg CG, Stegeman CA, and Heeringa P. Altered B cell balance, but unaffected B cell capacity to limit monocyte activation in anti-neutrophil cytoplasmic antibody-associated vasculitis in remission. *Rheumatology (Oxford)*. 2014;53(9):1683-92.
358. Cornec D, Berti A, Hummel A, Peikert T, Pers JO, and Specks U. Identification and phenotyping of circulating autoreactive proteinase 3-specific B cells in patients with PR3-ANCA associated vasculitis and healthy controls. *J Autoimmun*. 2017;84:122-31.
359. Fischer EG, and Lager DJ. Anti-glomerular basement membrane glomerulonephritis: a morphologic study of 80 cases. *Am J Clin Pathol*. 2006;125(3):445-50.
360. Kluth DC, and Rees AJ. Anti-Glomerular Basement Membrane Disease. *Journal of the American Society of Nephrology*. 1999;10(11).
361. Lerner RA, Glassock RJ, and Dixon FJ. The role of anti-glomerular basement membrane antibody in the pathogenesis of human glomerulonephritis. *J Exp Med*. 1967;126(6):989-1004.
362. Shen CR, Jia XY, Luo W, Olaru F, Cui Z, Zhao MH, et al. Laminin-521 is a Novel Target of Autoantibodies Associated with Lung Hemorrhage in Anti-GBM Disease. *J Am Soc Nephrol*. 2021;32(8):1887-97.

363. Nithagon P, Cortazar F, Shah SI, Weins A, Laliberte K, Jeyabalan A, et al. Eculizumab and Complement Activation in Anti-glomerular Basement Membrane Disease. *Kidney Int Rep*. 2021;6(10):2713-7.
364. Ooi JD, Holdsworth SR, and Kitching AR. Advances in the pathogenesis of Goodpasture's disease: From epitopes to autoantibodies to effector T cells. *Journal of Autoimmunity*. 2008;31(3):295-300.
365. McAdoo SP, and Pusey CD. Anti-Glomerular Basement Membrane Disease. *Clin J Am Soc Nephrol*. 2017;12(7):1162-72.
366. Prendecki M, Clarke C, Cairns T, Cook T, Roufosse C, Thomas D, et al. Anti-glomerular basement membrane disease during the COVID-19 pandemic. *Kidney Int*. 2020;98(3):780-1.
367. Pusey CD. Anti-glomerular basement membrane disease. *Kidney International*. 2003;64(4):1535-50.
368. Donaghy M, and Rees A. CIGARETTE SMOKING AND LUNG HAEMORRHAGE IN GLOMERULONEPHRITIS CAUSED BY AUTOANTIBODIES TO GLOMERULAR BASEMENT MEMBRANE. *The Lancet*. 1983;322(8364):1390-3.
369. Jayne DRW, Marshall PD, Jones SJ, and Lockwood CM. Autoantibodies to GBM and neutrophil cytoplasm in rapidly progressive glomerulonephritis. *Kidney International*. 1990;37(3):965-70.
370. Klinge S, Yan K, Reimers D, Brede K-M, Schmid J, Paust H-J, et al. Role of regulatory T cells in experimental autoimmune glomerulonephritis. *American Journal of Physiology-Renal Physiology*. 2019;316(3):F572-F81.
371. Paust HJ, Ostmann A, Erhardt A, Turner JE, Velden J, Mittrücker HW, et al. Regulatory T cells control the Th1 immune response in murine crescentic glomerulonephritis. *Kidney Int*. 2011;80(2):154-64.
372. Kluger MA, Luig M, Wegscheid C, Goerke B, Paust H-J, Brix SR, et al. Stat3 Programs Th17-Specific Regulatory T Cells to Control GN. *Journal of the American Society of Nephrology*. 2014;25(6):1291-302.
373. Anders H-J. Of Inflammasomes and Alarmins: IL-1β and IL-1α in Kidney Disease. *Journal of the American Society of Nephrology : JASN*. 2016;27(9):2564-75.
374. Swaminathan S, Leung N, Lager DJ, Melton LJ, III, Bergstralh EJ, Rohlinger A, et al. Changing Incidence of Glomerular Disease in Olmsted County, Minnesota: A 30-Year Renal Biopsy Study. *Clinical Journal of the American Society of Nephrology*. 2006;1(3).
375. Couser WG. Primary Membranous Nephropathy. *Clinical Journal of the American Society of Nephrology*. 2017;12(6).
376. Hoxha E, Reinhard L, and Stahl RAK. Membranous nephropathy: new pathogenic mechanisms and their clinical implications. *Nature Reviews Nephrology*. 2022;18(7):466-78.
377. von Haxthausen F, Reinhard L, Pinnschmidt HO, Rink M, Soave A, Hoxha E, et al. Antigen-Specific IgG Subclasses in Primary and Malignancy-Associated Membranous Nephropathy. *Frontiers in Immunology*. 2018;9.

378. Škoberne A, Behnert A, Teng B, Fritzler MJ, Schiffer L, Pajek J, et al. Serum with phospholipase A2 receptor autoantibodies interferes with podocyte adhesion to collagen. *European Journal of Clinical Investigation*. 2014;44(8):753-65.
379. Tomas NM, Hoxha E, Reinicke AT, Fester L, Helmchen U, Gerth J, et al. Autoantibodies against thrombospondin type 1 domain–containing 7A induce membranous nephropathy. *The Journal of Clinical Investigation*. 2016;126(7):2519-32.
380. Herwig J, Skuza S, Sachs W, Sachs M, Failla AV, Rune G, et al. Thrombospondin Type 1 Domain–Containing 7A Localizes to the Slit Diaphragm and Stabilizes Membrane Dynamics of Fully Differentiated Podocytes. *Journal of the American Society of Nephrology*. 2019;30(5).
381. Takano T, Elimam H, and Cybulsky AV. Complement-Mediated Cellular Injury. *Seminars in Nephrology*. 2013;33(6):586-601.
382. Coenen MJH, Hofstra JM, Debiec H, Stanescu HC, Medlar AJ, Stengel B, et al. Phospholipase A2 Receptor (PLA2R1) Sequence Variants in Idiopathic Membranous Nephropathy. *Journal of the American Society of Nephrology*. 2013;24(4).
383. Xie J, Liu L, Mladkova N, Li Y, Ren H, Wang W, et al. The genetic architecture of membranous nephropathy and its potential to improve non-invasive diagnosis. *Nature Communications*. 2020;11(1):1600.
384. Stanescu HC, Arcos-Burgos M, Medlar A, Bockenhauer D, Kottgen A, Dragomirescu L, et al. Risk HLA-DQA1 and PLA<sub>2</sub>R1 Alleles in Idiopathic Membranous Nephropathy. *New England Journal of Medicine*. 2011;364(7):616-26.
385. Motavalli R, Etemadi J, Soltani-Zangbar MS, Ardalan M-R, Kahroba H, Roshangar L, et al. Altered Th17/Treg ratio as a possible mechanism in pathogenesis of idiopathic membranous nephropathy. *Cytokine*. 2021;141:155452.
386. Cantarelli C, Jarque M, Angeletti A, Manrique J, Hartzell S, O'Donnell T, et al. A Comprehensive Phenotypic and Functional Immune Analysis Unravels Circulating Anti-Phospholipase A2 Receptor Antibody Secreting Cells in Membranous Nephropathy Patients. *Kidney Int Rep*. 2020;5(10):1764-76.
387. Moudgil A, Perriello P, Loechelt B, Przygodzki R, Fitzerald W, and Kamani N. Immunodysregulation, polyendocrinopathy, enteropathy, X-linked (IPEX) syndrome: an unusual cause of proteinuria in infancy. *Pediatr Nephrol*. 2007;22(10):1799-802.
388. Chuva T, Pfister F, Beringer O, Felgentreff K, Büttner-Herold M, and Amann K. PLA2R-positive (primary) membranous nephropathy in a child with IPEX syndrome. *Pediatr Nephrol*. 2017;32(9):1621-4.
389. Gentile M, Miano M, Terranova P, Giardino S, Faraci M, Pierri F, et al. Case Report: Atypical Manifestations Associated With FOXP3 Mutations. The "Fil Rouge" of Treg Between IPEX Features and Other Clinical Entities? *Front Immunol*. 2022;13:854749.
390. Burbelo PD, Joshi M, Chaturvedi A, Little DJ, Thurlow JS, Waldman M, et al. Detection of PLA2R Autoantibodies before the Diagnosis of Membranous Nephropathy. *Journal of the American Society of Nephrology*. 2020;31(1).
391. Remuzzi G, Chiurchiu C, Abbate M, Brusegan V, Bontempelli M, and Ruggenenti P. Rituximab for idiopathic membranous nephropathy. *Lancet*. 2002;360(9337):923-4.

392. Ruggenenti P, Chiurchiu C, Brusegan V, Abbate M, Perna A, Filippi C, et al. Rituximab in idiopathic membranous nephropathy: a one-year prospective study. *J Am Soc Nephrol*. 2003;14(7):1851-7.
393. Fervenza FC, Cosio FG, Erickson SB, Specks U, Herzenberg AM, Dillon JJ, et al. Rituximab treatment of idiopathic membranous nephropathy. *Kidney Int*. 2008;73(1):117-25.
394. Shi X, Qu Z, Zhang L, Zhang N, Liu Y, Li M, et al. Increased ratio of ICOS+/PD-1+ follicular helper T cells positively correlates with the development of human idiopathic membranous nephropathy. *Clinical and Experimental Pharmacology and Physiology*. 2016;43(4):410-6.
395. Zhang Z, Shi Y, Yang K, Crew R, Wang H, and Jiang Y. Higher frequencies of circulating ICOS+, IL-21+ T follicular helper cells and plasma cells in patients with new-onset membranous nephropathy. *Autoimmunity*. 2017;50(8):458-67.
396. Samuel SM, Takano T, Scott S, Benoit G, Bitzan M, Mammen C, et al. Setting New Directions for Research in Childhood Nephrotic Syndrome: Results From a National Workshop. *Can J Kidney Health Dis*. 2017;4:2054358117703386.
397. Maas RJ, Deegens JK, Smeets B, Moeller MJ, and Wetzels JF. Minimal change disease and idiopathic FSGS: manifestations of the same disease. *Nature Reviews Nephrology*. 2016;12(12):768-76.
398. Robins R, Baldwin C, Aoudjit L, Côté J-F, Gupta IR, and Takano T. Rac1 activation in podocytes induces the spectrum of nephrotic syndrome. *Kidney International*. 2017;92(2):349-64.
399. Tejani A. Morphological Transition in Minimal Change Nephrotic Syndrome. *Nephron*. 2008;39(3):157-9.
400. Nephrotic syndrome in children: prediction of histopathology from clinical and laboratory characteristics at time of diagnosis. A report of the International Study of Kidney Disease in Children. *Kidney Int*. 1978;13(2):159-65.
401. Canaud G, Dion D, Zuber J, Gubler M-C, Sberro R, Thervet E, et al. Recurrence of nephrotic syndrome after transplantation in a mixed population of children and adults: course of glomerular lesions and value of the Columbia classification of histological variants of focal and segmental glomerulosclerosis (FSGS). *Nephrology Dialysis Transplantation*. 2009;25(4):1321-8.
402. Hickson LJ, Gera M, Amer H, Iqbal CW, Moore TB, Milliner DS, et al. Kidney transplantation for primary focal segmental glomerulosclerosis: outcomes and response to therapy for recurrence. *Transplantation*. 2009;87(8):1232-9.
403. Artero ML, Sharma R, Savin VJ, and Vincenti F. Plasmapheresis Reduces Proteinuria and Serum Capacity to Injure Glomeruli in Patients With Recurrent Focal Glomerulosclerosis. *American Journal of Kidney Diseases*. 1994;23(4):574-81.
404. Gbadegesin RA, Adeyemo A, Webb NJA, Greenbaum LA, Abeyagunawardena A, Thalgahagoda S, et al. HLA-DQA1 and PLCG2 Are Candidate Risk Loci for Childhood-Onset Steroid-Sensitive Nephrotic Syndrome. *Journal of the American Society of Nephrology : JASN*. 2015;26(7):1701-10.

405. Ramanathan ASK, Senguttuvan P, Chinniah R, Vijayan M, Thirunavukkarasu M, Raju K, et al. Association of HLA-DR/DQ alleles and haplotypes with nephrotic syndrome. *Nephrology.* 2016;21(9):745-52.
406. Debiec H, Dossier C, Letouzé E, Gillies CE, Vivarelli M, Putler RK, et al. Transethnic, Genome-Wide Analysis Reveals Immune-Related Risk Alleles and Phenotypic Correlates in Pediatric Steroid-Sensitive Nephrotic Syndrome. *Journal of the American Society of Nephrology.* 2018;29(7).
407. Jia X, Horinouchi T, Hitomi Y, Shono A, Khor S-S, Omae Y, et al. Strong Association of the HLA-DR/DQ Locus with Childhood Steroid-Sensitive Nephrotic Syndrome in the Japanese Population. *Journal of the American Society of Nephrology.* 2018;29(8).
408. Dufek S, Cheshire C, Levine AP, Trompeter RS, Issler N, Stubbs M, et al. Genetic Identification of Two Novel Loci Associated with Steroid-Sensitive Nephrotic Syndrome. *Journal of the American Society of Nephrology.* 2019;30(8).
409. Jia X, Yamamura T, Gbadegesin R, McNulty MT, Song K, Nagano C, et al. Common risk variants in NPHS1 and TNFSF15 are associated with childhood steroid-sensitive nephrotic syndrome. *Kidney International*. 2020;98(5):1308-22.
410. Barry A, McNulty MT, Jia X, Gupta Y, Debiec H, Luo Y, et al. Multi-population genome-wide association study implicates immune and non-immune factors in pediatric steroid-sensitive nephrotic syndrome. *Nature Communications*. 2023;14(1):2481.
411. Downie ML, Gupta S, Voinescu C, Levine AP, Sadeghi-Alavijeh O, Dufek-Kamperis S, et al. Common Risk Variants in AHI1 Are Associated With Childhood Steroid Sensitive Nephrotic Syndrome. *Kidney Int Rep.* 2023;8(8):1562-74.
412. Christian MT, Webb NJA, Mehta S, Woolley RL, Afentou N, Frew E, et al. Evaluation of Daily Low-Dose Prednisolone During Upper Respiratory Tract Infection to Prevent Relapse in Children With Relapsing Steroid-Sensitive Nephrotic Syndrome: The PREDNOS 2 Randomized Clinical Trial. *JAMA Pediatr.* 2022;176(3):236-43.
413. Sellier-Leclerc AL, Baudouin V, Kwon T, Macher MA, Guerin V, Lapillonne H, et al. Rituximab in steroid-dependent idiopathic nephrotic syndrome in childhood--follow-up after CD19 recovery. *Nephrol Dial Transplant*. 2012;27(3):1083-9.
414. Shao XS, Yang XQ, Zhao XD, Li Q, Xie YY, Wang XG, et al. The prevalence of Th17 cells and FOXP3 regulate T cells (Treg) in children with primary nephrotic syndrome. *Pediatr Nephrol*. 2009;24(9):1683-90.
415. Liu LL, Qin Y, Cai JF, Wang HY, Tao JL, Li H, et al. Th17/Treg imbalance in adult patients with minimal change nephrotic syndrome. *Clin Immunol*. 2011;139(3):314-20.
416. Jaiswal A, Prasad N, Agarwal V, Yadav B, Tripathy D, Rai M, et al. Regulatory and effector T cells changes in remission and resistant state of childhood nephrotic syndrome. *Indian Journal of Nephrology.* 2014;24(6):349-55.
417. Prasad N, Jaiswal AK, Agarwal V, Yadav B, Sharma RK, Rai M, et al. Differential alteration in peripheral T-regulatory and T-effector cells with change in P-glycoprotein expression in Childhood Nephrotic Syndrome: A longitudinal study. *Cytokine*. 2015;72(2):190-6.

418. Tsuji S, Kimata T, Yamanouchi S, Kitao T, Kino J, Suruda C, et al. Regulatory T cells and CTLA-4 in idiopathic nephrotic syndrome. *Pediatr Int*. 2017;59(5):643-6.
419. Ye Q, Zhou C, Li S, Wang J, Liu F, Liu Z, et al. The immune cell landscape of peripheral blood mononuclear cells from PNS patients. *Scientific Reports*. 2021;11(1):13083.
420. Park E, Chang HJ, Shin JI, Lim BJ, Jeong HJ, Lee KB, et al. Familial IPEX syndrome: different glomerulopathy in two siblings. *Pediatr Int*. 2015;57(2):e59-61.
421. Hashimura Y, Nozu K, Kanegane H, Miyawaki T, Hayakawa A, Yoshikawa N, et al. Minimal change nephrotic syndrome associated with immune dysregulation, polyendocrinopathy, enteropathy, X-linked syndrome. *Pediatr Nephrol*. 2009;24(6):1181-6.
422. Benz K, Dötsch J, Rascher W, and Stachel D. Change of the course of steroid-dependent nephrotic syndrome after rituximab therapy. *Pediatric Nephrology*. 2004;19(7):794-7.
423. Iijima K, Sako M, Nozu K, Mori R, Tuchida N, Kamei K, et al. Rituximab for childhood-onset, complicated, frequently relapsing nephrotic syndrome or steroid-dependent nephrotic syndrome: a multicentre, double-blind, randomised, placebo-controlled trial. *The Lancet*. 2014;384(9950):1273-81.
424. Printza N, Papachristou F, Tzimouli V, Taparkou A, and Kanakoudi-Tsakalidou F. Peripheral CD19+ B cells are increased in children with active steroid-sensitive nephrotic syndrome. *NDT Plus*. 2009;2(5):435-6.
425. Colucci M, Carsetti R, Cascioli S, Casiraghi F, Perna A, Rava L, et al. B Cell Reconstitution after Rituximab Treatment in Idiopathic Nephrotic Syndrome. *J Am Soc Nephrol*. 2016;27(6):1811-22.
426. Colucci M, Carsetti R, Cascioli S, Serafinelli J, Emma F, and Vivarelli M. B cell phenotype in pediatric idiopathic nephrotic syndrome. *Pediatric Nephrology*. 2019;34(1):177-81.
427. Fribourg M, Cioni M, Ghiggeri G, Cantarelli C, Leventhal JS, Budge K, et al. CyTOF-Enabled Analysis Identifies Class-Switched B Cells as the Main Lymphocyte Subset Associated With Disease Relapse in Children With Idiopathic Nephrotic Syndrome. *Front Immunol*. 2021;12:726428.
428. Ling C, Wang X, Chen Z, Fan J, Meng Q, Zhou N, et al. Altered B-Lymphocyte Homeostasis in Idiopathic Nephrotic Syndrome. *Front Pediatr*. 2019;7:377.
429. Watts AJB, Keller KH, Lerner G, Rosales I, Collins AB, Sekulic M, et al. Discovery of Autoantibodies Targeting Nephrin in Minimal Change Disease Supports a Novel Autoimmune Etiology. *Journal of the American Society of Nephrology*. 2022;33(1):238.
430. Coward RJM, Foster RR, Patton D, Ni L, Lennon R, Bates DO, et al. Nephrotic Plasma Alters Slit Diaphragm–Dependent Signaling and Translocates Nephrin, Podocin, and CD2 Associated Protein in Cultured Human Podocytes. *Journal of the American Society of Nephrology*. 2005;16(3).
431. Salfi G, Casiraghi F, and Remuzzi G. Current understanding of the molecular mechanisms of circulating permeability factor in focal segmental glomerulosclerosis. *Front Immunol*. 2023;14:1247606.

432. Jamin A, Berthelot L, Couderc A, Chemouny JM, Boedec E, Dehoux L, et al. Autoantibodies against podocytic UCHL1 are associated with idiopathic nephrotic syndrome relapses and induce proteinuria in mice. *Journal of Autoimmunity.* 2018;89:149-61.
433. Ye Q, Zhang Y, Zhuang J, Bi Y, Xu H, Shen Q, et al. The important roles and molecular mechanisms of annexin A(2) autoantibody in children with nephrotic syndrome. *Ann Transl Med.* 2021;9(18):1452.
434. Chan EY-h, Yap DY-h, Colucci M, Ma AL-t, Parekh RS, and Tullus K. Use of Rituximab in Childhood Idiopathic Nephrotic Syndrome. *Clinical Journal of the American Society of Nephrology.* 2023;18(4).
435. Colucci M, Oniszczuk J, Vivarelli M, and Audard V. B-Cell Dysregulation in Idiopathic Nephrotic Syndrome: What We Know and What We Need to Discover. *Frontiers in immunology.* 2022;13:823204-.
436. Hada I, Shimizu A, Takematsu H, Nishibori Y, Kimura T, Fukutomi T, et al. A Novel Mouse Model of Idiopathic Nephrotic Syndrome Induced by Immunization with the Podocyte Protein Crb2. *Journal of the American Society of Nephrology.* 2022;33(11).
437. Alikhan MA, Huynh M, Kitching AR, and Ooi JD. Regulatory T cells in renal disease. *Clin Transl Immunology.* 2018;7(1):e1004-e.
438. Li Y, Liu H, Yan H, and Xiong J. Research advances on targeted-Treg therapies on immune-mediated kidney diseases. *Autoimmunity Reviews.* 2023;22(2):103257.
439. Ehrenstein MR, Evans JG, Singh A, Moore S, Warnes G, Isenberg DA, et al. Compromised function of regulatory T cells in rheumatoid arthritis and reversal by anti-TNFalpha therapy. *J Exp Med.* 2004;200(3):277-85.
440. Goodman WA, Levine AD, Massari JV, Sugiyama H, McCormick TS, and Cooper KD. IL-6 signaling in psoriasis prevents immune suppression by regulatory T cells. *J Immunol.* 2009;183(5):3170-6.
441. Schneider A, Long SA, Cerosaletti K, Ni CT, Samuels P, Kita M, et al. In active relapsing-remitting multiple sclerosis, effector T cell resistance to adaptive T(regs) involves IL-6-mediated signaling. *Sci Transl Med.* 2013;5(170):170ra15.
442. Dossier C, Jamin A, and Deschênes G. Idiopathic nephrotic syndrome: the EBV hypothesis. *Pediatric Research.* 2017;81(1):233-9.
443. Maruyama K, Tomizawa S, Shimabukuro N, Fukuda T, Johshita T, and Kuroume T. Effect of supernatants derived form T lymphocyte culture in minimal change nephrotic syndrome on rat kidney capillaries. *Nephron.* 1989;51:73-6.
444. Neuhaus TJ, Shah V, Callard RE, and Barratt TM. T-lymphocyte activation in steroid-sensitive nephrotic syndrome in childhood. *Nephrology Dialysis Transplantation.* 1995;10(8):1348-52.
445. Yap H-K, Cheung W, Murugasu B, Sim S-k, Seah C-C, and Jordan SC. Th1 and Th2 Cytokine mRNA Profiles in Childhood Nephrotic Syndrome: Evidence for Increased IL-13 mRNA Expression in Relapse. *Journal of the American Society of Nephrology.* 1999;10(3):529-37.
446. Cunard R, and Kelly CJ. T Cells and Minimal Change Disease. *Journal of the American Society of Nephrology.* 2002;13(5):1409-11.

447. Lama G, Luongo I, Tirino G, Borriello A, Carangio C, and Salsano ME. T-lymphocyte populations and cytokines in childhood nephrotic syndrome. *Am J Kidney Dis*. 2002;39(5):958-65.
448. Shimoyama H, Nakajima M, Naka H, Maruhashi Y, Akazawa H, Ueda T, et al. Up-regulation of interleukin-2 mRNA in children with idiopathic nephrotic syndrome. *Pediatr Nephrol*. 2004;19(10):1115-21.
449. Shalaby SA, Al-Edressi HM, El-Tarhouny SA, Fath El-Bab M, and Zolaly MA. Type 1/type 2 cytokine serum levels and role of interleukin-18 in children with steroid-sensitive nephrotic syndrome. *Arab J Nephrol Transplant*. 2013;6(2):83-8.
450. Wang L, Li Q, Wang L, Li C, Yang H, Wang X, et al. The role of Th17/IL-17 in the pathogenesis of primary nephrotic syndrome in children. *Kidney Blood Press Res*. 2013;37(4-5):332-45.
451. Yurasov S, Tiller T, Tsuiji M, Velinzon K, Pascual V, Wardemann H, et al. Persistent expression of autoantibodies in SLE patients in remission. *J Exp Med*. 2006;203(10):2255-61.
452. Yurasov S, Wardemann H, Hammersen J, Tsuiji M, Meffre E, Pascual V, et al. Defective B cell tolerance checkpoints in systemic lupus erythematosus. *J Exp Med*. 2005;201(5):703-11.
453. Kinnunen T, Chamberlain N, Morbach H, Cantaert T, Lynch M, Preston-Hurlburt P, et al. Specific peripheral B cell tolerance defects in patients with multiple sclerosis. *J Clin Invest*. 2013;123(6):2737-41.
454. Samuels J, Ng YS, Coupillaud C, Paget D, and Meffre E. Impaired early B cell tolerance in patients with rheumatoid arthritis. *J Exp Med*. 2005;201(10):1659-67.
455. Yang X, Tang X, Li T, Man C, Yang X, Wang M, et al. Circulating follicular T helper cells are possibly associated with low levels of serum immunoglobulin G due to impaired immunoglobulin class-switch recombination of B cells in children with primary nephrotic syndrome. *Molecular Immunology*. 2019;114:162-70.
456. Johnson JL, Rosenthal RL, Knox JJ, Myles A, Naradikian MS, Madej J, et al. The Transcription Factor T-bet Resolves Memory B Cell Subsets with Distinct Tissue Distributions and Antibody Specificities in Mice and Humans. *Immunity*. 2020;52(5):842-55.e6.
457. Russell Knode LM, Naradikian MS, Myles A, Scholz JL, Hao Y, Liu D, et al. Age-Associated B Cells Express a Diverse Repertoire of V(H) and Vκ Genes with Somatic Hypermutation. *J Immunol*. 2017;198(5):1921-7.
458. Woodruff MC, Ramonell RP, Haddad NS, Anam FA, Rudolph ME, Walker TA, et al. Dysregulated naive B cells and de novo autoreactivity in severe COVID-19. *Nature*. 2022;611(7934):139-47.
459. Mouat IC, Allanach JR, Fettig NM, Fan V, Girard AM, Shanina I, et al. Gammaherpesvirus infection drives age-associated B cells toward pathogenicity in EAE and MS. *Science Advances*. 2022;8(47):eade6844.
460. Zhang Q, Huang B, Liu X, Liu B, Zhang Y, Zhang Z, et al. Ultrasensitive Quantitation of Anti-Phospholipase A2 Receptor Antibody as A Diagnostic and Prognostic Indicator of Idiopathic Membranous Nephropathy. *Scientific Reports*. 2017;7(1):12049.

461. Watanabe K, Watanabe K, Watanabe Y, Fujioka D, Nakamura T, Nakamura K, et al. Human soluble phospholipase A2 receptor is an inhibitor of the integrin-mediated cell migratory response to collagen-I. *American Journal of Physiology-Cell Physiology.* 2018;315(3):C398-C408.
462. Hu M, Wang YM, Wang Y, Zhang GY, Zheng G, Yi S, et al. Regulatory T cells in kidney disease and transplantation. *Kidney International.* 2016;90(3):502-14.
463. Raffin C, Vo LT, and Bluestone JA. Treg cell-based therapies: challenges and perspectives. *Nature Reviews Immunology.* 2020;20(3):158-72.